



UNIVERSITAT DE
BARCELONA

Galenic development of a new sunscreen product for skin cancer prevention

Lola Amorós Galicia

ADVERTIMENT. La consulta d'aquesta tesi queda condicionada a l'acceptació de les següents condicions d'ús: La difusió d'aquesta tesi per mitjà del servei TDX (www.tdx.cat) i a través del Dipòsit Digital de la UB (diposit.ub.edu) ha estat autoritzada pels titulars dels drets de propietat intel·lectual únicament per a usos privats emmarcats en activitats d'investigació i docència. No s'autoritza la seva reproducció amb finalitats de lucre ni la seva difusió i posada a disposició des d'un lloc aliè al servei TDX ni al Dipòsit Digital de la UB. No s'autoritza la presentació del seu contingut en una finestra o marc aliè a TDX o al Dipòsit Digital de la UB (framing). Aquesta reserva de drets afecta tant al resum de presentació de la tesi com als seus continguts. En la utilització o cita de parts de la tesi és obligat indicar el nom de la persona autora.

ADVERTENCIA. La consulta de esta tesis queda condicionada a la aceptación de las siguientes condiciones de uso: La difusión de esta tesis por medio del servicio TDR (www.tdx.cat) y a través del Repositorio Digital de la UB (diposit.ub.edu) ha sido autorizada por los titulares de los derechos de propiedad intelectual únicamente para usos privados enmarcados en actividades de investigación y docencia. No se autoriza su reproducción con finalidades de lucro ni su difusión y puesta a disposición desde un sitio ajeno al servicio TDR o al Repositorio Digital de la UB. No se autoriza la presentación de su contenido en una ventana o marco ajeno a TDR o al Repositorio Digital de la UB (framing). Esta reserva de derechos afecta tanto al resumen de presentación de la tesis como a sus contenidos. En la utilización o cita de partes de la tesis es obligado indicar el nombre de la persona autora.

WARNING. On having consulted this thesis you're accepting the following use conditions: Spreading this thesis by the TDX (www.tdx.cat) service and by the UB Digital Repository (diposit.ub.edu) has been authorized by the titular of the intellectual property rights only for private uses placed in investigation and teaching activities. Reproduction with lucrative aims is not authorized nor its spreading and availability from a site foreign to the TDX service or to the UB Digital Repository. Introducing its content in a window or frame foreign to the TDX service or to the UB Digital Repository is not authorized (framing). Those rights affect to the presentation summary of the thesis as well as to its contents. In the using or citation of parts of the thesis it's obliged to indicate the name of the author.



UNIVERSITAT DE BARCELONA

FACULTAT DE FARMÀCIA I CIÈNCIES DE L'ALIMENTACIÓ

**GALENIC DEVELOPMENT OF A NEW SUNSCREEN
PRODUCT FOR SKIN CANCER PREVENTION**

LOLA AMORÓS GALICIA, 2022

UNIVERSITAT DE BARCELONA

FACULTAT DE FARMÀCIA I CIÈNCIES DE L'ALIMENTACIÓ

PROGRAMA DE DOCTORAT EN INVESTIGACIÓ, DESENVOLUPAMENT I
CONTROL DE MEDICAMENTS

**GALENIC DEVELOPMENT OF A NEW SUNSCREEN PRODUCT FOR SKIN
CANCER PREVENTION**

Memòria presentada per Lola Amorós Galicia per optar al títol de Doctor per la Universitat de Barcelona

Prof. Dr. Josep Maria Suñé Negre
Director i tutor

Lola Amorós Galicia
Doctoranda

Lola Amorós Galicia, 2022

El dolor que sents avui serà la força que sentiràs demà

-Dwayne Johnson-

Aportacions relacionades amb la Tesi Doctoral

Aquest projecte està emmarcat dins del programa de Doctorats Industrials concedit per la Generalitat de Catalunya en convocatòria pública competitiva:

Títol: “Desenvolupament d’una formulació d’aplicació tòpica amb nous fotoprotectors per a la prevenció de càncer de pell i melasma”

Número d’Expedient: 2019 DI 38

Data d’ inici: 25/07/2019

Data de finalització: 26/07/2022

Import atorgat a l’empresa: 33. 960,00 €

Import atorgat a la Universitat: 21.600 €

Empresa col·laboradora: Roka Furadada S.L.

Universitat col·laboradora: Universitat de Barcelona (Facultat de Farmàcia i Ciències de l’Alimentació).

Articles

- **Lola Amorós-Galicia**, Anna Nardi-Ricart, Clara Verdugo-Gonzalez, Carmen Martina Arroyo-Garcia, Encarna García-Montoya, Pilar Perez-Lozano, Josep Maria Suñé-Negre, Marc Suñé-Pou. “Development of a standardized method for measuring bioadhesion and mucoadhesion, applicable to various pharmaceutical forms”. *Pharmaceutics* **IF 6.525 (Q1)**.

Abstract

Sunscreen application is one of the best methods to prevent erythema, keratogenic cancer, melanoma and premature skin ageing. UV filters are the active substances preventing the harmful effects. Commercial UV filters exert its maximal effectiveness once they are applied on skin. Instead, progressive UV filters develop into its active form, which absorb UV-light in presence of UVB light. Although new UV filters were developed, still one of the old generation UV filters, avobenzene, is one of the most marketed sunscreens for its high absorbance in the UVA range. On the other hand, avobenzene can degrade upon exposure towards UV radiation. The aim was to evaluate the implications of the new technology in real sun exposure conditions. The absorbance of the progressive UV filters: PRE-A, PRE-B and PRE-C were evaluated at different concentrations in Emollient-A. PRE-A demonstrated the highest activation and absorbance and was characterized physico-chemically. Different batches of PRE-A were irradiated with a solar simulator. The batch with the highest absorbance was compared to avobenzene for four hours in Emollient-A solution. While PRE-A increased the absorbance with increased irradiation, avobenzene degraded converging both absorbances at 4 h irradiation. Mixtures of avobenzene and PRE-A were irradiated in solution obtaining for the combination 2:1 (avobenzene:PRE-A) the highest absorbance after 4 h irradiation. In emulsion this combination delivered higher Solar protection factor (SPF) and Protection in the UVA range (UVA-PF) at 2,5 and 5 minimal erhitemal dose (MED) compared to the same amount of avobenzene. Therefore, it could be used as avobenzene booster.

Experts recommend application of sunscreen products every 2 hours, as sweating and bathing contribute sunscreen film loss. This might be inconvenient to users and many of them admit not renewing sunscreen application, which decreases the effectiveness of the product. A bioadhesive sunscreen formulation with water resistant properties and SPF 30 was designed to ensure 100% stickiness of the UV filters after bathing. Moreover, the formulation should contain only photostable UV filters with no susception for being endocrine disruptors, bleaching of the coral reef or penetration potential. In addition, only non-comedogenic ingredients were used. The development process was made with a bioadhesive gel as starting

point and small modifications were done each time. The objective was to achieve cosmetical elegance as this is the most determinant factor in the compliance of sunscreen application. Cosmetic elegance was evaluated according to a survey. The final formulation obtained the maximal score in 5/6 evaluation criteria. Finally, a stability test was performed including in use stability concluding stability at 12 months at room temperature.

Resum

L'aplicació de protector solar és un dels millors mètodes per prevenir l'eritema, els diferents tipus de càncers de pell i l'envelliment prematur de la pell. Els filtres ultraviolats (UV) absorbeixen i reflecteixen la llum UV prevenint els seus efectes nocius. Els filtres UV comercials exerceixen la seva màxima eficàcia un cop s'apliquen a la pell. Així, la fotoprotecció s'exerceix independentment de la irradiació UV. En aquest treball s'han estudiat un nou tipus de filtres UV anomenats filtres UV progressius els quals evolucionen a la seva forma activa en presència de llum UVB.

Actualment l'avobenzona és un dels filtres solars més comercialitzats per la seva alta absorbència a l'espectre UVA. Tanmateix, és un filtre UV fotoinestable que disminueix la seva efectivitat degut a l'exposició solar continuada. L'objectiu era avaluar les implicacions de la nova tecnologia en condicions reals d'exposició solar. Es va mesurar l'absorbència dels filtres UV progressius: PRE-A, PRE-B i PRE-C a diferents concentracions en l'emol·lient-A en presència de llum solar simulada. PRE-A va demostrar una major activació i absorbència d'entre els tres filtres UV progressius i es van caracteritzar les seves propietats fisicoquímiques. Es van irradiar diferents lots de PRE-A i el lot amb major capacitat absorbent es va comparar amb l'avobenzona fins a quatre hores d'irradiació en solució d'emol·lient-A. L'absorbència de PRE-A va augmentar amb l'increment de dosi d'irradiació solar simulada mentre que l'avobenzona va decreixer i ambdues corbes d'absorbència van convergir a les 4 h d'irradiació. Posteriorment es van irradiar solucions de combinacions d'avobenzona i PRE-A. L'absorbència més alta es va produir amb la combinació 2:1 (avobenzona:PRE-A) després de 4 h d'irradiació. Finalment, es va formular una crema solar amb la combinació 2:1 (avobenzona:PRE-A) i es va mesurar la seva absorbència a diferents dosis eritemàtica mínima (MED). En emulsió, aquesta combinació suposa una millora del factor de protecció solar (SPF) i del factor de protecció en el rang UVA (UVA-PF) a 2,5 i 5 MED en comparació amb la mateixa quantitat d'avobenzona. Per tant, es podria utilitzar per a reforçar la fotoinestabilitat de l'avobenzona.

Els experts recomanen l'aplicació de productes de protecció solar cada 2 hores i després de banyar-se, ja que la sudoració i la immersió en aigua contribueixen a la pèrdua de la pel·lícula de protecció solar. Això suposa un inconvenient per als usuaris i molts d'ells admeten no renovar l'aplicació de protecció solar, la qual cosa disminueix l'eficàcia del producte. En aquest projecte es va dissenyar una formulació d'alta protecció solar (SPF 30), bioadhesiva i amb propietats resistents a l'aigua (100% dels filtres UV es mantenen a la formulació). A més, la formulació conté filtres UV fotoestables, sense potencial disruptió endocrina, blanqueig de l'escull de corall ni penetració a través de la pell. A més, es van utilitzar ingredients no comedogènics. El procés de desenvolupament es va fer amb un gel bioadhesiu com a punt de partida i es van fer petites modificacions cada vegada fins a obtenir un protector solar amb optimes propietats sensorials. L'elegància estètica es va avaluar segons una enquesta. La formulació final va obtenir la puntuació màxima en 5/6 criteris d'avaluació. Finalment, es va realitzar una prova d'estabilitat i l'estabilitat en ús. La crema bioadhesiva és estable als 12 mesos a temperatura ambient.

Agraïments

Primer de tot m'agradaria agrair al meu director de tesi, el Dr. Josep Maria Suñé i Negre per donar-me l'oportunitat de fer el doctorat a la Unitat de Tecnologia Farmacèutica del Departament de Farmàcia i Tecnologia Farmacèutica, i Físicoquímica de la Facultat de Farmàcia a la Universitat de Barcelona. Ha estat molt constructiu discutir els resultats dels experiments i valorar el mètode estadístic més escaient en cada cas. Gràcies per recolzar-me en cada pas del projecte i per la teva disponibilitat sempre que he necessitat consell.

També m'agradaria agrair a la Dra. Pilar Pérez Lozano per ensenyar-me el mètode de la solubilitat. També li agraeixo la seva disponibilitat per a comentar dubtes. A la Dra. Encarna García Montoya pel seu suport en temes d'estadística.

Al Dr. Marc Suñé Pou per la revisió dels articles i pòsters. Ha estat molt interessant discutir propostes i per donar-me suport. Al Sr. Roig per aconsellar-me en les formulacions galèniques. Al Dr. Alfons del Pozo per el seu consell en tècniques de formulació d'emulsions així com de productes cosmètics, determinació d'estabilitat i per estar sempre disposat a donar un cop de mà. A la Dr. Lyda Halbaut per ensenyar-me el funcionament del rheòmetre. Al Dr. Albert Manich del CSIC per ensenyar-me el mètode de la bioadhesivitat. Al Dr. Bernd Herzog per transmetre'm el seu ampli coneixement en filtres solars i fotoquímica, que des d'Alemanya, m'ha acompanyat en aquesta apassionant etapa.

M'agradaria agrair a Lúdia, Inma i Ester per la seva eficiència en les tasques administratives així com en el seu suport en tot moment.

Tanmateix, aprofito per agrair als meus companys de laboratori així com a tots els companys del SDM que he tingut el plaer de conèixer per fer la meva estada tan amena. Sempre recordaré els nostres esmorzars amb enyorança.

Finalment, als meus pares per donar-me sempre el vostre suport incondicional i ser el meu pilar. Mai us podré agrair prou tot el que feu per mi. Aquesta tesi es el resultat de l'esforç i constància que m'heu transmès sempre.

INDEX

AIMS	21
1 INTRODUCTION	27
1.1 SOLAR RADIATION	29
1.2 BIOLOGICAL EFFECTS OF SOLAR RADIATION ON THE SKIN	33
1.2.1 <i>Beneficial effects of solar radiation: Vitamin D</i>	33
1.2.2 <i>Negative health effects of solar radiation</i>	34
1.3 UV FILTERS	38
1.3.1 <i>Types of commercial UV Filters</i>	38
1.3.2 <i>Effectiveness measurements of UV filters</i>	40
1.3.3 <i>Concerns with UV filters</i>	44
1.3.4 <i>Progressive UV filters: PRE-A, PRE-B and PRE-C</i>	49
1.4 SEMISOLID FORMULATIONS AND SUNSCREEN PRODUCTS	55
1.4.1 <i>Emulsions</i>	55
1.4.2 <i>Stability of emulsions</i>	65
1.4.3 <i>The ideal sunscreen product</i>	67
2 PHOTOACTIVATION OF PROGRESSIVE UV FILTERS: PRE-A, PRE-B, PRE-C	75
2.1 INTRODUCTION	77
2.2 MATERIALS AND METHODS	78
2.2.1 <i>Materials</i>	78
2.2.2 <i>Solubility at 5% of progressive UV filters in different solvents</i>	80
2.2.3 <i>UV spectrophotometry- Cuvette method</i>	80
2.3 RESULTS AND DISCUSSION	83
2.3.1 <i>UV-filter solubility at 5%</i>	83
2.3.2 <i>Activation and characterization of photochemical behaviour at different irradiation doses and concentrations</i>	85
2.3.3 <i>Mixtures of progressive UV-filters and synergistic effect screening</i>	89
2.3.4 <i>Comparison of progressive UV-filters with commercial UV-filters</i>	94
2.4 CONCLUSION	97
3 PRE-A PHYSIC-CHEMICAL CHARACTERISATION	99
3.1 INTRODUCTION	101
3.2 MATERIALS AND METHODS	102
3.2.1 <i>Chemicals</i>	102
3.2.2 <i>Equipment</i>	102

3.2.3	<i>Content analysis by High Liquid Performance Chromatography (HPLC)</i>	103
3.2.4	<i>IR</i>	104
3.2.5	<i>UV</i>	105
3.2.6	<i>DSC</i>	106
3.2.7	<i>Solubility</i>	106
3.3	RESULTS AND DISCUSSION	107
3.3.1	<i>HPLC</i>	107
3.3.2	<i>IR</i>	113
3.3.3	<i>UV</i>	118
3.3.4	<i>DSC</i>	119
3.3.5	<i>Solubility</i>	120
3.4	CONCLUSION	121
4	PHOTOACTIVATION OF PRE-A IN DIFFERENT VEHICLES	125
4.1	INTRODUCTION	125
4.2	MATERIALS AND METHODS	127
4.2.1	<i>Materials</i>	127
4.2.2	<i>Cuvette method</i>	129
4.2.3	<i>Plate method</i>	132
4.3	RESULTS AND DISCUSSION	134
4.3.1	<i>Cuvette method</i>	134
4.3.2	<i>Plate method</i>	145
4.3.3	<i>SPF and UVA-PF</i>	151
4.3.4	<i>Synergic effect screening</i>	154
4.3.5	<i>Comparison of E1,1 with plate and cuvette method</i>	155
4.4	CONCLUSION	157
5	BIOADHESIVE SUNSCREEN EMULSION	161
5.1	INTRODUCTION	161
5.2	MATERIALS AND METHODS	162
5.2.1	<i>Chemicals</i>	162
5.2.2	<i>Equipment</i>	164
5.2.3	<i>Determination of the UV-filters combinations to reach an SPF 30 with the minimal amount of UV-Filters</i>	165
5.2.4	<i>Literature research: UV-filters and other ingredients with minimal toxicity, irritancy and comedogenicity</i>	166
5.2.5	<i>Formulation type finding</i>	166
5.2.6	<i>Evaluation of organoleptic properties of the formulations</i>	167
5.2.7	<i>pH</i>	169

5.2.8	<i>Microscopy</i>	170
5.2.9	<i>Rheology and viscosity</i>	170
5.2.10	<i>Extensibility</i>	171
5.2.11	<i>Bioadhesion</i>	172
5.2.12	<i>Active's product content and UVA in vitro determination</i>	173
5.2.13	<i>Water resistance</i>	177
5.2.14	<i>Centrifugation</i>	178
5.2.15	<i>Stability</i>	178
5.3	RESULTS AND DISCUSSION	189
5.3.1	<i>Literature search: UV-filters and other ingredients with minimal toxicity, irritancy and comedogenicity</i>	189
5.3.2	<i>Formulation process: trial and error</i>	190
5.3.3	<i>Formulation process: Organoleptic evaluation</i>	231
5.3.4	<i>Absorbance profile and stability of UV filters</i>	241
5.3.5	<i>SPF, UVA-PF and other parameters</i>	244
5.3.6	<i>pH</i>	249
5.3.7	<i>Microscopy</i>	249
5.3.8	<i>Rheology and viscosity</i>	250
5.3.9	<i>Extensibility</i>	254
5.3.10	<i>Bioadhesion</i>	255
5.3.11	<i>Water resistance</i>	258
5.3.12	<i>Centrifugation</i>	259
5.3.13	<i>Stability</i>	260
5.4	CONCLUSION	283
6	GLOBAL DISCUSSION	287
7	CONCLUSIONS	298
8	REFERENCES	305
	ANNEXES	325

AIMS

This thesis aimed to cover the following objectives:

1. Perform a physicochemical characterization of PRE-A by HPLC, UV, IR, DSC and assess its solubility in water.
2. Assess the photochemical activation of PRE-B, PRE-C and PRE-A alone or in combination and look for synergistic effects of the combinations. Compare the absorbance spectra of PRE-B, PRE-C and PRE-A to these of commercial UV filters.
3. Study the photochemical behaviour of different batches of PRE-A under simulated real life solar standard conditions and out of the match with the best activation capacity assess its absorption capacity with dependency of the solvent used to solubilize the UV filter and in combination with avobenzone.
4. Assess the absorption capacity of PRE-A alone and in combination with avobenzone by the cuvette method and plate method and compare the specific extinction for both methods. Moreover, assess synergic behaviour of the combinations and calculate the solar protection factor (SPF) and ultraviolet A (UVA) factor in formulation.
5. Design a bioadhesive sunscreen of high protection factor (SPF=30) using ingredients with high tolerability in respect to allergic sensitizers and non-comedogenicity with the focus on user's compliance.
6. Develop of an original, novel and systematic *in vitro* method for assessing bioadhesiveness of solid and semisolid forms that enables the comparison of results across studies mimicking real amounts of daily use.

BIBLIOGRAPHICAL PART

1. INTRODUCTION

1.1 Solar radiation

The sun emits energy in form of radiation to the Earth. The electromagnetic radiation is divided into three groups according to their wavelengths: the infrared light (IR) the (waves above 700 nm), visible light (400-700 nm), and UVR light (200-400 nm). The percentage of emitted light to the atmosphere are distributed in IR 56%, visible light 39% and UVR 5% (1). The UV light has the shorter wavelengths and therefore are the most energetical ones. The UV light is divided in three subgroups according to their wavelength; UVA (320-400 nm), which is further divided into UVAI (400- 340 nm) and UVAIL (340-320 nm), UVB (280-320 nm) and UVC (200-280 nm). UVB and UVA are important in sunscreen technology because both can produce harmful effects on skin like erythema, skin ageing and melanoma (2–4). Finally, UVC radiation with its shortest wavelength and therefore highest energy in electromagnetic spectrum is filtered by the ozone layer and avoids reaching the earth's surface (4,5).

The skin and UV radiation

The skin is an organ which is directly exposed to the external medium and has a protective function as it is the first immunological barrier. In adults its extension is about 2 m² and weights 4,1 kg and the thickness variates from 0,5 mm -4 mm. Structurally, it has three main layers: epidermis (outer layer), dermis and hypodermis. The epidermis is further divided into stratum corneum (SC), which is the most external part of the skin, and stratum granulosum, spinosum and basal layer (Figure 1-1).

Keratinocytes are produced in in the basal layer by keratinocyte stem cells and differentiate into all the other cells type from the different epidermis layers until they ascend to the stratum corneum forming corneocytes (6,7). The lifetime of a keratinocyte is four weeks (7).

Keratinocytes produce keratin which constitutes the hair and nails and contributes to the skin protective barrier, forming tight junctions between units. In the stratum corneum; keratinocytes of the granular layer die. Dead keratinocytes have no nucleolus and therefore no metabolism but form a compact intercrossed structure of corneocyte layers, which provide

the most efficient physical barrier. Corneocytes are continuously renewed by the differentiation of keratinocytes from the lower epidermis layer.

Melanocytes are positioned on the basal layer surrounded with keratinocytes. One every ten to twelve cells of the basal layer is a melanocyte but because of its finger shaped structure one melanocytes provides with pigment to 30-40 keratinocytes. Melanocytes exert a UV protective function by blocking the UVR and thus impeding its penetration to the dermis. The pigment which melanocytes produce is melanin and confers the color of the skin. Melanocytes produce two types of melanin: eumelanin and pheomelanin. Although all the people are provided with the same number of melanocytes (2400 each cm²), the percentage of one or the other type of melanin will determine the color. Eumelanin is dark brown and pheomelanin is yellow-red. In people with darker skin, eumelanin is at a greater proportion than pheomelanin. On the other hand, whiter skin people will be provided with more pheomelanin. The skin protection of eumelanin is superior than pheomelanin, blocking the UVR more efficiently. Therefore, dark skinned people will have a greater protection against UVR than fair skinned people (6,7).

Implications of the UVR radiation can be divided in UVB and UVA light. As already mentioned in section 1, shorter wavelengths (UVC, UVB) have higher energy. In the case of UVB and UVA which penetrate the atmosphere, UVB has a higher energy with more direct damage than UVA. On the other hand, the UVA penetrates more deeply into the skin dermis (Figure 1-1).

UVB rays are reflected in the stratum corneum and penetrate the epidermis producing erythema, commonly known as sunburn, and direct DNA lesions, which may develop in skin cancer if the DNA-reparation mechanisms fail and ultimately the cell does not undergo apoptosis. Cancer cells will then surpass control mechanisms and duplicate uncontrolled.

UVA rays can penetrate deeper into the dermis. Although, being a weaker mutagen than UVB, it contributes to skin cancer by indirect DNA-damage through reactive oxygen species (ROS) generation. Its radiation can penetrate window glasses and UVA is filtered also at cloudy days. Moreover, it promotes skin aging and causes damages of blood vessels (8–11).

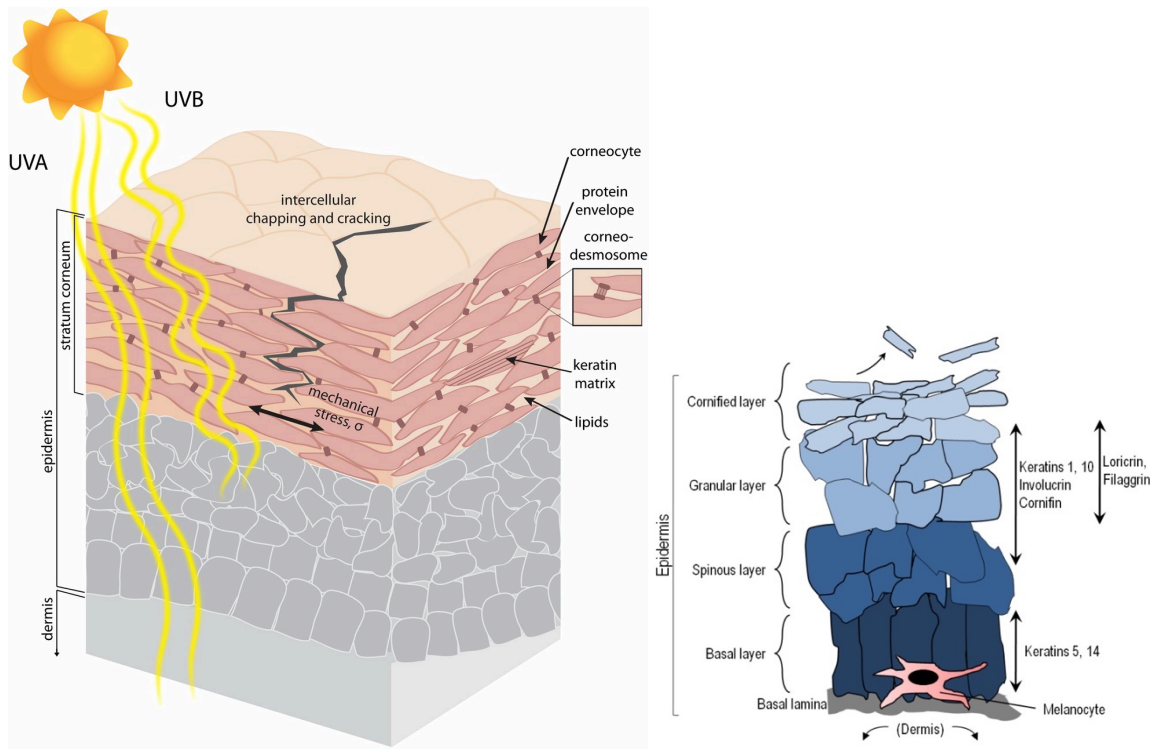


Figure 1-1. Structure of skin epidermis and dermis and the penetration of UVR through the layers (6,11).

Skin type classification

The magnitude of the harmful effects of continued ultraviolet radiation (UVR) depend on high extend on the skin type. There Fitzpatrick scale is a classification of the skin type which comprises the different skin tonalites linked to inherited sun protection (6,12) (Table 1-1).

Table 1-1. The Fitzpatrick scale of phototype classification (6).

Fitzpatrick phototype	Phenotype	Epidermal eumelanin	Cutaneous response to UV	MED (mJ/cm ²) *	Cancer risk
I	Unexposed skin is bright white Blue/green eyes typical Freckling frequent Northern European/British	+/-	Always burns Peels Never tans	15-30	++++
II	Unexposed skin is white Blue, hazel or brown eyes Red, blonde or brown hair European/Scandinavian	+	Burns easily Peels Tans minimally	25-40	+++ /++++
III	Unexposed skin is fair Brown eyes Dark hair Southern or Central European	++	Burns moderately Average tanning ability	30-50	+++
IV	Unexposed skin is light brown Dark eyes Dark hair Mediterranean, Asian or Latino	+++	Burns minimally Tans easily	40-60	++
V	Unexposed skin is brown Dark eyes Dark hair East Indian, Native American, Latino or African	++++	Rarely burns Tans easily and substantially	60-90	+
VI	Unexposed skin is black Dark eyes Dark hair African or Aboriginal ancestry	+++++	Almost never burns Tans readily and profusely	90-150	+/-

The six different phototypes are ranged from I-VI being I the less pigmented skin type and VI the most pigmented one. Fitzpatrick skin type I is most sensitive to erythema and therefore more prone to skin cancer at the same UVR dose. The higher the skin type (darker skin), the more eumelanin production, less risk of skin cancer and the higher the minimal erythemal dose (MED). The minimal erythemal dose (MED) is defined as the minimal time span or UVR dose required to produce redness (erythema) on skin (13,14).

The effect of melanin as natural photoprotector was calculated to be between 1.5-2.0 sun protective factors (SPF), meaning 1,5 to 2 times increased protection; up to 4 SFP, assuming that melanin UVR absorbance is 50-75% (15).

1.2 Biological effects of solar radiation on the skin

1.2.1 Beneficial effects of solar radiation: Vitamin D

The beneficial effects of solar irradiation are mainly the production of vitamin D. Vitamin D is a fat-soluble hormone, which our organism cannot produce per se. It must be consumed by solar exposure or by diet. Nevertheless, the diet provides only small amounts of vitamin D. Vitamin D production peak is around 300 nm, and therefore UVB radiation (290-320) is necessary for its production. The mechanism of absorbance of vitamin D by the sun involves the skin. Photons of UVB radiation interact with 7-dehydrocholesterol (7-DHC), which is found in the plasma membrane of keratinocytes and fibroblasts forming previtamin D₃. An isomerization of previtamin D₃ converts it thermally to vitamin D₃ (cholecalciferol). From the keratinocyte or fibroblast, the place where it is produced, it is transported by the serum vitamin D binding protein to the liver, where it will transform it to 25(OH)D₃ (calcidiol). An hydroxylation of the molecule in the kidney activates calcidiol to the active calcitriol.

Calcitriol is key in genome transcription and its beneficial effects are observed in bone homeostasis, immune mechanisms with stimulation of immune cells with cancer prevention and reducing progression of infections, and cardiovascular disease prevention. Recommended plasma concentration of serum 25(OH)D levels is 50 nmol/mL. Lower concentration levels will indicate a vitamin D insufficiency and below 30 nmol/L to a vitamin D deficiency. Vitamin D deficiency will develop in rickets in children together with other musco-skeletal diseases like fractures and muscle weakness. Moreover, association with vitamin D deficiency have been linked with diseases. Some examples are autoimmune diseases like rheumatoid arthritis, Alzheimer and cardiovascular diseases (16–18).

Although some population groups with skin diseases like xeroderma pigmentosum, which apply daily high photoprotection show vitamin D deficiency in winter, all in all recurrent sunscreen product application seems not to interfere with vitamin D homeostasis (17).

1.2.2 Negative health effects of solar radiation

Erythema

The solar spectral irradiance (19) is depicted in Figure 1-2. Out of the total UVR which penetrates the stratosphere, the 95% correspond to UVA light (20). However, the erythemal action spectrum (21) is almost exclusive of the UVB range. The multiplication of the solar spectral irradiance and erythemal action spectrum results in the erythemal effectiveness spectrum, which is the zone in the spectra where humans are most susceptible to develop erythema. Erythema is produced near 90% by UVB radiation, while UVA is by 10% responsible of sunburn (22). Figure 1-2 shows the erythemal action spectrum, solar action spectrum and erythemal effectiveness spectrum (23).

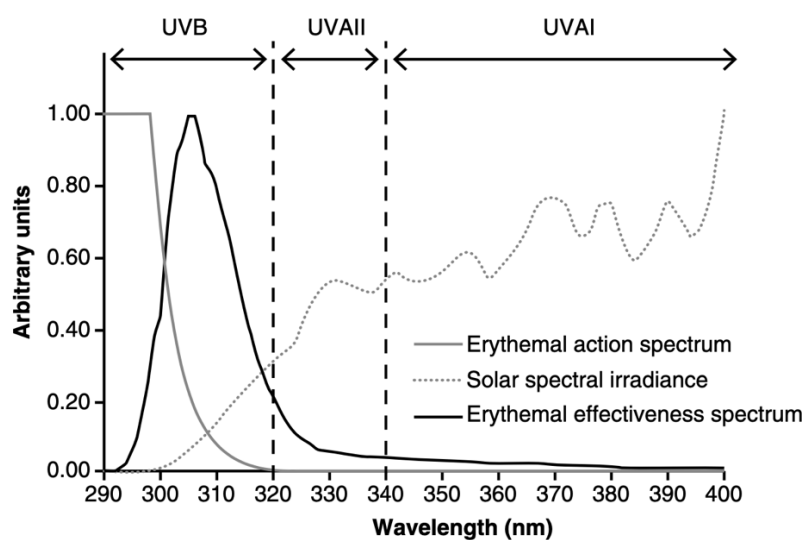


Figure 1-2. Erythemal action spectrum, solar action spectrum and erythemal effectiveness spectrum (23).

Premature skin ageing

Facial ageing was suggested to be produced 80% by UVR radiation, although smoking and air pollution are other factors which may play a role as well in facial wrinkling (24). Premature skin ageing is mainly attributed to UVA although UVB radiation might contribute. UVA radiation penetrates deeper into the dermis at different levels of skin interacting with keratinocytes,

melanocytes, endothelial cells and fibroblasts. The clinical effects of photoaging manifest before the age of 50 and are mostly due to chronic UVA radiation. Clinical manifestations appear in areas which are daily exposed like face, neck, forearms and dorsal hands. Most common signs of aging are pigmentary alterations and wrinkling. Lighter skinned phototypes and continued exposure in areas with high UV indexes during the year are mostly affected (25). Caucasian and Asiatic of Mongolian ethnicities are at higher risk of developing solar lentigines and pigmentary alterations. This alteration of the melanin is more prone in phototype II and III and in women which tan easily becoming a dark to very dark sun tanning. This points out to the efficient production of melanin in Caucasians and also to more risky behaviour towards the sun (26,27). Other manifestations are roughness, dyspigmentation and dry skin, laxity and telangiectasia (27).

Figure 1-3 shows the clinical signs of photoaging. The photograph of the 61-year-old twins reflect the signs of 40 years suntanning in Florida east coast (with 16 years of smoking history), right photograph. The twin on the left minimized her sun exposure (28).



Figure 1-3. Signs of photoaging during lifetime of twin females at 61 years. On the left: Avoidance of high sun exposure; on the right: Suntanning over 40 years (28).

Skin cancer

Skin cancer is the worst effect of sunscreen overexposure. It is the type of cancer with the highest incidence in the United States. Every year around five million citizens in the United States are treated with a cost exceeding the \$8 billion. Skin cancers are classified into non-melanoma, with the subtypes basal cell carcinoma (BCC) and squamous cell carcinoma (SCC), and melanoma. The non-melanoma cancers have a much higher incidence (95%) compared to melanoma (5% incidence) although the effects of melanoma have a much worse prognosis (29,30).

The non-melanoma skin cancers are localized on the skin and normally spreading of the cancerous cells does not occur. BCC is less aggressive than SCC with a 5% maximal dissemination probability, commonly to the lymph nodes. Different treatments are cryotherapy (local freezing), application of anti-cancer creams, radiotherapy and photodynamic therapy (a form of light application). Not treated tumors may cause skin damage. All in all, the non-melanoma have a cure percentage of 90% (30).

Melanoma incidence in the 21st century is in constant increase. In many western countries the risk of incidence to melanoma has increased 1 in 50. The increased risk correlates with sun exposure during lifetime and specially at young ages (31). A study conducted in Australia showed that children migrated from England before the age of 10 developed as adults 4 times more melanomas than a homologous population of English immigrants arriving to Australia at the age of 16 year or later. Surprisingly, native Australians developed the same incidence rate than those British people that were born or came as children to Australia (32). The most frequent melanoma type, the superficial spreading melanoma which appears at 70% of the cases diagnosed shows at places in the body which are commonly hidden and sporadically exposed, rather than in chronic places like hand or neck. Melanoma are localized typically on the back of the legs in women and in the trunk in men. Genetic factors play a role in the development of melanoma. First, Caucasians are at higher risk rather than people with a darker skin, especially for phototypes I and II (29). Second, masculine gender is at 1,5 higher risk to develop melanoma compared to females. However, females younger than 40 are at higher risk than men. Nevertheless, this tendency inverts at the age of 75 as men have a 3-fold risk compared to women of the same age (33).

As it is esteemed that unprotected exposure to sunlight is linked to skin cancers development by 80-90% (34). Therefore, many countries promote the application of sunscreens to prevent skin cancers. Sunscreen application have demonstrated to reduce the non-melanoma and melanoma cancer incidence. In a randomized trial with ten-year follow-up study, a 50% risk of incidence reduction to melanoma was measured for 4,5 years daily application of sunscreen product (35,36).

1.3 UV Filters

1.3.1 Types of commercial UV Filters

UV filters are the active ingredients in sunscreens because of the effect of absorbing UVR. UV filters are classified depending on the spectrum band they cover namely into UVB (290-320), UVA (320-400) and broad-spectrum filters (UVA and UVB). To be effective and protect against the whole UV spectrum, sunscreens normally contain a mixture of different filters. The concentration of every filter is limited by the regulatory authorities. UV filters are commonly named by its INCI name, which stands for Internal Nomenclature of Cosmetic Ingredients. It was established in the 1970's by the Personal Care Products Council to list ingredients on cosmetic products labels (37). There are two types, the organic and inorganic UV filters:

Organic UV filters

Organic UV filters present a chromophore, which acts by absorbing UVR. When UV filters absorb a UV photon the molecule is excited from the ground state to an excited singlet state. The energy must then dissipate in form of heat so that the molecule can go back to its ground state. Excited molecules can dissipate energy by fluorescence, vibrational relaxation and in some cases they get excited to the triplet state through intersystem crossing. In this case the relaxation to the ground state of the UV absorbers is through phosphorescence and intersystem crossing (Figure 1-4) (38,39). Degradation of the absorbing molecule can happen if the energy is not effectively dissipated into heat. In these cases, a break of the molecule would produce degradation of the UV filter (39).

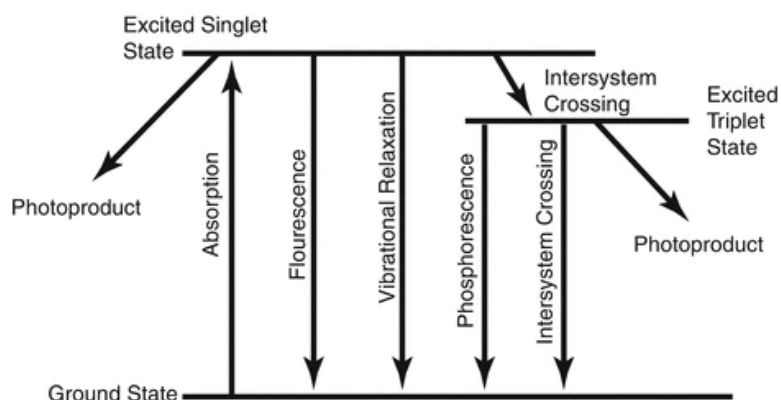


Figure 1-4. Energetic and ground states with relaxation pathways (38).

Organic UV filters are the most used type of sunscreens for its aesthetical properties. Most of the UV filters are lipophilic and therefore are incorporated into the oil phase of the formulation.

Inorganic UV filters

Inorganic UV filters are also called physical filters or mineral filters. Zinc oxide and titanium dioxide (ZnO and TiO₂) are minerals, which are milled as fine particles (7). Technologically, mineral particles are formulated as dispersions or suspensions (40). They are semiconductors with a high band gap energy between the valence and conduction band (8,9). However, rather than absorbing UV light, which contributes only small to its protective effect, they mainly act by blocking UV radiation through reflection and scattering producing a mirroring effect of incident light. The main disadvantage of inorganic UV filters in formulation is the white trash on the skin (also called white cast effect) due to the difference of the refractive index between the particles and water (7,10,38,41). This whitening ghostly effect is perceived as aesthetically unappealing (10).

Otherwise, due to its big particle size, the penetration into the epidermis is low. Compared to organic UV filters, inorganic UV filters have fewer irritation and allergenic potential, and endocrine disruption effects are not under consideration (7,10,40). Therefore, the FDA consider ZnO and TiO₂ as the safest UV filters (42). Among adult population, formulations made only of inorganic filters are not that well tolerated. The reasons are its whitish effect on skin and the fact that formulations use to be greasy. However, inorganic UV filters are an optimum option for products directed to babies (7).

1.3.2 Effectiveness measurements of UV filters

One of the highest importance of UV filters is effectiveness. From the mid 30's there has been an increasing demand for high protection sunscreen products. This tendency was reflected in the development of the new-generation UV filters in the 1990s. The need to cover the entire UV spectrum and to achieve SPF 30-50+ high UV filter amounts is linked with the increased awareness towards the dangerous effects of the sun (23,43). High effectiveness means mainly a high absorbance among the UV spectrum (9). The specific extinction at the maximum wavelength ($E_{1,1(\lambda_{max})}$), SPF and UVA-PF are parameters to define effectiveness.

Specific extinction and wavelength of maximum absorbance

The specific extinction at 1 cm pathlength at 1% concentration ($E_{1,1}$) is a parameter used to quantify the performance of UV filters in solvents. The wavelength of maximum absorbance (λ_{max}) is the wavelength, at which the maximum absorption of the UV filter takes place and the ($E_{1,1(\lambda_{max})}$) is the absorbance of 1% substance (w/v) in 1 cm path length at the wavelength of maximum absorbance of the UV filter. $E_{1,1(\lambda_{max})}$ is based on the extinction (E), which can be calculated with the Beer-Lambert equation; 1-1 (44).

$$E_{\lambda} = -\log\left(\frac{I}{I_0}\right) = \epsilon_{\lambda} \cdot c \cdot d \quad \text{Equation 1-1}$$

where,

E_{λ} is the extinction or absorbance. It is the capacity of a sample to attenuate light at a given wavelength (45),

I_0 is the incident light and I_1 the transmitted light (light that passed through a sample),
 ϵ_{λ} in corresponds to the extinction coefficient and is the measurement of the energy loss of a radiation passing through a sample and has the units $\left(\frac{L \cdot cm^2}{mol}\right)$. It depends on the sample and on the wavelength, at which the sample is irradiated.

C is the molar mass (mol/L) of the solution,

d is the length in cm^2 of the solution the light passes through.

$E_{1,1(\lambda_{max})}$ can be calculated with Equation 1-2 :

$$E_{1,1\lambda_{max}} = \epsilon_{\lambda_{max}} \cdot \frac{1g \text{ substance}}{100ml \text{ solution}} \cdot 1cm \quad \text{Equation 1-2}$$

The principle of the spectroscopic measurement is depicted in Figure 1-5 where an incident light I_0 passed through a sample, absorbing partially the incident light. The transmitted light I is the percentage of light that effectively passes the sample.

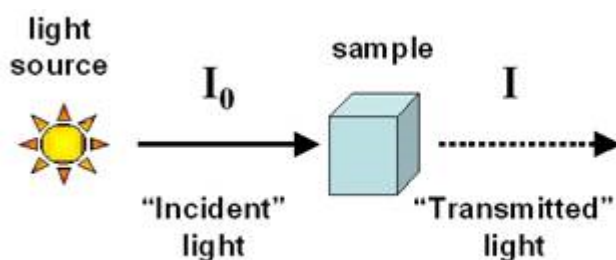


Figure 1-5: Principle of the spectroscopic measurement with an incident light and a transmitted light passing through a sample

Solar protection factor (SPF) *in vivo*

The solar protection factor (SPF) was a term coined by Franz Greiter in 1974 and it is the validated methodology to quantify the effectiveness of a sunscreen product (46). The SPF is a measure of the UVR needed to cause a minimal erythematous sign compared to unprotected skin. Volunteers are irradiated with simulated solar light on unprotected skin until an erythema is observed. After quantifying the minimal dose at which an erythema is observed ($MED_{unprotected \text{ skin}}$), the process is repeated after application of the sunscreen product and the dose to produce the erythema is quantified ($MED_{protected \text{ skin}}$) (47). The SPF is obtained by Equation 1-3.

$$SPF = \frac{MED_{protected}}{MED_{unprotected}} \quad \text{Equation 1-3}$$

A minimum of ten volunteers of phototype I-III according to Fitzpatrick classification are selected for the experiment. Six different UVR doses are applied on the back of the volunteers in clearly defined segments as spots. Every spot corresponds to a specific UVR dose. After 16-24 h the back of the volunteers is visually inspected and the spot where erythema was observed determines the $MED_{unprotected}$. With the known specific $MED_{unprotected}$ for each volunteer, 2 mg/cm² of sunscreen formulation are applied on the back and according to the dose needed to develop erythema the SPF is calculated. As an example, an SPF 10 will be obtained if the protected skin requires 10 times more irradiation dose as the unprotected skin, meaning the erythema appears after 10 minutes UVR in unprotected and 100 minutes in protected skin.

The SPF is a standardized *in vivo* method. To date no *in vitro* method was approved by the health authorities. Therefore, before the commercialization of a sunscreen product an SPF *in vivo* test is required. This presents ethical controversies since volunteers are exposed to simulated solar radiation, until an erythema is produced. This erythema exerts a damage of the skin (20). Moreover, the SPF *in vivo* do not reflect the entire UVR as only erythema produced by UVB and UVAII radiation is quantified. In addition, it is expensive and time consuming (1). Therefore, sunscreen product developers before conducting the SPF *in vivo* assess the SPF using *in vitro* technologies.

Solar protection factor (SPF) *in vitro*

SPF *in vitro* is based on spectroscopical measurements. The sunscreen film is spread on a synthetical matrix and the amount of UVR passing through the sample is analyzed. The SPF *in vitro* is calculated using Equation 1-4.

$$SPF = \frac{\sum_{290}^{400} S_{er}(\lambda) \cdot S_s(\lambda)}{\sum_{290}^{400} S_{er}(\lambda) \cdot S_s(\lambda) \cdot T(\lambda)} \quad \text{Equation 1-4}$$

where $S_s(\lambda)$ stands for the intensity of the light source, $s_{er}(\lambda)$ is the erythral action spectrum and $T(\lambda)$ stands for the transmittance of the UV filter at a specific wavelength. $S_s(\lambda)$ and $s_{er}(\lambda)$ values are given in literature (48). Nevertheless $T(\lambda)$ must be measured.

There are different parameters which influence the SPF value: type of substrate, amount of sunscreen product and spreading technique. Important for this method is that the substrate has a roughened surface to simulate the irregularities of skin surface. The preferred substrate of the cosmetic industry for assessing the UVA *in vitro* are the polymethylmethacrylate (PMMA) plates. These are easy to handle, unexpensive and therefore, there can be rejected after use. Other commonly used substrates are Vitro-Skin, Roughened Quartz Plate and PTFE (Teflon). Although these materials are good predictors of the SPF, main throwbacks of the first two substrates are the high cost and the need of cleaning the surfaces (1). In addition, Vitro-skin has to be hydrated the day before the experiment using a very specific approach (49).

UVA-PF

UVA protection factor is calculated *in vitro* based on the same methodology of transmittance of the SPF *in vitro*.

$$UVA - PF = \frac{\sum_{320}^{400} S_{PPD}(\lambda) \cdot S_{UVA}(\lambda)}{\sum_{320}^{400} S_{PPD}(\lambda) \cdot S_{UVA}(\lambda) \cdot T(\lambda)} \quad \text{Equation 1-5}$$

The UVA-PF is calculated by Equation 1-5. Instead of 290-400 nm of the range comprised by the SPF measurement, the UVA-PF is calculated alongside the UVA spectra (320-400 nm).

Further,

S_{PPD} corresponds to the permanent pigment darkening and

$S_{UVA}(\lambda)$ is the spectral irradiation received from a radiation UVA light source.

In Europe, to label the sunscreen products with UVA protection, the proportion of UVA-PF towards SPF has to be 1/3 (0,33), at least.

Water resistance *in vivo*

The water resistance retention (WRR) test is an *in vivo* method to prove the efficiency after water immersion of the formulation on skin. First the SPF *in vivo* is established for every individual participating in the test according to equation 1-3 and after the immersion the water resistance of the formulation is calculated as the percent remaining after bathing (Equation 1-6)

$$WRR\% = \frac{SPF_w - 1}{SPF_s - 1} * 100 \quad \text{Equation 1-6}$$

where: SPF_w is the wet SPF after water immersion
 SPF_s is the static SPF

The ISO 16217:2020 (50) describes the immersion procedure of minimum ten volunteers and ISO 18861:2020 (51) describes the percentage of water resistance. Volunteers have two immersion periods of 20 minutes each with 15 minutes out of the water in-between. For a sunscreen product to be claimed water resistant, the WRR% must be 50% at least (52,53).

1.3.3 Concerns with UV filters

Photodegradation

The photodegradation is a problem in sunscreen care. Photodegradation of UV filters is produced by mechanisms which produce adducts of the molecules and break the filters apart making the UV filter less effective. Moreover, metabolites with unknown effects may appear in the degradation process. Some of the substances are still unknown and therefore, its effects in ecosystems and individuals are still not studied.

The most common UV filters known for their photoinstability are avobenzene (BMDBM), ethylhexyl methoxycinnamate (EHMC) and Terephthalidene Dicamphor Sulfonic Acid (TDSA):

- **BMDBM**

BMDBM is an unstable UV filter in presence of ultraviolet radiation (UVR). After 1 h avobenzene can lose up to 36% of its initial absorbance (54)

- **Other photolabile UV-filters: EHMC (55)TDSA (56,57)**

EHMC and TDSA are UV filters which degrade in presence of UVR. As an example, EHMC recovery after 4 h irradiation is 72% (57)

Moreover, BMDBM exerts a destabilizing effect on the filters EHMC and DHHB, causing its degradation. Therefore, the following combinations of UV filters should be avoided:

- EHMC and BMDBM: Is a combination which should be avoided as it causes a degradation of EHMC.

In a study where both UV filters were in formulation, there was only a 35% recovery EHMC while avobenzene's degradation was comparable to the degradation of avobenzene alone in formulation after an irradiation dose of 30 MED (58)

In addition, another study reported a 72% EHMC recovery after irradiation of EHMC alone in a caprylic/capric triglyceride solution in quartz cell at 765 W/m² for 4 h. However, EHMC in presence of BMDBM, in the same conditions and in a 1:1 proportion, showed only 52% recovery while BMDBM were 60% recovered. Although the recovery of BMDB could seem low, it is worth mentioning, that the recovery of BMDBM alone was only 44% (57). Therefore, an increased degradation of EHMC was caused by BMDBM (Figure 1-6).

- DHHB and BMDBM: This combination should be avoided as well for causing degradation of DHHB.

In a solution of 3% DHHB in caprylic/capric triglyceride in quartz cell at 765 W/m² for 4 h UVR, reported a 100% recovery. However, in presence of BMDBM in a 1:1 proportion of EHMC and DHHB only 38% of DHHB recovered while BMDBM showed 57% recovery (Figure 1-6) (57).

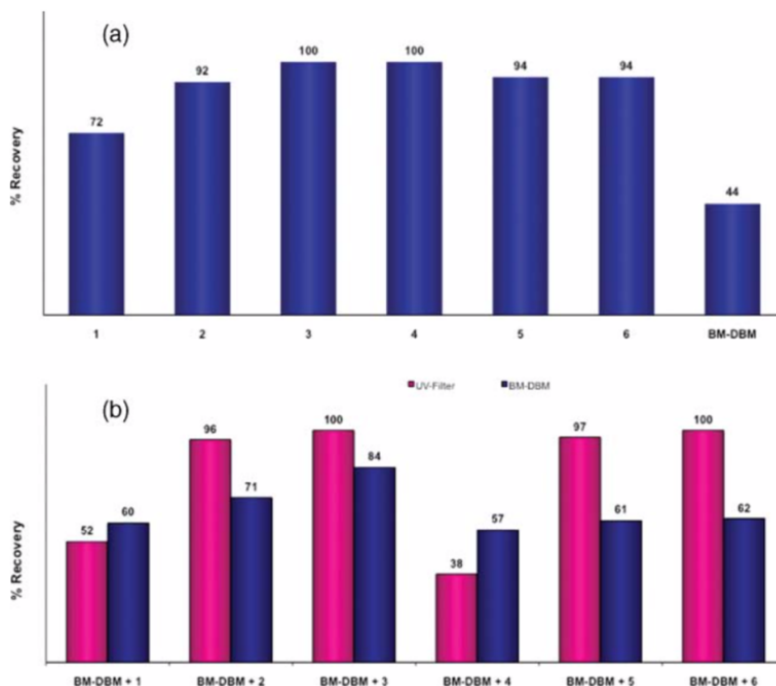


Figure 1-6. UV filter photodegradation: a) Recoveries of filter 1-6; 1. EHMC, 2. BEMT, 3. OCR, 4. DHHB, 5. EHT, 6. DBT and BMDBM b) Recoveries of filters 1-6 and BMDBM when filter X is combined with BMDBM (57).

On the other hand, some UV filters have been shown to contribute to the photostabilization of BMDBM (Table 1-2).

Table 1-2. UV filters which stabilize avobenzone with references of literature.

UV filters with stabilization capacity for avobenzone
BEMT (57–61)
OCR (57,59,61,62)
MBC (59,61)
PS15 (59,61)

Contact allergy and endocrine disruption

Some organic UV filters have shown penetration through the skin. Oxybenzone was found in the urine, breast milk, semen (63–65) and plasma at concentrations that exceed more than 400 times the maximal systemic concentration of 0,5 ng/mL dictated by the FDA (66). A guideline by the FDA on non-prescription sunscreen products states that nonclinical toxicology studies should be performed in sunscreens showing a steady state above this threshold (67,68). Other organic filters: octocrylene, avobenzene and ethylhexyl methoxycinnamate exceeded the systemic plasma threshold as well, however at lower concentrations than oxybenzone. The data was obtained from a randomized clinical trial in which 24 human volunteers applied sunscreen formulations. The UV filter composition was oxybenzone, octocrylene, avobenzene and ethylhexyl methoxycinnamate. Volunteers had to apply the sunscreen formulation four times a day during four consecutive days at 75% of their body area (66). These results were confirmed by another similar randomized clinical trial with 48 participants (69) All the six UV filters in formulation: octocrylene, avobenzene, ethylhexyl methoxycinnamate, ethylhexyl salicylate, homosalate, and octocrylene were found at plasma concentrations surpassing the threshold after a single exposure at the first day of the trial (69). The implications of these findings are yet unknown. However, there are no evidence of increased risk of toxicity for humans (10).

However, it is thought, that penetration of some UV filters through the skin may induce sensitivity reactions. Contact allergy is the most wide adverse effect of UV filters being oxybenzone the major photoallergen. Although there were reported photoallergenicity cases, in view of the high number of exposed people to oxybenzone through sunscreen products, the rate is low (39).

It is important mentioning that UV filters in (66,69) had a molecular mass between 228 and 362 g/mol. Many new generation of UV filters have a molecular mass of > 500 g/mol. The 500 Dalton (Da) rule postulates that molecules higher than 500 g/mol are unable to cross the stratum corneum of the skin, excluding systemic exposure (70). UV filters with >500 Da are listed in Table 1-3.

Table 1-3. New generation of UV filters (39).

Filter	Peak absorption (nm)	500 Da
UVA		
Ecamsule (Mexoryl SX)	345	+
UVB		
Octyl triazone = ethylhexyl triazone	314	+
Amiloxate = isoamyl methoxycinnamate	308	
Diethylhexyl butamido triazone	311	+
Enzacamene = 4 methyl benzylidene camphor	300	
UVA/UVB		
Drometrizole trisiloxane (Mexoryl XL)	303/341	+
Bemotrizinol (Tinosorb S)	310/343	+
Bisotrizole (Tinosorb M)	305/360	+

UVA ultraviolet A, UVB ultraviolet B

Endocrine disruption was reported in some animal studies for octocrylene. However, the experiments were performed by exposing oxybenzone to the animals at extreme high concentrations, which did not correspond to reality (39). All in all, oxybenzone tends to be avoided by the cosmetic industry in Europe due to the bad press that have been facing since these studies were published. Another organic UV filter, ethylhexyl methoxycinnamate have been suspected of endocrine disruption potential. Some studies reported estrogenic and anti-thyroid activity in humans and estrogenic, anti-androgenic and anti-thyroid activity in rats. However, most human studies were performed *in vitro*. In epidemiologic studies ethylhexyl methoxycinnamate was found in breast milk thus a possible exposition of the newborn to the molecule was considered. All in all, more evidence is needed to support the endocrine disruption effect of ethylhexyl methoxycinnamate both at acute and chronic exposure (71).

Despite these concerns for endocrine disruption, the beneficial effect of sunscreens outweighs the harmful overexposure to UVR. Moreover, at a daily base the intake of phytoestrogens in food is much higher than the obtained oestrogen activity due to sunscreen use (7).

1.3.4 Progressive UV filters: PRE-A, PRE-B and PRE-C

Progressive UV filters were developed patented in 2005 with the patent application number 05102228.3 (72) and consist of a class of UV filter precursors with a benzoic acid ester structure whose absorbance capacity increases with increasing irradiation dose. Classical UV filters block a fraction of photons from UV light. Instead, progressive UV filters are precursors of other compounds with increased absorbance in the UV spectrum. The transition to the active substances occurs through UVB light. Mechanistically, the phototransposition or activation of the precursors to the active substances is mediated by UV light in a reaction called Foto-Fries (Figure 1-7) (72–74).

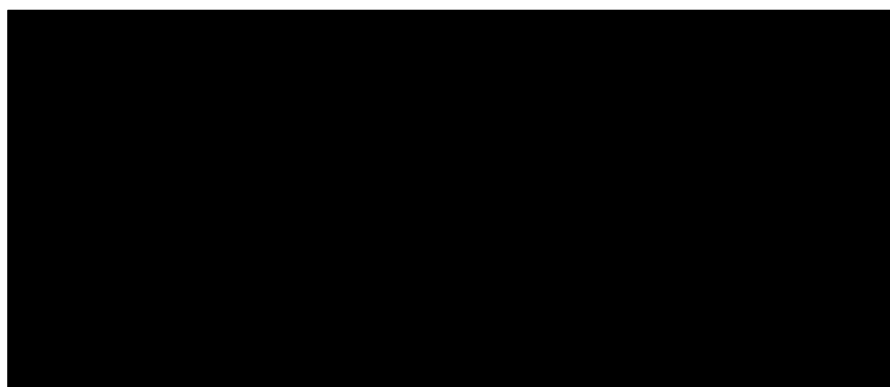


Figure 1-7. Mechanism of reaction and core structures of precursors and active substances (73)

In a Foto-Fries reaction, aryl benzoate precursors will react with UVB light to form β -hydroxycetone-type molecules.

According to this reaction the precursor is subjected to UVB radiation. Therefore, the transposition to the active substance can variate according to the received UVB exposure. This technology would have as consequence that at sunny days the conversion of the precursor to the active substance would be much faster than at cloudy days. The results would be higher protection with increasing sun exposure. Thus, the photoprotection could be adjusted to the climate conditions (74).

This technology has another advantage. After a review on the classical UV filters, it was observed that benzophenone-type and dibenzoylmethane-type UV filters (Figure 1-8) have in its structure a β -hydroxyketone. This characteristic β -hydroxyketone is crucial for the photoprotection activity of the molecules. The molecules on Figure 1-8 are approved by the regulatory authorities as UV filters to be used in humans.

A further advantage of this technology is that the Foto-Fries reaction can be implemented on β -hydroxyketone-type UV filters with proven effectiveness by designing compatible aryl benzoate precursors (74).

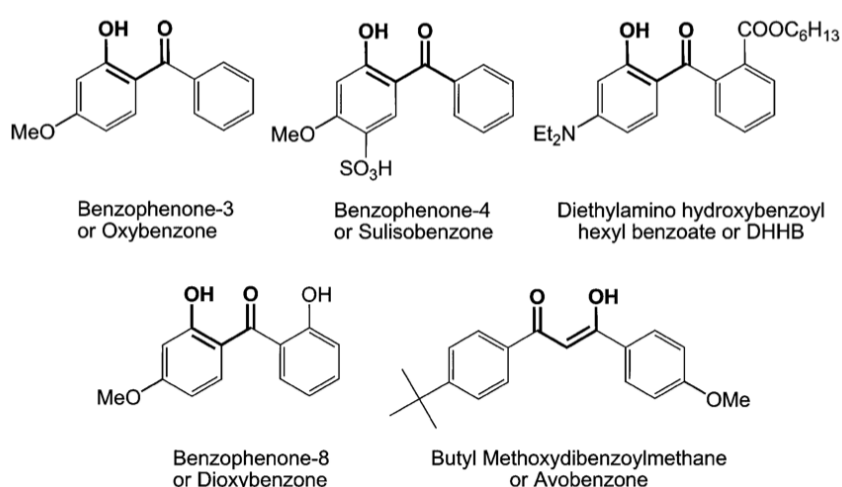


Figure 1-8. Classical UV filters with an β -hydroxyketone structure (74).

- **PRE-A**

PRE-A is the precursor molecule of avobenzone. Avobenzone or Butyl Methoxydibenzoylmethane (BMDBM) (see Figure 1-7) is one of the widely used UVA sunscreens worldwide. It offers a wide spectrum in the UVA range with a maximum around 360 nm. Moreover, it is the only organic UVA filter approved by all regulatory agencies over the world (38)

According to the findings described in (72) the activation of PRE-A in methanol is fast, reaching at 358 nm about four times its initial absorbance after 5 minutes with a complete phototransposition with UVB irradiation. PRE-A concentration was around 0,00046% as 4 mL

of a solution containing 0,231 mg was diluted in 50 mL methanol. The irradiation was performed on a Luzchem LZC-4 equipment with UVB lamps (LES-UVB-01)(74). The irradiation intensity was 60 W/m² in the UVB range (72)

PRE-A has a maximal absorbance in the UVC spectrum which extends to the UVB range. With increasing UVB radiation, the absorbance in the UVC-UVB spectra decreases while the absorbance in the UVA spectrum increases (Figure 1-9). This photoactive behavior in the UVA spectra coincides with the formation of avobenzene.

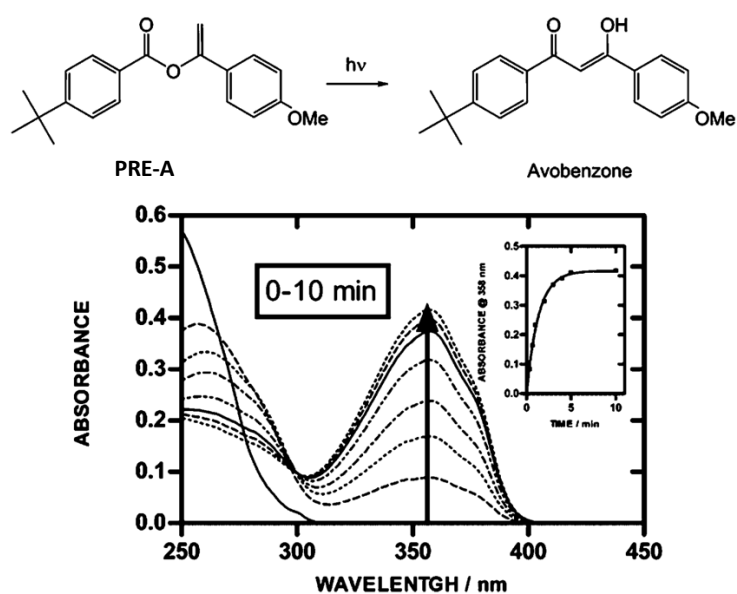


Figure 1-9. Phototransformation of PRE-A in methanol (74)

Silylated progressive UV filter precursors

This type of progressive UV absorbers is a new generation of precursors of active substances with increased photostability. The international patent WO2015/177064 (75) describes the invention. Structurally the molecules consist of mono-silylated polymeric benzoic acid ester compounds. The silylated chain is attached to the acyl ring of the benzoic group. Between the silyl group and the benzoic acid ester group, an imine or carbamate group links both structures (75).

The residue R in molecular core I can be in a para (i), meta (ii) or ortho (iii) position (Figure 1-10) (75).

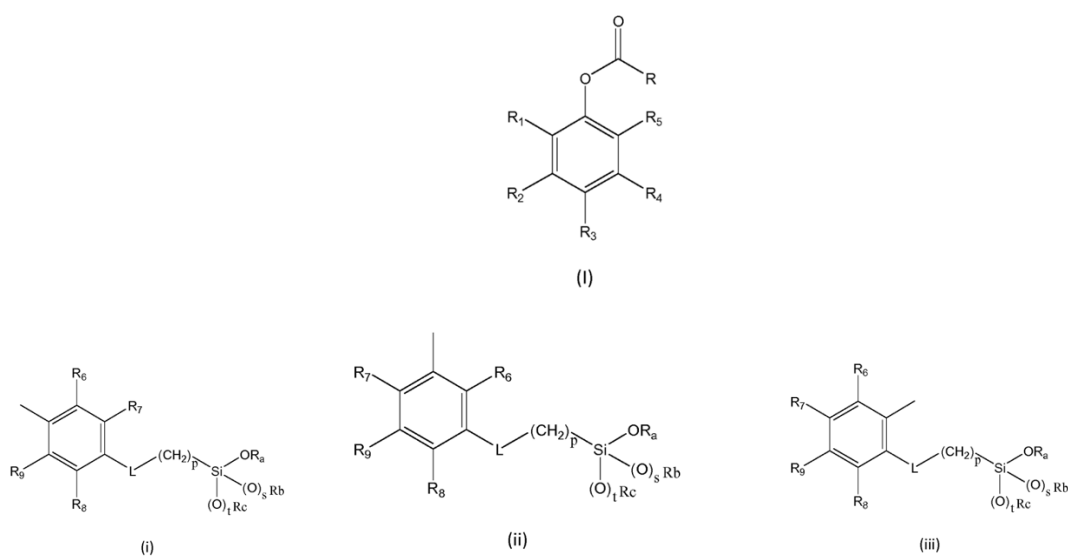


Figure 1-10. Structures of silylated compounds (I) core and (i-iii) residues (75).

- **PRE-B**

Particles of PRE-B have been assessed photochemically. PRE-B with its chemical name; X is a substance with moderate absorbance in the UVB spectrum. Like other aryl benzoate precursors, PRE-B is activated with UVB light to another compound with increased absorbance in the UVB and UVA spectrum. It has a UVB irradiation dose dependency with increasing absorbances the higher the irradiation dose. Figure 1-11 shows the photokinetics of PRE-B at different irradiation times. The particles were dispersed in 3% PEG 300 and spread on PMMA plates at 1,3 mg/cm². For the photoconversion PRE-B was irradiated on a Luzchem reactor with UVB light at an intensity of 70 W/m². The measurement of the absorbance was performed with a UV /Vis spectrophotometer (76).

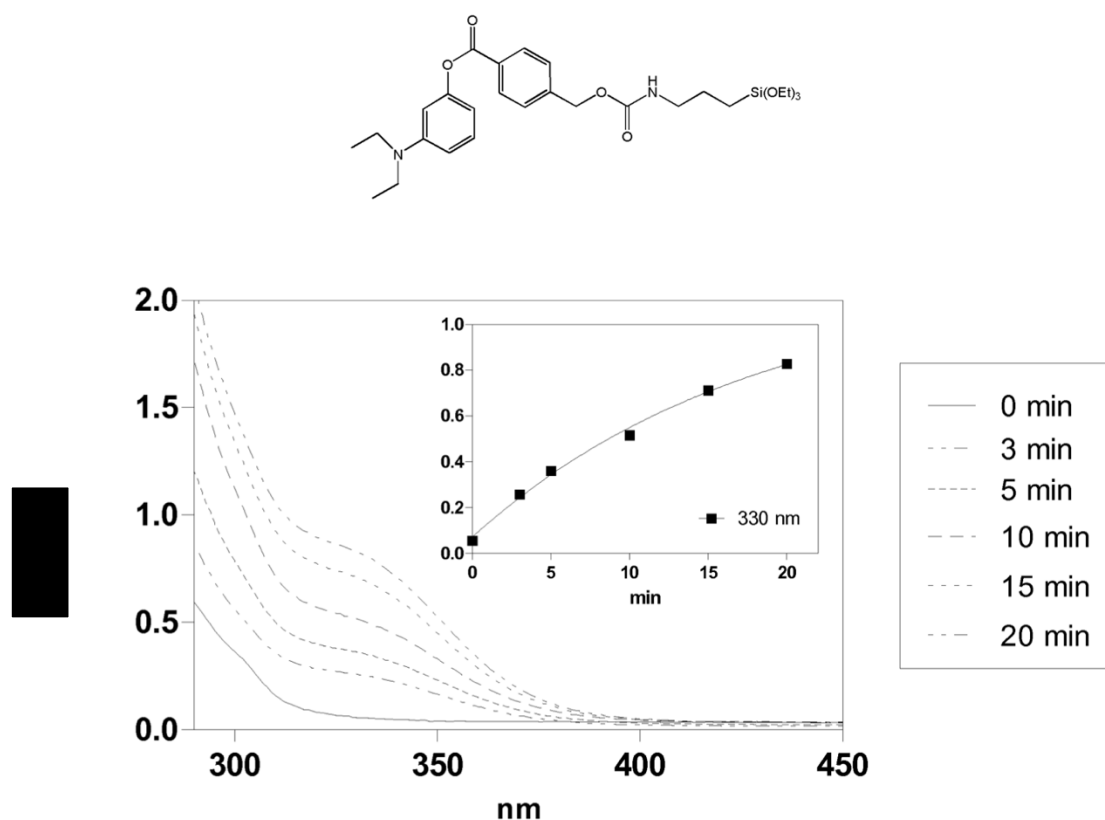


Figure 1-11. Molecular structure and photoactivation of PRE-B at 3% in PEG 300 (76).

- **PRE-C**

The chemical name of PRE-C is Y. The mechanistical activation process of the precursor and the preparation and irradiation conditions are identic to PRE-B. The precursor presents moderate absorbance capacity in the UVB spectrum. However, with increasing UVB dose the absorbance in the UVA spectrum increases (Figure 1-12) (76).

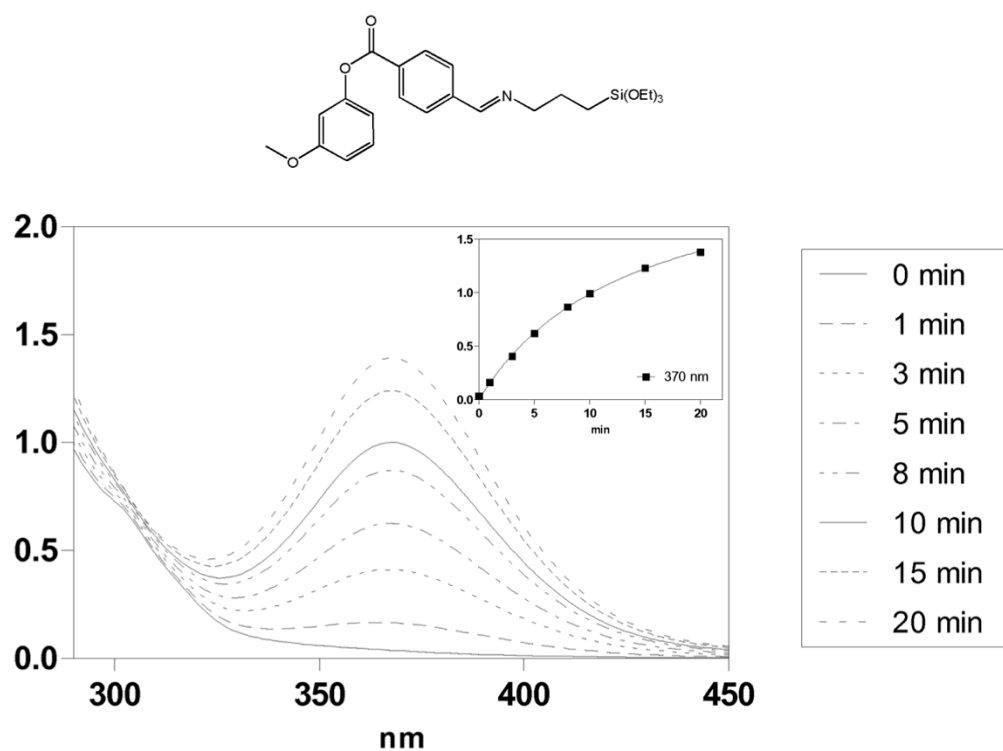


Figure 1-12. Molecular structure and photoactivation of PRE-C at 3% in PEG 300 (76).

1.4 Semisolid formulations and sunscreen products

1.4.1 Emulsions (77–79)

Emulsions are dispersions of two immiscible liquids. The liquids forming the two phases are water and oil and each phase can contain multiple components. The process of formation of an emulsion is called emulsification and consists of the dispersion of one of the phases, in form of droplets, into the other phase. The dispersed phase forming droplets is called discontinuous or intern and the other phase is the continuous, dispersant or extern (80). The size of the droplets of the dispersed phase varies from 0,5 to 100 μm .

Emulsions are thermodynamic instable systems, which are not stable with only mechanical stirring. Consequently, at some point the two phases will separate (81).

This instability is caused due to the area in the emulsification process, which produces a free Gibbs enthalpy increase according to Equation 1-7.

$$\Delta G = \gamma \cdot \Delta A \qquad \text{Equation 1-7}$$

where,

γ is the interfacial tension

ΔA is the area in the emulsification process

ΔG is the Gibbs free enthalpy

The higher the mechanical energy given during the emulsification, the smaller the particles and the smaller the interfacial tension.

The strategy to maintain two immiscible phases together is with the addition of an emulsifier to the biphasic system. The emulsifier is a compound which has affinity to hydrophilic (water phase) and lipophilic (oil phase) medium. The amphiphilic property of emulsifiers is attributed to its chemical structure, which is made of a hydrophobic head and a hydrophobic tail (Figure 1-13A). The emulgent because of its amphiphilic character will go is in the interphase, the border between both immiscible phases (red line in Figure 1-14). The emulsifier has the property to decrease the interfacial tension between both phases. With agitation, the biphasic system will homogenise allowing the internal phase to be dispersed into the external

phase. Structures in form of droplets, will originate. Micelles are the association of few tenside/emulgent molecules (82). Figure 1-13B shows a spherical micelle where the oil droplets (internal phase) are trapped by emulgents in a water medium (external phase) (83).

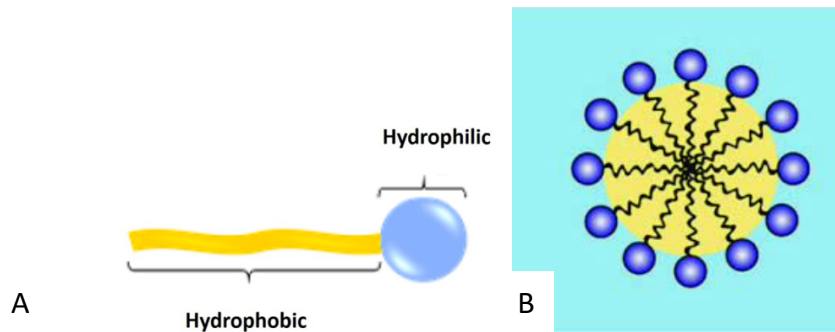


Figure 1-13. A) Structure of an emulsifier B) Emulsifier at the interface of water and oil (83).

According to the Bancroft rule, the external phase of an emulsion will be this in which the emulgent is most soluble. Depending to the solubility of the emulsifier to one of the phases, the emulsion will be an:

- Oil in water emulsion (O/W Emulsion), oil droplets in water as external phase, or
- Water in oil emulsion (W/O Emulsion), water droplets in an oil medium.

The classification of the type of emulsion is greatly determined by the hydrophylic-lipophylic balance (HLB) of the emulgent. It was determined by Griffin in 1949 and 1954 and determines the extent of an emulgent to be lipophilic or hydrophilic. The scale of HLB goes from 0 to 20 being 0 a completely hydrophobic molecule and 20 a completely hydrophilic molecule. For non-ionic surfactants the HLB is defined as Equation 1-8:

$$HLB = 20 \cdot \frac{Mh}{M} \quad \text{Equation 1-8}$$

where,

Mh is the molecular mass of the hydrophilic portion

M is the molecular mass of the whole molecule

It was established that HLB values from 4-6 are W/O emulgents, and 8-18 are optimum O/W emulgents.

From this classification, formulators could calculate the HLB value of the formulation by the HLB of the emulgent. In the case of a mixture of emulgents, the final HLB of the formulation was calculated by the fraction (X) and value (HLB req.) of the single HLB emulgents in the emulsion (1-9).

$$HLB \text{ requirement} = (HLB \text{ req. } A \cdot XA) + (HLB \text{ req. } B \cdot XB) + \dots \quad \text{Equation 1-9}$$

Griffin postulates that each substance or mixture of substances to be emulsified can be attributed a required HLB value, which is the HLB value that has to bear the emulsifier to design a stable emulsion. Therefore, the required HLB of the emulsifier has to be the same than the required HLB for a mixture of emollients (oily compounds). The HLB of every emollient can be found in literature. The HLB required can be calculated by 1-9, for the fraction of each emollient in the greasy phase.

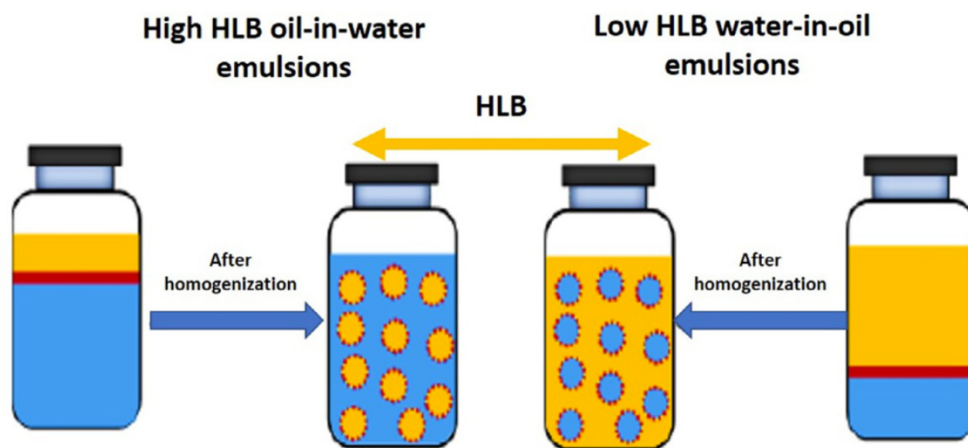


Figure 1-14. Formation of a O/W emulsion (left) and a W/O emulsion (right) (83).

The HLB system is a useful strategy in the formulation of emulsions, which provides a theoretical HLB value for the emollients with the required fraction of the emulgent. However, it does not give information on the necessary amount of the emulgent to develop stable emulsions. A detriment of emulgent can cause unstable emulsions and excessive amounts will cause the formation of structures in the formulation. This can be solved whether empirically with the formulation of emulsions or through the commercial information provided for the emulsifier or mixture of emulsifiers.

Before the manufacturing of a semi-solid product, many aspects must be considered. First, the target population is crucial. Young adults with acne prone skin will prefer non-to-low-oily or at least non-comedogenic formulations whereas older people with dry skin will prefer formulations with great moisturizing properties. For acne prone costumers' gels, lotions and O/W light creams are preferred. However, in dry skins the loss of water is unwanted and therefore an W/O heavy cream with great amount of emollients will give a protective hydration of the skin (82).

The water loss is necessary to maintain a correct water homeostasis (5 mL/h/m^2) in the skin. It is regulated by the stratum corneum, which is in contact with the external medium. In damaged skin the water loss increments. Therefore, the W/O emulsions can contribute to the retain of water loss while creating a water repellent film on the skin. This occlusive effect may cause a swelling of the skin due to water increase. On the other hand, in hydrophilic external phase formulations volatile components like alcohol will evaporate producing a cooling effect. Moreover, these formulations allow a transference of water to the external medium cause an increased water exchange from the skin to the medium by osmotic effects. According to the penetration capacity through the skin the classification is (from lower to higher penetration): wet pack, powder, solution, hydrogel, paste, O/W milk, O/W cream, cooling ointment, W/O emulsion-systems, oleogel, patch, okklusive dressing (82).

Emulsions are the predominant forms so far in the field of solar protection (84) and approximately 80% of the emulsions in the market are O/W emulsions (85).

Ingredients

Hydrophilic components

Water constitutes the principal ingredient in the water phase. However, other ingredients are appreciated for its moisturizing and smoothness properties and for the ability to decrease the contact angle (77). These ingredients are called moisturizers. Moisturizers decrease the surface tension with water and therefore emulsification energy decreases. Some of the most common moisturizers are:

- **Propylene glycol:** It is a water miscible cosolvent with antimicrobial properties, stabilizer for vitamins and humectant.
- **Glycerin:** Antimicrobial preservative, emollient, humectant and tonicity agent
- Other moisturizers are **Polyethylene glycols (PEGs)** or **buthylenglycol**. For PEGs, the number that comes next to PEG (example PEG-200 or PEG-400) refers to its mean molecular mass in Dalton (Da). PEGs with a higher molecular mas have a higher viscosity than lower molecular mass polymers.

Emollients (77,82)

Emollients constitute the main ingredient in the oil phase. Emollients give not only pleasant feeling but also maintain the hydration and protection of the skin. The main groups of emollients are:

- **Hydrocarbons:** Paraffin, is a mixture of purified hydrocarbons from petroleum. They can be viscous or non-viscous. Another example is vaseline, which is constituted of a mixture of hydrocarbons from petroleum.
- **Fatty alcohols:** Cetearylalcohol, Stearylalcohol
- **Glycerides:** They are produced semi-synthetically or synthetically. Representative for medium chain glycerides (C8-C10) are caprylic/capric triglycerides (Mygliol-types). Long chain glycerides (C14, C16, C18).

- **Natural glycerides** (with or without hydrogenisation): Castor oil, Jojoba oil, Hydrogenated castor oil.
- **Waxes:** Constituted of alcohol acid esters, mainly long chain. Some representative groups are lanolin, beeswax, Emollient-A, C12-C15 Alkyl benzoate, Isopropyl myristate.

Some physicochemical properties of an emollient to take into account for the design of a formulation are; spreading value, spreading rate, polarity, refractive index and viscosity. The use of this properties provides a hint to choose the most suitable emollient in the formulation. As an example, the polarity of the emollient can give a hint on the possibility to solubilize the Active Pharmaceutical Ingredient (API). Medium-to-high polar emollients are commonly used to provide a best solubility and performance of UV filters (86). Moreover, important sensorial aspects are smoothness, extensibility, occlusive properties, adequate consistency for each skin type and overall perception of the formulation. The combination of more emollients can provide optimum extensibility and polarity in a formulation.

- **Extensibility (77,87):**

- **High extensibility emollients:** undecane (and) tridecane, isononyl isonanoate, isodecyl neopentanoate, coco caprylate-caprate, Emollient-A, isopropyl myristate
- **Medium extensibility;** capryc-caprylic triglycerides, ocylpalmitate.
- **Low extensibility;** Mineral oil, liquid paraffin, dipentaerythryl pentaiononanoatem, C12-C15 alkylbenzoate

- **Polarity (77,87):**

- **Apolar emollients:** Mineral oil, liquid paraffin
- **Low polarity emollients:** undecane (and) tridecane, diethylhexylcyclohexane, Dicaprylyl ether
- **Medium polarity:** Coco-caprylate, dicaprylyl carbonate, propylheptyl caprylate, capryc-caprylic tryglicerides
- **High polarity:** Dibutyl adipate, isononyl isonanoate, C12-C15 alkylbenzoate.

Emulgents (77)

O/W Emulgents have an high HLB from 10-15. Allow a wide range sensorial adjustment with emollients, viscosity enhancers and polymers. Moreover, different textures can be obtained and have an hydration effect. The main groups are non-ionic, anionic and cationic emulgents.

- **Non ionic:** Are not charged. They are divided into:
 - Ethoxylated fatty alcohols: Cetareth-10, -20, -30, Steareth-20, -30 or mixtures (Glyceryl stearate and Cetareth-20 and cetareth-12 and cetaryl alcohol and Cetyl palmitate)
 - Ethoxylated glycerides: Glyceryl stearate (and) PEG-100 Stearate
 - Alkylpolyglucosides: Cetaryl glucoside, lauryl glucoside
 - Sucroesters: Sucrose polystearate

- **Anionic:** Are negatively charged. The most representative groups are:
 - Soaps: Sodium stearate, Potassium stearate
 - Alkyl sulfate: Sodium cetaryl sulfate
 - Alkyl phosphate: Sodium cetaryl phosphate
 - Alkyl glutamate: Sodium stearyl glutamate

- **Cationic:** Are positively charged. They have a powdery touch and some examples are:
 - Distearaldimonium chloride, Palmitamidopropyltrimonium chloride

On the other hand, W/O emulgents have low HLB of 5-9. The main properties of W/O emulsions are a better water resistance, rich and moisturizing emulsions with high hydration a better bioavailability of the API through the skin and higher protective effect. Some examples of W/O emulgents are:

- Sorbitan esters: Sorbitan isostearate, Sorbitan stearate, sorbitan oleate
- Polyglycerin derivatives: Polyglyceryl -3 diisostearate, -4 isostearate
- PEG-30 dipolyhydroxystearate, PEG-30 Polyhydroxystearate, PEG-7 Hydrogenated castor oil

There are other type of emulsions which need no emulgent. These are called polymeric emulsions. There is no need to calculate the HLB as the stabilization of the emulsion is produced by steric impairment. Commonly used stabilizers with emulgent effect are:

- Sodium polyacrylate
- C10-30 Acrylates/Alkylacrylates crosspolymer
- Carbomer
- Galactoarabinan

Stabilization agents (77,88)

Stabilization agents can be added in addition to the emulsifiers to increase the stability of emulsions. These compounds increase the viscosity of emulsions by forming a tridimensional network. These are consistence factors and rheology modifiers.

Consistence factors are greasy components of vegetal sources. Some examples are waxes, large chain fatty alcohols, high molecular weight esters, which build a tridimensionality network of lamellar structure with emulgents (Figure 1-15A).

Rheology modifiers are jelling compounds which increase in volume and increase the viscosity of creams while maintaining the non-greasy feeling. They form a tridimensionality network of organopolymers (Figure 1-15B). Some examples are cross-linked polyacrylates, hydroxyethylcellulose and xanthan gum. Some polyacrylates need slight neutral pH to form the network and swell. Normally to adjust the pH a weak base like triethanolamine or a strong base like sodium hydroxide (NaOH) is added.

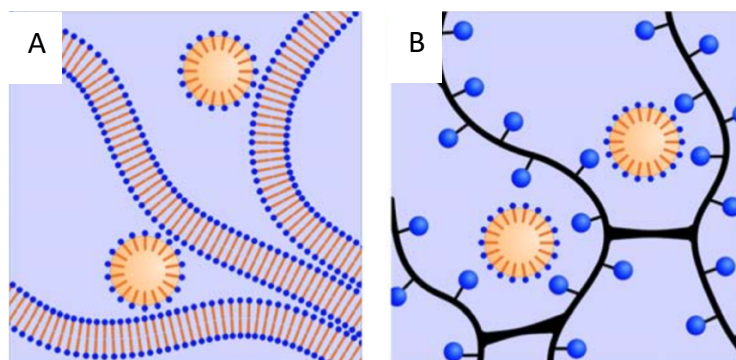


Figure 1-15. A) Lamellar structure, B) Polymeric structure (77).

Preservatives (82)

Preservatives are used in formulation to avoid microbial proliferation. According to the Ph. Eur. 10th edition on microbiological quality of cutaneous preparations (89) the total aerobic microbiological count is limited to 200 and the total combined yeasts/moulds count is limited to 20 as maximal acceptable count. Sources of microbiological contamination are air, water, devices, raw material and personnel. Factors contributing to microbial contamination are water, temperature (18-25 °C, ideal growth of fungus 30-37 °C), pH (between pH 3,5-10 possibility to grow), nourishment (carbohydrates, oils, proteins) (82).

Used preservatives in cosmetics are methyl paraben, phenoxyethanol, benzyl alcohol, potassium sorbate, sodium benzoate and sorbic acid. Other ingredients which are not preservatives, like ethylhexyl glycerin are combined to preservatives like phenoxyethanol for boosting the antimicrobial effect (77,90).

Chelating agents

Chelating agents like disodium EDTA, trisodium EDTA and tetrasodium EDTA are components which increase the stability of formulations by neutralizing the metals of the formulation which commonly precede from water (91).

Manufacturing (82)

The manufacturing process is determinant in the formulation. The process is a little different for O/W and W/O emulsions:

- **Direct method:** The direct method consists of mixing the internal phase into the external phase. Therefore, in an O/W emulsion the oil phase will be added under stirring into the water phase Figure 1-16A. In the case of an W/O emulsion the water phase will be added dropwise to the oil phase under strong stirring Figure 1-16 B.

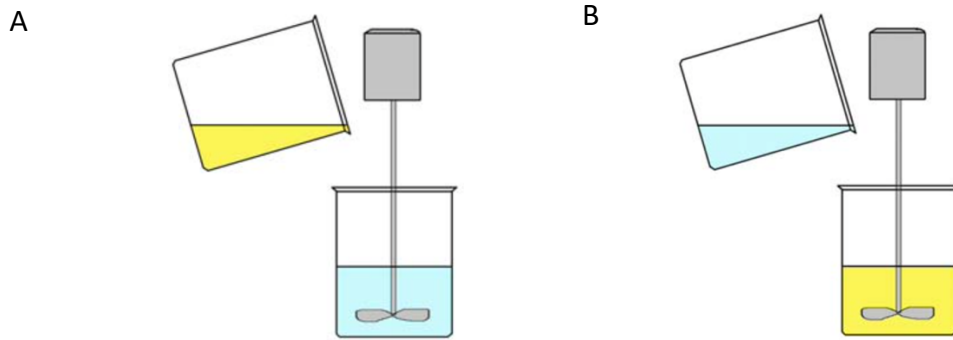


Figure 1-16. Direct method; Emulsification process of A) O/W emulsion B) W/O emulsions (92)

- **English method:** It consists of mixing the emulgent in the external phase and adding the internal phase afterward slowly (82).
- **Continental method:** First, the emulgent is added in the internal phase and afterwards the external phase is added stepwise. Under some circumstances it can come to phase inversion during the emulsification process (82).
- **Temperature dependent phase inversion/indirect method:** Are both phases mixed at a temperature higher than the phase inversion temperature (PIT), then it can come to a phase inversion of the W/O into O/W after cooling down the emulsion. The PIT depends from emulgent, the mass-phase relationship of the emulgent, the required HLB value and from the HLB value of the emulgent or mixture of emulgents.

The emulsification process is usually performed using an helix stirrer. Afterwards, the homogenisation is performed with a homogenizer or turrax, and in formulations which need high temperatures (when some ingredient needs to be dissolved) a cooling process with plate stirring is performed.

1.4.2 Stability of emulsions (93)

The stability of an emulsion is determined by the capacity of an emulsion to maintain the homogeneity during its shelf life. However, emulsions are thermodynamically unstable systems, in which the biphasic system tends to separate. Instability depends on many factors:

- **Homogenisation degree and mechanical stress:** The degree of mechanical energy will contribute on small droplet size of the internal phase. A formulation with small droplets tends to be more stable
- **Viscosity:** High viscosity formulations are more stable than less viscous formulations. This happens as the movement of the droplets in viscous formulations is slowly and the probability of interaction between droplets decreases.
- **Temperature:** Higher temperatures destabilize the emulsions. It contributes to a decrease in the viscosity and to a higher mobility of the droplets with higher interaction probability.
- **Density differences** of the two phases can contribute to destabilization of the system. A creaming will be formed if the density of the internal phase is lower than these of the external phase. If the density of the internal phase is higher than that of the external phase, sedimentation will occur.

In a destabilization process some physical appearances of the emulsion can be observed:

- **Creaming or sedimentation:** This happens do to gravitational or centrifugal external forces. Larger droplets migrate faster to the surface (creaming) due to they have lower densities than the external phase. In the opposite case, higher densities of the droplets, then the droplets migrate to the bottom (sedimentation) due to differences in density. It is a reversible process by agitation. The size and distribution of the droplets is constant.

- **Flocculation:** Droplets come together without merging as a result of attraction between droplets. It is an intermediate state between creaming and sedimentation, and it is caused because of a high amount of the internal phase. It is a reversible process which can be solved with agitation. The use of non-ionic emulsifiers can mitigate the repulsion of the biphasic system.
- **Phase inversion:** A W/O emulsion can turn to a O/W emulsion due to interactions with the ingredients, a high percentage of internal phase (higher than 74,048%), wrong HLB of the emulgent and high temperatures. The droplet size does not change.
- **Coalescence:** The mobility of the droplets in the medium can contribute to the collision of two or more with each other. In some cases due to these collisions the thin layer of the external phase can break. As a result, the droplets can form immediate collisions merging together to form a larger molecule. This process can lead to complete phase separation in the worst case (94).
- **Oswald ripening:** Smaller droplets have a higher solubility than larger ones. In the Oswald ripening, the smaller droplets will disappear and other droplets will increase in size (94).

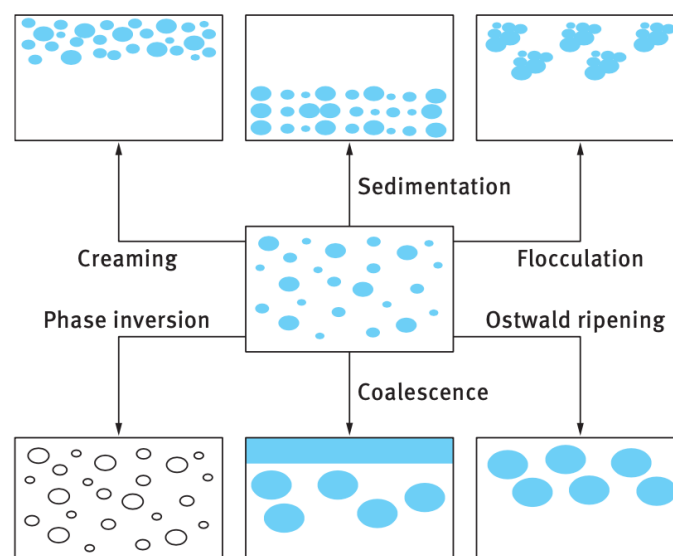


Figure 1-17. Break-down processes in emulsions (94).

1.4.3 The ideal sunscreen product

The most marketed sunscreen products globally are those with high solar protection factor (SPF). The highest SPF sunscreens have 50-60% share of the retail market (9). However, more education is needed for better user compliance, given that many users still seem to underestimate the negative effects caused by UVR (95). Moreover, the SPF and the UVA protection factor (UVA-PF) specified on sunscreen packaging is often not achieved because users do not apply enough of the product to protect their skin against UVR.

For a sunscreen to be efficient, a dose of 2 mg/cm² should be applied (7). If less is applied, the user would be overestimating the solar protection, since the SPF specified on the product packaging will not be reached (95,96). This has indeed been observed in some studies where participants generally applied doses ranging from 0,4 to 1,13 mg/cm² (median values). Other factors contributing to a decrease in sunscreen user compliance include

1. Greasy formulation and sticky perception on the skin;
2. Requirement for frequent reapplication of the product; public health agencies recommend to reapply sunscreen products every two to three hours (97,98);
3. Requirement for reapplication after bathing;
4. White cast effect on skin (98,99).

These weak factors which contribute to poor user compliance are often directly or indirectly influenced by sunscreen formulation technology. Seeking to address consumers' priorities, commercial brands offer a wide range of claims, UV filter combinations, ingredients, SPF, UVA-labeling among others. However, these wide range of sunscreen product properties may be overwhelming for the consumer. Skin care experts often refer to several factors that should be considered when purchasing a sunscreen (7,98,100). These include:

1. Fluidity (e.g., with an aqueous base or oil in water formulation, which increases user compliance);
2. High SPF;
3. UVA-labelling (which ensures protection in the UVA range);

4. Water resistance;
5. Preference for photostable UV-filters in sunscreen blends (as photolabile UV-filters producing unknown breakdown, whose biological consequences are not yet documented);
6. Absence of hormone activity in UV-filter;
7. Avoidance of UV-filters that may penetrate the skin through systemic distribution;
8. Absence of parabens (7,98,100).

Bioadhesion

The term of bioadhesion was first defined in early 80th decade where formulations with great retention on biological surfaces start becoming of great interest (101). Mucoadhesion is a word derived from bioadhesion and defines the contact of the bio-adhesive formulation when the biological surface is mucosa (102).

Bioadhesive substances are polymers, which are normally added to pharmaceutical formulations to make them adherent to biological membranes. This is of high interest when a contact for a long time period of the product on the skin is desired (103). The increase in retention time of pharmaceutical formulations promotes the absorbance of the pharmacological active ingredient contained in the formulation through biological membranes. At this way, the pharmacological treatment can be improved increasing the user compliance by decreasing the reapplication frequency. Another advantage of bioadhesive formulations, especially if the target is reached systemically, is the decreased amount of drug needed to ensure a stable therapeutic plasma concentration. Therefore, the steady state persists for a longer time compared to non-bioadhesive formulations where there is the risk of peaks and tails above and below the therapeutic range. Thus, it can cause toxicity due to high drug concentrations (104).

The mechanism of adhesion is still not fully elucidated. However, scientific community agree that the polymers are tridimensional structures which crosslink and increase in volume in presence of solvents. Many forces are involved in the conformation of polymer structures

that confer bioadhesion. Most common are covalent bonds but also physical entanglement, ionic forces, hydrophilic interactions and van der Waals forces (105).

The implications of polymers as bioadhesive excipients on formulations are extremely important in medicine. Bioadhesive formulations are not only highly valued in drug delivery but also in the dental and within the surgical field. Some examples include the repair of a broken teeth by adhesion of the two dentin fragments and adhesion of a mesh to a peritoneum with a bioadhesive glue (106).

In drug delivery, the most common application sites include dermal, buccal, peroral, nasal, ocular, rectal and vaginal where the pharmacologic effect can be locally or systemic. The conditions of the different application sites may differ substantially from each other. As an example, gastric mucosa differs from epidermis. While epithelial skin of the gut has mucus, which is mainly composed of water, and it is constantly in contact with acidic medium (pH 1,2), skin epidermis is in a dry environment, and it is composed of a lipidic barrier made of ceramides, cholesterol and fatty acids (107). These differences play a role in the bioadhesive measurement and therefore test conditions need to be as close as possible to the application site to simulate real conditions. Also, the animal selected in the adhesion test is of interest. Pig or rat mucosa, excised vaginal cow or pig skin are generally preferred in scientific literature (104).

Different methods to assess the bioadhesion degree of final products or excipients have been performed so far. The methods can be divided according to *in vitro* and *in vivo* methods. *In vitro* methods are generally preferred for being cost-effective, relatively easy to perform and less time consuming. They are commonly used to screen for bioadhesive excipients prior to formulation development or in the case of testing new bioadhesive product candidates with different bioadhesive agents (104).

Among the *in vitro* tests, the measurement of the vertical detachment strength tests are usually employed. This technique can be analyzed by modified balance, tensile device, dynamic angle analyzer, electromagnetic transducer system but texture analyzer is the most employed method (104,108).

This system consists of the quantification of the detachment strength needed to break the internal forces which link the bioadhesive material with the biological surface. Commonly two parameters are measured; the detachment force or peak force, which is the maximal force needed to detach the surface from the bioadhesive material, and the work of adhesion, which is calculated from the area of the force-distance curve after the contact of the bioadhesive material and the biological surface under a constant force during a fixed time. However, again there are critical factors that may influence results and contribute negatively to the harmonization within the same type of method.

The parameters to assess the bioadhesive capacity are indeed slightly different from study to study and this makes comparison between different formulations and adhesive polymers difficult (108). Some of the critical parameters are:

1. the force applied
2. contact time
3. detachment speed (108)
4. amount of test material (109) and
5. temperature could be a possible factor influencing bioadhesion.

To illustrate the difference in the parameters only for gel semisolid formulations some examples are given: while in (103,109) studies the speed was 0,1 mm/s, the contact time 2 min, the amount varied between 70 mL, 15 mL or 100 μ L at 0,001 N force and nasal pig mucosa 0,5 mL sample and two rat skin sheets were put together for 2 min before separating them with a withdrawal speed of 1 mm/s. Otherwise, in (110) rabbit vaginal mucosa was let set for 10 min in vaginal fluid previous to the experiment and the experimental conditions were 0,2 N force applied during 150 s and the detachment speed was 0,1 mm/s. Also, in (111) the contact time was 10 min for an experiment in which rabbit small intestine was used as substrate. The force of 0,1 N was applied and the test speed was 0,1 mm/s. However, there are also differentiated experimental settings as in (112) where one piece of pig skin attached to a rubber ring was immersed into a water beaker. No force was applied during the contact of the skin with the water bath and the skin-water contact was maintained for 60 s.

Afterwards, the upper part of the texture analyzer was detached from the water at a speed of 0,5 mm/s.

Moreover, although some studies about the bioadhesive capacity of topical forms have been performed, these focused mainly on intestinal mucoadhesion rather than on the skin (112). All in all, until now there is still no standardized method to assess bioadhesion (113).

Some insights on the critical aspects have been made which contribute to the development of the optimization of a standardized method. *Hägeström et al., 2004* (113) concluded that a small amount of bioadhesive gel in contact with two mucosa sheets was preferred to a large volume of bioadhesive gel in contact with one piece of mucosa. Moreover, in respect to the detachment speed, and after testing different speeds (0,1-0,5 mm/s), they came to the decision that a lower detachment speed of 0,1 mm/s conduced to higher precision in the detachment force and work compared to 0,5 mm/s (113). However, although some studies (114,115) suggest that the work of adhesion has a higher predictive value compared to peak force, it seems to be the opposite for a small sample amount (113).

Comedogenicity

Comedogenesis is the abnormal differentiation of the follicular epithelium to forms microcomedons. Microcomedons are horny plugs which can develop to comedons (116). This lesion can lead to open or closed comedons (blackheads or whiteheads) and to pustules of papules due to inflammation (117). The conditions for a comedon to be formed are greasy skins with an increment of sebaceous production with hyperkeratinization of the cells that surround the pilosebaceous hole or pore. The result is an obstruction of the pore with superficial oxidation. The production of microcomedones is the first stage for the acneic lesions (118). Acne is a disease of the pilosebaceous follicle of multifactorial ethiology that affects mainly those skin areas with highest sebaceous glands like face (90%), higher part of the bag (60%) and breast (15%). It is most frequent in teenagers and young adults (between the ages 11-30 years with 80% prevalence). It has a hormonal etymology as androgens promote the enlargement of the sebaceous glands (119). Typical structures of acne are macules, papules, pustules, atrophic scars, macular erythema and hyperpigmentation (120).

Cosmetic products can have some components in the formulations which may obstruct the pore. The use of those comedogenic promoting substances may worsen acne (121). Some studies have been conducted to classify widely used components in cosmetics according to the degree of comedogenicity. *Fulton et al.* (122) conducted studies to grade comedogenic substances according to its comedogen potential using the rabbit ear assay. This assay is a sensitive and it was argued to be a conservative method as human skin is not as sensitive as rabbit ear (123).

EXPERIMENTAL PART

2. PHOTOACTIVATION OF PROGRSSIVE UV FILTERS: PRE-A, PRE-B AND PRE-C

2.1 Introduction

PRE-B, PRE-C and PRE-A are so called progressive UV filters as its absorbance capacity increases by increasing irradiation dose. Structurally, PRE-B and PRE-C have a silica coating attached to the molecule, while PRE-A was no coating according to the molecules in Table 2-1.

For PRE-B, PRE-C and PRE-A to be used in the way commercial UV filters do, should be able to be solubilized or suspended in a suitable solvent. Commonly, in the EU commercial UV filters are allowed in a 5% concentration at least.

The aim was to study and compare the activation of PRE-B, PRE-C and PRE-A. Therefore, PRE-B and PRE-A were first solubilized at 5% concentration in different solvents of various log P value. The solvent with the best solubilization abilities was chosen for the further activation characterization of progressive UV filters.

Further, PRE-B, PRE-C and PRE-A (batch 1) were solubilized in this solvent at different concentrations (from 1% to 0,008%). PRE-A was additionally solubilized at a concentration of 0,001%. Therefore, all three progressive UV filters were compared in the optimum concentration (the concentration in which PRE-B, PRE-C and PRE-A showed the highest activation and absorbance). The absorbance was expressed in E1,1 to compare the activation between concentrations. Finally, the progressive filter at the determined concentration were compared according to:

- PRE-B at 0,008%
- PRE-C at 0,008%
- PRE-A at 0,008%

Moreover, the progressive UV filters were combined to cover the entire UV spectra. It is known, that PRE-B is a UVB filter while PRE-C and PRE-A are UVA filters. Therefore, PRE-B was combined with PRE-C and/or PRE-A, resulting in the following combinations:

- PRE-B at 0,008% & PRE-C at 0,008%
- PRE-B at 0,008% & PRE-A at 0,008%
- PRE-B at 0,008% & PRE-A at 0,008% & PRE-C at 0,008%

At this way, the progressive UVA filters were complemented by the progressive UVB filter resulting in the entire UVR coverage. The results of the combinations might be taken into considerations in future formulation designs.

At this point, the absorbance values ($E_{1,1}$) of the combinations of progressive UV filters, obtained empirically, were compared to the $E_{1,1}$ of the summation of the single progressive UV filters, obtained in silico. As an example: $E_{1,1(\lambda_{max}), (PRE-B \text{ at } 0,008\%)} + E_{1,1(\lambda_{max}), (PRE-C \text{ at } 0,008\%)}$ VS. $E_{1,1(\lambda_{max}), (PRE-B \text{ at } 0,008\% \text{ \& } PRE-C \text{ at } 0,008\%)}$. The aim of this procedure was to find some synergistic behaviour of the combinations towards the single UV filters.

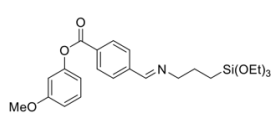
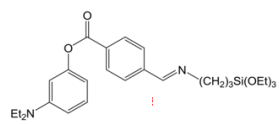
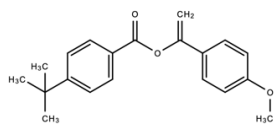
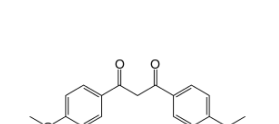
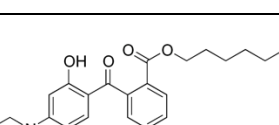
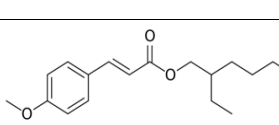
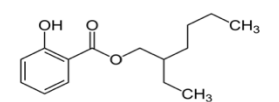
Finally, it was important to outweigh the protective effect of the progressive UV filters. For the progressive UV filters to be effective they needed to be activated by UV light. The effectiveness of the progressive UV filters was assessed by plotting the absorbances spectra in a graph together with the absorbance spectra of the commercial UV filters. The $E_{1,1}$ values from 290-400 nm of the single progressive UV filters after maximal activation (10 h irradiation) were compared with the absorbance of widely used commercial UVA and UVB filters after 2 h irradiation at 765 W/m². The type and structure of the commercial UV filters are listed in Table 2-1.

2.2 Materials and methods

2.2.1 Materials

Chemicals: PRE-A (UVA-filter), PRE-B (UVB-filter) and PRE-C (UVA-filter) by Company P. INCI name, trade name and supplier, UV-filter classification and chemical structure are listed in Table 2-1.

Table 2-1: UV-Filters: Ingredient nomenclature (INCI), Trade name and supplier, classification by the range of maximal absorbance and chemical structure.

INCI	Trade name and supplier	UV-Filter classification	Chemical structure
"PRE-B" (INCI unknown)	"PRE-B" (Company P)	Progressive UVB-filter, Silica coating	
"PRE-C" (INCI unknown)	"PRE-C" (Company P)	Progressive UVA-filter, Silica coating	
"PRE-A" (INCI unknown)	PRE-A (Company P)	Progressive UVA-filter	
Buthyl methoxydibenzoyl methane	Uvinul BMBM (BASF)	Commercial UVA-filter	
Diethylamino Hydroxybenzoyl Hexyl Benzoate	Uvinul A Plus (BASF)	Commercial UVA-filter	
Ethylhexyl methoxycinnamate	Uvinul MC 80 (BASF)	Commercial UVB-filter	
Ethylhexyl Salicylate	Neo Heliopan OS (Symrise)	UVB-filter	

Emollient-A as solvent by BASF (Emollient-A)

Volumetric flasks

Quartz cuvettes 1 cm by Hellma

Devices: Magnet stirrer (IKA Rh digital), analytical balance BP 211 D (Sartorius), Solar simulator Atlas CPS+ (Ametek), UV/Vis spectrophotometer specord 205 (Analytik Jena) and software WinASPECT.

2.2.2 Solubility at 5% of progressive UV filters in different solvents

Before starting with the activation of the UV filters, the appropriate solvent was chosen to perform the activation experiments of the progressive UV filters. A total of 10 solvents were selected: six lipophilic (Emollient-A, Undecane (and) Tridecane, Emollient-C, Decyl oleate, Emollient-B and Caprylic/ capric triglyceride) and 4 hydrophilic (Ethanol, PEG 200, PEG 400, and water) solvents. PRE-B and PRE-A were diluted in the correspondent solvent at 5% solution in a volumetric flask. PRE-A in crystalline form and PRE-B as dense liquid were stirred for 20 minutes by magnetic stirring. Should the solution be still heterogenic, then the flask was placed for 20 min into an ultrasonic bath. Finally, if the solution was still heterogenic, the flask was heated to 80 °C under magnetic stirring. The solution should optically be homogenic afterwards to be soluble. PRE-C solubility at 5% PRE-C was not performed as only limited amount of PRE-C was available. A 5% concentration was determined as most of the UV filters are limited to a 5% concentration in formulation.

2.2.3 UV spectrophotometry- Cuvette method

a Preparation of solutions

PRE-B, PRE-C and PRE-A were prepared separately at 1%, 0,008% and/or 0,001% (w/v) solution in Emollient-A. In the solutions where two or three UV-filters were combined, the concentration of each UV filter was 0,008%. The following solutions were prepared:

- PRE-A at 0,008% (w/v) & PRE-C at 0,008% (w/v),
- PRE-B at 0,008% (w/v) & PRE-C at 0,008% (w/v),
- PRE-B at 0,008% (w/v), PRE-A at 0,008% (w/v) & PRE-C at 0,008% (w/v)

b Spectroscopic measurements

A volume of 2,5 mL of the described solutions in 2.2.3a were filled in 1 cm quartz cuvettes and irradiated in a solar simulator (Atlas CPS+, Ametek) with a filter system (COLIPA standard sun). This filter system simulates the natural sun light covering a UV range from 290 to 400 nm with a total irradiance of 765 W/m². The solar simulator was equipped with a water cooled-sample table supplement (Ametek) which was connected to an external thermostat

(Lauda ECO RE 630 S) programmed at -20 °C to ensure that the samples did not surpass the 40 °C temperature during irradiation. The temperature inside the solar simulator was monitored with a digital thermometer datalogger (K 202 Datalogger, Voltcraft). The irradiation time of each UV-filter-solution was 0, 5 min, 20 min, 1 h, 2 h, 4 h and 10 h corresponding to 0.4, 1.7, 5, 10, 20 and 50 MED (minimal erythemal dose), respectively; which is equivalent to 225 kJ/m², 900 kJ/m², 2700 kJ/m², 5400 kJ/m², 10800 kJ/m².

The 1 cm quartz cuvettes were placed horizontally at the cooling table of the solar simulator with its transparent quartz side upwards to the solar simulator (oriented towards the lamp) to avoid absorbances by the glass. To assess the absorbance, the solutions at 1% (w/v) were not able to be measured directly by the spectrophotometer as they exceeded the limit of detection of the device and therefore a dilution was needed; PRE-C and PRE-B 0,625/100, PRE-A 1/100. The single UV filter solutions at 0,008% were measured directly (without dilution). However, the combinations PRE-B & PRE-C and PRE-B & PRE-A for 4 and 10 h were diluted 1/2 PRE-B, and for the combination PRE-B & PRE-A & PRE-C the dilution was 1/2 for 20 min, 1 h, 2 h, 4 h and 1/4 for 10 h.

The UV-filter's absorbance was measured in quartz cuvettes of 1 cm pathlength from 290-400 nm in 1 nm steps with the spectrophotometer (Specord 205 analytik Jena), software (WinASPECT).

The average in absorbance for each UV-filter concentration and radiation time was calculated out of the three measurements per combination.

c Calculation of E_{1,1}

The method to calculate the specific extinction (E_{1,1}) is explained in section 4.2.2- Computational analysis- conversion of A to E_{1,1}.

d Statistical analysis

A statistical analysis was performed to find synergistic behaviour of the progressive UV filters mixtures on the absorbance capacity compared to the single progressive UV filters. The combinations were PRE-B (progressive UVB filter) and PRE-C and/ or PRE-A (progressive UVA

filter) to cover the entire UV spectrum. The absorbance values of the single progressive UV filters were added for the two or three filter combinations: PRE-B & PRE-C, PRE-B & PRE-A and PRE-B & PRE-C & PRE-A. The resulting absorbance spectra were defined as in silico measurements. In silico spectra were compared to the measured experimental spectra of the combinations. A two way-ANOVA turkey multiple comparisons test was performed at a specific wavelength; PRE-B&PRE-C at 365 nm, PRE-B & PRE-A at 360 nm and PRE-B & PRE-C & PRE-A at 360 nm.

2.3 Results and discussion

2.3.1 UV-filter solubility at 5%

Emollient-A was the only solvent able to solubilize PRE-B and PRE-A at 5% concentration without the need of heating the solution. It was therefore chosen for the activation tests of both progressive UV filters. PRE-B and PRE-A were able to solubilize in Emollient-A at 5% concentration solely with the with the help of magnetic stirring. Indeed, Emollient-A is not only one of the most employed emollients in the formulation of sunscreen products but also increased the protection capacity of some lipophilic commercial UV filters: EHMC, DHHB, BEMT and EHS. These UV filters achieve higher absorbances compared to other current emollients in sunscreen formulation (59).

On the other hand, Undecane (and) Tridecane was a suitable solvent to solubilize 5% PRE-A, however it was not able to solubilize PRE-B weather by ultrasounds nor under stearring up to 80 °C.

Finally, PEG 400 was able to solubilize 5% PRE-A and 5% PRE-B, nevertheless solubilizing PRE-A was only possible under heat. Therefore, the solubility of PRE-B in PEG 400 was lower compared to the solubility of in Emollient-A (Table 2-2).

All in all, Emollient-A was the only emollient in which PRE-B and PRE-A solubilized at 5% without the need of heat. Therefore, Emollient-A were used to solubilize the progressive UV filters.

Table 2-2. Solubilities at 5% PRE-A and PRE-B in different solvents.

	Ethanol	Propilenglycol	PEG 200	PEG 400	Emollient-A	Undecane (and) Tridecane	Emollient-C	Decys oleate	Emollient-B	Water (distilled)	Caprylic/ capric triglyceride
PRE-A	Non-soluble at 5%, (soluble at 2%)	Not soluble weather ultrasounds nor stearring up to 80 °C. (Soluble at 1% at 80 °C under magnetic stirring.)	Soluble with magnetic stearring and heating up to 80 °C	Soluble with magnetic stearring and heating up to 80 °C	Soluble with magnetic stirring	Soluble with magnetic stirring				Not soluble	
PRE-B	Not soluble weather ultrasounds not stearring			Soluble with stearring	Soluble with stearring	Not soluble weather ultrasounds nor stearring up to 80 °C. (also 1% PRE-B not solubles)	Not soluble weather ultrasounds nor stearring up to 80 °C.	Not soluble weather ultrasounds nor stearring up to 80 °C.	Not soluble weather ultrasounds nor stearring up to 80 °C.	Not soluble weather ultrasounds nor stearring up to 80 °C.	Not soluble weather ultrasounds nor stearring up to 80 °C.

2.3.2 Activation and characterization of photochemical behaviour at different irradiation doses and concentrations

The activation of the progressive UV filters investigated under different concentrations is shown in the following subsections a, b and c.

a *PRE-B*

The wavelength at the maximal absorbance was 290 nm. From the three concentrations 0,008% was the only one at which PRE-B showed higher absorbance with increasing irradiation dose. At 0,8% PRE-B concentration, only until 20 minutes irradiation a 10% increase in at 290 nm in respect to non-irradiation was observed. However, from 1 h irradiation the absorbance decreased to levels of “non-irradiation”. Similarly, at 1% only at 5 min some very small activation (6%) was measured (Figure 2-1 A).

In contrast, PRE-B at 0,008% concentration increased with increasing irradiation dose (Figure 2-1A and B). The wavelength of the maximal absorbance of PRE-B was at 290 nm. However, it was observed that at 335 nm the activation was more pronounced compared to 290 nm. Therefore, 335 nm was found to be a more representative wavelength for the increase in absorbance after irradiation (Figure 2-1C). While at 290 nm there was a 25%, 26% and 28% increase in absorbance after 2 h, 4 h and 10 h irradiation, respectively; at 335 nm the increase was 90%, 91% and 92%, respectively (Figure 2-1B and Figure 2-1C).

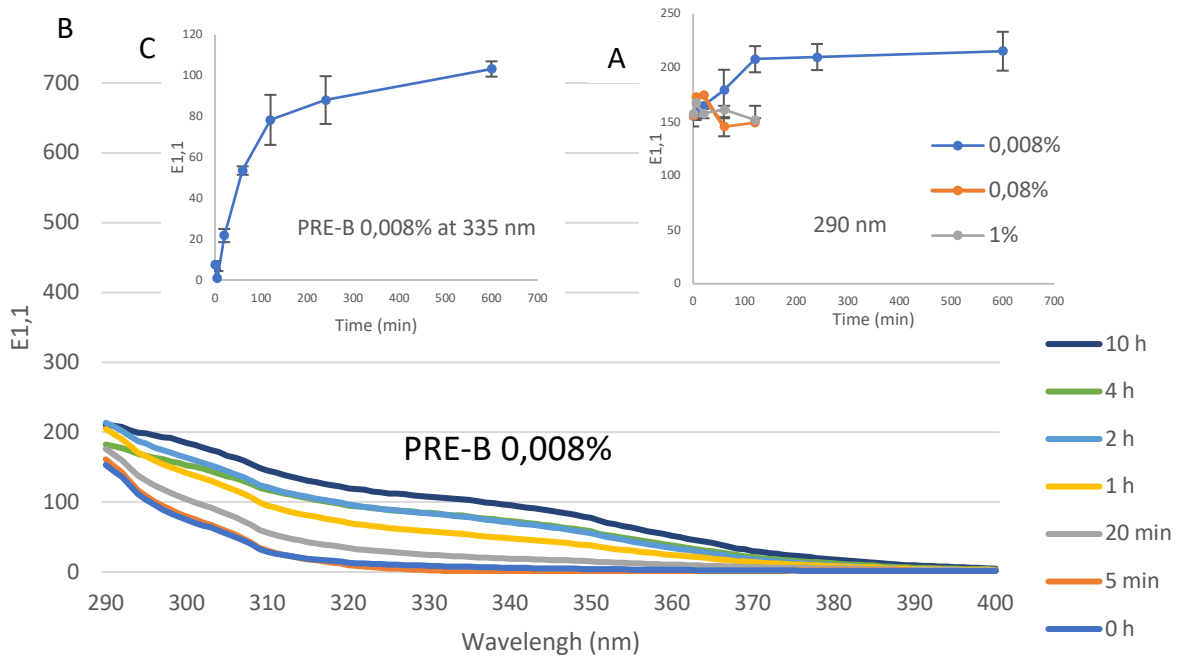


Figure 2-1. A) $E_{1,1}$ at its maximal wavelength (290 nm) of PRE-B in Emollient-A solution at different concentrations (0,008%, 0,08% and 1%) as a function of time. B) $E_{1,1}$ from 290-400 nm C) $E_{1,1}$ at 335 nm of PRE-B 0,008% in Emollient-A solution after different irradiation times (0, 5 min, 20 min, 1 h, 2 h, 4 h and 10 h) at 765 W/m^2 .

b PRE-C

PRE-C activation in Emollient-A solution was observed at 0,008% concentration while at 1% concentration the activation was much slow (Figure 2-2A). While the $E_{1,1}$ was 74,78 (at 0,008% PRE-C concentration) after 1 h irradiation the, at 1% concentration the $E_{1,1}$ was 10,19 at the same irradiation time. The increase in absorbance was of 892% and 98%, respectively. Therefore, the irradiation dose was increased for 0,008% concentration compared to 1% concentration.

For the 0,008% concentration, the result was an increase in absorbance with increasing irradiation dose. After 10 h irradiation an $E_{1,1}$ of 168 was achieved. However, the activation velocity of PRE-C decreased with increasing irradiation dose. From 0 to 1 h irradiation dose the slope of the equation was 1,13, from 1 h to 4 h the slope of the equation decreased to 0,41 and from 4 h until 10 h it decreased to 0,054.

Moreover, it was observed, that while in the UVA spectrum the absorbance increased, in the UVB spectrum the absorbance decreased (Figure 2-2B).

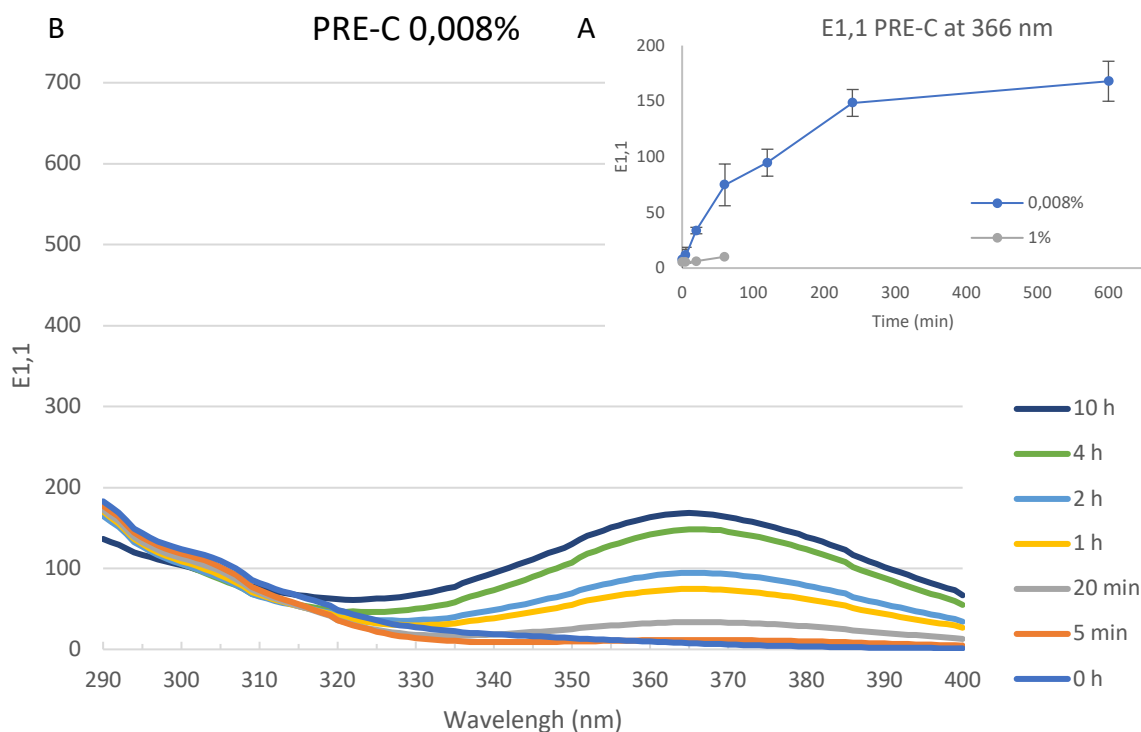


Figure 2-2. A) E1,1 at its maximal wavelength (366 nm) of PRE-C in Emollient-A solution at different concentrations (0,008% and 1%) as a function of time. B) E1,1 of PRE-B 0,008% in Emollient-A solution after different irradiation times (0, 5 min, 20 min, 1 h, 2 h, 4 h and 10 h) at 765 W/m².

c PRE-A

PRE-A activation was analysed for three different concentrations (1%, 0,008% and 0,001%). Like PRE-C, PRE-A showed at 0,008% concentration higher absorbance with increasing irradiation dose compared to 1% concentration. However, it was observed, that the smaller the concentration of PRE-A in solution, the higher and faster conversion to avobenzene (Figure 2-3A). Therefore, PRE-A at 0,001% concentration in Emollient-A solution showed higher E1,1 than 0,008% concentration. In turn, 0,008% concentration of PRE-A showed higher E1,1 than 1% PRE-A concentration in Emollient-A concentration. To show the difference in absorbance of the three different concentrations, the times 2 h, 4 h and 10 h were compared. Numerical results of E1,1 value are presented in Table 2-3.

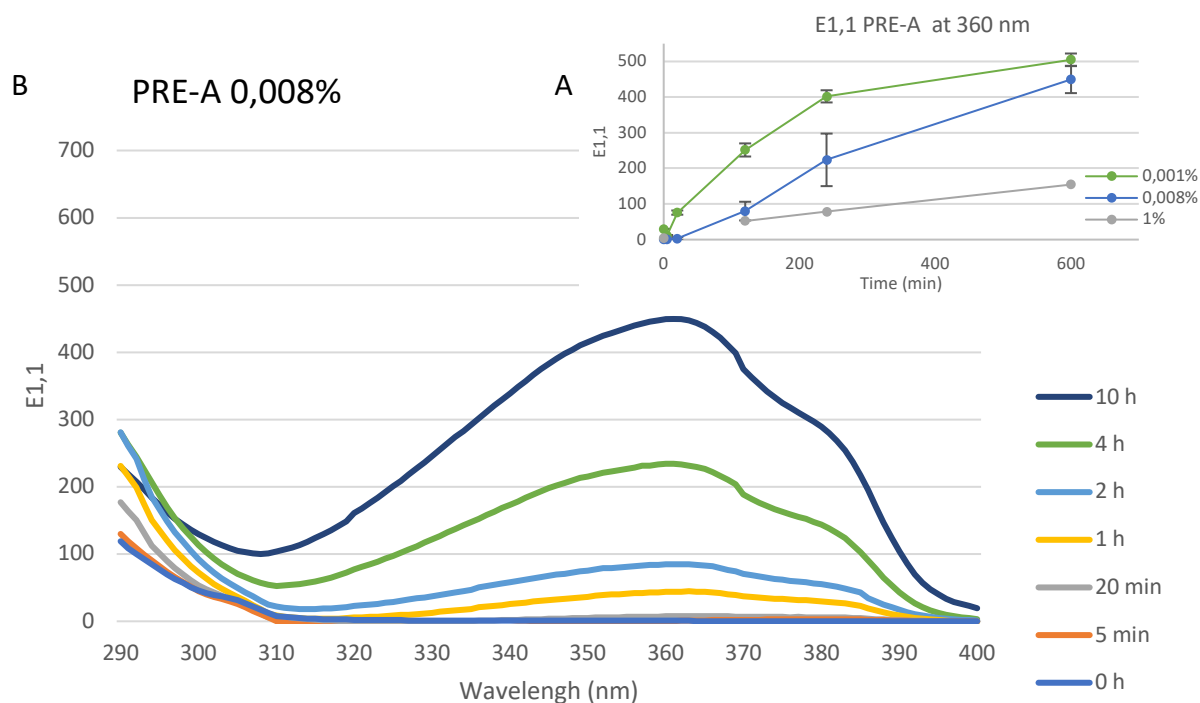


Figure 2-3. A) E1,1 at its maximal wavelength (290 nm) of PRE-A in Emollient-A solution at different concentrations (0,001%, 0,008% and 1%) as a function of time. B) E1,1 of PRE-A at 0,008% in Emollient-A solution after different irradiation times (0, 5 min, 20 min, 1 h, 2 h, 4 h and 10 h) at 765 W/m².

At 0,001% the E1,1 was 3,1 times higher than 0,008% and in turn 0,008% was 1,5 times higher than 1% at 120 min irradiation. The difference between 0,001% and 0,008% was smaller with increasing irradiation with a factor 1,8 and 1,1 for 240 and 600 min, respectively. On the other hand the distance between 0,008% and 1% increased with increasing irradiation time. A factor of 2,9 for both 240 and 600 minutes was obtained between these both concentrations.

The concentration of PRE-A in solution seems to be determinant for the activation of PRE-A to avobenzone. Smaller concentrations like 0,001% of PRE-A are activated faster than higher concentrations like 0,008% or 1%. The slopes of the trendlines of equations of the three concentrations of absorbance vs time reveal this behaviour. The slopes for 1%, 0,008% and 0,001%, and are 0,2, 0,7 and 0,8 respectively (Figure 2-3A).

Table 2-3. E1,1 values of PRE-A at 360 nm at 0,001%, 0,008% and 1% concentration in Emollient-A solution at 120, 240 and 600 min, and potency factors between concentrations for each time point.

Time (min)	PRE-A E1,1 at 360 nm			0,001% vs 0,008%	0,008% vs 1%
	0,001%	0,008%	1%		
	E1,1	E1,1	E1,1	Factor	Factor
120	251,6	80,0	52,2	3,1	1,5
240	402,1	223,8	78,3	1,8	2,9
600	504,6	449,5	154,5	1,1	2,9

The absorbance spectrum of PRE-A at 0,008% is shown in Figure 2-3B. PRE-A is a molecule that has absorbance properties in the UVB spectrum with a maximum in the UVC range (see section 3.3.3). With increasing irradiation dose, PRE-A turns progressively to avobenzone thus increasing the absorbance in the UVA range and UVB. This activation started between 5 and 20 minutes (E1,1 at 0, 5 and 20 min for 0,008% were 0,8, 0,8 and 2,4, respectively).

All in all, PRE-A showed a higher E1,1 in the UVA range compared to PRE-C. PRE-C and PRE-B reached similar maximal E1,1 values; 167 PRE-C and 214 PRE-B. On the other hand, PRE-A maximal E1,1 value at 10 h irradiation was 449,5. This is more than two times higher the maximal E1,1 of PRE-B and PRE-C. The concentration of 0,008% was further used for the mixtures of progressive UV filters.

2.3.3 Mixtures of progressive UV-filters and synergistic effect screening

a PRE-B and PRE-C

Figure 2-4A show the E1,1 in silico results of the combination of PRE-B and PRE-C and in Figure 2-4B, the real experimental results of this combination are presented. Both graphs show the results at the same irradiation doses.

First, in graphs obtained by in silico calculations two peaks were observed, one peak at 290 nm and another at 366 nm. The spectra of the PRE-B and PRE-C mixture was like the PRE-C spectra ($ITB \lambda_{max} = 366 \text{ nm}$, $ITM\&ITB \lambda_{max} = 365 \text{ nm}$) and E1,1 of the mixture of PRE-B and PRE-C was higher compared to PRE-C alone.

However, the results of experimental measurements reveal no maximal absorbance (E1,1) in the UVA range, although the mixture continued showing an irradiation dependent absorbance. Comparing the theoretic (in silico) $E_{1,1(\lambda_{max}), 2 h} = 212$ with the experimental $E_{1,1(\lambda_{max}), 2 h} = 84$ of the PRE-B&PRE-C mixture, it was observed, that the average absorbance at the maximal wavelength was lower than expected in the calculations.

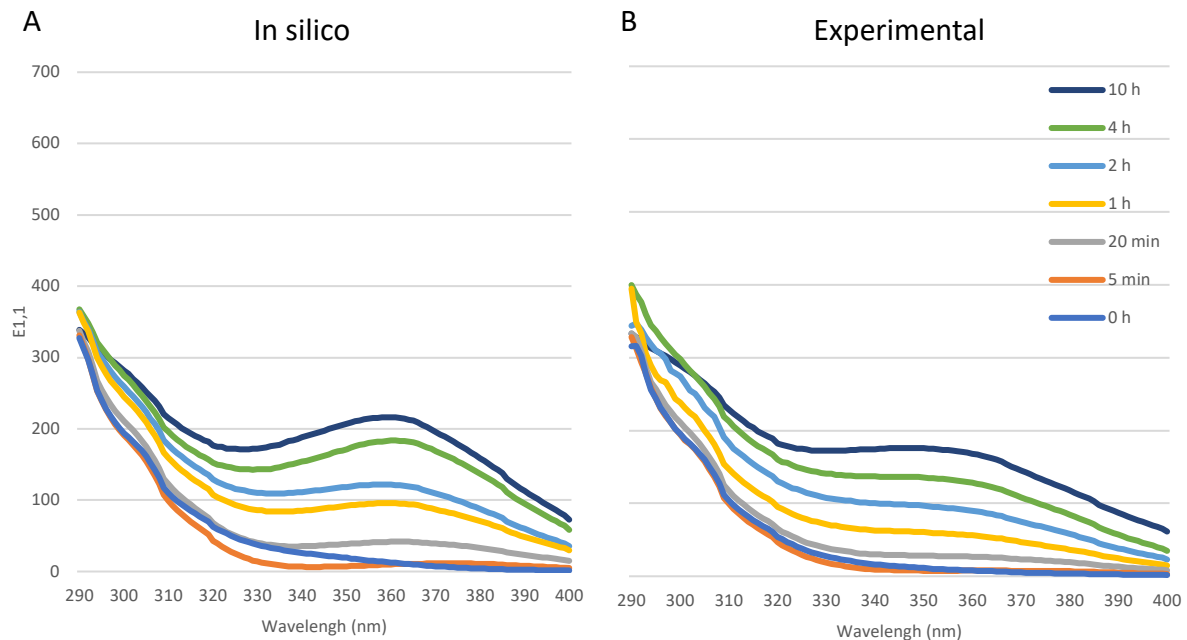


Figure 2-4. $E_{1,1}$ of the mixture PRE-B 0,008% and PRE-C 0,008% in Emollient-A solution after different irradiation times (0, 5 min, 20 min, 1 h, 2 h, 4 h, 10 h) at 765 W/m^2 . A) In silico values B) Experimental values.

b PRE-B and PRE-A

The in silico and experimental results of the mixture of the progressive UVB-filter PRE-B (0,008%) and the progressive UVA- filter PRE-A (0,008%) were compared (Figure 2-5A and B).

At first sight, the $E_{1,1}$ values at 360 nm after 10 h, 2 h and 1 h irradiation showed were on average higher compared to in silico values. However, a more accurate comparison was needed to determine the significance of the obtained results, which was statistically analysed in Figure 2-5 and will be discussed below in this subsection.

On the other hand, at 290 nm the E1,1 showed almost identical results for all the irradiation times, except for 10 h ($E_{1,1}(\lambda_{max}), 10 \text{ h, in silico} = 440$ and $E_{1,1}(\lambda_{max}), 10 \text{ h, experimental} = 365$). The maximal wavelength of the mixture PRE-B & PRE-A was 360 nm, like for PRE-A alone.

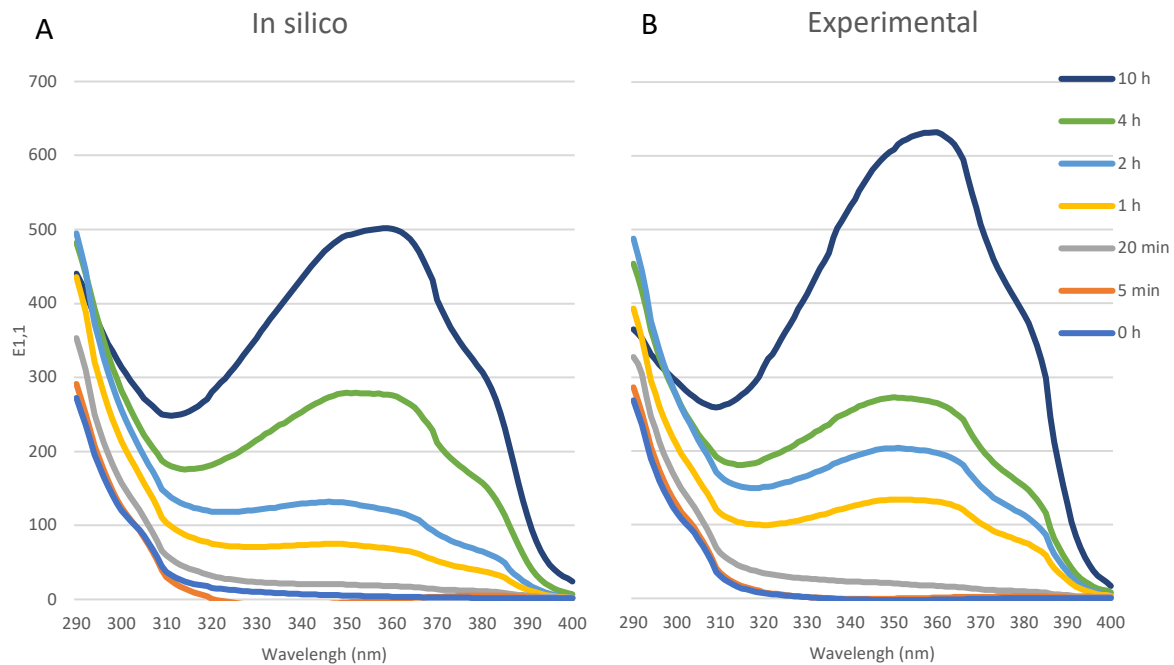


Figure 2-5. $E_{1,1}$ of the mixture PRE-B 0,008% and PRE-A 0,008% in Emollient-A solution after different irradiation times (0, 5 min, 20 min, 1 h, 2 h, 4 h, 10 h) at 765 W/m^2 . A) In silico values B) Experimental values.

c PRE-B, PRE-C and PRE-A

The mixture of the three progressive UV filters: PRE-B, PRE-C and PRE-A, each at 0,008% in Emollient-A solution showed an absorbance spectrum which reassembled the spectrum of the mixture PRE-B & PRE-A 0,008% with a higher absorbance spectrum.

The maximal wavelength in the UVB range was 290 nm, and 360 nm in the UVA range. In silico and experimental absorbance spectrum showed comparable absorbance curves. However, the average absorbance maximum at 290 and 360 nm showed differences. In the PRE-C range, the *in silico* graph (Figure 2-6A) show higher absorbances. On the other hand, experimental results (Figure 2-6B) showed higher absorbances in the UVA range at 4 h, 2h and 1h.

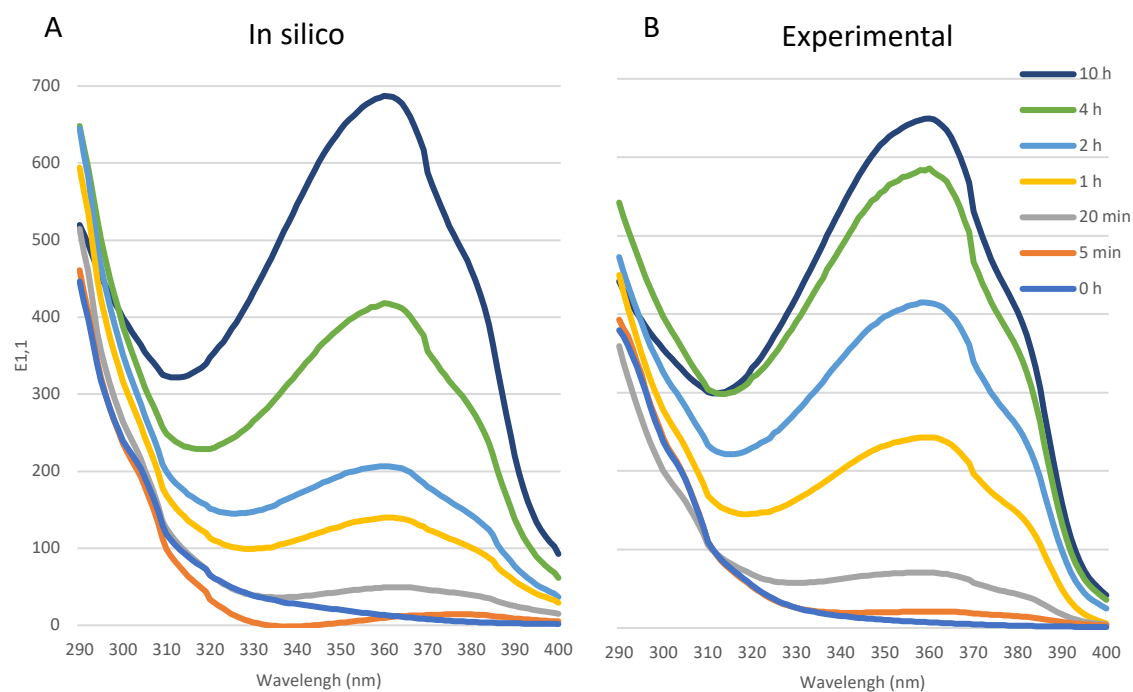


Figure 2-6. E1,1 of the mixture PRE-B 0,008%, PRE-C 0,008% and PRE-A 0,008% in Emollient-A solution after different irradiation times (0, 5 min, 20 min, 1 h, 2 h, 4 h, 10 h) at 765 W/m². A) In silico expected values B) Experimental values.

The obtained results from the mixtures *in silico* and experimental were compared at the maximal wavelength of the mixtures; PRE-B & PRE-C λ_{\max} =365 nm, PRE-B & PRE-A λ_{\max} =360 nm, PRE-B & PRE-C & PRE-A λ_{\max} =360 nm (Figure 2-7).

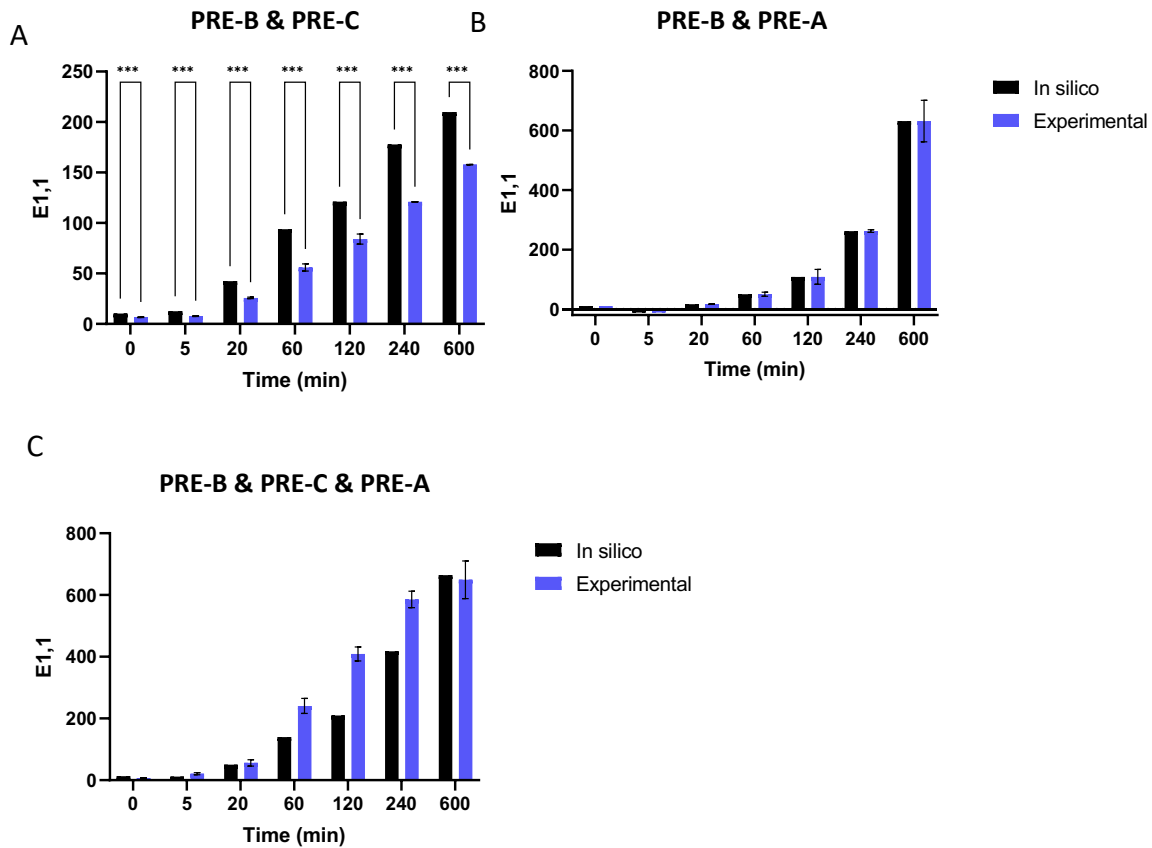


Figure 2-7. E1,1 of *in silico* and experimental of progressive UV filter combinations A) PRE-B & PRE-C B) PRE-B & PRE-A C) PRE-B & PRE-C & PRE-A. Statistical analysis: Two-way ANOVA (turkey multiple comparisons test).

Results showed no significant difference between the *in silico* and the experimental results in the mixtures containing PRE-A (PRE-B & PRE-A and PRE-B & PRE-C & PRE-A) at any irradiation time. Therefore, no synergistic effect was observed.

In contrast, the mixture of PRE-B and PRE-C at 0,008% in Emollient-A solution was statistically significant from the *in silico* values at $p > 0,001$ for all the irradiation times (0, 5 min, 20 min, 1 h, 2 h, 4 h and 10 h). Results showed that the *in silico* E1,1 of the mixture was higher than the experimental E1,1 at 365 nm. Therefore, the mixture of PRE-B & PRE-C show an antagonistic effect at all the irradiation times tested.

2.3.4 Comparison of progressive UV-filters with commercial UV-filters

According to the results in Figure 2-8, the E_{1,1} of the four commercial UV filters revealed, that after 2 h irradiation at 765 W/m² the tested UV filters degrade. The straight line represents the E_{1,1} of the UV filters before irradiation and the dotted lines are the E_{1,1} after 2 h irradiation. Among the tested commercial UV filters, avobenzene (AVO) and ethylhexyl methoxycinnamate (EHMC) showed a higher degradation than DHHB and EHS. The recoveries were of 52% and 78% for AVO and EHMC, respectively. On the other hand, DHHB and EHS had recoveries of 92% and 81%, respectively. The photoactive instability of AVO and EHMC is widely reported in literature and was explained in section 1.3.3. According to Figure 2-8, commercial UV filters start degrading with UVR while the absorbance of progressive UV filters increases with UVR. As both types of UV filters were measured at the same concentration, solvent, method and irradiation intensity, the E_{1,1} spectra were compared.

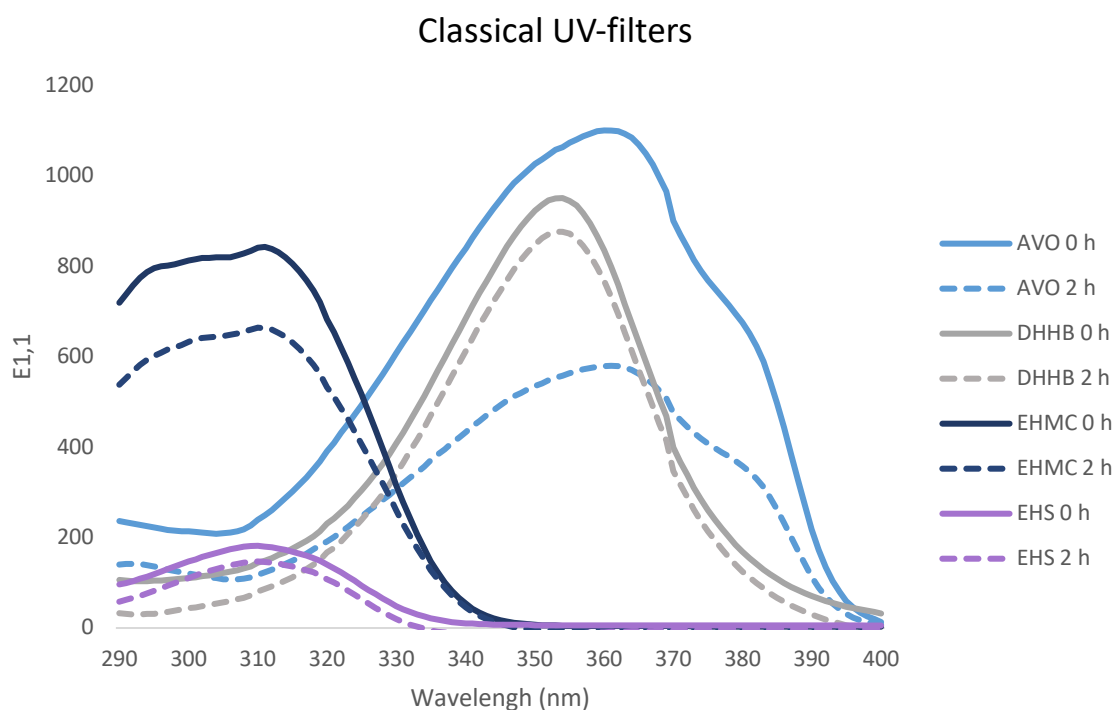


Figure 2-8. E_{1,1} of commercial UV filters; Avobenzene (AVO), Diethylamino Hydroxybenzoyl Hexyl Benzoate (DHHB), Ethylhexyl methoxycinnamate (EHMC) and Ethylhexyl Salicylate (EHS) after 0 and 2 h irradiation at 765 W/m².

The E1,1 spectra of the commercial UV filters after 2 h irradiation were plotted in a graph. On the other hand, the E1,1 spectra of the maximal tested irradiation (10 h) were plotted in the same graph (Figure 2-9).

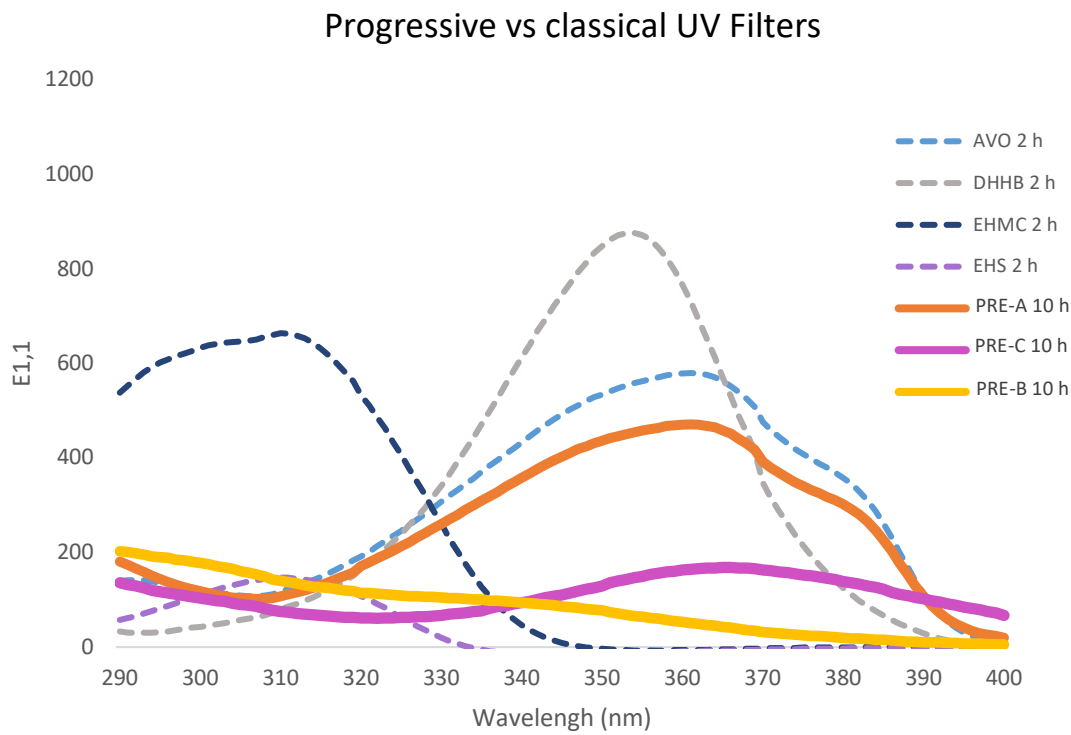


Figure 2-9. E1,1 of commercial UV filters; Avobenzon (AVO), Diethylamino Hydroxybenzoyl Hexyl Benzoate (DHHB), Ethylhexyl methoxycinnamate (EHMC) and Ethylhexyl Salicylate (EHS) after 2 h irradiation at 765 W/m² and E1,1 of progressive UV filters: PRE-A, PRE-C and PRE-B.

According to the results in Figure 2-1-Figure 2-7, the progressive UV filters need to be activated by UV light of high intensity during a long period of time to be effective. The irradiance of 765 W/m² is the maximal irradiation of the UV simulator. However, frequently in real life lower irradiances are measured during sunny days. The dose 11,6 MED was the average irradiation dose of three so-called beach days from 8 a.m. to 5 p.m. in Hawaii (124). In the used solar simulator 765 W/m² during 2 h irradiation equals 10 MED. Therefore, 10 MED is approximately the same irradiation dose of the sunniest hours at a sunny day in Hawaii.

On the other hand, 10 h at 765 W/m² equals to 50 MED, which is five times higher the irradiation of a beach day in Hawaii. Knowing that higher irradiation benefits the activation of the progressive UV filters, 10 h is their best version in terms of effectiveness. All in all,

extreme irradiation conditions of the progressive UV filters do not reflect reality. However, under this conditions progressive UV filters are favorized.

Figure 2-9 shows that after 10 h irradiation, weather PRE-B, PRE-C nor PRE-A could not reach the E_{1,1} values of EHMC, DHHB and AVO. PRE-A showed the highest absorbance among the other two progressive UV filters and its maximal E_{1,1} was the nearest to avobenzone.

On the other hand, PRE-B reached almost the E_{1,1(λ_{max})} of the low-absorbing UV filter EHS at 310 nm. Moreover, from 290 to 310 nm and from 320 nm to 400 nm it reached a higher E_{1,1} spectrum than EHS. The last progressive UV filter PRE-C showed absorbance in the UVB and UVA range. However, this absorbance was low compared to PRE-A.

2.4 Conclusion

- 2.4.1 Emollient-A solubilizes PRE-A and PRE-B at 5% concentration only with magnetic stirring without heat, making it a suitable solvent for sunscreen product formulation.
- 2.4.2 PRE-B, PRE-C showed activation at 0,008% in Emollient-A solution and no activation at 1%. PRE-A (batch 1) showed a faster activation and a higher absorbance the smaller the PRE-A concentration (0,001% > 0,008% and >>1%).
- 2.4.3 At 0,008% concentration, the representative wavelengths for the activation were 335 nm, 366 nm and 360 nm for PRE-B, PRE-C and PRE-A, respectively in Emollient-A solution. The $E_{1,1(\lambda_{max})}$ after 10 h irradiation were 210,5, 167,9 and 449,5 for PRE-B, PRE-C and PRE-A, respectively.
- 2.4.4 PRE-B & PRE-C show an antagonistic effect at $E_{1,1(\lambda_{max})}$, in the UVA range at the irradiation times 0, 5 min, 20 min, 1 h, 2 h, 4 h and 10 h.
- 2.4.5 After 10 h irradiation PRE-A (batch 1) showed a higher $E_{1,1(\lambda_{max})}$, than PRE-C and PRE-B and a lower absorbance than avobenzone after 2 h irradiation, at the same concentration.
- 2.4.6 PRE-B showed at 10 h irradiation a similar $E_{1,1(\lambda_{max})}$, to EHS after 2 h irradiation, at the same concentration.

3. PRE-A PHYSIC-CHEMICAL CHARACTERISATION

3.1 Introduction

PRE-A was analysed physicochemically. The methods employed for the characterisation of avobenzene were used with the objective to study the identity and purity of PRE-A. Three references manufactured in 2015, five years previous to the analysis, were measured. However, only limited information of this substance was available. The references were: R-81, R-80 and R-90. All three references were from different synthesis. Two of them; R-81 and R-80 were named after precursor of avobenzene nr. X and R-90 was labelled as precursor of avobenzene like nr. Y. Therefore, it was suspected, that the references R-81, R-80 had a different structure from R-90. Results of the three references were measured by HPLC and compared with the HPLC results from 2015 thus, results could be compared to previous obtained data. PRE-A is a precursor of avobenzene, which is activated by UVB light (125) However, before submitting the precursor to simulated solar radiation, a characterization of the molecule previous to the transformation to avobenzene was done and results are presented in this chapter.

Five different methods were used to characterize PRE-A: HPLC chromatography, IR-and UV-spectroscopy, DSC and solubility. Purity of the three PRE-A references were determined by HPLC. Moreover, as the same method was used as in 2015, the degradation after five years of the molecule could be assessed. On the other hand, the identity was proven by IR- and UV-spectroscopy.

The three PRE-A samples were firstly analysed by HPLC and IR. The reference with the highest purity was then used to perform further characterization experiments of PRE-A. First it was measured by spectrophotometry before irradiation to characterize the UV spectrum of PRE-A before the conversion to avobenzene. Moreover, a DSC was done to reveal incompatibilities with future excipients in formulation. Finally, the solubility in water at three different pH was done and compared with the avobenzene solubility.

3.2 Materials and Methods

Ingredients and equipment used are listed in Table 3-1 and Table 3-2, respectively.

3.2.1 Chemicals

Table 3-1. Chemicals used in the characterization of PRE-A

Name and reference nr.	Supplier	Category
PRE-A R-81	Company L	Active substance
PRE-A R-80	Company L	Active substance
PRE-A R-90	Company L	Active substance
Acetonitrile	Panreac (Spain)	Solvent
Methanol	Panreac (Spain)	Solvent
Water for HPLC	Panreac (Spain)	Solvent

3.2.2 Equipment

Table 3-2. Equipment used for the characterization of PRE-A.

Devices	Model	Supplier
Analytic balance	Sartorius BP211D	Sartorius (Germany)
Magnetic stirrer	Ikamag RCT	IKA (United Kingdom)
Cuvettes	10mm High Precision Cell, Quartz SUPRASIL	Hellma Analytics (Germany)
Electronic pipettes	EDP3-Plus	Rainin (Switzerland)
UV/Vis spectrophotometer	Specord 205	Analytik Jena (Germany)
Spectrophotometer Software	WinASPECT®	Analytik Jena (Germany)
HPLC	Series 1100 (UV-Vis detector G135A, Injector G1313A , software ChemStation)	Hewlett Packard (USA)
HPLC-column	Kromasil 100 C18 5 µm 150 x 4,6 mm	Teknokroma (Spain)
IR	Spectrum IR version 10.6.	Perkin Elmer (USA)
DSC	DSC-822e	Mettler Toledo (USA)

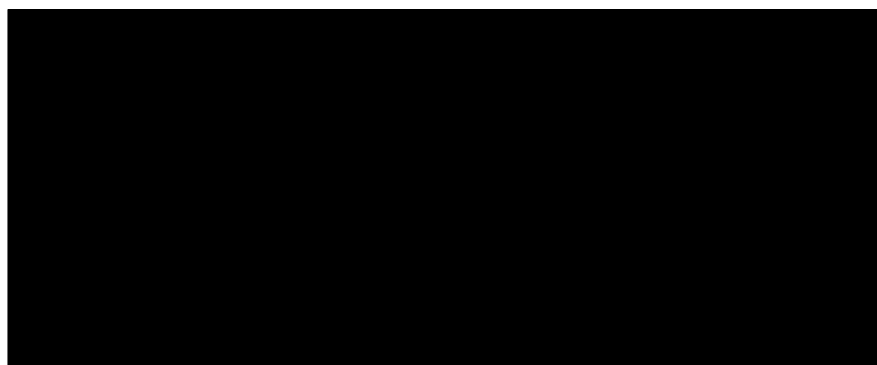
3.2.3 Content analysis by High Liquid Performance Chromatography (HPLC)

The high-pressure liquid chromatography (HPLC) is a device made of a pump, an injector, a column and a detector. Small molecule particles are separated depending on their polarity through the HPLC column and the substances are quantified. In the reversed-phase chromatography, the mobile phase is a polar solvent. This solvent elutes through the stationary phase in the columns, which is made of a solid or an immiscible liquid. The analytes which are carried by the solvent in the mobile phase will pass through the system at different times conditioned by the polarity interactions or affinity with the stationary and the mobile phase (polar molecules will pass faster than apolar molecules in the reverse-phase method) (126). PRE-A in crystal form must be solubilized and the sample needs to be filtered to avoid obstruction of the system. It is a high precision technique, which allow to separate and detect small amounts of impurities and degradation from the main molecule.

The content of PRE-A of three different samples with references; Ref: R-80, Ref: R-81 and Ref: R-90 were analyzed by HPLC chromatography (Hewlett Packard Series 1100) using an UV-Vis detector G135A. Each of the three PRE-A references were diluted in acetonitrile: H₂O (80:20) in a 100 µg/mL concentration. Before the injection, it was filtered through a 10 mL syringe with a 0,45 µm PTFE filter membrane.

An established method (127) was used to quantify PRE-A with the following parameters:

Column:
Mobile Phase:
Flow rate:
Gradient:
Injection volume:
Detection:



All the peaks were quantified by the HPLC-software.

3.2.4 IR

PRE-A was measured with a Perkin Elmer Spectrum IR version 10.6. For the measurement 1 mg of PRE-A was grounded in a mortar with 100 mg of anhydrous KBr. The mixture was then pressed under a pressure of several bars in a vacuum to form a compact layer of about 1 mm thickness. The individual KBr grains were melt into a uniform, crystal-clear mass. The compact mass was placed in the beam path of the spectrometer using a special sample holder.

The infrared (IR) radiation is originated from a coil of wire surrounded by a ceramic capsule. It is heated electrically, so that it gives out a IR radiation, which is heat, over a whole range of frequencies. The irradiation goes by a series of mirrors to the sample. The radiation not absorbed by the sample arrives to the detector. The interferogram that arrives to the detector can be decoded by a mathematical technique called Fourier transformation. This gives the intensity of the IR radiation at each frequency separately. A graph is originated by the software program of the IR spectrophotometer in which the percentage transmission is given against the wavelength.

IR spectroscopy is vibrational spectroscopy. Vibrations of covalent chemical bonds are in the energy range of the IR spectrum. The large number of vibrational degrees of freedom of organic molecules can be surveyed if they can be assigned to specific structural elements of the molecules.

IR measurements were performed by de Pharmaceutic Chemical Unit of the Faculty of Pharmacy and Food Sciences, University of Barcelona.

3.2.5 UV

The Ultraviolet (UV) spectrometry consists of the measurement of the absorbance of UV/Vis radiation (light source) through molecules.

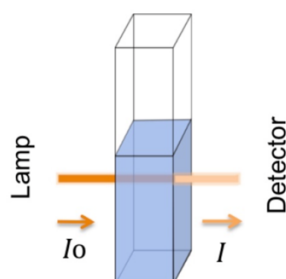


Figure 3-1. Principle of the spectroscopic measurement with an incident light (I_0) and a transmitted light (I) passing through a sample (38).

According to the Lambert Beer's law, if a light beam penetrates a homogeneous medium (sample), it can lose intensity through absorption. The transmission is the percentage of light that passes through the sample (Figure 3-1) subtracting the absorbance of the reference. The absorbance is inversely proportional to the transmission and is calculated by Equation 3-1.

$$A = \frac{I_0}{I} = \log \frac{1}{T} = \epsilon \cdot c \cdot d \quad \text{Equation 3-1}$$

where,

A stands for the absorbance,

I_0 corresponds to the incident light, and I is the intensity of the light after leaving the sample,

c is the concentration of the sample,

d is the thickness of the layer, and

ϵ is the coefficient of absorption. It is a proportionality factor and corresponds to the slope of the straight line if A is plotted against c in a diagram.

The spectrometer is represented by absorbance against the wavelength.

For the analysis, a 0,03% stock solution of PRE-A in methanol was prepared. Further, a 1/50 dilution of the stock solution in methanol was made. The dilution was measured in a UV/Vis spectrophotometer with a quartz cuvette of 1 cm pathlength (Hellma) 1nm stepwise.

3.2.6 DSC

Differential scanning calorimetry (DSC) is based on the difference in temperature of the sample and a reference (empty container, air) after application of a controlled temperature cycle. This test is used to study the physical-chemical behavior of substances exposed to temperature increase. The results of the heat flux are plotted against the temperature. Two different reactions can take place: endothermic or exothermic. Exothermic peaks in the graph are the result of interactions between the components of the sample and, in the first instance, an incompatibility of those components (38).

In this study, PRE-A was exposed to a temperature increase starting from 30 °C to 300 °C, with an increase of 10 °C / min. Thus, the equipment used for the measurement performs a differential tracking calorimetry by the heat flux method. This method consists on the measurement of the difference in temperature of the sample and the reference, converting as a function of heat. The test was performed by applying a dry nitrogen flow of 50 mL/min (38,39).

The DSC measurement was performed by the Polymorphism and Calorimetry Unit, Scientific and Technological Centers of the University of Barcelona.

3.2.7 Solubility

For the solubility of PRE-A in water: Firstly, a stock solution of 100 µg/mL of PRE-A in methanol was prepared and seven dilutions (16, 12, 10, 8, 6, 4 and 2 µg/mL) were made in water at pH 1, 6 and 7. Second, the absorbance of PRE-A was measured at its maximal wavelength (λ_{max} PRE-A in MeOH=247 nm, section 3.3.3). Water at the respective pH-value was used as blank. Three calibration lines, corresponding to pH 1, 6 and 7 were drawn by plotting the absorbance values against the concentrations. The confidence of variation of a minimum of five dilutions was less than 5 %. Further, a solution of PRE-A was made under saturation in water at pH 1, 6 and 7 and let under stirring for 24 h at 37 °C. The solution was then filtered through a 10 mL syringe and the absorbance was read under the spectrophotometer.

3.3 Results and discussion

3.3.1 HPLC

R-80

The main peak came after 7,992 minutes and its area under the curve (AUC) was 71,65% out of the total peak areas in the sample (Figure 3-2, Table 3-3). Comparing the current results with previous HPLC results of another batch of PRE-A measured in 2015 by Company L, in which both were measured using the same method (131) both peaks came at around 8 min (7,992 minutes for batch R-80 and 8,154 minutes for the same batch measured in 2015). This peak corresponds to the active substance, PRE-A, according to the results of Company L. Moreover, the same batch was measured by another HPLC-method using gradient and some differences in retention times and purity were observed. While its purity was of 93,4% in 2015 (Figure 3-3) our measurements conducted 5 years later showed a purity of 71,65%. The purity of this batch had decreased by around 23%. The difference in the retention time might be due to the differences of the methods; while in 2015 a mobile phase composition made of 80% acetonitrile and 20% water was used with an isocratic pump, in the current study a gradient with a mobile phase of 60% acetonitrile, 40% water was used. This explains the differences in the retention times.

In addition to the second bigger peak that appeared at 28,302 minutes, which was already characterized by Company L and named as impurity nr. Z (Figure 3-3), small new peaks appeared. These small peaks may have appeared due to a partial degradation of PRE-A, considering the long storage time.

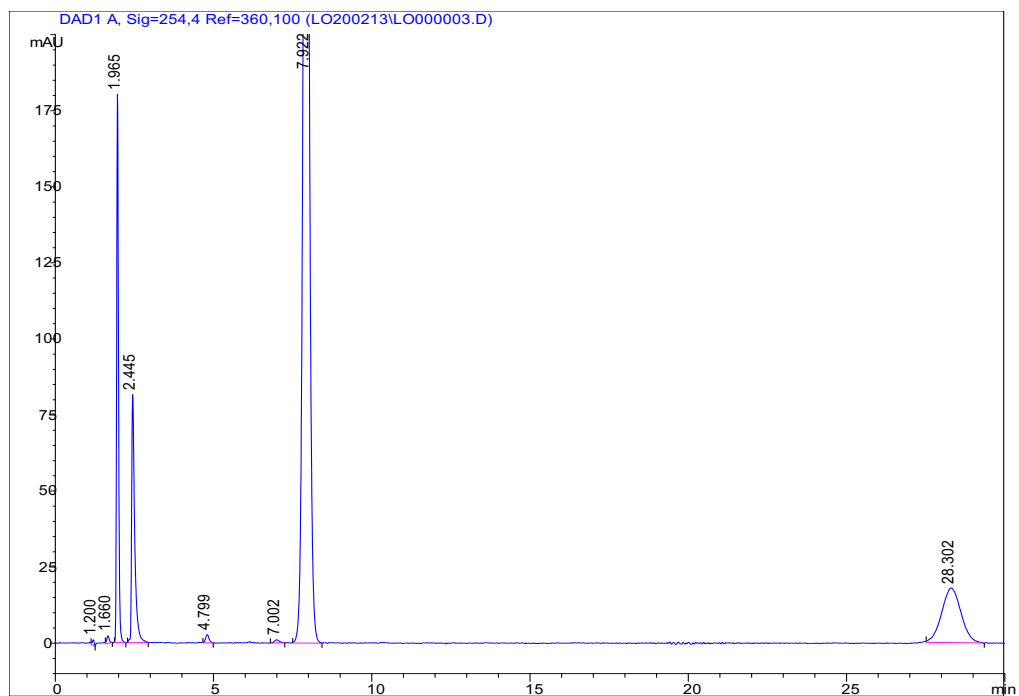


Figure 3-2. HPLC chromatogram of Ref: R-80 of PRE-A at 254 nm.

Table 3-3. Retention time and area of the peaks in ref. R-80 of the HPLC chromatogram at 254 nm.

Peak	Retention time	Area (%)
1	1,200	0,10
2	1,660	0,17
3	1,965	10,01
4	2,445	7,38
5	4,799	0,28
6	7,002	0,14
7	7,992	71,65
8	28,302	10,25

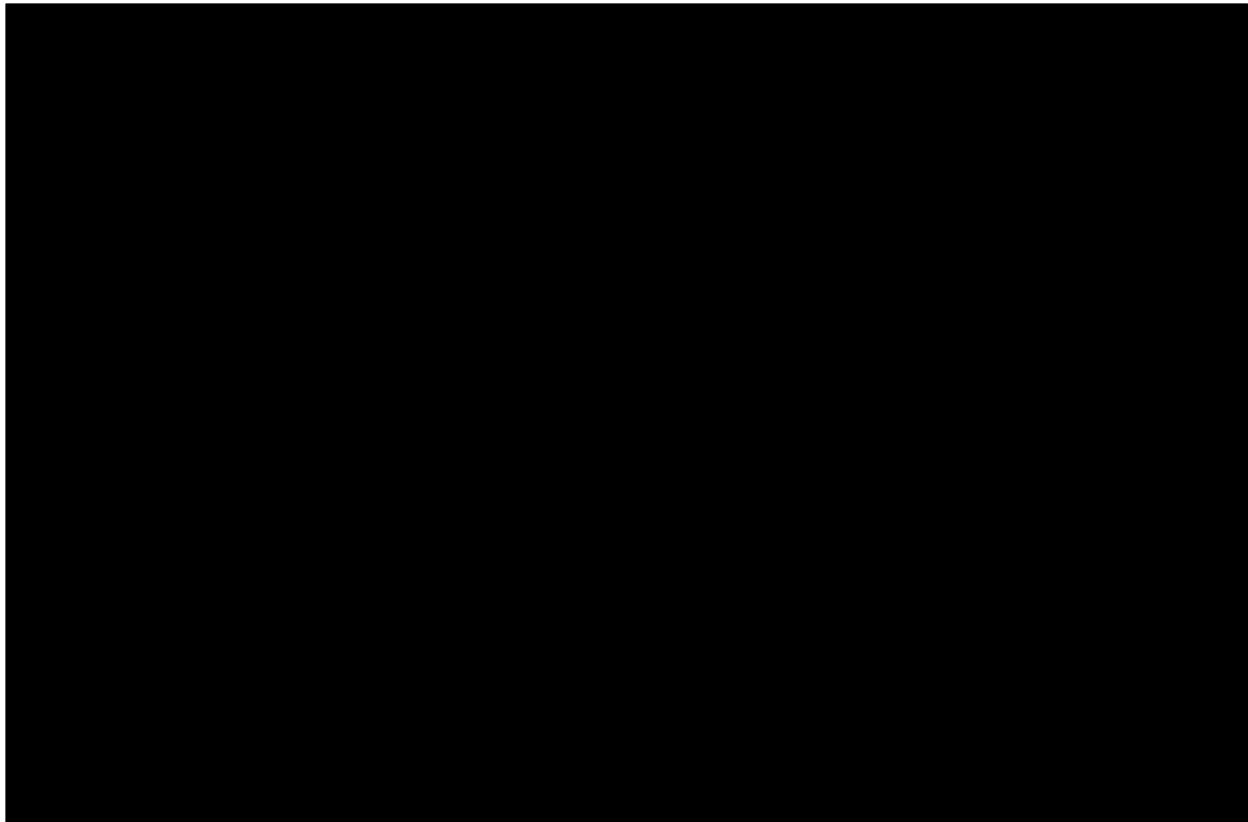


Figure 3-3. Retention time and area of the peaks in ref. R-80 of the HPLC chromatogram at 254 nm. Measurements of 2015 by Company L.

R-81=batch 1

The main peak came after 7,917 minutes and its AUC was 94,6% out of the total peak areas in the sample (Figure 3-4, Table 3-4). According to the results obtained in 2015 (127), the main peak might be PRE-A as the retention time of both studies were at around 8 min (7,917 minutes for the present study and 8,154 minutes for the measurement in 2015). However, after comparing the same batch with 5 years difference, although by another method (using a mobile phase of 60% acetonitrile and 40% water with gradient), the purity of the sample had decreased by around 5%. Also new small peaks appeared in addition to the already identified peak as impurity (impurity nr. Z) by Company L in 2015 (Figure 3-5). Taking previous classifications of the peaks into consideration the new peaks identified in the recent analysis, may be impurities as well.

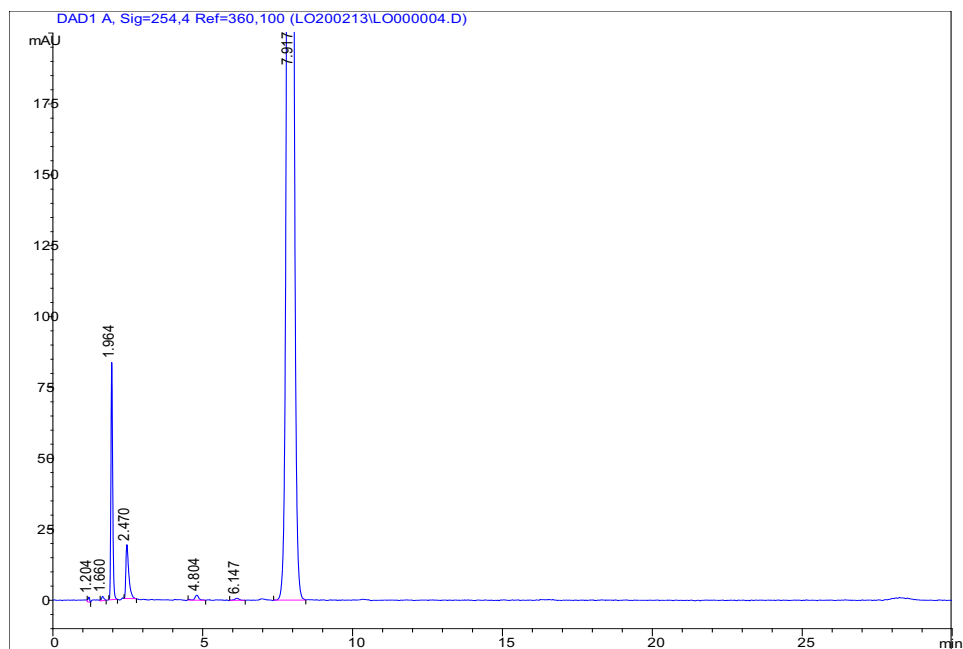


Figure 3-4. HPLC chromatogram of Ref: R-81 of PRE-A at 254 nm.

Table 3-4. Retention time and area of the peaks in ref. R-81 of the HPLC chromatogram at 254 nm.

Peak	Retention time	Area (%)
1	1,204	0,07
2	1,660	0,08
3	1,964	3,63
4	2,470	1,36
5	4,804	0,17
6	6,147	0,08
7	7,917	94,60

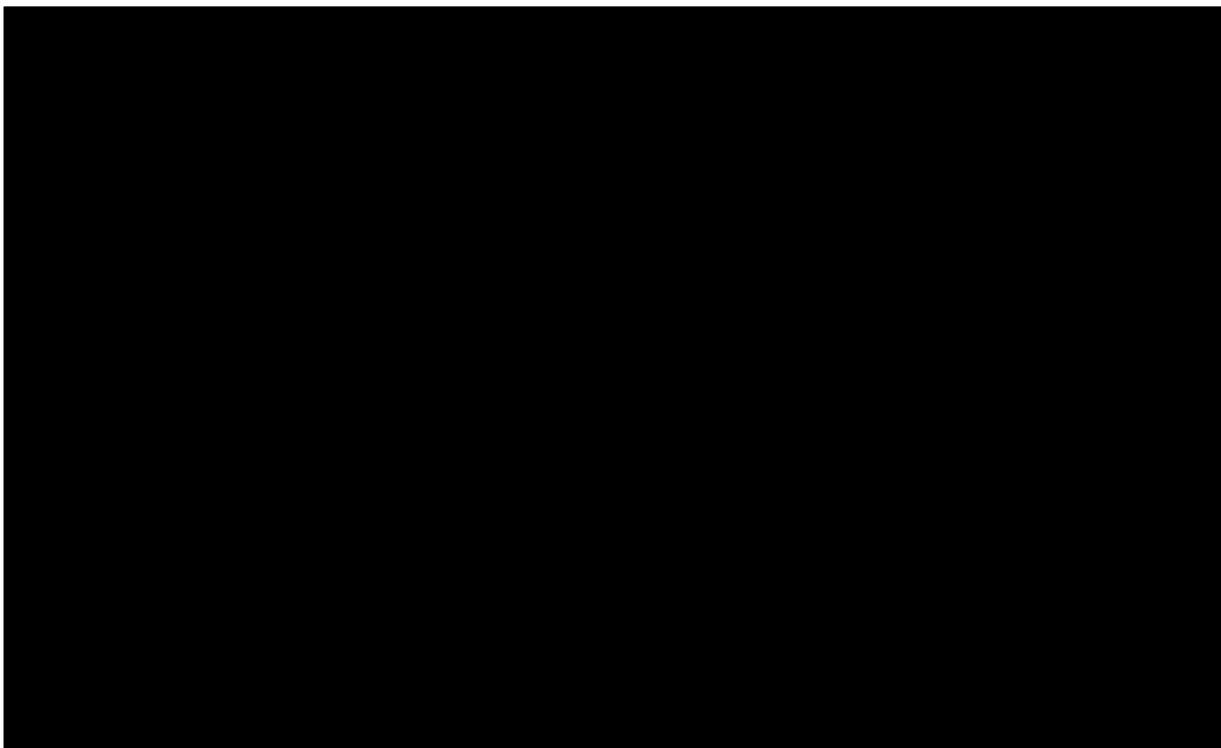


Figure 3-5. Retention time and area of the peaks in ref. R-81 of the HPLC chromatogram at 254 nm. Measurements of 2015 by Company L.

R-90

The AUC of the main peak was 92,70 % out of the total peak areas in the sample (Figure 3-6, Table 3-5). Results of previous HPLC measurements by Company L showed a purity of 99,0% (132). Therefore, around 9% in purity has been lost after 5 years storage. However, neither information about the method nor the HPLC peaks were shown in the report. Only the purity of PRE-A was available.

All in all, reference R-81 showed the highest purity from the three analyzed samples. Comparing reference R-90 with R-81 and R-80, some differences in the retention times were observed. While the peak of PRE-A (references R-81 and R-80), came after 7,9 minutes, the peak of PRE-A like nr. Y (reference R-90) came after only 3,5 minutes. This difference in retention times gives a hint, that both molecules may be different in structure. To confirm this assertion the sample was analyzed by IR.

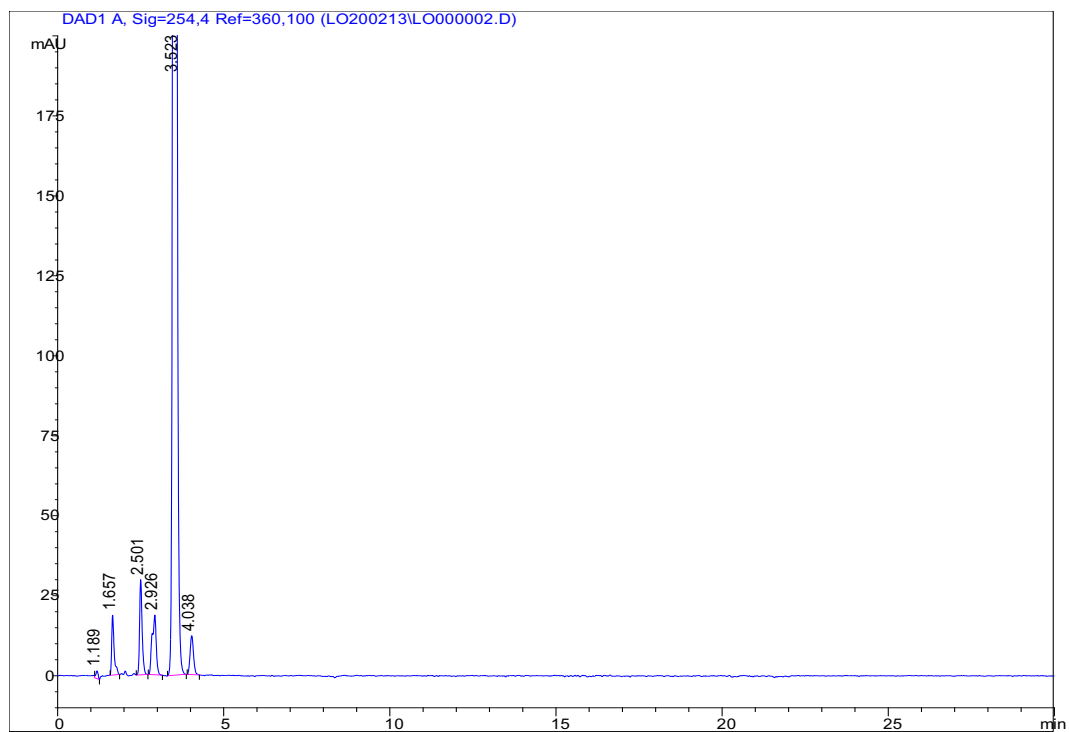


Figure 3-6. HPLC chromatogram of Ref: R-90 PRE-A at 254 nm.

Table 3-5. Retention time and area of the peaks in ref. R-90 of the HPLC chromatogram at 254 nm.

Peak	Retention time	Area (%)
1	1,189	0,16
2	1,657	1,36
3	2,501	2,25
4	2,926	2,27
5	3,523	92,70
6	4,038	1,24

3.3.2 IR

The IR spectroscopical results confirm the assertions made after the HPLC analysis. The IR spectra of Ref: R-80 and Ref: R-81 are similar (Figure 3-8 and Figure 3-7), and different to Ref: R-90 (Figure 3-9). This confirms the assertion that the sample with reference R-90 differs in structure with the other two references.

The infrared spectra of reference R-81 and (B) depicted the molecular structure of PRE-A. Characteristic groups in the IR spectra were identified corresponding to the investigated molecule, PRE-A. The following most characteristic groups were identified:

R-81

First, the small peak at 3074 cm^{-1} was attributed to the aromatic C-H-bond or to the alkene (C=C-H) because as a rule of thumb stretching vibrations, which are bigger than 3000 cm^{-1} correspond to H-atoms at unsaturated C-atoms (like aromatic C-H bonds) while smaller-than- 3000 cm^{-1} -stretching vibrations correspond to aliphatic C-H bonds. Therefore, the sharp peak at $2964,8\text{ cm}^{-1}$ corresponds to an alkane group (C-H). This group could be attributed to the C-H bonds of the tert-butyl group (CH_3) of PRE-A. (Figure 3-7).

Second, the sharp peak at 1720 cm^{-1} is characteristic for carbonyl (C=O) group and might correspond to the keto group of the molecule (Figure 3-7).

Third, the peak at 1642 cm^{-1} , appear when the molecules present alkenes (C=C) or aromates. This reflected the two aromatic groups and the alkene group of PRE-A (Figure 3-7).

A band at 1460 cm^{-1} (here 1457 cm^{-1}) is typical for CH_3 -groups due to bending vibrations of the molecule.

Last, the peaks at 1286 , 1241 and 1177 cm^{-1} corresponded to the (C-O) group contained inside the ester or ether group of the molecule (Figure 3-7).

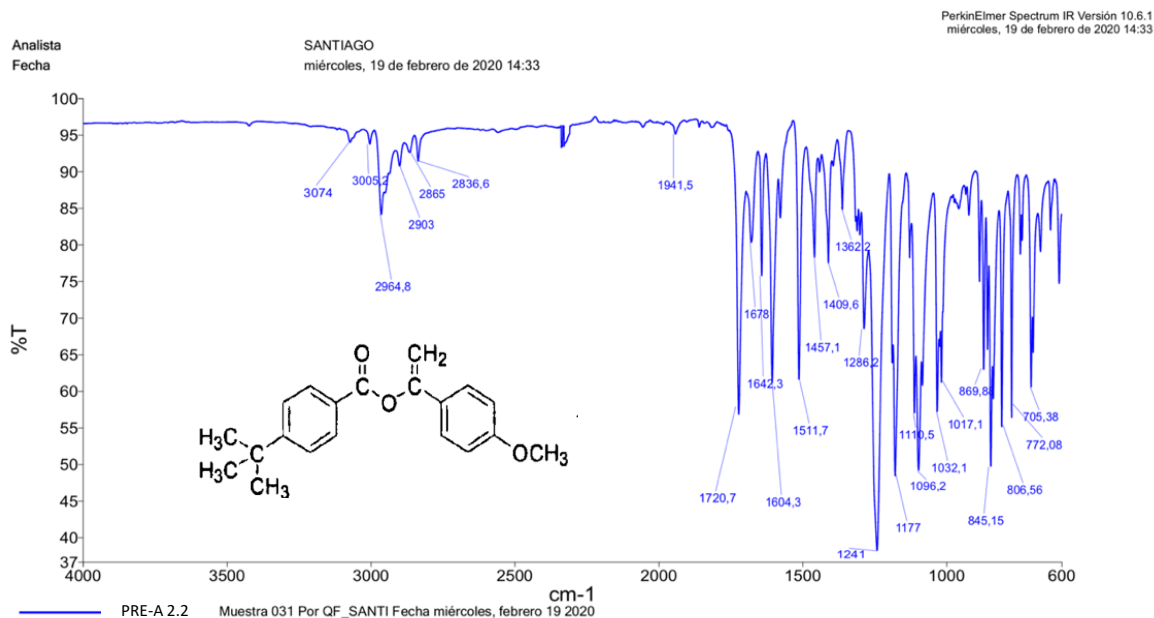


Figure 3-7. IR spectrum of ref: R-81 (internal ref: PRE-A 2.2)

R-80

The characteristic bonds and groups for the spectrum of reference R-80 (Figure 3-8) are presented in Table 3-6.

Table 3-6. IR absorption bands of ref. R-80.

Wavenumber (cm ⁻¹)	Chemical group
≈ 3074 (band not scored in IR spectrum)	C=C-H, alkene stretching vibration
2964, 2903, 2867, 2836	C-H aliphatic stretching
1716	C=O carbonyl
1675	C=C aromatic
1604, 1511	C=C stretching vibration
1459	-C-H ₃ -group, bending vibration
1279, 1241, 1178	C-O ether, ester

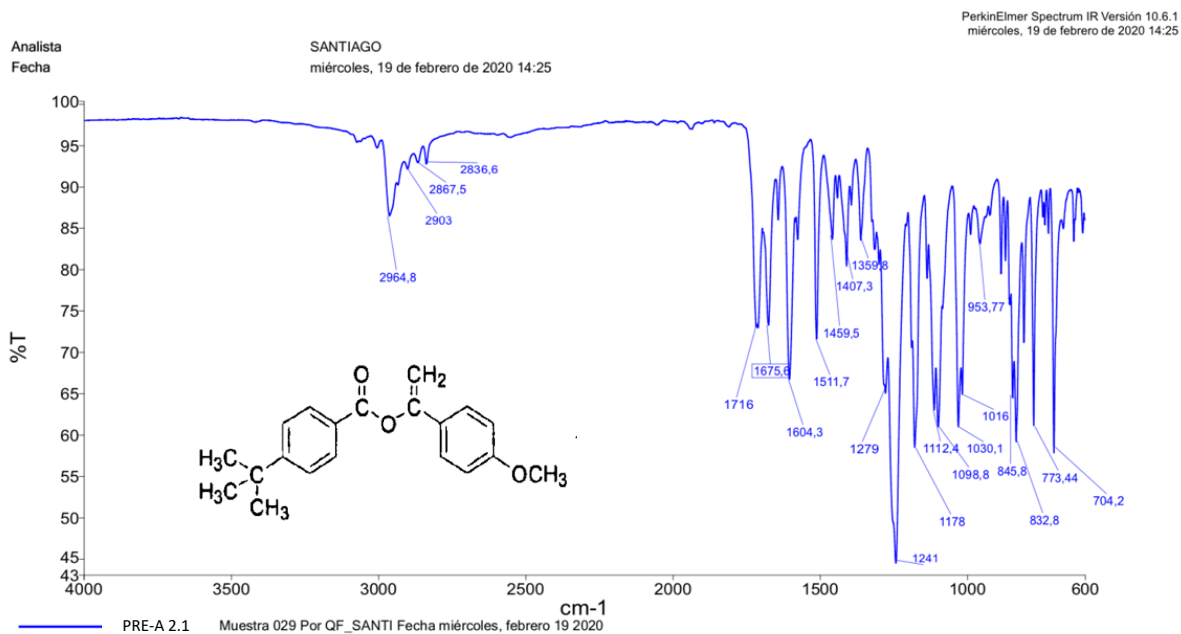


Figure 3-8. IR spectrum of ref: R-80 (internal ref: PRE-A 2.1)

R-90

As previously mentioned after analyzing this molecule by HPLC, the difference in the retention time from R-81 and R-80 there was the suspicion, that reference R-90 would be a different molecule from the previous two. To confirm this statement, also an IR spectroscopic measurement of this molecule (Figure 3-9) was performed and results are presented in Table 3-7.

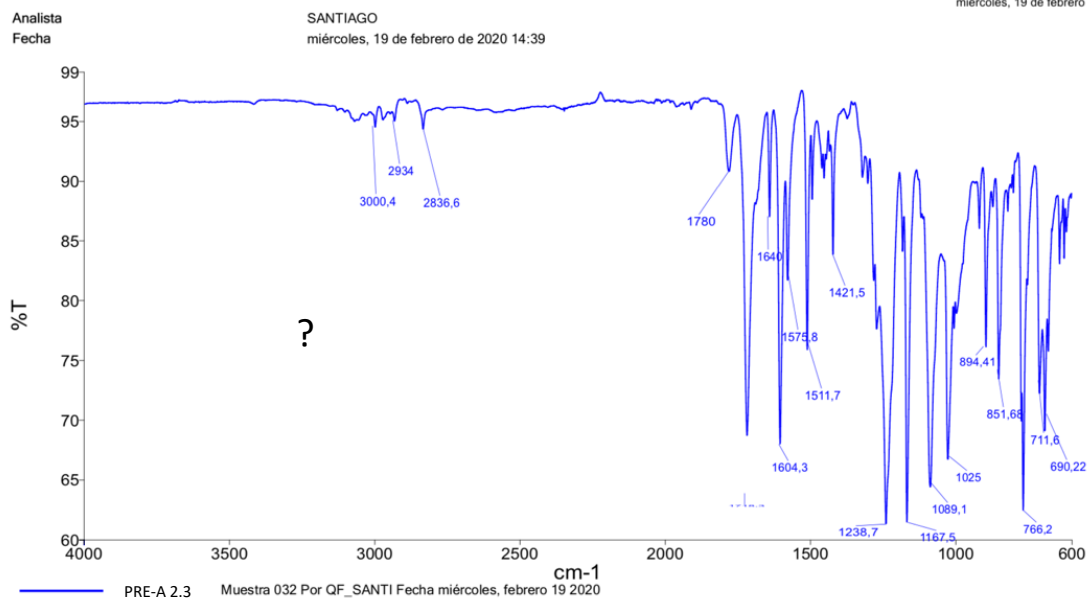


Figure 3-9. IR spectrum of ref: R-90 (internal ref: PRE-A 2.3)

Table 3-7. IR absorption bands of ref. R-90.

Wavenumber (cm ⁻¹)	Chemical group
≈ 3074 (band not scored in IR spectrum)	C=C-H, alkene stretching vibration
3000, 2934, 2836	C-H aliphatic stretching
≈ 1716 (band not scored in IR spectrum)	C=O carbonyl
1640	C=C aromatic
1604, 1575, 1511	C=C stretching vibration
1238	C-O ether, ester

Comparison of the three references

The references R-81 and R-80 have identical IR spectra and, other than reference R-90. The main difference is that while R-81 and R-80 have a sharp band at 2964 cm⁻¹, this band was not observed in R-90. Moreover, the band at 1460 cm⁻¹, which is characteristic for the bending vibration of the -C-H₃-group did not show in the IR spectrum of R-90.

After careful revision of the existing literature about dose-dependent progressive sunscreens, a US patent with number US 8,545,816 B2 (133) presented three molecules that lead to avobenzone or to avobenzone-like conversion after irradiation. These three molecules with

its conversions after ultraviolet light extracted from (133) are presented in Figure 3-10.

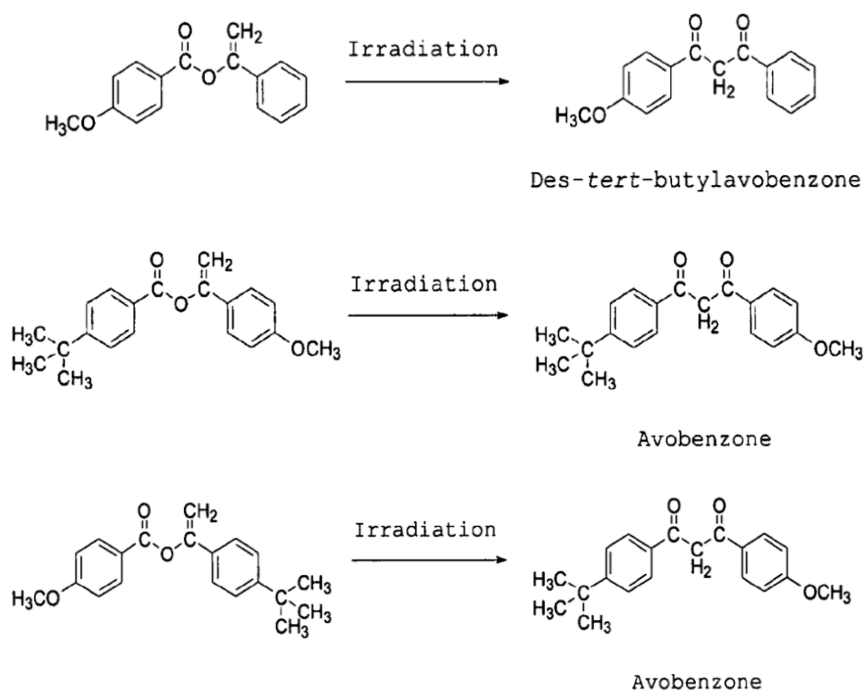


Figure 3-10. Dose-dependent progressive sunscreens that lead to avobenzone or avobenzene-like compounds (43).

From the three molecules only the molecule that produced des-tert-butylavobenzone fitted in the results obtained by IR spectrum. As this molecule did not have 3x -CH_3 groups this would explain the little absorbance around 2900 cm^{-1} and the lack of the band at 1460 cm^{-1} .

3.3.3 UV

The reference with the highest purity was R-81 according to HPLC results (section 3.3.1) and was therefore characterized further by UV-spectroscopy, DSC and its solubility in water was measured. The UV reference R-81 of PRE-A at 0,0006% in methanol without UV-light activation shows two peaks at 204 nm and 247 nm with an absorbance of 0,95 and 0,49, respectively (Figure 3-11).

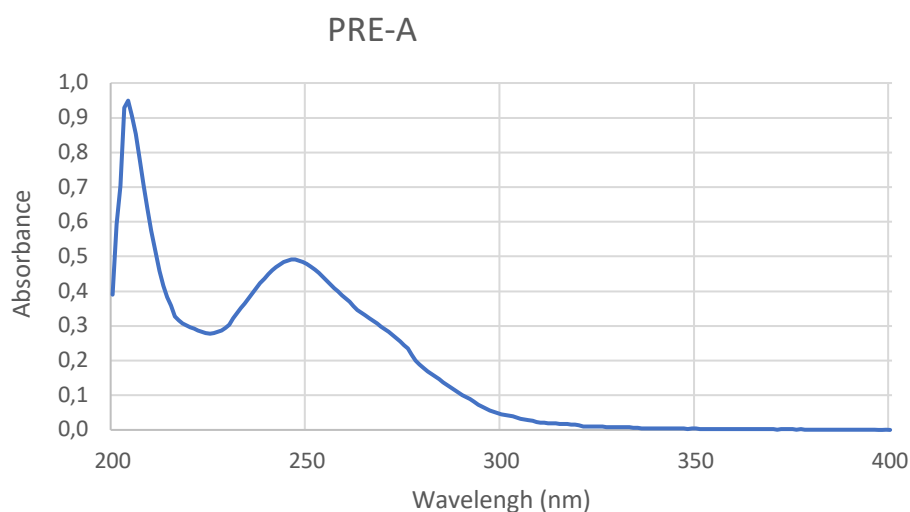


Figure 3-11. PRE-A ref. R-81, UV-spectra measured in methanol.

The obtained UV spectra was like the PRE-A spectra depicted in a previous publication (38), where the absorbance curve of PRE-A was represented for 250-400 nm.

Here in this publication of PRE-A the absorbance presented a peak around 250 nm. However, any other peak of PRE-A could not be identified as the measurement was limited to 250-400 nm. In our measurement, the absorbance was measured from 200-400 nm resulting in two peaks, at 247 and 204 nm (Figure 3-11).

3.3.4 DSC

Two endothermic peaks were found at 73, 3 °C and at 232 °C, corresponding to the two melting points of PRE-A. This means, that the structure, which can be crystalline or endomorph, has been melted turning into liquid state. The onset of the first peak starts at 52,55 °C with a peak at 73,25 °C. The integral is -178,30 mJ with an enthalpy of -60,87 Jg⁻¹).

The second second melting point was detected with an onset at 152,4 °C, with a peak at 232 °C (integral of -215 mJ with an enthalpy of -73,4 J/g) (Figure 3-12). This diagram is important in order to formulate the emulsion of a sunscreen as the state of PRE-A (liquid starting at 52 °C) could be ideal in formulation as typically crystalline UV filters need to be heated until 70-80 °C to make them solubilize and reach homogeneity of the sunscreen formulation.

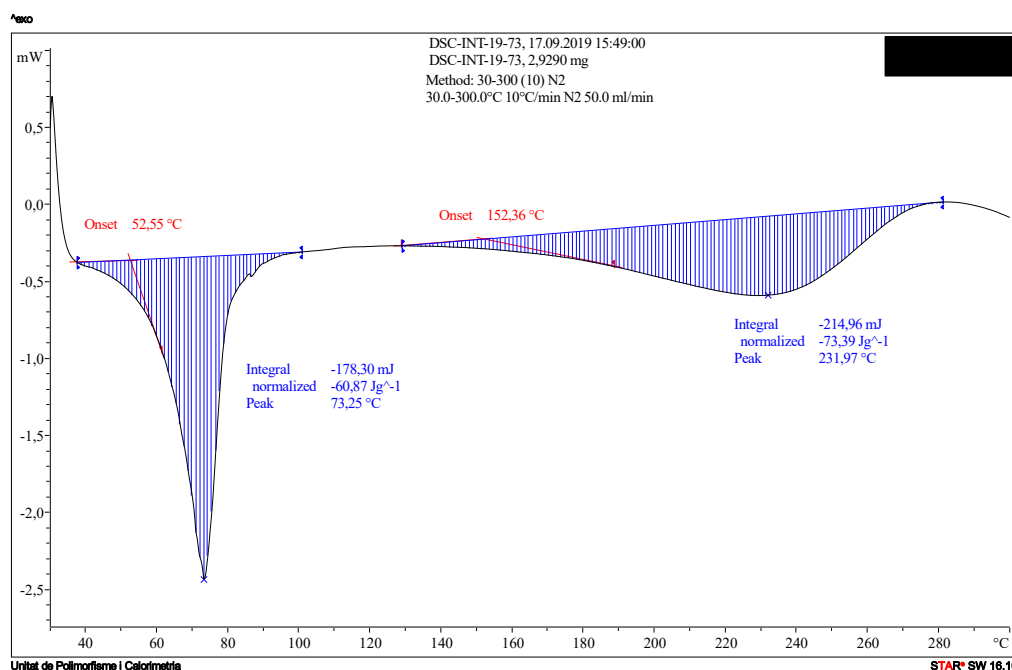


Figure 3-12. DSC of PRE-A ref. R-81.

3.3.5 Solubility

The solubility of PRE-A is dependent on the water-pH. Figure 3-13, shows that the solubility of PRE-A in water increases the lower the water pH. The solubility of PRE-A in water at pH 1, 6 and 7 was 0,02 mg/mL, 0,018 mg/L and 0,011 mg/L, respectively.

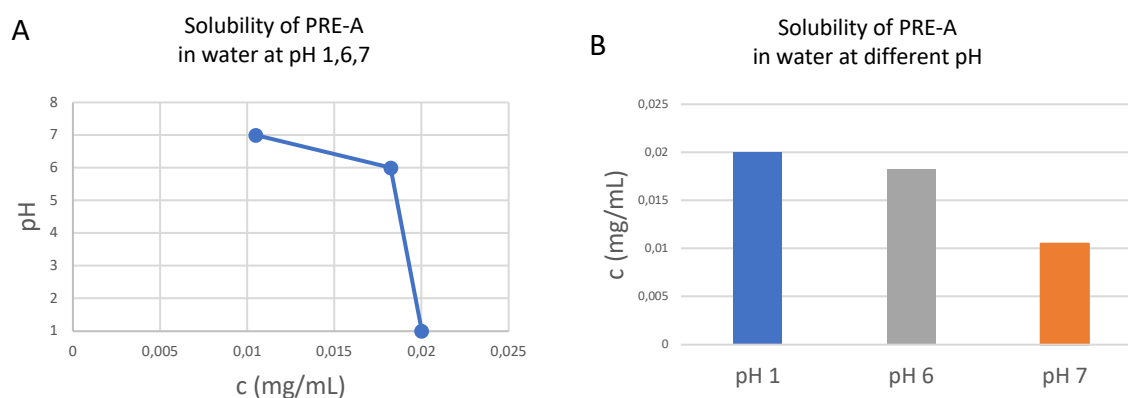


Figure 3-13. A) Regression curves and B) Solubility of PRE-A in water of pH 1, 6 and 7.

According to the results, the highest solubility of PRE-A in water at pH 1 (0,02 mg/mL). Avobenzone has almost the same structure as PRE-A and as only small amounts of the synthesized PRE-A were available, the solubility was compared with avobenzone for further solubility tests in other solvents.

Avobenzone has a solubility of 0,0015 mg/mL (135) to 0,0022 mg/mL (136) in water depending on the literature source. Comparing both solubilities, PRE-A has a ten times higher solubility in water. Avobenzone's solubility is tiny and therefore it is considered to be not soluble in water. Although PRE-A solubility is higher than avobenzone's, it is practically insoluble according to Ph. Eur. as the required part of solvent (mL) to solubilize 1 g solute exceeds 10.000 (137). Moreover, it is not enough to be solubilized in the current filter concentrations (up to 5% for avobenzone in Europe (138)) as PRE-A maximal concentration would be 0,018 %. Therefore, it is not soluble in water.

From this it can be stated, that although the solubility of PRE-A and avobenzone is similar as both are insoluble in water, the solubility of avobenzone can give some hints about the solubility of PRE-A. However, the solubility of PRE-A needs to be studied specifically for each solvent.

3.4 Conclusion

- 3.4.1 References R-81 and R-80 showed similar retention times in the HPLC. In both references the peak came after 7,9 min. However, in reference R-81 this peak was higher corresponding to a higher pureness of PRE-A.
- 3.4.2 The references R-81 and R-80 showed similar IR spectra.
- 3.4.3 UV/Vis spectra from 200-400 nm showed absorbance peaks; at 204 and 247 nm.
- 3.4.4 Two peaks at 73 and 232 °C were observed in the DSC, corresponding to the melting points of PRE-A.
- 3.4.5 PRE-A's solubility in water showed a pH dependency. At the low pH 1 a higher solubility was observed compared to pH 6 and 7. However, it was practically insoluble in water in terms of the Ph. Eur.

4. PHOTOACTIVATION OF PRE-A IN DIFFERENT VEHICLES

4.1 Introduction

Progressive UV filters is a new technology in UV filters, which act similar to prodrugs. Progressive UV filters have initially low absorbance properties, however in presence of UV radiation, they get activated to its active conformation, which absorbs UV-light (Figure 4-1). This reaction, called Foto-Fries, consists of a keto-enol tautomerization (being the enol form the active conformation)(139).

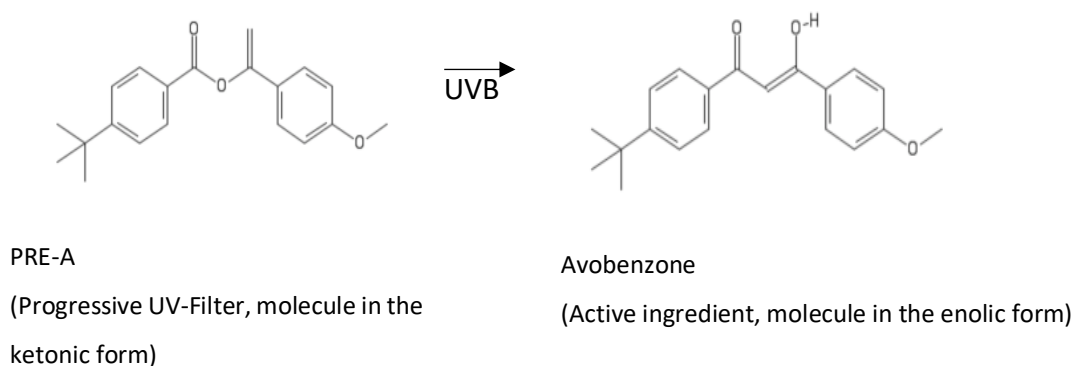


Figure 4-1. Foto-transposition of PRE-A to the active form avobenzone by UVB light: Foto-Fries reaction

In this chapter, two different experimentation set ups (cuvette method, plate method) were performed to address different questions, namely:

- Which batch of PRE-A is the one with the highest absorbance?
- Does solvent viscosity influences the kinetics of PRE-A activation?
- Could PRE-A be used as a stabilization product for avobenzone?

Comparison in PRE-A photoactivation of five batches (1, 2, 3 and 7) and avobenzone at 0,001% in Emollient-A

Firstly, the absorbance properties of four different batches was assessed.

The aim of the study was to evaluate the implications of the progressive UV filters technology in real sun exposure conditions. By a constant source of simulated solar exposure, the absorbance of PRE-A irradiation-dependent photoactivation was assessed at different times. Between batches there were small modifications in the manufacturing process resulting in a different physical aspect. A high and fast absorbance was the criteria to assess the quality of a product. The batch with the highest absorbance should serve as pattern for further scalability of PRE-A. Moreover, its increase in irradiation-dependent absorbance was compared with the well-known irradiation-dependent photodegradation of the commercial UVA-filter avobenzone.

Previous literature report avobenzone degradation until 2 h because of the recommendation to reapply sunscreens after this time (140). In this study the authors decided to extend the tested irradiation time up to 10 h, because of the also well-known poor compliance regards reapplication of the sunscreen users (141).

PRE-A in emollients of different viscosity

PRE-A photoactivation and avobenzone photostability were assessed on solvents with different viscosity: ethanol (1,10 mPa·s), Emollient-A (5 mPa·s), cocoglycerides (40 mPa·s) and PEG 400 (120 mPa·s) (87,142,143). The emollient Emollient-A, an emollient proved to produce an increase in absorbance of PRE-A after irradiation (AFE=16,61) in the UVA range (320-400 nm)(144) is one of the most frequently used emollients in formulation of sunscreen products (145).

PRE-A as stabilization product of avobenzone

Once the batch of PRE-A with the highest absorbance was identified, this batch was combined with avobenzone at different proportions. The absorbance at different irradiation doses was monitored. Finally, the absorbances of the mixtures for every irradiation dose were compared with the absorbance of avobenzone. The aim was to choose the proportion in which the highest stability of avobenzone was achieved. This was determined by the cuvette method (section 4.2.2) and afterwards by this optimal proportion was assessed by the plate method (section 4.2.3).

4.2 Materials and Methods

4.2.1 Materials

Ingredients and equipment used are listed in Table 4-1 and Table 4-2.

Table 4-1. Ingredients used in the cuvette method with popular name, INCI (international nomenclature of cosmetic ingredients) name and batch number, supplier and commercial name and category of the ingredient.

Name & INCI name and Batch nr.	Supplier	Category
PRE-A batch 1	Company L	UV-Filter
PRE-A batch 2	Company M	UV-Filter
PRE-A batch 3	Company M	UV-Filter
PRE-A batch 7	Company M	UV-Filter
Avobenzone (Butyl Methoxydibenzoylmethane)	Neo Heliopan 357 (Symrise) ¹	UV-Filter
Ethanol	Merck	Solvent
Emollient-A	Emollient-A (BASF) ¹	Solvent
Cocoglycerides	Myritol 331 (BASF) ¹	Solvent
PEG 400	Fagron	Solvent

¹Ingredients, which were a gift of the supplier.

Table 4-2. Devices used in the cuvette method listing the model and supplier.

Devices	Model	Supplier
Analytic balance	Sartorius BP211D	Sartorius (Germany)
Magnetic stirrer	Ikamag RCT	IKA (United Kingdom)
Cuvettes	10mm High Precision Cell, Quartz SUPRASIL	Hellma Analytics (Germany)
Electronic pipettes	EDP3-Plus	Rainin (Switzerland)
Solar simulator	ATLAS CPS+ equipped with water cooling plate	Ametek (EEUU)
Thermostat	ECO Silver	Lauda (Germany)
Thermometer datalogger	K 202 Datalogger	Voltcraft (Germany)
Suntest Lamp Filter	Solar Standard COLIPA Ident-Nr. : 5607 7759	Ametek (EEUU)
UV/Vis spectrophotometer	Specord 205	Analytik Jena (Germany)
Spectrophotometer Software	WinASPECT®	Analytik Jena (Germany)

Materials used in the three types of experiments as listed in Table 4-2. Results are shown in sections 4.3.1a, 4.3.1b, and 4.3.1c:

1) Section 4.3.1a, active ingredients: PRE-A (batch 1, batch 2, batch 3 and batch 7), and avobenzone. Emollient: Emollient-A.

2) Section 4.3.1b. Active ingredients: PRE-A batch 7, emollients: ethanol, Emollient-A, Cocoglycerides and PEG 400.

3) Section 4.3.1c. Active ingredients: PRE-A batch 7 and avobenzone. Emollients: Emollient-A.

4.2.2 Cuvette method

Solution preparation and irradiation

Concentrations of 0,001% of PRE-A (batches 1, 2, 3 or 7) or avobenzone in Emollient-A solution were prepared (section 4.3.1a).

A volume of 2,5 mL of the solutions was filled in 1 cm quartz cuvettes. The cuvettes were placed in horizontal position in the middle of the sample holder table (Figure 4-B). The sample holder table was equipped with a water cooling system connected to an external thermostat (Lauda ECO Silver) programmed at -40 °C to prevent the plates surpassing the temperature of 40 °C during irradiation (Figure 4-2A). The temperature inside the solar simulator was monitored with a digital thermometer datalogger. The 10 mm quartz cuvettes were placed horizontally at the cooling table of the solar simulator with its transparent quartz side upwards to the solar simulator (oriented towards the lamp). Quartz cuvettes were used to avoid absorbances by the glass in the UVB range.

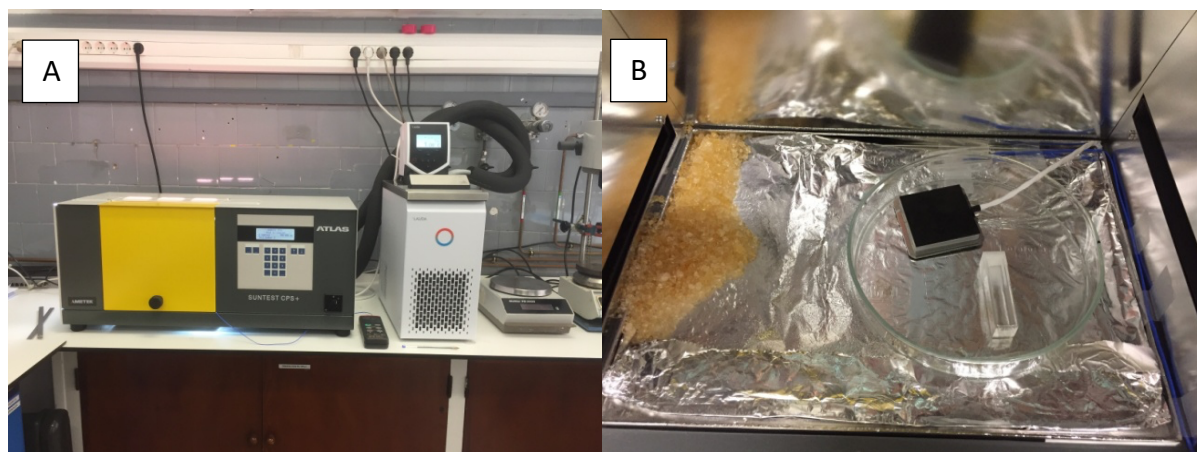


Figure 4-2. A) Irradiation Chamber, ATLAS CPS+ with the external thermostat, Lauda ECO Silver, external thermometer to monitor temperature of the cuvettes inside the chamber. B) Cuvette containing the sample inside the irradiation chamber. The position of the cuvette is upwards the xenon lamp.

The xenon lamp of the solar simulator was equipped with a filter system, which is the recommended COLIPA Standard Sun emitting a radiation of 765 W/m² (from 300-800 nm), of which 76,5 W/m² correspond to (300-400 nm). The intensity of the light source is represented

in Figure 4-2. The cuvettes were measured for 0, 5 min, 20 min, 2 h, 4 h and 10 h. This corresponds to 0, 0.5, 1.5, 10, 20 and 50 MED (minimal erythemal doses), respectively, which is equivalent to 0 kJ/m², 270 kJ/m², 810 kJ/m², 5400 kJ/m², 10800 kJ/m² and 27000 kJ/m², respectively. The purpose was to test the initial activation of the batches (0, 5 and 20 min) and after longer periods of irradiation time (2 h, 4 h and 10 h).

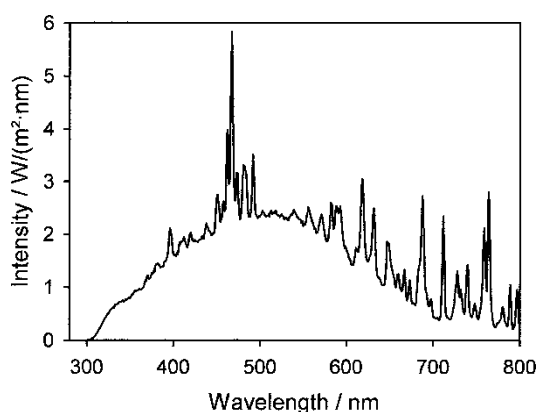


Figure 4-2. Spectrum of the radiation of the ATLAS Suntest CPS+ with standard sun filter at sample position (41).

Two different stock solutions for each batch of PRE-A and avobenzone were measured ($t=0$) and afterwards irradiated simultaneously. In total 10 cuvettes (2 x batch 1 PRE-A, 2 x batch 2 PRE-A, 2 x batch 3 PRE-A, 2 x batch 7 PRE-A and 2 x avobenzone) were irradiated simultaneously to minimize errors. After each irradiation dose, the cuvettes had a rest in the dark of 15 minutes before the absorbance was measured. The same two cuvettes corresponding to the two stock solutions of a batch were used for all the irradiation doses.

The absorbance of the UV filters was measured from 250-400 nm in 1 nm steps by spectrophotometry (UV/Vis spectrophotometer specord 205, Analytik Jena) and software WinASPECT. The samples (solutions of active ingredients in quartz cuvettes) were measured in the spectrophotometer 15 min after irradiation.

In the case of the PRE-A activation depending on different solvents (section 4.3.1b), concentrations of 0,001% of PRE-A batch 7 in ethanol, Emollient-A, cocoglycerides or PEG 400 were prepared. The experimental procedure was identical to the previous experimental set (section 4.3.1a) and the irradiation time was 0 h, 5 min, 20 min 2 h and 4 h.

In the case of PRE-A (batch 7) as stabilization product of avobenzone, mixtures with the proportions 1:1, 1:2, 1:4, 2:1 and 4:1 of PRE-A (batch 7) and avobenzone were prepared at 0,001% in Emollient-A. The experimental procedure was identical to set 4.3.1a and the irradiation time was 0 h, 5 min, 20 min 2 h and 4 h.

In all tests, the respective pure emollient was used as blank.

Computational analysis- conversion of A to E1,1

Out of the average value of absorbance of the two stock solution with a confident value of 95%, the average specific extinction (E1,1) was calculated from 250-400 nm with Equation 4-1 and Equation 4-2.

$$\varepsilon = \frac{A_{\lambda}}{c \cdot d} \quad \text{Equation 4-1}$$

where A_{λ} corresponds to the absorbance at a specific wavelength, c is the concentration of the solution in (mol/L) and d is the optical path length (cm).

$$E1\%, 1cm = \frac{\varepsilon \cdot 1\%}{MM} \quad \text{Equation 4-2}$$

where ε is the extinction coefficient and MM is the molecular mass of the active substance. The $E1,1$ is an optimal parameter to compare absorbances taking into account the exact weighted mass of the solution. Therefore, the $E1,1$ of the different stock solutions before and after irradiation were compared for all the samples.

Further the extinction at the maximal wavelength ($E_{(\lambda_{max})}$) and the wavelength of maximal absorbance (λ_{max}) were identified.

Finally, for the experiment of section 4.3.1c, the real $E1,1$ was compared with the theoretical $E1,1$, which was calculated from the single $E1,1$ results from PRE-A (batch 7) and avobenzone.

4.2.3 Plate method

Formulation's preparation

Formulations were prepared according to Table 4-3, were

- PRE-A 5%
- Avobenzene 5%
- Avobenzene 3,34% and PRE-A 1,67% (2:1 avobenzene: PRE-A, total 5%)
- Avobenzene 5% and PRE-A 2,5% (2:1 avobenzene : PRE-A)

were added to the oil phase (phase A) of the formulations.

Table 4-3: Formulation composition without active ingredients

	INCI	Amount (%)
A	PEG-6 Stearate (and) Ceteht-20 (and) Glyceryl Stearate (and) Steareth-20	5,00
	Emollient A	15,00
	Cetyl alcohol	3,00
	Phenolxyethanol & Ethylhexylglycerin	1,00
B	Aqua	ad. 100
	Disodium EDTA	0,20
	Glycerin	3,00

Procedure:

1. Phase A was heated to 75 °C with helix stirrer at 50 rpm
2. Phase B was heated to 75 °C with helix stirrer at 50 rpm
3. Phase A was added to phase B under stirring
4. The emulsion was homogenized under turrax for 1 minute
5. The emulsion was cooled down to 25 °C under U plate stirring.

The absorbance of each of the formulations was measured separately on a PMMA plate. First, the correspondent emulsion was spread on a PMMA plate and measured on the spectrophotometer Labsphere 2000S (see subsection 5.2.12). The ISO 24443:2012 was not followed for this absorbance measurements as there were no *in vivo* SPF data for PRE-A. The PMMA plate was measured at three different spots to obtain the absorbance UV-spectra. Plates were irradiated at 0 MED, 2,5 MED, 5 MED, 7,5 MED and 10 MED with the ATLAS CPS+ Sunscreen simulator under controlled temperature of 30 °C. After each irradiation, the plate was measured at the same spots of previous measurement and the absorbance for every irradiation dose was collected. All measurements were performed in triplicate. In all tests, the PMMA plate with 15 mg Glycerin spread on the plate as a thin film was used as blank.

Computational analysis- conversion of the absorbance to the SPF and UVA-PF

The SPF and UVA-PF was given by the software of the spectrophotometer Labsphere 2000S. The absorbance values of avobenzone 5%- and PRE-A 5%- emulsions were used to calculate the theoretical SPF and UVA-PF of the mixtures. The procedure to calculate the SPF and UVA-PF is explained in section 5.2.3.

Computational analysis- conversion of A to E1,1

The E1,1 was calculated from the absorbance values with Equation 4-1 and Equation 4-2.

Statistical analysis

Statistical significance of experimental results of the ingredient mixtures compared to theoretical expected values were determined at $p < 0,05$ using GraphPad Prism v.9 by two-way ANOVA.

4.3 Results and discussion

4.3.1 Cuvette method

a Batches (Comparison of PRE-A photoactivation of four batches (1, 2, 3, 7) and avobenzone at 0,001% in Emollient-A)

Avobenzone

Avobenzone has a decrease in absorbance by almost the half of its initial value after 10 h. Moreover, after 5 min irradiation, degradation was observed. The higher the irradiation, the more the absorbance increased at the wavelengths 270-290 nm. This value is not relevant for sun protection applied for human use because this spectral range corresponds to UVC. However, it helps for understanding of the photochemical transformation of the molecule (Figure 4-3).

PRE-A batch 1-7

The absorbance of the batches of PRE-A increased with increasing irradiation energy. While in batch 1 and 2 the maximal absorbance was at 10 h, batch 3 and 7 had a maximal absorbance at 4 h and between 4 h and 10 h absorbance decreased. Batch 3 and 7 reached its maximal absorbance faster than batches 1 and 2. Moreover, the absorbance high was superior in batch 3 and 7 (E1,1 between 700-800) than in batch 1 and 2 (E1,1 between 500-600).

It is important mentioning, that PRE-A at 0 h has a little absorbance reaching its maximum at 327-329 nm. However, after 5 min irradiation its absorbance decreases and shows a maximum at 359 nm. From 5 min on, its maximal absorbance is at 359 nm (Figure 4-4-Figure 4-7).

Batch 1 at 359 nm has the lowest absorbance compared to the other batches followed by batch 2 for all the irradiation doses. At 20 min batch 3 has the highest absorbance. However, batch 7 achieves the highest absorbance for 2 h to 10 h of irradiation time (Figure 4-8).

Avobenzone vs. PRE-A batch 1-7

Avobenzone has a higher absorbance than PRE-A. However, from 4 h irradiation, PRE-A batch 3 and batch 7 have a higher absorbance than avobenzone (Figure 4-8).

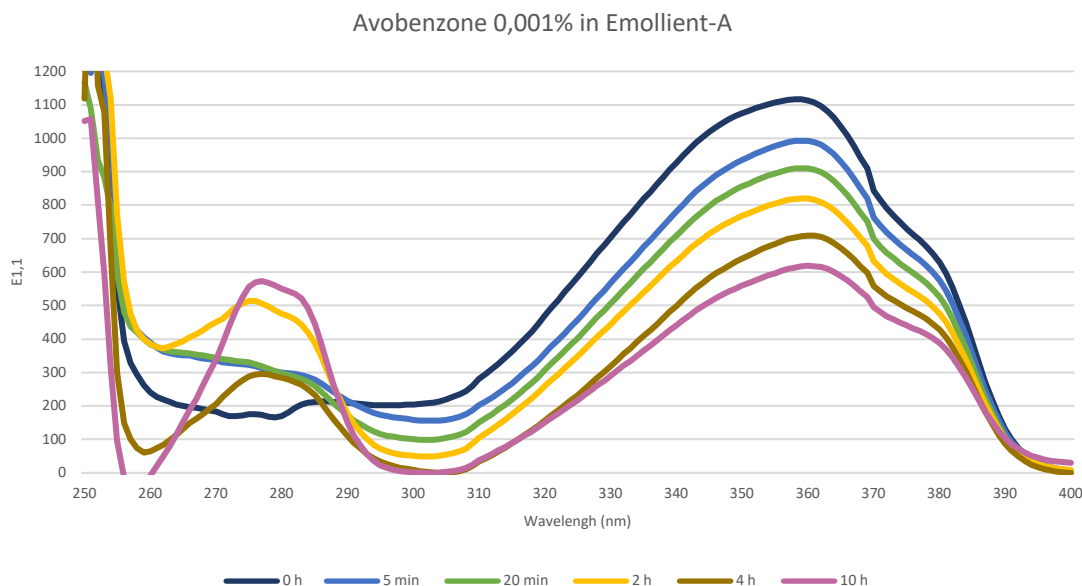


Figure 4-3. Specific extinction ($E_{1,1}$) of avobenzone from 250-400 nm in a 0,001% solution with Emollient-A after different irradiation times (0, 5 min, 20 min, 2 h, 4 h and 10 h) at 765 W/m².

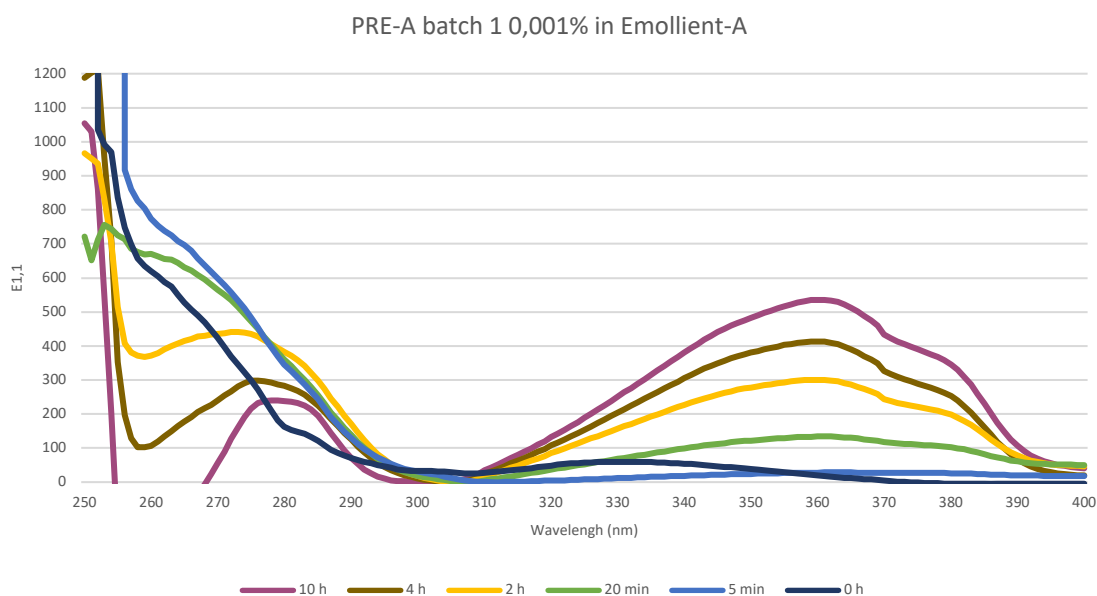


Figure 4-4. $E_{1,1}$ of PRE-A lot 1 from 250-400 nm in a 0,001% solution with Emollient-A after different irradiation times (0, 5 min, 20 min, 2 h, 4 h and 10 h) at 765 W/m².

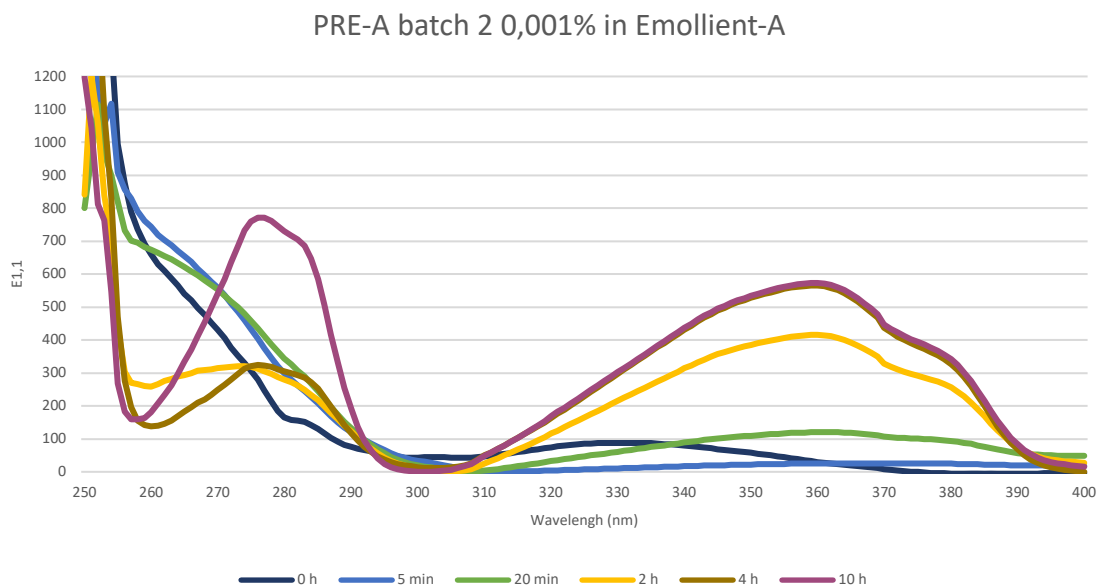


Figure 4-5. E_{1,1} of PRE-A (batch 2) from 250-400 nm in a 0,001% solution with Emollient-A after different irradiation times (0, 5 min, 20 min, 2 h, 4 h and 10 h) at 765 W/m².

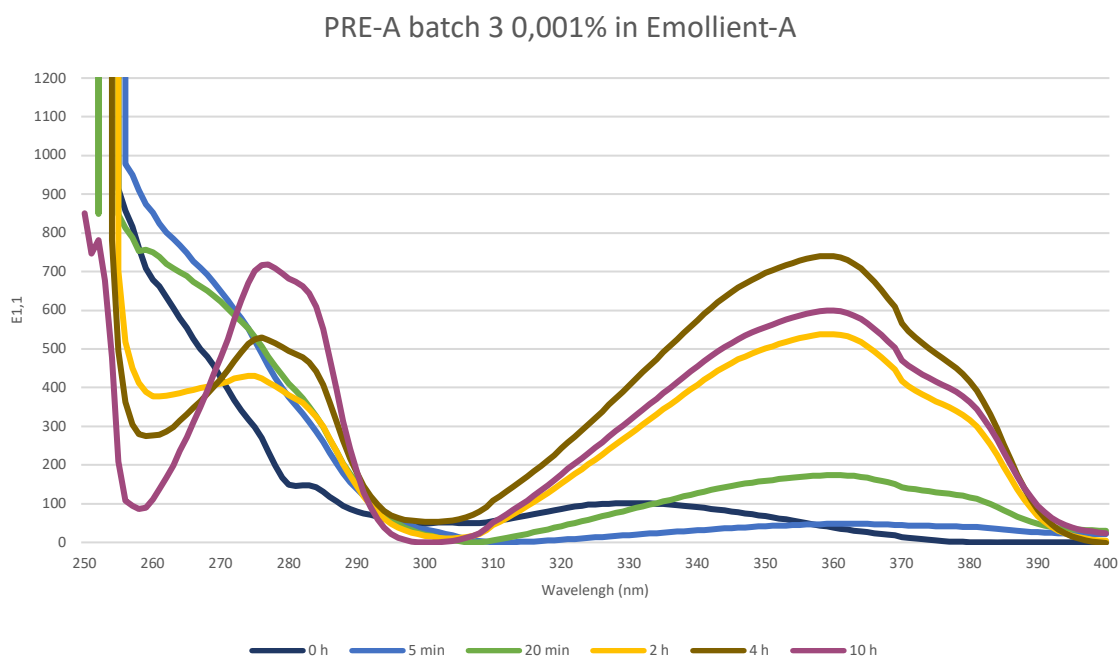


Figure 4-6. E_{1,1} of PRE-A batch 3 from 250-400 nm in a 0,001% solution with Emollient-A after different irradiation times (0, 5 min, 20 min, 2 h, 4 h and 10 h) at 765 W/m².

PRE-A batch 7 0,001% in Emollient-A

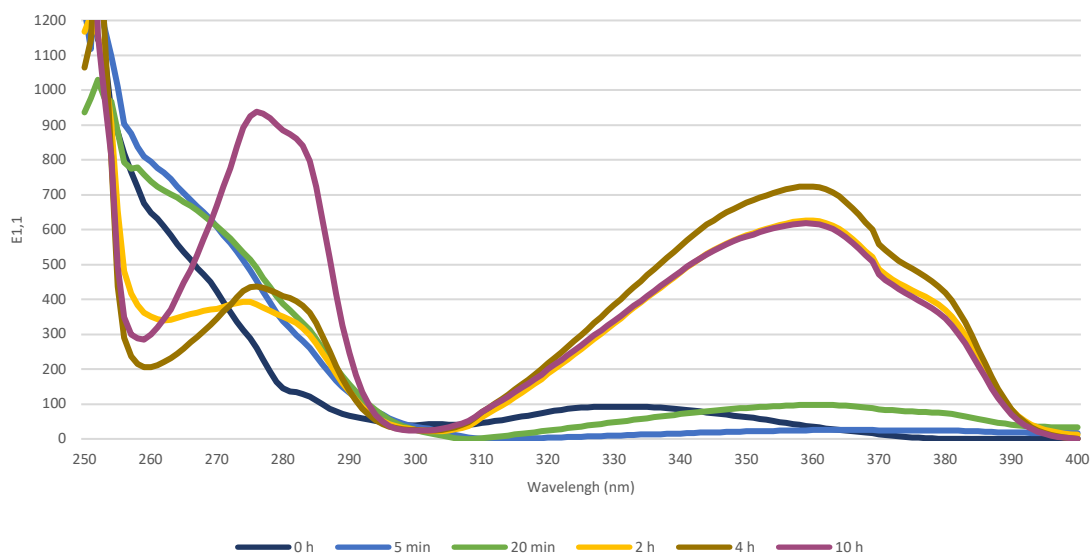


Figure 4-7. E1,1 of PRE-A batch 7 from 250-400 nm in a 0,001% solution with Emollient-A after different irradiation times (0, 5 min, 20 min, 2 h, 4 h and 10 h) at 765 W/m².

Avobenzone and PRE-A batches 1, 2, 3, 7 at 0,001% in Emollient-A at 359 nm

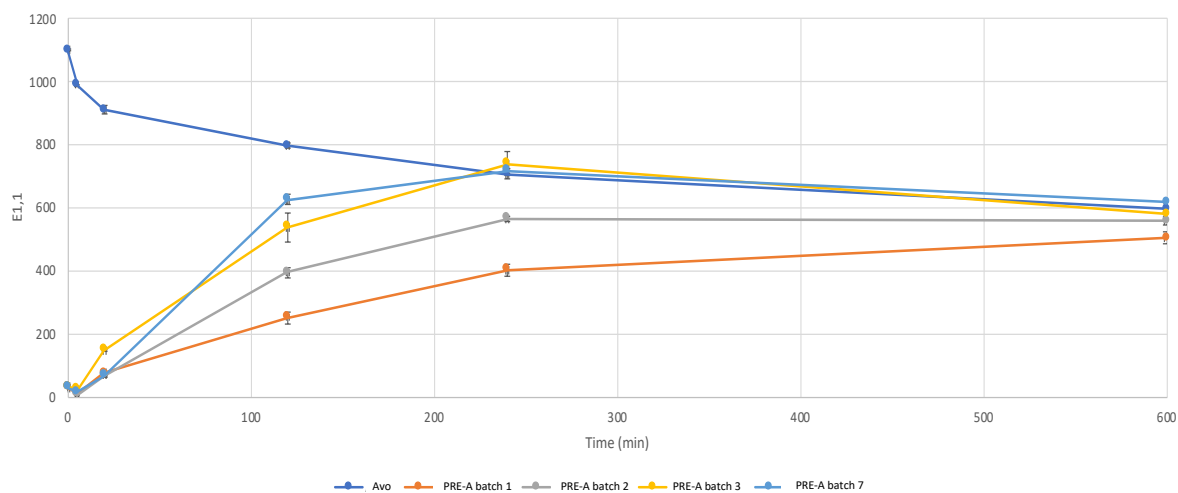


Figure 4-8. E1,1 at 359 nm of avobenzone, batch 1, 2, 3 and 7 of PRE-A in a 0,001% solution with Emollient-A after irradiation at 765 W/m² for 0, 5 min, 20 min, 2h, 4 h and 10 h.

b *PRE-A photoactivation in different solvents*

Ethanol was the solvent in which PRE-A had the highest absorbance at different irradiation times followed by Emollient-A, cocoglycerides, myritol and PEG 400. The results obtained suggest that viscosity is inversely proportional to the activation of PRE-A. On the other hand, it should be mentioned that ethanol is not a suitable solvent for solubilizing PRE-A, as PRE-A solubility in ethanol is only 2%, section 2.2.2. Therefore, Emollient-A is confirmed as a suitable solvent for PRE-A activation (Figure 4-9).

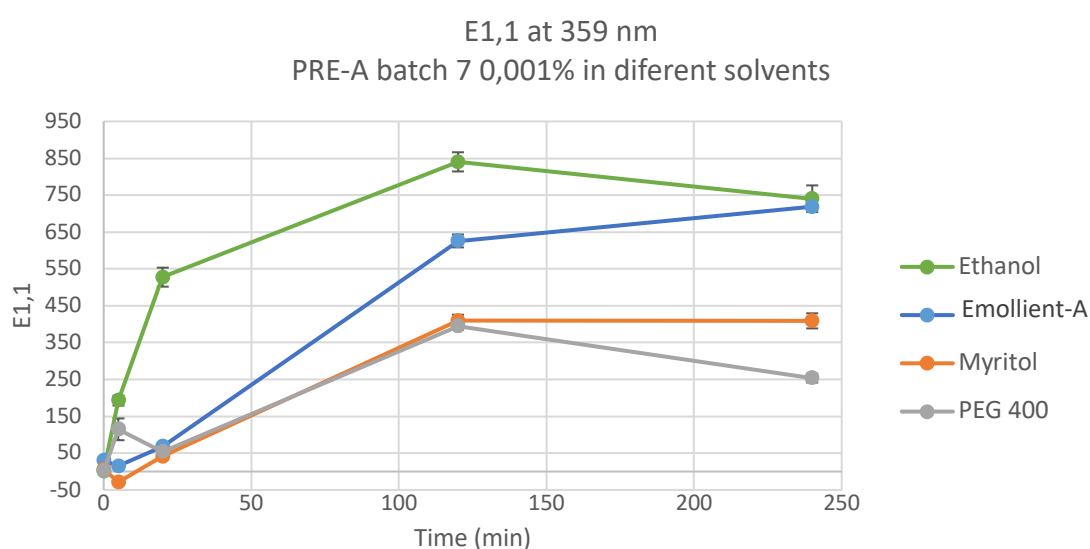


Figure 4-9. Progression of E1.1 in maximum absorbance wavelength; 359 nm of PRE-A at 0.001% ethanol, Emollient-A, Cocoglycerides Myritol and PEG 400.

c *Proportions of avobenzene and PRE-A (Comparison of PRE-A and avobenzene photoactivation and degradation at 0,001% in different proportions of PRE-A and avobenzene)*

PRE-A (batch 7) as a stabilisation product (booster) of avobenzene

The different combinations of avobenzene with PRE-A showed predictable results. The $E_{1,1(\lambda_{max})}$ in the combinations in which PRE-A were predominant (1:2 and 1:4, avobenzene: PRE-A) the initial absorbance (0 h irradiation) was lower than in the combinations in which

avobenzene were predominant (4:1 and 2:1, avobenzene: PRE-A) but increased with increasing irradiation time. The proportions 1:1, 1:2 and 1:4, avobenzene: PRE-A had a different initial absorbance (1:1 higher absorbance, 1:4 lower absorbance) but converged at 4 h irradiation. Therefore, the increase in absorbance was higher in 1:4 but in the counterpart its initial absorbance was the lowest from all the combinations. This is not surprising, as on the one hand, the absorbance of PRE-A has a maximal value at 0 h (without irradiation). On the other, PRE-A needs to be activated by UVB light.

Further, the combination 4:1 shows the highest absorbance from all the combinations (4:1, 2:1, 1:1, 1:2, 1:4) not only without irradiation but also at 5 and 20 min. However, despite its satisfactory initial absorbances, this is the only combination in which at 2 h its absorbance decreases. Nevertheless, its absorbance is still much higher than 1:1, 1:2 and 1:4. From 2 h to 4 h irradiation, there is a slight increase in absorbance being the second highest absorbance at 4 h. Finally, comparing the proportions 4:1 and 2:1, which have the highest absorbances. The combination 4:1 had higher absorbance at 0-, 5- and 20-min irradiation. However, this tendency inverts around at 75 min. The measured absorbance of 2:1 at 2 h and 4 h is not only higher than 1:4 but also than all the other combinations (Figure 4-10).

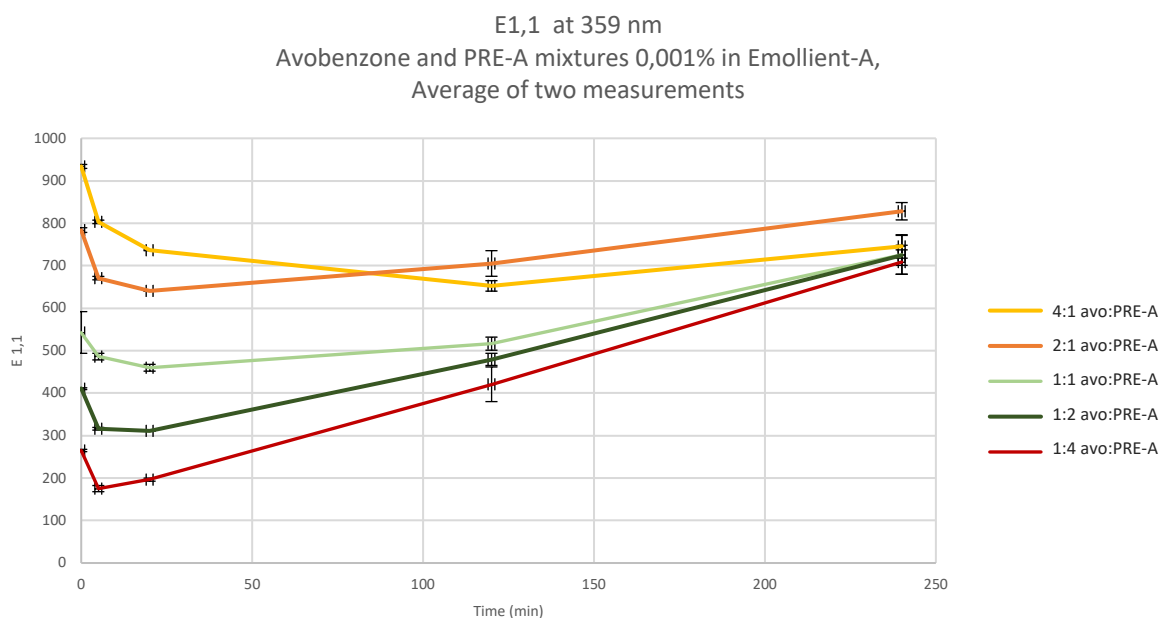


Figure 4-10. E1,1 of different proportions (1:1, 1:2, 1:4, 2:1, 4:1) of avobenzene and PRE-A batch 7 at 359 nm after irradiation at 765 W/m² for 0, 5 min, 20 min, 2h and 4 h.

When comparing the combinations of avobenzone: PRE-A with the single filters, avobenzone has a higher absorbance in almost every irradiation time instead of 4 h. At around 3 h irradiation, the combination 2:1 had a higher absorbance than avobenzone (Fig. 12). Therefore, the addition of PRE-A in formulations containing avobenzone, in the proportion 2:1 (avobenzone: PRE-A) demonstrates having a stabilization effect for avobenzone at higher sun exposition times.

On the other hand, PRE-A measured as a single filter has from 0 h to 2 h a fast increase in absorbance. However, from 2 h to 4 h it seems to have a slower conversion of PRE-A to avobenzone. This may be the reason for the slower increase in absorbance in the time interval 2 to 4 h. It seems that the combinations 4:1 and 2:1 are beneficial for the stabilization of avobenzone at 4 h irradiation (Figure 4-11).

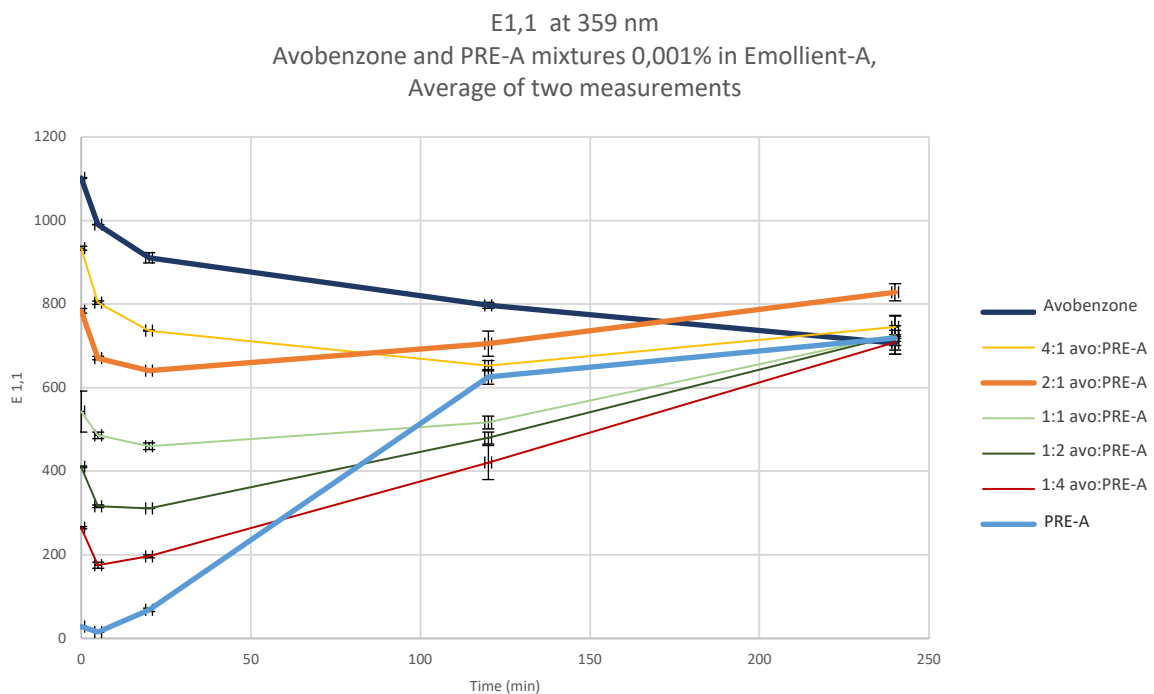


Figure 4-11. E1,1 of different proportions (4:1, 2:1, 1:1, 1:2, 1:4) of avobenzone and PRE-A batch 7 and single measurements of avobenzone and PRE-A batch 7 at 359 nm after irradiation at 765 W/m² for 0, 5 min, 20 min, 2 h and 4 h.

Exploration of synergistic behaviour

The behaviour of the combination (experimental values) in comparison to the sum of the empirical values of avobenzone and PRE-A in the different combinations combination (theoretical values) were analysed (Figure 4-12-Figure 4-17). A synergistic behaviour of the combinations could not be proven in the majority of the cases. However, the experimental E1,1 at 0 MED of the combinations was higher than in the theoretical values. Therefore, a synergistic effect of the combinations compared to the single values in the UVC (200-280) and UVB (280-320) ranges was observed (Figure 4-12-Figure 4-16). However, at 5 min, 20 min, 2 h and 4 h irradiation there was no synergistic effect. Theoretic and experimental E1,1 at the wavelength of 359 nm show similar values. Although, on the one hand at 0 h and 4 h there is a tendency that the experimental values of the combinations have a higher E1,1 than the theoretical. On the other, for the irradiation times 5 min, 20 min and 2 h the theoretical values have a higher E1,1 than the experimental ones (Figure 4-17).

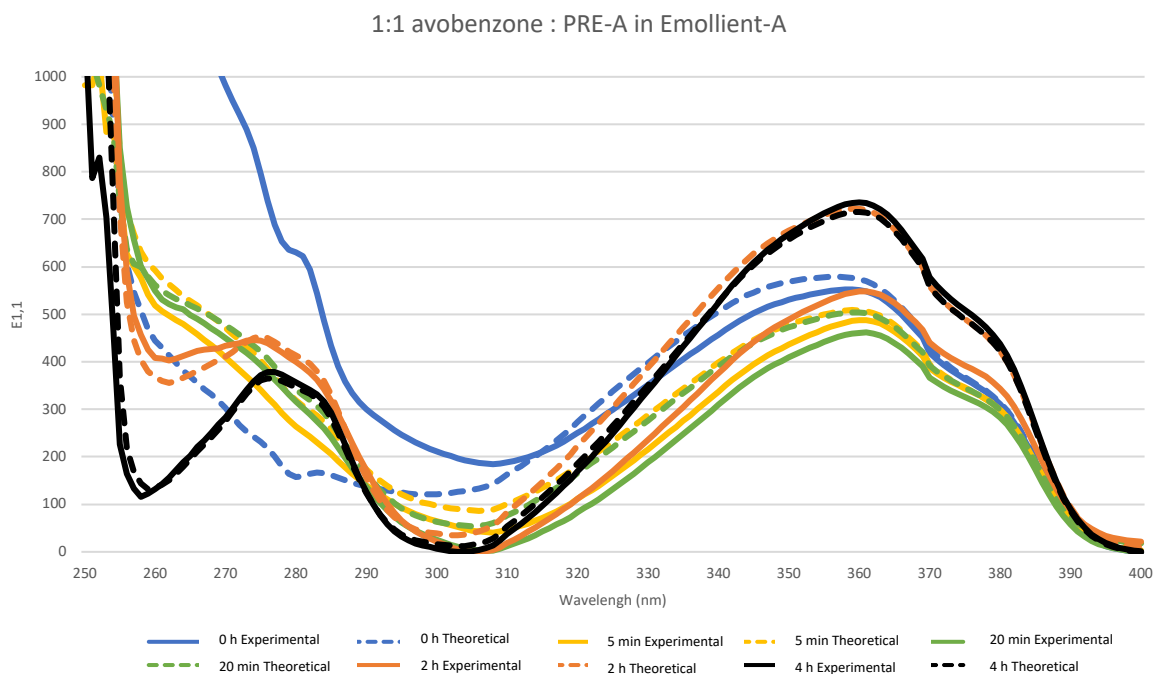


Figure 4-12. E1,1 of a 0,001% solution of a mixture of avobenzone and PRE-A in a 1:1 proportion in Emollient-A. Irradiation was set at 765 W/m² during 0, 5 min, 20 min, 2h and 4 h. Experimental value — , Theoretical value ---.

1:2 avobenzene : PRE-A in Emollient-A

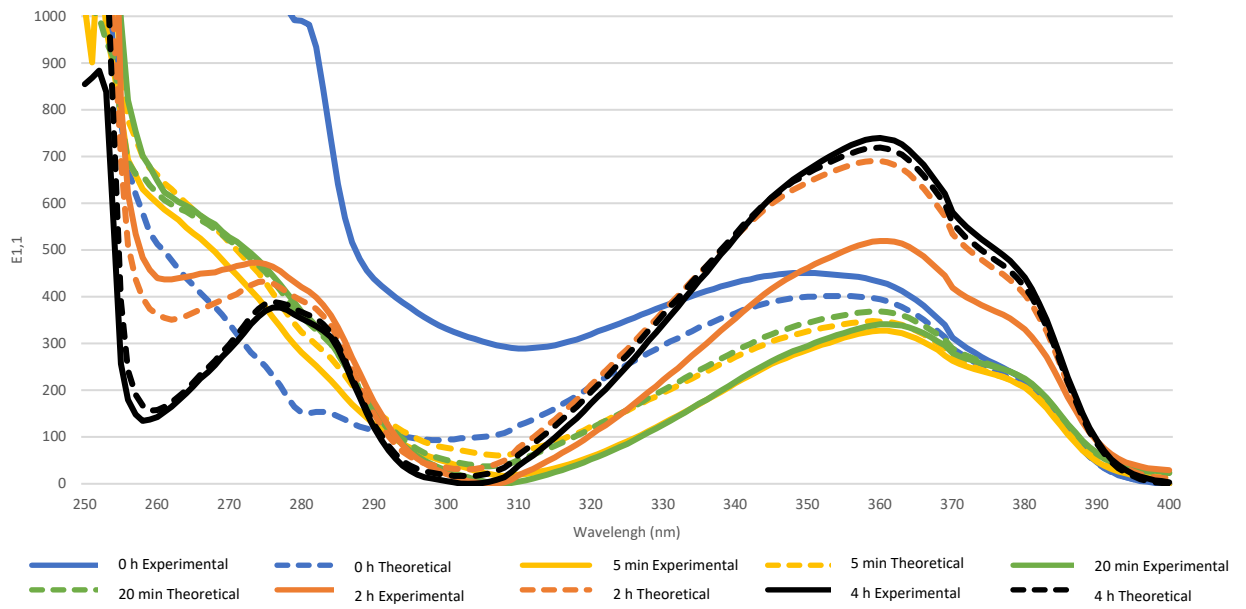


Figure 4-13. E1,1 of a 0,001% solution of a mixture of avobenzene and PRE-A in a 1:2 proportion in Emollient-A. Irradiation was set at 765 W/m² during 0, 5 min, 20 min, 2h and 4 h. Experimental value —, Theoretical value ---.

1:4 avobenzene : PRE-A in Emollient-A

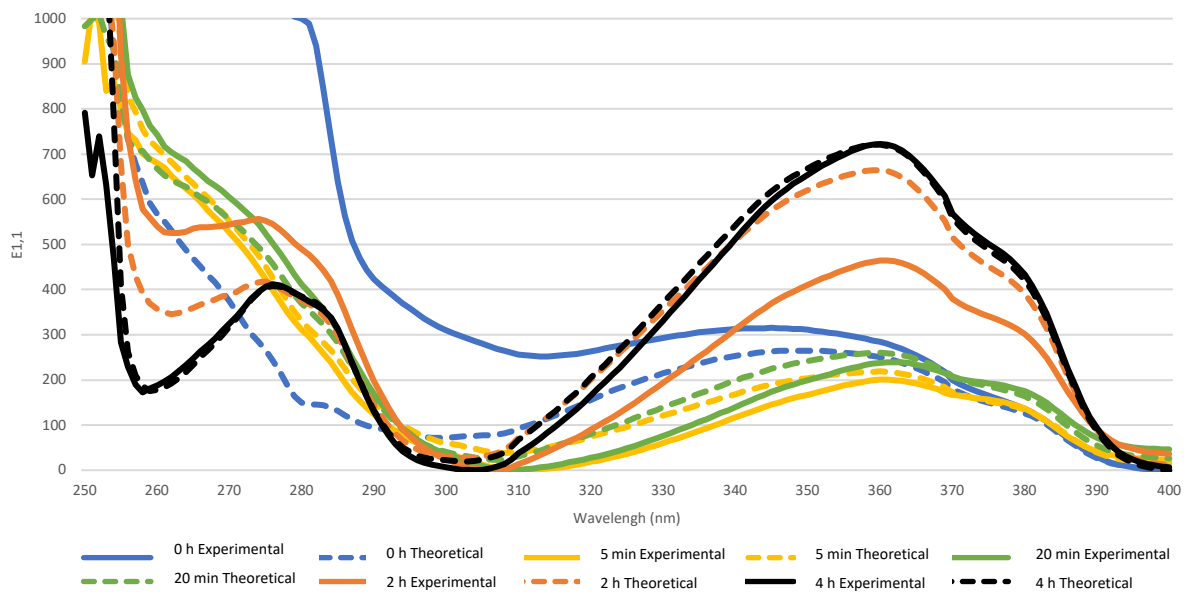


Figure 4-14. E1,1 of a 0,001% solution of a mixture of avobenzene and PRE-A in a 1:4 proportion in Emollient-A. Irradiation was set at 765 W/m² during 0, 5 min, 20 min, 2h and 4 h. Experimental value —, Theoretical value ---.

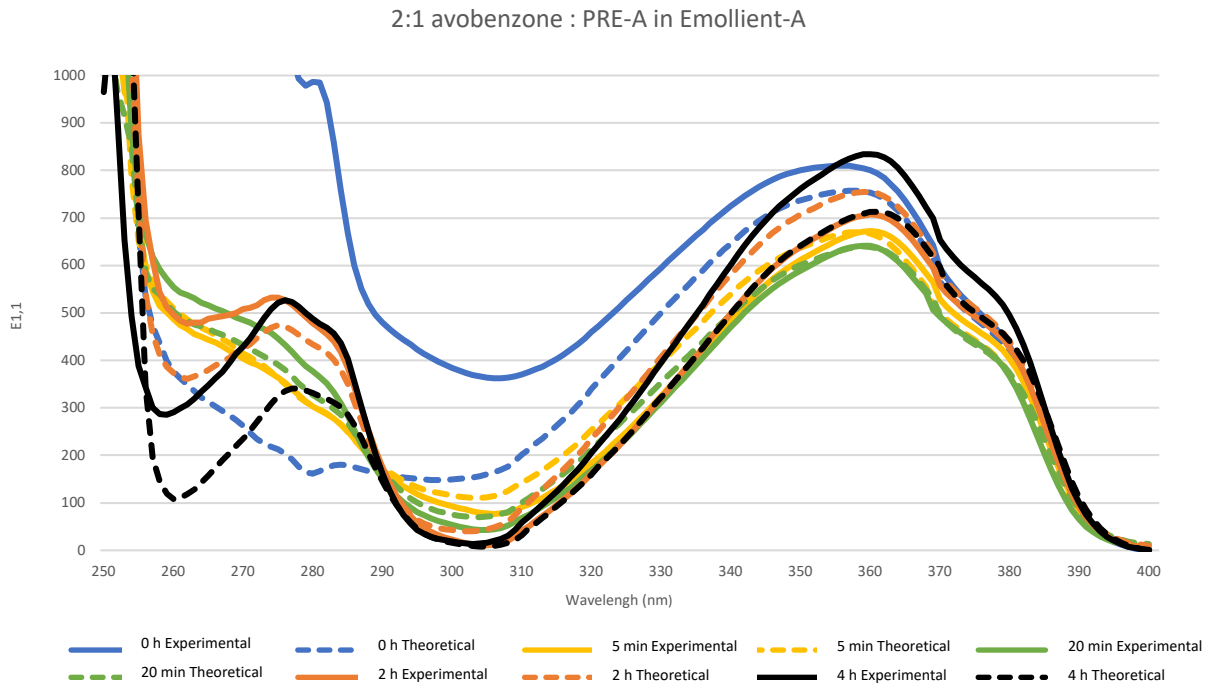


Figure 4-15. E1,1 of a 0,001% solution of a mixture of avobenzone and PRE-A in a 2:1 proportion in Emollient-A. Irradiation was set at 765 W/m² during 0, 5 min, 20 min, 2h and 4 h. Experimental value —, Theoretical value - - -.

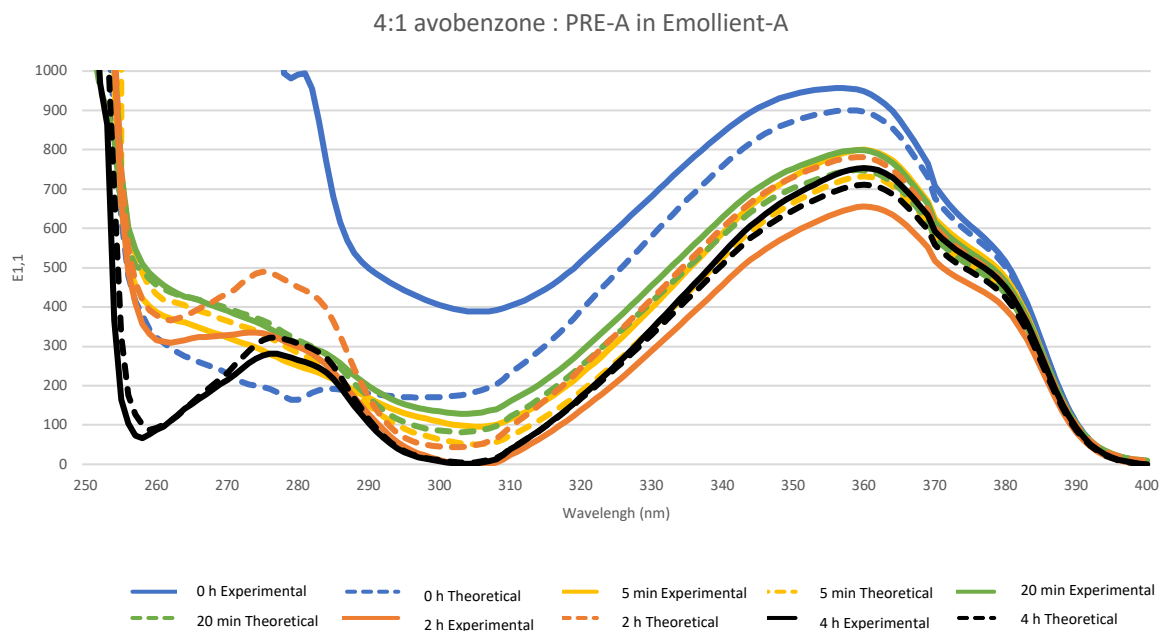


Figure 4-16. E1,1 of a 0,001% solution of a mixture of avobenzone and PRE-A in a 4:1 proportion in Emollient-A. Irradiation was set at 765 W/m² during 0, 5 min, 20 min, 2h and 4 h. Experimental value —, Theoretical value - - -.

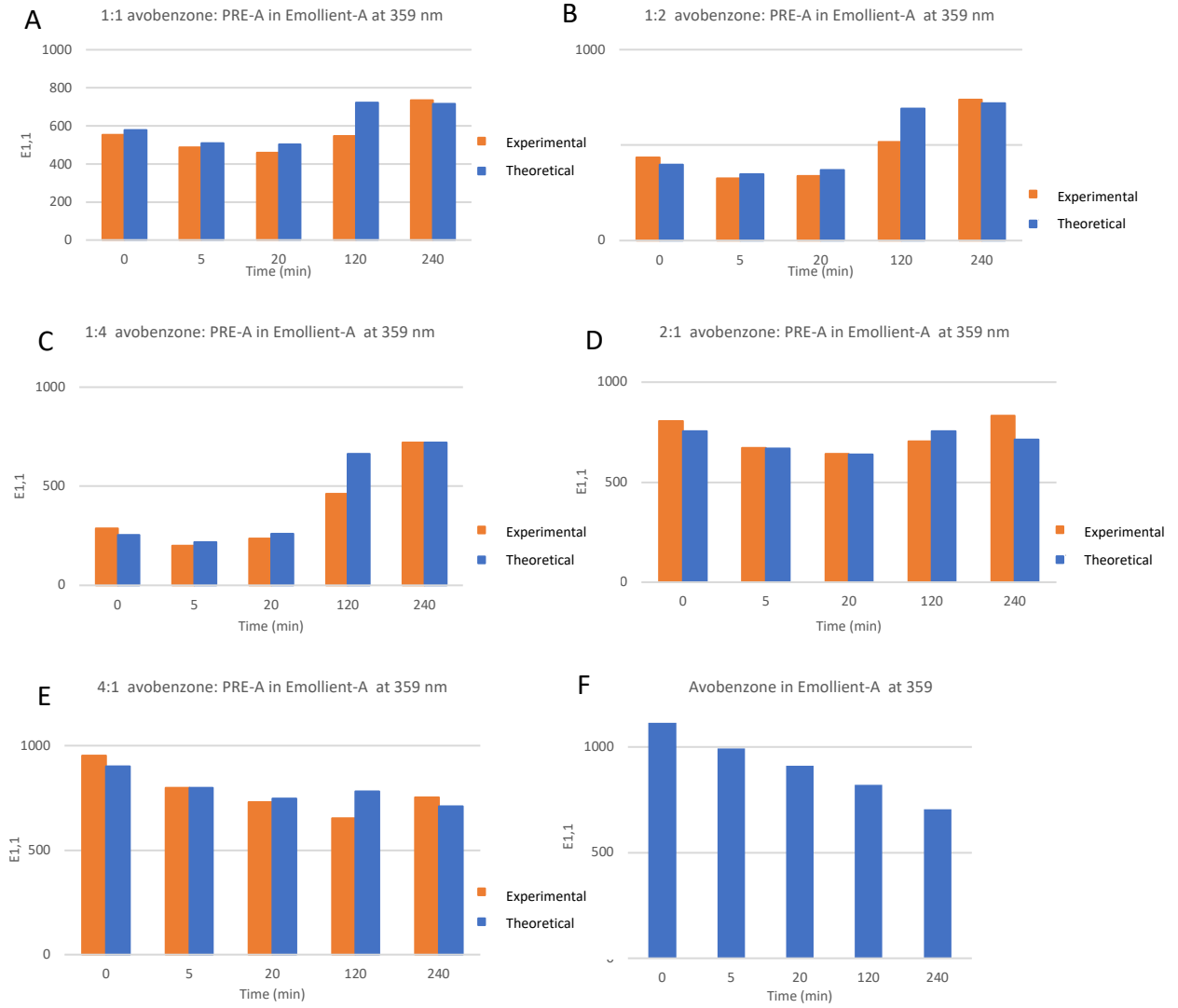


Figure 4-17. $E_{1,1}$ of a 0,001% solution of a mixture of avobenzone and PRE-A at different proportions (A) 1:1 (B) 1:2 (C) 1:4 (D) 2:1 (E) 4:1 in Emollient-A solution. (F) $E_{1,1}$ of avobenzone 0,001% in Emollient-A. Irradiation of the samples at 765 W/m^2 during 0, 5 min, 20 min, 2 h and 4 h. Experimental value in orange vs theoretical value in blue.

4.3.2 Plate method

a PRE-A 5%

PRE-A has a fast activation from 0 to 1 MED. From 1 MED on the activation speed decreases reaching its maximal absorbance at 7,5 MED, which equals to 1,5 h at 765 W/m² irradiation. The differences in the activation are most visible at its maximal wavelength (359 nm), while in the UVB range (especially at 300 nm), only small differences in the absorbance capacity were observed (Figure 4-18).

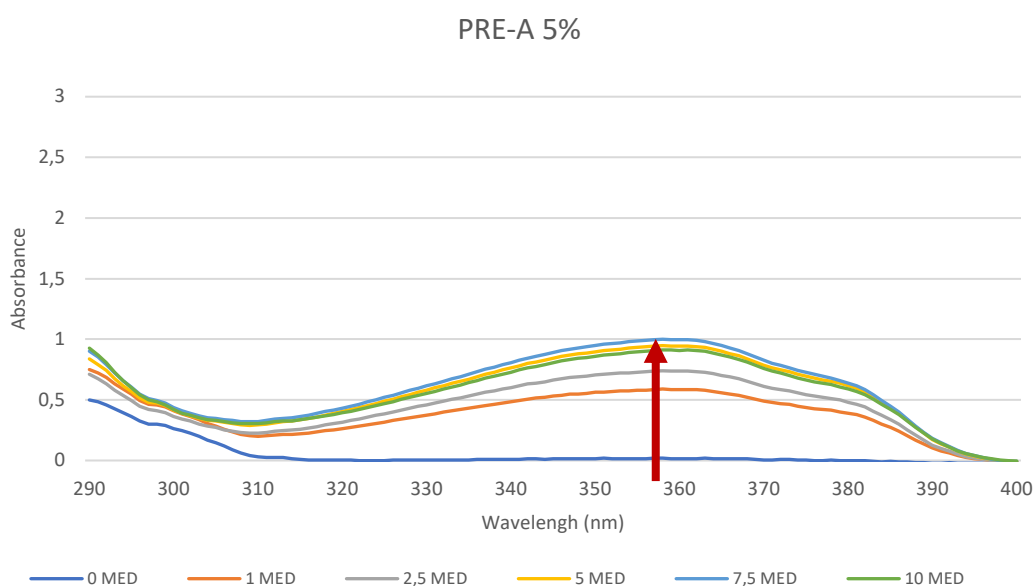


Figure 4-18. UVR absorbance spectra of PRE-A 5% at 0, 1, 2,5, 5, 7,5 and 10 MED in emulsion measured on a PMMA plate.

b Avobenzone 5%

The degradation of avobenzone was assessed photochemically and it is presented in Figure 4-19. Surprisingly, the absorbance of avobenzone 5% in PMMA substrate increased from 0 MED to 2,5 MED. This effect was not observed in the cuvettes, which were dissolved in Emollient-A as well (Figure 4-8 and Figure 4-11). The absorbance at 5 MED was however decreased compared to 0 MED (Absorbance at 5 MED was 2,04 and at 0 MED was 2,18 at 359

nm, Figure 4-19). From 5 MED until 10 MED the absorbance decreased in the UVA range. On the other hand, from 290-300 nm, the absorbance at 5, 7,5 and 10 MED increased.

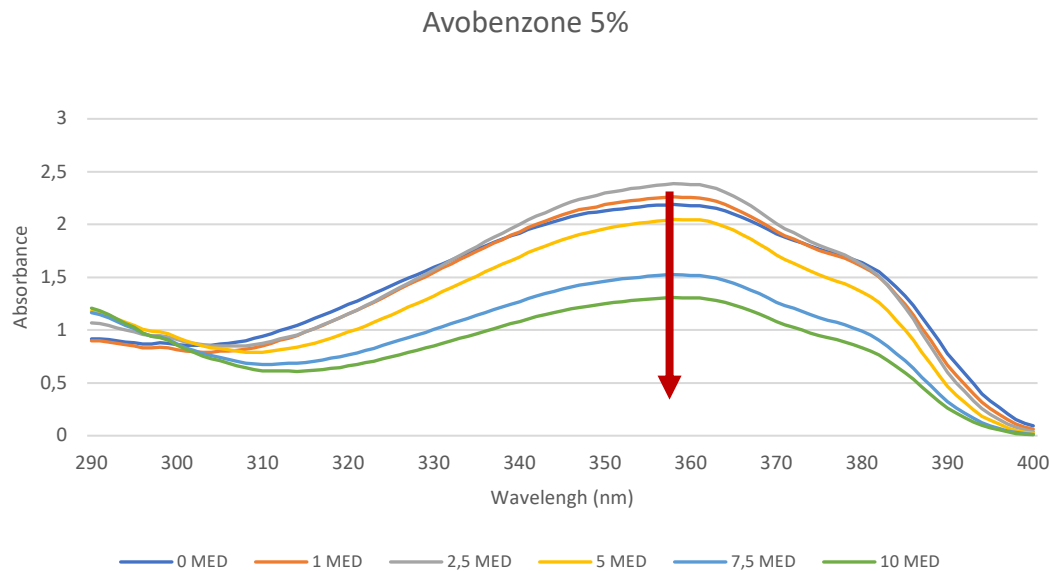


Figure 4-19. UVR absorbance spectra of avobenzone 5% at 0, 1, 2,5, 5, 7,5 and 10 MED in emulsion measured on PMMA plate.

c Avobenzone 5%, PRE-A 2,5% (2:1)

In the mixture of avobenzone 5% and PRE-A 2,5%, the absorbance spectrum at 1 MED was close to the absorbance spectrum at 0 MED (2,27 and 2,28, respectively at 359 nm). At 2,5 MED the mixture of avo:PRE-A reached its maximal absorbance (2,63 at 359 nm) and at 5 MED was still higher than at 0 MED (2,42 at 5 MED at 359 nm). Compared to 5% avobenzone, this mixture of 5% avobenzone and 2,5 % PRE-A seems to contribute to a stabilization of avobenzone. While avobenzone 5% shows a decrease in absorbance somewhere between 2,5 and 5 MED (Figure 4-20), the mixture avobenzone 5% and PRE-A 2,5% shows still at 5 MED an increase in absorbance compared to 0 MED. Otherwise, the absorbance at 290-300 nm generally increases with increasing irradiation (10 MED> 5MED>2,5 MED> 0 MED) (Figure 4-20).

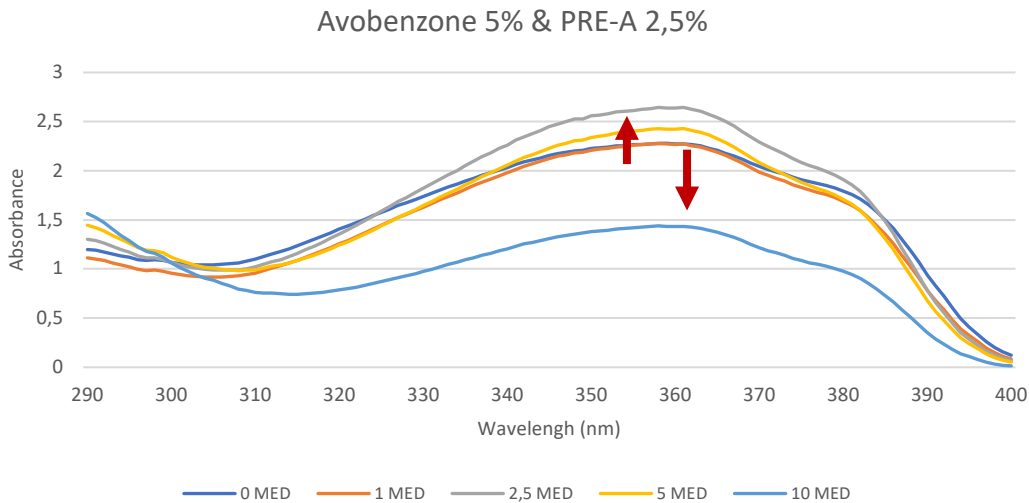


Figure 4-20. UVR absorbance spectra of avobenzon 5% and PRE-A 2,5% at 0, 1, 2,5, 5 and 10 MED in emulsion measured on a PMMA plate.

d Avobenzon 3,3% PRE-A 1,6% (2:1)

In the mixture of avobenzon 3,3% and PRE-A 1,6%, the absorbance spectrum at 1 MED increased a 21% respect to 0 MED (1,85 and 2,25, respectively at 359 nm). At 2,5 MED the mixture of avo:PRE-A reached its maximal absorbance (2,53 at 359 nm) and at 5 MED was still higher than at 0 MED (2,18 at 5 MED at 359 nm). Compared to 5% avobenzon, this mixture of 3,3% avobenzon and 1,6 % PRE-A seems to contribute to a stabilization of avobenzon. While avobenzon 5% shows a decrease in absorbance somewhere between 2,5 and 5 MED (Figure 4-20), the mixture avobenzon 3,3% and PRE-A 1,6% shows still at 5 MED a 17% increase in absorbance compared to 0 MED (Figure 4-21).

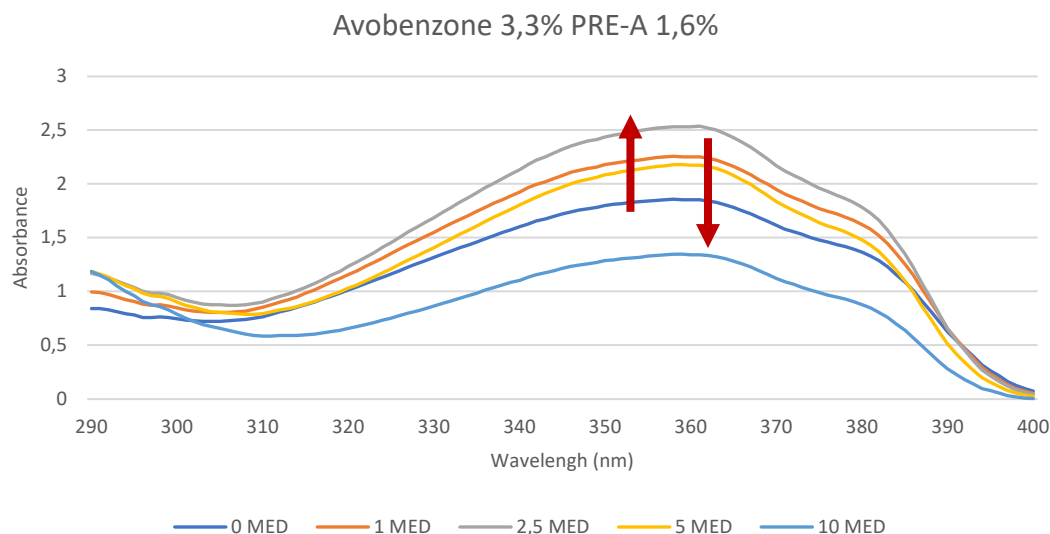


Figure 4-21. UVR absorbance spectra of avobenzone 3,3% and PRE-A 1,6% at 0, 1, 2,5, 5 and 10 MED in emulsion measured on a PMMA plate.

Figure 4-22 shows the activation and degradation of the four emulsions with the different ingredients (avobenzone, PRE-A) and combinations of ingredients at its maximal wavelength, 359 nm at different irradiation doses (0,1, 2,5 5, 7,5 and 10 MED). The results corresponding to 7,5 MED for the two avo: PRE-A mixtures were not measured but predicted from 5 and 10 MED results.

It comes into eye, the great difference in absorbance between PRE-A 5% to the other assessed emulsions. While the 5% PRE-A emulsion shows a maximal absorbance of 1 at 7,5 MED, the other three emulsions show its maximal absorbances (2,38, 2,53 and 2,64) at 2,5 MED. These maximal absorbances correspond to 5% avobenzone, 5% avo & 2,5% PRE-A and 3,3% avo & 1,6% PRE-A, respectively. Therefore, avobenzone's maximal absorbance is more than two times higher the PRE-A's maximal absorbance. This higher absorbances are most probably determined by the absorbance curve of avobenzone, weather alone or in combination with PRE-A.

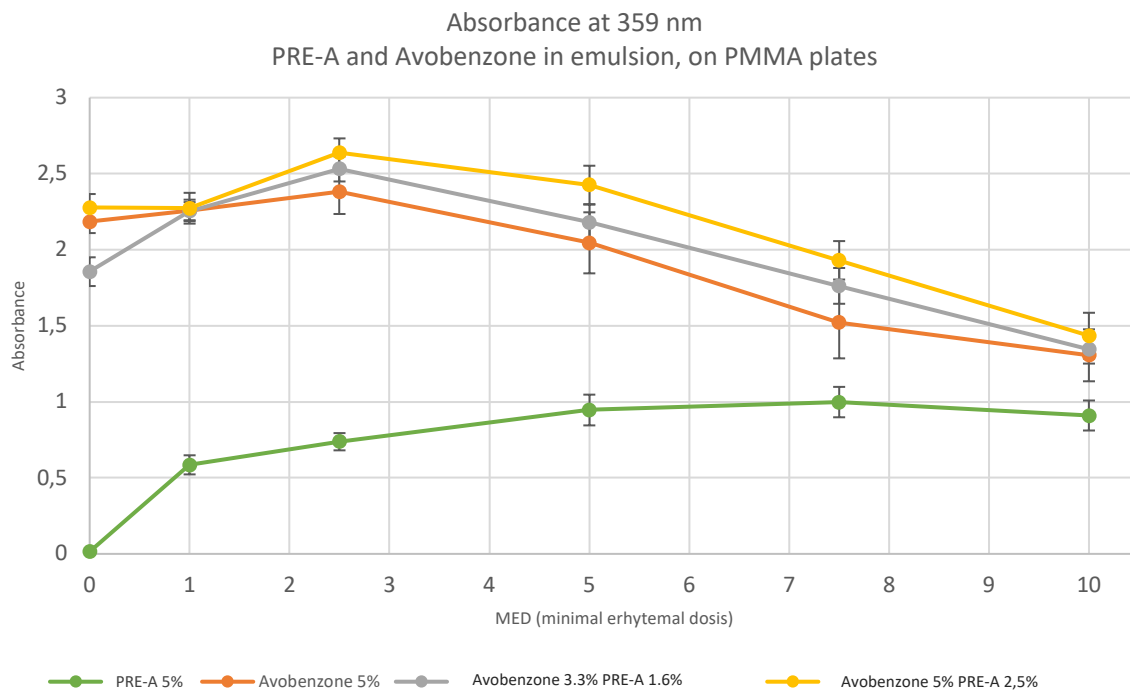


Figure 4-22. Absorbance of emulsions with 1) PRE-A 5%, 2) avobenzone 5%, 3) avobenzone 3,3% and PRE-A 1,6% and 4) avobenzone 5% and PRE-A 2,5% at 0, 1, 2,5, 5, 7,5 and 10 MED.

PRE-A at the same concentration as avobenzone does not reach at any dose (0 MED to 10 MED) the absorbance high of avobenzone. Therefore, although PRE-A shows some irradiation dose dependant activation, this absorbance increase is not high enough to compete with avobenzone's absorbance. At least from 0 to 10 MED irradiation dose at its maximal permitted amount (5% in cosmetics) in this O/W emulsion.

Based on these results (Figure 4-22), the idea to use PRE-A alone in formulation instead of avobenzone was rejected. However, PRE-A could be used as a booster in combination with avobenzone to decrease its inherent degradation.

According to section 4.3.1c, the mixture 2:1 (avobenzone: PRE-A) showed the highest absorbance. Therefore, this combination was also measured in emulsion. The combination 5% avobenzone and 2,5% PRE-A was considered in sunscreen formulation, if PRE-A would be seen a booster (not as UV filter) by the cosmetics regulation. The combination of 3,3% avobenzone and 1,6% PRE-A (5% active substance) was measured in the case the cosmetics regulation would consider PRE-A as avobenzone, because PRE-A is the precursor of avobenzone and

after radiation PRE-A converts to avobenzene. In this case, the regulation would limit the total amount of the mixture to 5% active substance (=avobenzene).

Avobenzene showed in general lower absorbance compared to the mixtures. The mixture of 5% avo 2,5% PRE-A showed the highest absorbance followed by the mixture of 3,3% avo 1,6% PRE-A (Figure 4-22). Increased absorbances compared to 5% PRE-A are listed in Table 4-4.

Table 4-4. Absorbances and percentage increase taking 5% avobenzene as reference.

MED	Avobenzene 5%	%	Avobenzene 5% PRE-A 2,5%	%	Avobenzene 3,3% PRE-A 1,6%	%
0	2,2	100,0	2,3	104,3	1,9	85,0
1	2,3	100,0	2,3	100,6	2,3	99,8
2,5	2,4	100,0	2,6	110,8	2,5	106,3
5	2,0	100,0	2,4	118,6	2,2	106,5
7,5	1,5	100,0	1,9	126,8	1,8	115,8
10	1,3	100,0	1,4	109,9	1,3	103,0

4.3.3 SPF and UVA-PF

The increase in absorbance of the mixtures compared to 5% avobenzone show an increase in the SPF and UVA-PF as well. While at 5% avobenzone an SPF 10, 8,9, 8 and 5 was measured for 0, 1, 2,5, 5 and 10 MED, respectively in general, higher SPF values were obtained for the mixtures 5% avo 2,5% PRE-A: 14, 11, 13, 12, 7 for the same irradiation doses. This is not surprising, as 2,5% PRE-A were added to the 5% avobenzone in formulation. Therefore, higher SPF values were expected. On the other hand, the SPF values of the mixture 3,3% avo 1,6% PRE-A delivered SPF values very similar to 5% avobenzone: 7, 8,10,8, 5. Specially at 0 MED, the SPF was even lower than at 5% avobenzone.

SPF values of 5% PRE-A were very small, in the order of 1 and 2, compared to 5% PRE-A (Figure 4-23).

The results of the UVA-PF had the same tendency as for the SPF values. Moreover, the UVA-PF difference of 5% PRE-A compared to 5% avobenzone was even higher than for the SPF values (Figure 4-24).

All in all PRE-A had less protection capacity than avobenzone. Avobenzone had a 3x to 9x higher SPF compared to PRE-A. Moreover, in the UVA-PF the difference of avobenzone compared to PRE-A was overall higher (63x higher UVA-PF at 0 MED) also although avobenzone's photodegradation (1,8x higher UVA-PF at 10 MED). PRE-A showed a faster conversion to avobenzone in the plate method than in cuvette. However, PRE-A's conversion to avobenzone was less successful than it should to reach the absorbance, SPF and UVA-PF values of avobenzone from 0 to 10 MED.

PRE-A should therefore be used as booster to prevent or reduce avobenzone's photodegradation. The combination avobenzone 3,3% and PRE-A 1,6% showed a similar SPF and a slightly higher UVA-PF at 2,5 and 5 MED. However, this combination was at 0 MED two times lower in the UVA-PF and 1,7 times lower in the SPF compared to 5% avobenzone (Figure 4-23 and Figure 4-24).

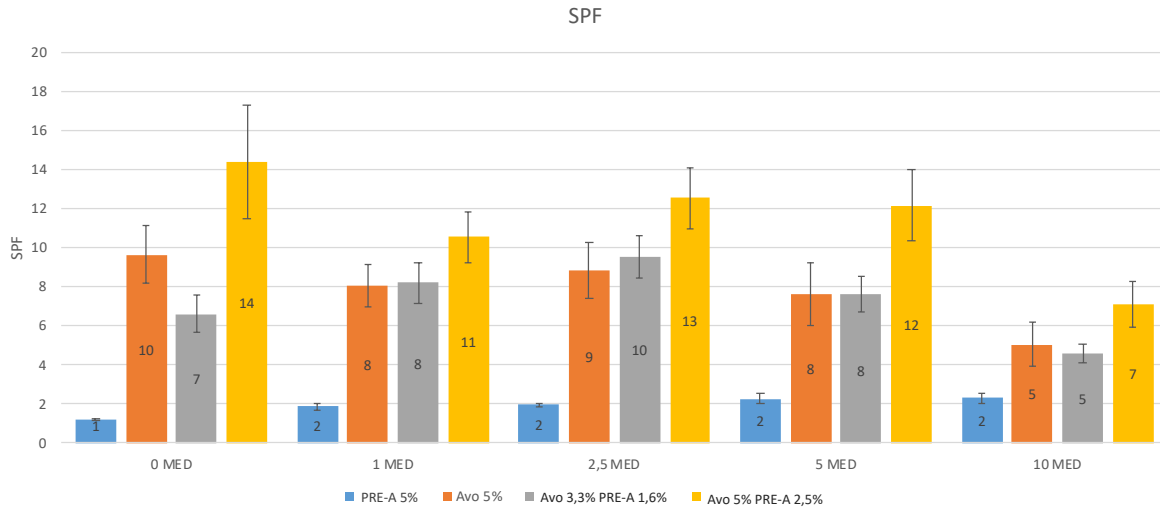


Figure 4-23. SPF values of emulsions with 1) PRE-A 5%, 2) avobenzone 5%, 3) avobenzone 3,3% and PRE-A 1,6% and 4) avobenzone 5% and PRE-A 2,5% at 0, 1, 2,5, 5 and 10 MED.

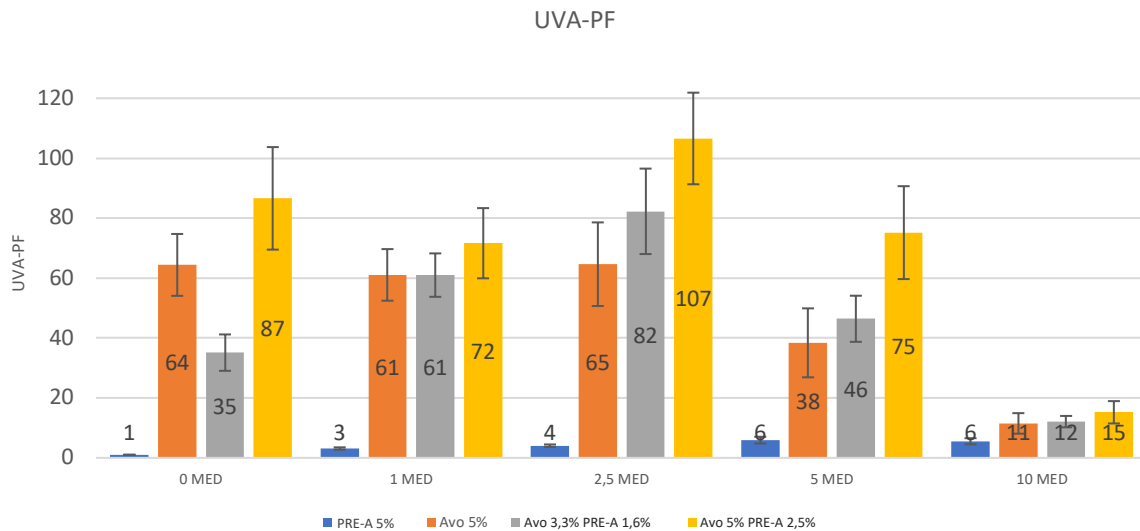


Figure 4-24. UVA-PF values of emulsions with 1) PRE-A 5%, 2) avobenzone 5%, 3) avobenzone 3,3% and PRE-A 1,6% and 4) avobenzone 5% and PRE-A 2,5% at 0, 1, 2,5, 5 and 10 MED.

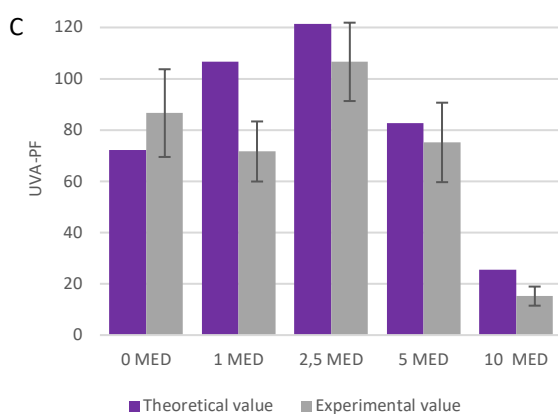
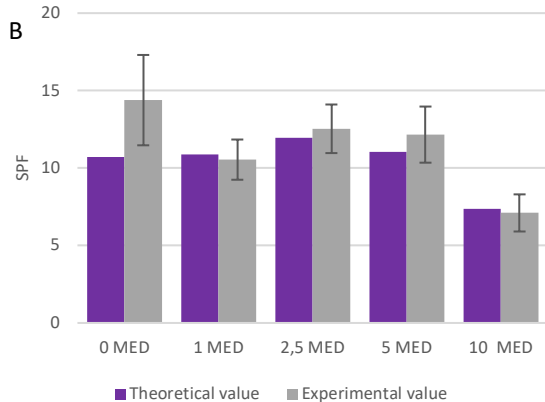
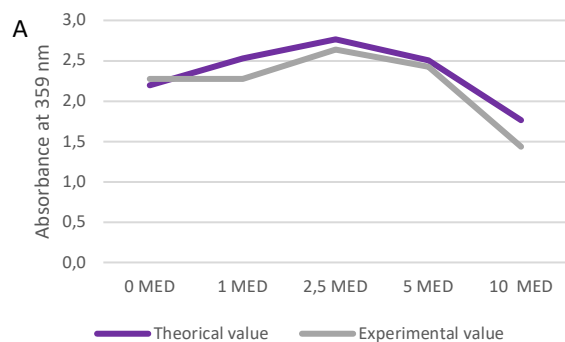
However, what are the implications of 1 MED to 10 MED? 1 MED was defined as the minimal erythral dose to cause sunburn. For a phototype II the minimal erythral dose (MED) is defined at 250 J/m². Therefore, 10 MED means the 10x dose to cause erythema (2500 J/m²). It is however difficult to imagine what the implications of 10 MED are. For sure it will cause sunburn to an individual with phototype II. However, it is difficult to imagine 10 MED as a magnitude of damage if the skin. Instead, the maximal cumulative dose in a day was searched.

In a study (147) the mean sun irradiance of three days, from 8 am to 5 pm, at the beach in Hawaii was 2890 J/m². This corresponds to 11,6 MED. However, the mean exposure of beachgoers in this study were exposed to 4,2 MED for 2-3 h in full sun. According to the high irradiation doses in a beach day in Hawaii, the fixed 10 MED of this study is high enough to simulate the conditions on a beach day and study the absorbance of PRE-A.

4.3.4 Synergic effect screening

The synergic effect of the mixtures was studied. Results of the theoretic (calculated) and experimental values are shown in Figure 4-25.

5% avobenzone & 2,5% PRE-A



3,3% avobenzone & 1,6% PRE-A

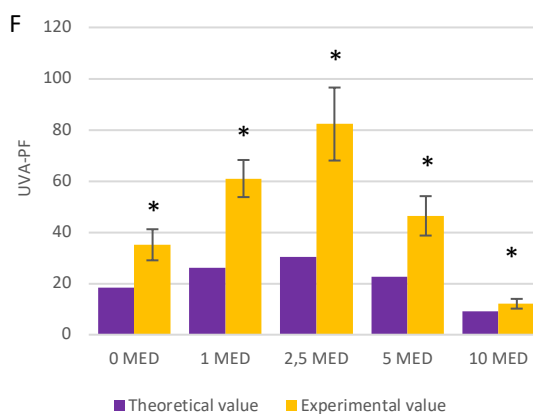
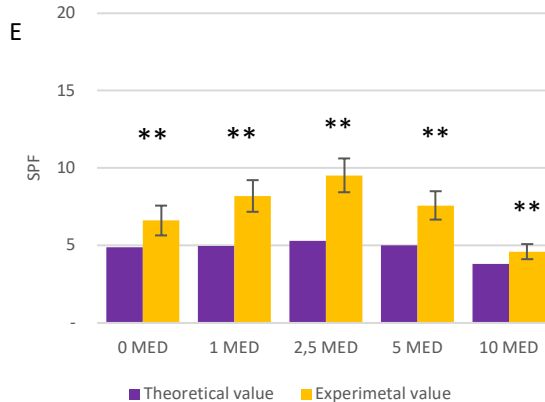
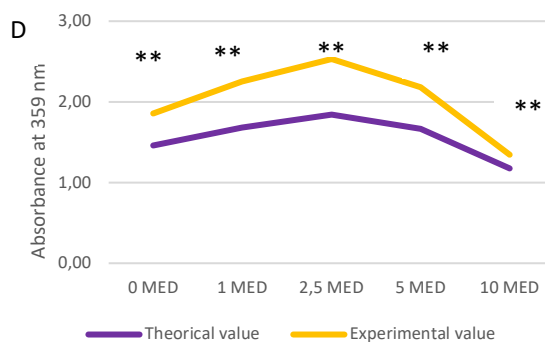


Figure 4-25. Emulsions with 5% avobenzone & 2,5% PRE-A: Theoretical and experimental a) absorbance at 359 nm b) SPF and c) UVA-PF values. Emulsions with 3,3% avobenzone & 1,6% PRE-A: Theoretical and experimental d) absorbance at 359 nm e) SPF and f) UVA-PF values.

A synergic effect is produced when the combination of two substances produces a higher outcome than when the same substances are exposed or administrated individually. In other words, the sum of both substances has a higher effect than expected with normal arithmetic calculation (42). The absorbance of avobenzonone 5% and PRE-A 5% were adjusted to the corresponding percentage in the mixture and were added. These values were named as theoretic values.

The absorbance spectra of the experimental values of 5% avobenzonone and 2,5% PRE-A for 1, 2,5, 5 and 10 MED were slightly decreased compared to the theoretical values and slightly increased for 0 MED. The results of the absorbance spectra were reflected in the SPF and UVA-PF. An overall decrease of the experimental SPF and UVA-PF was observed except for 0 MED. However, experimental values showed no statistical significance ($p= 0,16$, for absorbance, $p=0,18$ for the SPF and $p= 0,25$ for UVA-PF) with theoretic values and therefore no synergistic effect was observed.

On the other hand, in the emulsion with 3,3% avobenzonone and 1,7% PRE-A the experimental absorbance-, SPF- and UVA-PF values were significantly higher than theoretical values ($p=0,0078$ for absorbance, $p=0,0084$ for the SPF and $p=0,035$). For this reason, according to the results, a synergistic effect was observed for 3,3% avobenzonone and 1,7% avobenzonone and PRE-A, respectively.

4.3.5 Comparison of E1,1 with plate and cuvette method

To compare both methods, the irradiation time at which avobenzonone and PRE-A's absorbance was measured, was converted into MED-units. According to the irradiation source of the ATLAS CPS+, 12,7 minutes corresponded to 1 MED. The irradiation dose in MED's were calculated for all the times avobenzonone and PRE-A's were irradiated in solution.

The specific extinction (E1,1) at 359 nm for the different irradiation doses of avobenzonone and PRE-A differed from method to method. In emulsion, using the PMMA plates, avobenzonone experienced an increase from 0 to 2,5 MED. Afterwards the E1,1 decreased and reached a

lower E1,1 at 10 MED compared to the avobenzone's E1,1 in solution (cuvette method). In contrast, avobenzone in solution showed a decrease in absorbance from the beginning (once it was exposed to UV radiation). This would be the expected behaviour of avobenzone. The increase in absorbance at 1 and 2,5 MED in the plate method is most probably due to a change of the structure of the emulsions-film on the PMMA plates (149).

PRE-A in emulsion experienced a fast increase showing its maximal absorbance around 7,5 MED while in solution the conversion of PRE-A to avobenzone was still in process. According to Figure 4-8 at 4 h (18,9 MED) PRE-A's absorbance was higher than at 2 h (9,6 MED), suggesting that the maximum absorbance could be between 2-4 h (9,6-18,9 MED) or 4-10 h (18,9-48 MED) (Figure 4-26).

Therefore, it seems that the form in which the ingredients are exposed to UV radiation (solution or emulsion) influences its absorbance.

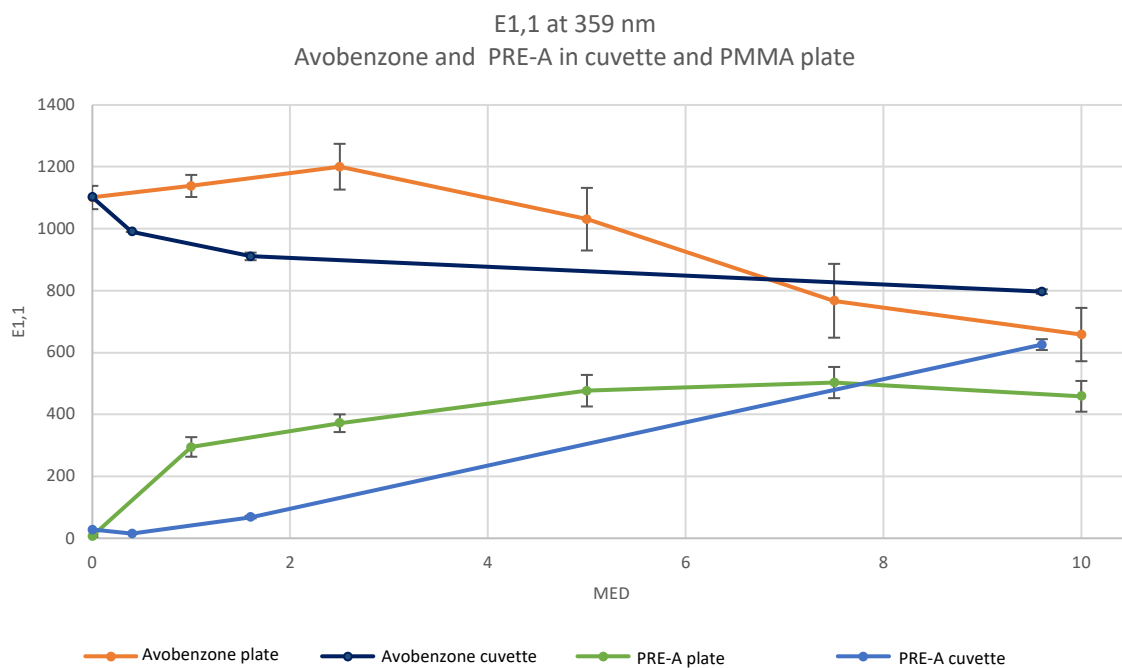


Figure 4-26. E1,1 at 359 nm of avobenzone and PRE-A with the cuvette and PMMA plate method.

4.4 Conclusion

- 4.4.1 PRE-A batch 7 has the highest absorbance compared to the other batches of PRE-A. Therefore, it was chosen for further combination experiments with avobenzone.
- 4.4.2 The proportion of avobenzone and PRE-A with the highest stability until 4 h was the proportion 2:1 avobenzone: PRE-A.
- 4.4.3 A synergistic effect with the combination of avobenzone and PRE-A for the proportions 4:1, 2:1, 1:1, 1:2, 1:4 compared to single measurements of avobenzone and PRE-A could not be proven.
- 4.4.4 PRE-A has a maximal increase at 7,5 MED in emulsion. However, avobenzone showed overall higher absorbances. PRE-A was used in combination with avobenzone as booster ingredient.
- 4.4.5 The absorbance of the plate method showed a faster activation of PRE-A and a faster degradation of avobenzone and PRE-A compared to the cuvette method.
- 4.4.6 It exists a synergistic effect for 3,3% avobenzone and 1,6% PRE-A.

5. BIOADHESIVE SUNSCREEN EMULSION

5.1 Introduction

In view of the high demand of highly efficient, safe and formulation attractiveness of sunscreen products, our aim was to design a sunscreen product to be used together with PRE-A.

The objective was to develop a bioadhesive sunscreen formulation with pleasant organoleptic properties. In the sunscreen formulation development process, the point of departure was a bioadhesive gel which was redesigned to be used as sunscreen product. The optimization of the bioadhesive sunscreen was gradual. A sunscreen formulation with no bioadhesive properties was merged with the bioadhesive gel. First an explorative development based on trial and error was performed. In a second phase, a more formulation development based on the feedback of 20 volunteers assessing the organoleptic properties of the formulations was performed. The optimization of the final product was gradual and small modifications were done to each formulation to improve people's compliance.

The sunscreen formulation had to achieve:

- i. High efficiency of the UV-filters: reaching a SPF 30 with broad spectrum protection and UVA-labeling.
- ii. Maximal quality UV-filters and excipients: ingredients should be safe for humans and oceans, photostable and non-comedogenic; and avoid endocrine disruptors and skin penetration.
- iii. Best user compliance: by focusing on formulation attractiveness and adherence on the skin to minimize loss of the UV-filters from bathing or sweating.

Each formulation was evaluated organoleptically; spreadability, fluidity, pleasant feeling on skin, appearance, non-stickiness and white cast effect were evaluated. Formulations was scored from 1-5 (1 worse quality, 5 better quality) for every organoleptic parameter. The

formulations, which supposed an improvement on its organoleptic properties compared to the previous ones were presented graphically.

The bioadhesive emulsion 6-13 was submitted to different tests; centrifugation at 5000 rpm for 15 min, microscopical evaluation, rheology, viscosity and extensibility. After 12 months storage at room temperature in plastic tube a re-evaluation of the formulation was done. Additionally, its SPF and UVA-PF were measured *in vitro*, its bioadhesive behavior and water resistance potential were tested. The in-use stability of the formulation was tracked by adapting the semi-solid control diagram to an accelerated and longtime stability of the bioadhesive emulsion 6-13 instead of stress conditions. The samples were stored at 5 °C, 25 °C and 40 °C for six months and in this period critical stability parameters (organoleptic properties, viscosity, extensibility, rheology, and pH) were tested for all the conditions.

Finally, a stability test was performed using the control diagram. Samples were stored at 5 °C, 25 °C and 40 °C for six months closed in glass vials.

At the time the bioadhesive emulsion 6-13 was developed there was not enough PRE-A necessary to be added in the formulation. Therefore, the bioadhesive emulsion 6-13 was designed in view of a future addition of PRE-A.

5.2 Materials and Methods

5.2.1 Chemicals

The chemicals used are given in Table 5-1 with the corresponding trade name, supplier, international nomenclature of cosmetic ingredients (INCI) name. The ingredients used from BASF, Croda, Gatefossé, SEPPIC, Schülke Inc., Merck and Nouryon were a kind gift of these suppliers. The other ingredients were purchased.

Table 5-1. List of ingredients used in the formulation. For each main classification, trade name, supplier and INCI name is given.

Main classification	Trade name	Supplier	INCI ¹ name
Emulsifiers	Span™ 60	Croda	Sorbitan oleate
	Tween™ 20	Croda	Polysorbate 20
	Emulsifier-A	Company Q	Emulsifier-A
Emollient	Emollient-B	BASF	Emollient-B
	Caprylic/Capric Triglyceride	BASF	Caprylic/Capric Triglyceride
	Mygliol 812	BASF	Caprylic/capric Triglyceride
	Emollient-C	Company Q	Emollient-C
	Solvent-G	Fagron	Solvent-G
	Glycerin	Fagron	Glycerin
	Goma xantana/ Rheocare XGN	Fagron/ BASF	Xanthan gum
Preservative	Euxyl® PE9010	Schülke Inc	Penoxyethanol & Ethylhexylglycerin
UVA-Filter	Uvinul® A Plus	BASF	Diethylamino Hydroxybenzoyl Hexyl Benzoate (DHHB)
UVA & UVB-Filter	Tinosorb® S	BASF	Bis-Ethylhexyloxyphenol Methoxyphenyl Triazine (BEMT)
	Tinosorb® S Lite Aqua	BASF	Bis-Ethylhexyloxyphenol Methoxyphenyl Triazine (and) Acrylates/C12-22 Alkyl Methacrylate Copolymer (BEMT aqua)
	Tinosorb® M	BASF	Methylene Bis-Benzotriazolyl Tetramethylbutylphenol (and) Aqua (and) Decyl Glucoside (and) Propylene Glycol (and) Xanthan Gum (MBBT)
	Tinosorb® 2AB	BASF	Tris-Biphenyl Triazine (and) Aqua (and) Decyl Glucoside (and) Butylene Glycol (and) Disodium Phosphate (and) Xanthan Gum (TBPT)
UVB-Filter	Uvinul® T150	BASF	Ethylhexyl Triazone (EHT)
Adhesive agent booster	BA-booster-1	Company H	BA-BOOSTER-1
Basic buffer	BASE-1	Termo Fisher Scientific	BASE-1
Adhesive agent	BA1	Company E	BA1
Film former/ Thickener/ water resistance	Eudragit® L 100	Evonik	Polymethacrylates

¹ International nomenclature of cosmetic ingredients

5.2.2 Equipment

The equipment used is listed in Table 5-2.

Table 5-2. Equipment used, type of equipment, model and supplier

Type	Model	Supplier
Semi analytic balance	Mettler PB3000	Mettler Toledo (Switzerland)
Semi analytic balance	Mettler PJ360 Delta Range	Mettler Toledo (Switzerland)
Magnetic stirrer and heater	Ikamag RCT	IKA (United Kingdom)
Magnetic stirrer and heater	Heidolph MR2002	Heidolph (Germany)
Stirrer	Heidolph CG5	Heidolph (Germany)
Stirrer	Hei-Torque Core C665	Heidolph (Germany)
Turrax	Silverson L4RSA4	Silverson (United Kingdom)
Rheometer	Haake RheoStress 1	Haake (Germany)
Optical microscope	Leica DM 1000LED	Leica (Germany)
Strain gauge	SUÑÉ ARBUSSÀ/ DEL POZO OJEDA	University of Barcelona (Spain)
SPF & UPF Tester	Labsphere 2000S	Labsphere (EEUU)
Solar simulator	ATLAS CPS+ equipped with water cooling plate	Ametek (EEUU)
Thermostat	ECO Silver	Lauda (Germany)
Thermometer datalogger	K 202 Datalogger	Voltcraft (Germany)
Suntest Lamp Filter	Solar Standard COLIPA Ident-Nr. : 5607 7759	Ametek (EEUU)

5.2.3 Determination of the UV-filters combinations to reach an SPF 30 with the minimal amount of UV-Filters

The SPF of the UV-filter combinations was assessed with a free available computational tool (150) whose algorithm is given in Equation 5-1.

$$SPF = \frac{\sum_{290}^{400} s_{er}(\lambda) \cdot S_s(\lambda)}{\sum_{290}^{400} s_{er}(\lambda) \cdot S_s(\lambda) \cdot T(\lambda)} \quad \text{Equation 5-1}$$

where $S_s(\lambda)$ stands for the intensity of the light source, $s_{er}(\lambda)$ is the erythral action spectrum and $T(\lambda)$ stands for the transmittance of one UV-filter at a specific wavelength. $S_s(\lambda)$ and $s_{er}(\lambda)$ values are given in literature (48). Nevertheless $T(\lambda)$ must be measured. The transmittance $T(\lambda)$ can be also calculated with Equation 5-2 from the absorbance ($E(\lambda)$) of the UV-filter at a specific wavelength.

$$T(\lambda) = 10^{-E(\lambda)} \quad \text{Equation 5-2}$$

The filter efficiency (FE) is a value to measure the efficacy of the combination of UV-filters in respect to the used amount (in %) and its resulting SPF. In other words, it shows how much the UV-filters are contributing to reach a specific SPF value. The higher this value, the less UV-filter amount is necessary to reach a particular SPF value.

The filter efficiency was obtained from a computational tool (150)(151) designed to simulate the *in vivo* SPF by adjusting *in vitro* measurements of the UV-filters (151)(152).

$$UVA - PF = \frac{\sum_{320}^{400} S_{PPD}(\lambda) \cdot S_{UVA}(\lambda)}{\sum_{320}^{400} S_{PPD}(\lambda) \cdot S_{UVA}(\lambda) \cdot T(\lambda)} \quad \text{Equation 5-3}$$

The UVA-PF (Equation 5-3) is like the SPF equation with slight modifications. Instead of 290-400 nm, the UVA-PF was calculated alongside the UVA spectra (320-400 nm). Further, S_{PPD} corresponds to the permanent pigment darkening and $S_{UVA}(\lambda)$ is the spectral irradiation received from a radiation UVA light source.

To label the sunscreen products with UVA protection, the proportion of UVA-PF towards SPF must be 1/3 (0,33), at least. When this proportion was achieved, it was marked with a PASS.

5.2.4 Literature research: UV-filters and other ingredients with minimal toxicity, irritancy and comedogenicity

The comedogenicity and irritancy of the ingredients used was assessed alongside the existing literature, particularly, by a report on cosmetic ingredients (153). Only those ingredients classed as non-comedogenic (graded 0-1) by this report were selected. Toxicity of the ingredients were reviewed with the reports of:

- Scientific Committee on Consumer Safety- European Commission (154);
- The Cosmetic Ingredient Review (155);
- Safety Assessment of the supplier of each ingredient;
- Breast cancer prevention partners- Campaign for safe cosmetics (156)

5.2.5 Formulation type finding

The bioadhesive gel developed by the SDM was the starting point for the initial formulation whose ingredients are listed in Table 5-3.

Table 5-3. Ingredients of bioadhesive gel. Internal reference: PLC-19-001-3-1.

Ingredients	Amount (%)
BA1	3
BA-BOOSTER-1	6
Menthol crystal	0,1
BASE-1	3
Glycerin	2
Solvent-G	30
Deionized water	55,9
TOTAL	100

As the original formulation was a gel, it was intended to develop a gel as well including PRE-A and other UV-filters to reach the desired SPF. However, a gel is made of hydrophilic components and therefore, when making a hydrophilic formulation the formulation expert must know the solubility of the UV-filter in polar as well as in apolar solvents. Because of the poor solubility of PRE-A in water (see section 3.4), it was not difficult to state that PRE-A is lipophilic as well as avobenzone, whose poor solubility equals to 2,3 mg/L (157).

PRE-A is even more lipophilic than avobenzone (0,02 mg/L) (see section 3.4). The first idea was to develop a formulation made from only one phase, alongside with the original formulation (Table 5-3).

However, the use of a lipophilic phase in the formulation was necessary due to the low solubility of PRE-A in water (see section 3.4). Therefore, two phases were chosen.

5.2.6 Evaluation of organoleptic properties of the formulations

A sensory test was carried out. This test sought to develop a formulation using feedback on sensory performance. Sensory performance plays an important role in determining a product's shelf-life and its acceptance by the consumer. It is also essential for the selection of

ingredients and optimization of formulations. Finally, good sensorial performance influences the choice of the cosmetic by the consumer (158)

The tests were carried out following a similar procedure as in ISO 11136:2014 guidelines. Twenty volunteers were asked to report on the same product according to their preferences, using different organoleptic parameters. No information on the ingredients composition of the product was provided (159–161). The selection of participants was made by age, skin phototype and sex. Candidates were aged 25-65, with half aged 25-35; 55% of participants were men; 45% were women; and all were phototype II-III.

Participants evaluated two/four emulsions per session depending on the needs of the test: gel 1 and gel 2: two; type of formulation, e.g., O/W, W/O: four; optimization of the O/W emulsion: two emulsions simultaneously. Each session was carried out on a different day. Particularly, participants were asked to evaluate the organoleptic properties of each emulsion by ranking them from 1-5 (1 for the worst to 5 for the best). These properties were:

- Spreadability;
- Fluidity (very fluid, sprayable =1; medium fluidity =3; high viscosity=5);
Pleasant feeling on skin;
- Appearance (refers to homogeneity and color of the formulation, were transparent and white tones were preferred over yellow ones);
- Non-stickiness;
- White cast effect.

Participants signed a written consent form to participate in the test. In view of the harmless characteristics of the emulsions, the ethical aspect of the test was guaranteed. Moreover, in cosmetics, the approval of an ethics committee is not required to carry out sensory performance studies.

Before starting the experiment, participants agreed that a very fluid consistency would be given a rate of 1, a medium consistency a rate of 3 and a greater consistency of the emulsion

a rate of 5. It was also agreed that a medium consistency would be perceived as better for a high protection sunscreen.

A “pair test” was carried out (where two products were compared). Clear guidelines were given for its execution. Participants were first asked to wash and dry their hands and subsequently apply a hydro-alcoholic solution (waiting for a minute for it to evaporate). They subsequently applied a sample of 0,3 mg of the emulsion to the back of one hand and were asked to distribute it evenly over ten seconds with the palm of their index finger. During this period, they were asked to evaluate the spreadability and the consistency of the emulsion. The non-greasy texture of the emulsion was then evaluated. Evaluation of the white cast effect followed a minute later, and the latter was followed by the evaluation of the non-stickiness texture (one and a half minutes later). After two minutes participants were then asked to wash their hands to evaluate the appearance of the emulsion. The same procedure was carried out on the back of the other hand to evaluate the second product in this “pair test”.

First, the gels were evaluated for their organoleptic properties 1-5. The ingredients of the gel with the highest score were used in the subsequent formulations. The same proceeding was used for assessing the emulsion type (A, B) and base (O/W, W/O). The formulation with the highest average score was selected and continued to be optimized. Participant’s feedback informed some gradual changes in terms of the formulation process and ingredients. A sensory evaluation was carried out after each new formulation. Before starting the test, participants were reminded of their previous emulsion score.

The volunteer’s feedback informed subsequent decisions made to improve the organoleptic properties of the formulation.

5.2.7 pH

The pH was determined using a calibrated pH meter (CRISON MICROPH 2002). An amount of 3 g of emulsion was diluted in 30 mL of distilled water in a beaker. The pH value should be between 5,5 and 6,5.

5.2.8 Microscopy

For the sample preparation approximately 5 mg of sample emulsion were deposited in microscope slides (75 by 25 mm) and a cover slip was carefully placed at the bottom of the sample. The samples were examined under a light microscope (Leica DM 1000 LED, Wetzlar, Germany) with an objective of 40x magnification. The images were captured with a camera Leica EC3 (Leica Microsystems, Wetzlar, Germany).

5.2.9 Rheology and viscosity

Rheological measurements were performed using a Haake Rheostress 1 rheometer (Thermo Fisher Scientific, Karlsruhe, Germany) (Figure 5-1A). Two measurements were performed for the characterization of the rheological behavior and viscosity of the bioadhesive emulsion, 24 h after formulation preparation. The emulsion was placed at a fixed lower plate and was tempered at $25 \pm 0,2$ °C with a thermostatic circulator Thermo Haake Phoenix II + Haake C25P (Thermo Fischer Scientific, Waltham, MA, USA) which was connected to the rheometer. Only after achieving the temperature of 25 ± 0.2 °C the experiment was run and the mobile upper cone Haake C60/2° Ti (60 mm diameter, 2° angle) was attached (Figure 5-1B). Between the cone and the plate there was a 0,105 mm gap, which was filled by the emulsion. The rheometer was connected to a computer with the Haake Rheowin® Job Manager v. 4 software (Thermo Electron Corporation, Karlsruhe, Germany) for test execution and Haake Rheowin® Data Manager v. 4 software (Thermo Electron Corporation, Karlsruhe, Germany) for evaluation of the recorded data. This data consisted on the viscosity ($\eta = f(\dot{\gamma})$) as function of shear stress (γ) the and flow curves ($\tau = f(\dot{\gamma})$) which were obtained after a ramp-up period from 0 to 50 s^{-1} for 3 min; constant shear rate period of 50 s^{-1} for 1 min; and a ramp-down period from 50 to 0 s^{-1} for 3 min. The data from the flow curves were fitted to different mathematical models' equations: Newton, Bingham, Ostwald-de-Waele, Herschel-Bulkley, Casson and Cross. Best fit of mathematical models was based on the correlation coefficient value (r). The viscosity mean value (Pa·s) was determined from the constant share section at 50 s^{-1} . Two measurements were conducted and the measurement with best fit for r was determinant for the rheological behavior.

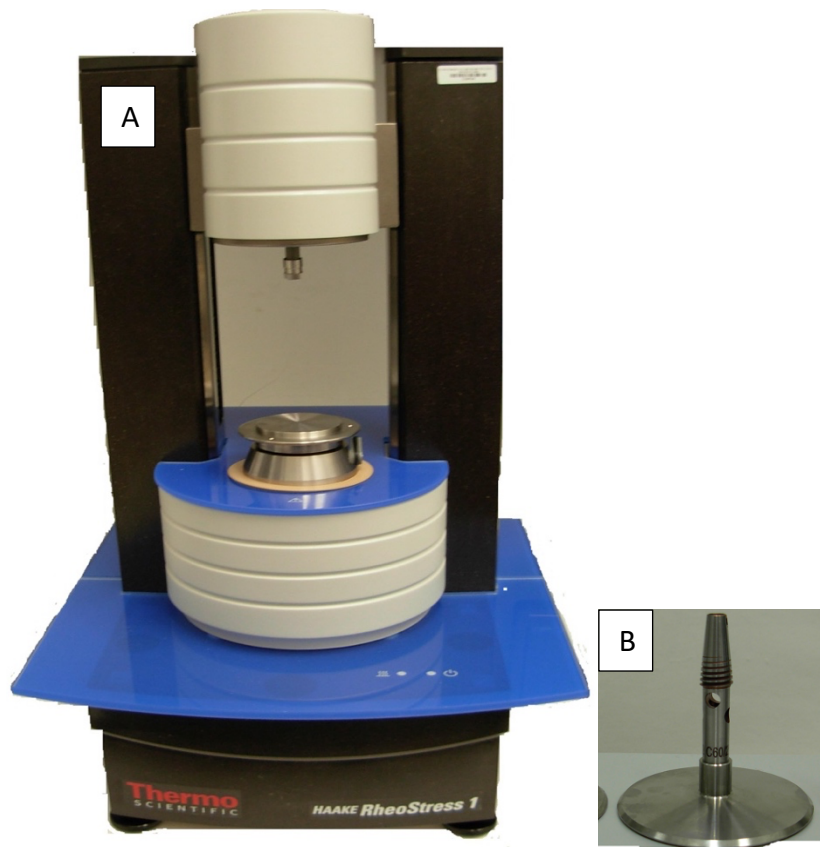


Figure 5-1. A) Haake Rheostress 1 rheometer (Thermo Fisher Scientific, Karlsruhe, Germany). B) Upper cone Haake C60/2° Ti.

5.2.10 Extensibility

The used extensometer is an equipment designed by Dr. Alfonso del Pozo Ojeda and Dr. Josep Maria Suñé Arbussà (162,163). The cylinder has two positions. The first position has a volume of approximately 1 cm³ (Figure 5-2A) and the second position is flat, without volume. From the first position by rotating the extensometer to an angle of 90°, the second position appears. From the first position the necessary amount of emulsion to cover the surface of the cylinder of the extensometer was placed. Any excess of emulsion is cleaned with a spatula to make the base of the extensometer even. The hard plastic coverage is placed above and on top goes a weight of 100 g (Figure 5-2B). Then the extensometer rotates to the second position and the cream does up and spreads to the base of the extensometer. After one minute the weight

is taken away and the diameter is measured with a vernier calliper. The area of the circle is calculated using Equation 5-4. The measurements were performed in triplicate.

$$S(\text{mm}^2) = \pi \cdot \left(\frac{d(\text{mm})}{2}\right)^2 \quad \text{Equation 5-4}$$



Figure 5-2. Extensometer designed by Dr. Alfonso del Pozo Ojeda and Dr. Josep Maria Suñé Arbussà. A) first position: cylinder has approximately 1 cm capacity volume. B) Second position: cylinder with no volume (even to the base) with the plastic coverage and 100 g weight.

5.2.11 Bioadhesion

The bioadhesive method is an original method specifically developed and set-up for this assay, reason of the annexed publication. The bioadhesive force between the pig ear skin and the bioadhesive cream UV-19-001-06-13 was assessed using MT-LQ Materials Test Texture analyzer (SET19002, Stable Micro Systems, Surrey, England) and analysis was performed with the software materials master. The texture analyzer was provided by the *Consejo Superior de Investigaciones Científicas* (CSIC).

Frozen ears were obtained from 40 Kg weight pigs from a laboratory animal facility (Estabulari de la UB, Campus Universitari de Bellvitge). The ears were cleaned with water (25 ± 0.5 °C),

and the skin (epidermis and dermis) was separated from the cartilage of the pig ear with a scalpel and stored in the freezer at $-20\text{ }^{\circ}\text{C}$ for two weeks.

The skins were defrosted 24 h before the start of the study. They were cut into square pieces ($3 \times 3\text{ cm}$) and placed on Petri dishes. These skin portions were the substrates for the sample vehicles. A total of 80 mg of the emulsion was spread homogeneously on the substrate skin sheets. In addition, another skin sheet was attached to the lower end of a cylindrical probe (1 cm in diameter) facing downward, opposite the substrate skin with a rubber ring (attached skin) as shown in Figure 5-3. The test was performed lowering the probe at a constant speed ($0,1\text{ mm/s}$) until the skin and sample made contact. The skin and the sample were kept in contact for 60 s at a force of 0,5 N. After 60 s, the skin was drawn upwards (0.1 mm/s) until the contact between the surfaces was broken. The peak force, which is the force needed to separate the two skin sheets, was calculated. The more force needed, the stronger bioadhesion of the sample measured. At least three replicates were analyzed per sample at $25 \pm 0.5\text{ }^{\circ}\text{C}$.

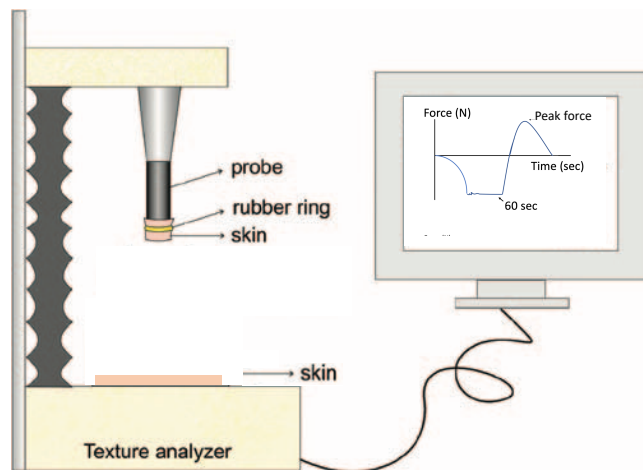


Figure 5-3. Schematic picture of the skin adapted to the texture analyzer probe and a typical force vs. time curve obtained from the detachment measurements of the bioadhesive test. Adaptation of (105).

5.2.12 Active's product content and UVA *in vitro* determination

The bioadhesive emulsion 6-13 was spread on the plates, accordingly to ISO 24443: 2012: *Determination of sunscreen UVA protection in vitro* (164) in which $32,5 \pm 0,5\text{ mg}$ were spread on a $5 \times 5\text{ cm}^2$ PMMA plate HD6 ($6\text{ }\mu\text{m}$ rugosity). This roughness simulates skin surface, and

the emulsion application equals (1,3 mg/cm²). Droplets of similar size were spread on the plate with a fingertip in two phases. First the distribution over the plate consisted of touching the surface of the plate to distribute the material. Afterwards, a small circular spreading technique was employed (30 sec), and finally the emulsion was spread horizontally and vertically until it was visibly uniformly distributed (20-30 seconds) with a slight increment of the pressure on the PMMA plate. The sample was dried during 30 minutes in a dark place. The PMMA plate with 15 mg Glycerin spread on the plate as a thin film was used as blank.

To minimize the error between measurements, previous training was required. A standard emulsion given by the ISO 24443:2012 was formulated. The measured *in vitro* SPF and UVA-PF were compared to these given by the ISO. The obtained *in vitro* UVA-PF should be within the limits of acceptance.

In vitro SPF calculation

The absorbance spectrum of the emulsion on the PMMA plate was measured with the spectrophotometer Labsphere 200S and the SPF was calculated with Equation 5-5.

$$SPF \text{ in vitro} = \frac{\int_{290 \text{ nm}}^{400 \text{ nm}} E(\lambda) * I(\lambda) * d\lambda}{\int_{290 \text{ nm}}^{400 \text{ nm}} E(\lambda) * I(\lambda) * 10^{-A_0(\lambda)} * d\lambda} \quad \text{Equation 5-5}$$

where,

$E(\lambda)$ is the erythemal spectrum (data in ISO 24443:2012)

$I(\lambda)$ is the received spectral irradiance of the UV source (RSS for SPF calculation)

$A_0(\lambda)$ is the averaged film product monochromatic absorbance of the assay before UV exposure

$d\lambda$ is the wavelength interval

The calculated *in vitro* SPF was then adjusted to fit the *in vivo* SPF. The *in vivo* SPF was taken from an *in-silico* tool (151). The adjusted *in vitro* SPF was made by multiplying the initial absorbance curve by the adjustment coefficient, "C" value.

Therefore, the adjusted *in vitro* SPF was calculated by Equation 5-6.

$$SPF \text{ in vitro, adj} = \frac{\int_{290 \text{ nm}}^{400 \text{ nm}} E(\lambda) * I(\lambda) * d\lambda}{\int_{290 \text{ nm}}^{400 \text{ nm}} E(\lambda) * I(\lambda) * 10^{-A_0(\lambda)C} * d\lambda} \quad \text{Equation 5-6}$$

where, C is the adjustment coefficient

In order for the PMMA plates to be accepted as valid performance, the “C” value need to in the range 0,8-1,6. Would there be any of the four plates out of the range, new plates should be added so that at least four plates would lay in the required range of the “C” value.

In vitro UVA-PF

The initial value for the UVA-PF was calculated based on the measured absorbance spectrum with the “C” value. It was calculated like the *in vitro* SPF, with slight modifications. Instead of a erythematic spectrum $E(\lambda)$, the permanent pigment darkening $P(\lambda)$ was used. Moreover, the spectral irradiation received from a radiation UVA source $I(\lambda)$ was used for the calculations instead of the RSS). In addition, the values for the wavelengths 320-400 nm were integrated.

The *in vitro* UVA-PF was calculated with Equation 5-7.

$$UVA - PF_0 = \frac{\int_{320 \text{ nm}}^{400 \text{ nm}} P(\lambda) * I(\lambda) * d\lambda}{\int_{320 \text{ nm}}^{400 \text{ nm}} P(\lambda) * I(\lambda) * 10^{-A_0(\lambda)C} * d\lambda} \quad \text{Equation 5-7}$$

$P(\lambda)$ and $I(\lambda)$ values were taken from the listed values in the ISO 24443:2012.

Irradiation of the plates and UVA calculation

For these calculations, the photodegradation of the filters are also considered. Therefore, plates need to be irradiated at a given dose based on the initial UVA-PF. The dose of irradiation is calculated by Equation 5-8.

$$D = UVA - PFA_0 \cdot 1,2 \quad \text{Equation 5-8}$$

Each PMMA plate was irradiated on a solar simulator ATLAS CPS+ 75,6 W/m² (290-400 nm), according to the specifications of the UV source in ISO 24443: 2012 (Table 5-4). The value of the UV source was calculated and calibrated by a specialized technician.

Table 5-4. Specifications of the UV source (21).

Especificaciones de la fuente de exposición al UV medidas con un espectroradiómetro	
Irradiancia UV total (290 nm a 400 nm)	40 W/m ² a 200 W/m ²
Relación de irradiancia de UVA ^a a UVB ^b	8:22
^a 320 nm a 400 nm.	
^b 290 nm a 320 nm.	

During the irradiation the temperature needs to be between 25-30 °C. Finally, the UVA-PF is calculated from the absorbance of the irradiated plates by Equation 5-9.

$$UVA - PF = \frac{\int_{320 \text{ nm}}^{400 \text{ nm}} P(\lambda) * I(\lambda) * d\lambda}{\int_{320 \text{ nm}}^{400 \text{ nm}} P(\lambda) * I(\lambda) * 10^{-A_e(\lambda)c} * d\lambda} \quad \text{Equation 5-9}$$

where, A_e is the mean absorbance of the monochromatic film product of the measurement after plates irradiation.

5.2.13 Water resistance

The water resistance is an *in vivo* test subjected to regulation, which is obligatory when claiming of a water-resistant sunscreen. The obtained data has to be presented to the authorities that will authorize the labeling of the sunscreen product to be water resistant if the sunscreen product passes the test for water resistance. There are two ISO standards which need to be followed; ISO 16217:2020 (165) which defines the water immersion procedure for determining WR, and ISO 18861:2020 (166) which defines the percentage of water resistance. There is no standardized test for water resistance *in vitro* as the predictability of this method needs to be improved. However, an *in vitro* test method could be used for an initial screening of the water resistance of the sunscreen product. Based on an *in-vitro* method described in (167) which consisted of simulating *in vivo* conditions with the use of ethylene methacrylate acid copolymer (EMA) plate instead of the skin of volunteers a new method was proposed. The method proposed in this study was identical to the described method except on the plates as HD6 polymethacrylate (PMMA) plates were used instead of the EMA plates.

Immersion conditions

Four PMMA plates were fixed with a Tesa Hook & Loop tape fixing system to the inner part of 1 L glass beaker, with a gap of 2 cm from the ground. The bioadhesive emulsion was previously spread on the plates, accordingly to ISO 24443: 2012 (164) in which firstly circular and secondly spreading techniques are used to cover homogenously the PMMA plate in a way to ensure the standardized amount of 1,3 mg/cm². The plates were dried for 30 min and then fixed by the fixing system to the glass beaker with 500 mL water by a constant temperature of 30 °C. The water was under a constant flow using a propeller stirrer at 300 rpm. As described in *in vivo* measurements the plates were kept for two periods of 20 minutes under immersion separated by 15 minutes out of the water. The plates were then taken out from the water and let dry for 30 minutes.

Water resistance determination

The standardized test ISO 24443: 2012 (164) for evaluation of *in vitro* UVA PF was used for determination of the SPF before and after immersion of the plates, which is directly linked to the amount of filters which are still present on the PMMA plate. The resulting water resistance is presented in percentage and is calculated according to Equation 5-10, meaning the percentage of filter protection which is still on the plate after immersion. The experiment was done four times for statistical significance.

$$\% WR = \frac{\text{Post immersion SPF} - 1}{\text{Pre immersion SPF} - 1} \quad \text{Equation 5-10}$$

The conditions for water resistance in Europe state that sunscreen products after immersion need to carry at least more than 50 % recovery respect to the pre immersion SPF (168).

5.2.14 Centrifugation

In a period between 24-48 h after emulsion formulation, centrifugation was performed using HERAFUS MEGAFUGE 16R centrifuge. Approximately 5 g of sample at 25 °C was weighted and filled in a falcon tube of 14 mL diameter and centrifuged at 5000 rpm for 15 minutes. This method was established by the Pharmaceutical Technology department of the university of Barcelona and mentioned in (169). For an optimal stability, the sample should be homogenic and without phase separation after the centrifugation procedure.

5.2.15 Stability

Stability tests for cosmetical products are currently not subjected to a defined regulation. However, cosmetic industries have designed their own accelerated stability conditions to perform a predictive assessment of the product durability. Despite there are no strict guidelines for cosmetics to assess stability of the products under investigation, it is not uncommon, that the ICHQ1A guideline: stability testing of new drug substances and products (170), that applying to pharmaceutical products are followed for cosmetic products are used

as well. This ICH regulation state that drug products need to be stored in three conditions of temperature and relative humidity as described in Table 5-5:

Table 5-5. Storage conditions of drug products: long term, intermediate and accelerated studies (climate zone II).

Study	Storage condition	Minimum time-period covered by data at submission
Long term	25 °C ± 2 °C/60% RH ± 5% RH or 30 °C ± 2 °C/65% RH ± 5% RH	Expiration time (max. 60 months)
Intermediate	30 °C ± 2 °C/65% RH ± 5% RH	12 months
Accelerated	40 °C ± 2 °C/75% RH ± 5% RH	6 months

The testing of the drug products should be performed every 3 months. Long term studies for products that are intended to have a shelf life of at least 12 months, should be tested at least for the 12 months. During the first year the product should be tested every 3 months for the first 12 months, every 6 months for the second year and annually from the third year on.

In the case of accelerated stability, a 6-month study is recommended. Three time points, including the initial and final time point should be included. Therefore, in most cases are tested at 0, 3 and 6 months.

The intermediate test applies in case of a result of significant change observed in the accelerated test condition. In this case four test measurements including the initial and final points of a 12-month test are needed (170).

Accelerated stability tests designs are mostly performed in cosmetic industry for formulations which have previously fulfilled the centrifugation criteria (see section 5.2.14). Therefore, the accelerated stability is mostly performed in definitive formulations and pilot scale formulations (171). Every cosmetic industry has its own protocols for its semisolid products under development. However, there are some differences on temperature conditions,

storage time, testing time periods and critical endpoints to test the final products. Therefore, literature research on different cosmetic industry protocols on stability of three different cosmetic companies was conducted (171–173).

This research together with the ICH guidelines as reference, an own study protocol was designed. For conducting this protocol on the stability of the final cosmetic product a selection of the most relevant criteria was chosen and are presented as follows.

For the temperature, storage time and period for re-test are listed in Table 5-6.

Table 5-6. Stability of the bioadhesive emulsion. Storage conditions: temperature, storage time and period for re-test.

Temperature	Storage time	Re-test
5 °C	6 months	1 st , 2 nd , 3 rd , 6 th month
25 °C	12 months	1 st , 2 nd , 3 rd , 6 th , 12 th month
40 °C	6 months	1 st , 2 nd , 3 rd , 6 th month

Three samples of a same batch were stored in glass jars and vials depending on the method. Then these samples were kept at different temperature conditions (5 °C, 25 °C and 40 °C) for six months in the case of 5 °C and 40 °C (0, 1, 2, 3, 6) and for 12 months in the case of 25 °C (0, 1, 2, 3, 6 and 12) to assess its stability. The stability was tested in two ways:

- The in-use stability consists of testing the same sample every time the experiment is performed, in other words, for the different storage times (for example in this study, for 25 °C the same sample would be tested after 0, 1, 2, 3, 6 and 12 months). In the present study, the same batch of the product was divided in three different glass jars and stored at 5 °C, 25 °C and 40 °C. The glass jars were closed with a plastic cap with a rotational system, which could be reopened easily.
- The stability method consists of testing the sample only once. Therefore, one sample is tested for a specific storage temperature at a specific storage time (for example in

this study, for 25 °C one samples would be tested for 0 months, another sample would be tested for 1 months, and so on with a total of six samples to cover all the time-sets. It is the method described by the ICH Q1A: stability testing of new drug substances. Moreover, it is the traditional, widespread test in cosmetic industry to assess the stability of cosmetic products. The batch of a product is stored in different sealed vials. In this study, five different vials were stored at 5 °C (corresponding to the stability measurements after 0, 2 and 3 months storage), six different vials were stored at 25 °C (corresponding to the stability measurements after 0, 2, 3 and 12 months storage) and five different vials were stored at 40 °C (corresponding to the stability measurements after 0, 2 and 3 months storage).

The in-use stability is stressing much more the product than the stability method. In the in-use stability the product is exposed to not only to different changes in temperature and humidity, but also to continuous human manipulation. These factors may decrease the stability of the product.

Finally, the critical parameters to evaluate the stability were:

1. Organoleptic properties
2. Viscosity
3. Rheology
4. Extensibility
5. pH

Five measurements were performed (t=0, 1 month, 2 month, 3 months, 6 months) for the set of critical parameters.

These properties define the physicochemical behaviour of the sunscreen emulsion and were chosen to assess the stability by comparing these critical aspects at the initial time (t= 0) vs the evaluation time (t= X months).

To quantify the quality of the product each critical parameter was evaluated by a score system from 1-10, in which 1 was the lowest grade whereas 10 was the highest.

Finally, all the scores from each critical parameter were represented graphically in a diagram radius. This proposed model in which stability is tracked by comparing the diagrams of different months to the initial diagram is based on a study conducted by the Pharmacy and Pharmaceutical Technology, and Physical Chemistry Department of the University of Barcelona and published at PLOS one (169). In this validated study, referred as Semi-solid Control Diagram (SSCD), stress was applied to the final semisolid formulation instead of different temperature and storage time conditions. Despite some critical parameters were extracted from the article like organoleptic properties, extensibility and viscosity, others (pH and rheology) were changed as these two parameters are widely used for assessing stability of final products in cosmetic the industry.

The objective of the approach is to assess stability by scoring the formulation and compare each stability condition (5 °C, 25 °C, 40 °C) and storage time (t= 1, 2, 3, 6 and 12 months) to the initial time point (t=0) for the same stability condition.

1. Organoleptic properties

Organoleptic properties are classified into five groups:

- Homogeneity
- Color
- Flowability
- Absence of air
- Texture

Each characteristic was given the same weight and therefore had the same value. In other words, one characteristic counted 1/5 of the final score. Each property parameter was determined by adding together the experimental values (eV) of each of the five following properties:

a. Homogeneity (spreading the sample on a glass plate): limit value (eV) = 2

The criteria for maximum homogeneity (2) were no physical discontinuities (oil, water) or no clumps visible in the sample with the naked eye and under a microscope.

If small discontinuities appeared (only visible under a microscope, not with the naked eye), a value of 1 was assigned.

If some discontinuities were visible with the naked eye, a value of 0 is assigned.

b. Color: limit value (eV) = 2

The color was checked with the naked eye.

If color was uniform throughout the sample: 2.

If there were non-uniform parts, but they were almost imperceptible: 1.

If different shades of color were visible: 0.

c. Flow through a tube or cannula: limit value (eV) = 2

The sample's flow through a cannula with a diameter of 4.80 mm using manual force was studied and its dispersion was observed.

If it passed smoothly: 2.

If it flowed with some difficulty and force was required: 1.

If it did not flow or excessive force was required: 0.

d. Absence of air: limit value (eV) = 2

If there was absence of air with the naked eye and under a microscope: 2.

If there was presence of air (only visible under a microscope, not with the naked eye): 1.

If there was presence of air with the naked eye: 0.

e. Texture (on glass): limit value (eV) = 2

If the texture was as expected and it could be spread properly: 2.

If the texture was not as expected and it was difficult to spread: 0.

The value of the radius was calculated by adding together the organoleptic valuations in Equation 5-11 (169):

$$eV=r=(P_1+P_2+P_3+P_4+P_5)$$

Equation 5-11

2. & 3. Viscosity and rheology

The viscosity and rheology method are described in section 5.2.9. The viscosity which was set as reference was 1000 mPa·s, which corresponds to a medium gel viscosity. This value reference (V1) and the viscosity of the cream (v2) the equation to score the formulation ($r = 10 - (v^1/100 - v^2/100)$.) was calculated.

The rheological behavior which was considered optimal was pseudoplastic, as creams usually have this behavior. Therefore, if this was the case a score of 5 was given. If the formulation, additionally showed a thixotropic effect, it was scored 10 as a reduction in force by spreading is wanted in a cream which must be spread, and even more to a wide surface as this is the case in sunscreen products. Did the cream not present weather pseudoplastic behavior not thixotropy, a 0 was given.

4. Extensibility

The extensibility (E) method is described in section 5.2.10. The r value for extensibility was calculated using Equation 5-12.

$$r = 10 - (E^1/100 - E^2/100) \quad \text{Equation 5-12}$$

where E1 is the target extensibility (ideal extensibility or goal) and E2 is the experimental extensibility obtained from the average of three extensibility measurements.

The ideal extensibility (E1) was 1000 mm², which corresponds to a high extensibility which is characteristic of fluid semisolid forms.

5. pH

The method to measure the pH of a semisolid form is described in section 5.2.7.

The skin's ideal pH is 5,5 (174). An increased pH could be detrimental causing inflammatory diseases like acne and psoriasis or dry skin (175). Therefore, the optimal pH of a semisolid form goes from acidic pH to near to neutral pH 6 (176). However, some cosmetic companies accept a wider pH range until the neutral pH. It is not uncommon to consider a neutral pH value if the eye is taken into consideration. The tears have an average pH which fluctuates between 7.25 and 7.45 depending on morning or the afternoon measurements, respectively (175). Taking all this information in view, the pH of the formulations should be between 5,5 and 6,5. Once the pH was adjusted for this range, the obtained pH value at t=0 was compared with the pH value of the same formulation measured time after in stability conditions.

Although the obtention of the identical pH value is an optimal parameter to determine the stability of a product, small variation in pH over time and under accelerated stability are not uncommon and therefore accepted. In line with this statement the scores for evaluating the pH were:

If the pH obtained in stability conditions (P2) was compared to the initial pH value (P1):

equaled or had a deviation of ± 1 , then r=10

had a deviation of $> \pm 1$, then r=5

if the pH was <4 or >7 , then r=0

All the parameters with its specifications are summarized in Table 5-7.

Table 5-7. Conversion of the critical parameters into radius values

Parameter		Limit value	Conversion to radius
Organoleptic properties	-Homogeneity	0-2	$eV=r=(P_1+P_2+P_3+P_4+P_5)$
	-Color	0-2	
	-Flow (cannula)	0-2	
	-Absence of air	0-2	
	-Texture	0-2	
Viscosity		100-100000 mPa·s (1000mPa·s)	$r= 10- (v^1/100 - v^2/100)$
Extensibility		100-1000mm ² (1000mm ²)	$r= 10- (E^1/100- E^2/100)$
pH	$pH_2= pH_1 \pm 1$	10	$r= 10$
	$pH_2= pH_1 \pm >1$	5	$r=5$
	$pH_2= <4 \text{ or } >7$	0	$r=0$
Rheology	Pseudo-plastic with thixotropy	10	$r=10$
	Pseudo-plastic without thixotropy	5	$r=5$
	Not Pseudo-plastic	0	$r=0$

The graphical representation of the stability parameters is a pentagonal diagram, named radius diagram (Figure 5-4).

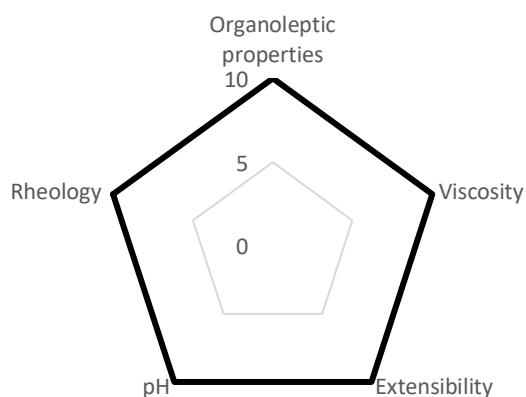


Figure 5-4. Radius diagram obtained with the application of Semi-solid Control Diagram (SSCD).

Calculation an index to establish the quality of the final product

The radius diagram, see Figure 5-4, is a graphical representation on the quality of the final product based on the five parameters described in section 5.2.15. Although the radius diagram is helpful when comparing between formulations or as in the present study comparing the same formulation at different times and stability conditions, the quality of the final product can be calculated as well. Three indexes were calculated based on the five parameters. These indexes are:

a. Parametric Index (PI)

which was calculated with Equation 5-13

$$PI = \frac{\text{n}^\circ \text{ of parameters with value } \geq 5}{\text{n}^\circ \text{ of total parameters}} \quad \text{Equation 5-13}$$

where n° of parameters with value ≥5 means the number of parameters equal to 5 or higher, and where n° of total parameters means the total number of parameters, which is always five in this study.

The formulation must be between >0,5-1,

as the limit of acceptance of a formulation > 0,5 and the maximum value 1.

b. Parametric Profile Index (PPI)

Is the sum of all the r values of the parameters divided by the total number of parameters, which in this case is 5. It is described by Equation 5-14.

$$PPI = \frac{\sum r}{\text{n}^\circ \cdot r} \quad \text{Equation 5-14}$$

The limit of acceptance is limited from 5 to 10 (being 10 the maximal value) .

c. Good Quality Index (GQI):

The GQI was calculated with Equation 5-15.

$$GQI = PPI \cdot f \qquad \text{Equation 5-15}$$

where f is the reliability factor, corresponding to a polygon area/circle area, which in this case is 0,75. The polygon area refers here to the area of the radius diagram, which is a pentagon.

The limit of acceptance should be higher than 5 and its maximum value is 10. ($LioA \geq 5-10$).

A quality formula is one that occupies half of the graph's area or, in other words, one with a GQI of 5.

5.3 Results and discussion

5.3.1 Literature search: UV-filters and other ingredients with minimal toxicity, irritancy and comedogenicity

Safety parameters as dermal toxicity, comedogenicity and irritancy were assessed for the ingredients used in the formulations (Table 5-8).

Moreover, only ingredients and UV-filters which were not listed in the *Red list of Chemicals of Concern for safe cosmetics* by the Breast Cancer Prevention Partners (177) were used.

Table 5-8. Safety assessments, comedogenicity and irritancy of different ingredients

INCI ¹ name	Toxicity	Comedogenicity/ Irritancy
Sorbitan stearate	Safe dermal (178)	Irritancy 1 Comedogenicity 0 (153)
Polysorbate 80	Safe dermal (179)	Irritancy 0, Comedogenicity 0 (153)
Emollient-B	Safe dermal (180)	Non-comedogenic (181)
Caprylic/Capric Triglyceride	Safe (max. leave on conc. is 95,6% (182)	Irritancy 0, Comedogenicity 0
Solvent-G	Safe (86% has no evidence of sensitization) (183)	Irritancy 0, Comedogenicity 0 (153)
Glycerin	Safe dermal (184)	Irritancy 0, Comedogenicity 0
Xanthan gum	No sensitization at 0,1% (185)	Non-irritant at 1% in rabbits (185)
Phenoxyethanol	Safe up to 1% (186)	
Ethylhexylglycerin	No phototoxic and photoallergic at 100%, no genotoxic, no reproductive and developmental toxicity (187)	Mild skin irritating when undiluted (187)
DHHB	Permitted use up to 10% except US and Canada (188)	
BEMT	Permitted use up to 10% except US and Japan (188), photostable, no skin penetration (140)	
BEMT aqua	Permitted use up to 10% except US and Japan (188)	

MBBT	Permitted use up to 10% except US and Japan (188), No skin penetration, photostable (140)	
TBPT	Permitted use up to 10% in EU (188)	
EHT	Permitted use up to 5% except US and Canada (188)	
BA-BOOSTER-1	No information on concentration limits (189)	
BA1		
Polymethacrylates		slight irritant effect - does not require labelling in rabbit (190)

Moreover, any ingredients and UV-filters used in the formulations is listed in the red list of cosmetics under concern- campaign for safe cosmetics by the breast cancer prevention partners (191).

5.3.2 Formulation process: trial and error

Preliminary emulsions

a) Emulsion 1-1)

To start, a first formulation containing UV-filters to reach an SPF of 30 was made. The use of UV filters was thought to be essential to determine that all the components could cope with the UV filters and produce an homogenic emulsion. It needs to be outlined, that the more UV-filters used, the difficult it is to solubilize those UV-filters, being the stability of the formulation of major concern. Therefore, three UV-filters were considered the best option to start with.

Table 5-9. Emulsion 1-1. Oil in water (O/W) emulsion.

	Ingredient family	Trade name	INCI	1-1
A	Emulsifier	Emulium delta	Cetyl Alcohol, Glyceryl Stearate, PEG-75 Stearate, Ceteht-20 , Steareth-20	4,00
	Emollient	Emollient-B	Emollient-B	7,00
	Emollient	Cetio IV	Decyl oleate	3,00
	Preservative	Euxyl PE9010	Phenolxyethanol, Ethylhexylglycerin	1,00
	Broad spectrum filter	Tinosorb S	Bis-ethylhexyloxyphenol methoxyphenyl Triazone	5,00
B		Water	Aqua	ad. 100
	UVB-filter	Eusolex 232	Phenylbenzimidazole sulfacid	2,00
	UVA-filter	Neo Heliopan AP	Disodium Phenyl Dibenzimidazole Tetrasulfonate	4,00
	Strong base	NaOH (10 % sol.)	NaOH (10 % sol.)	5,00
C	Moisturing agent	Glycerin	Glycerin	5,00
	Chelating agent	EDTA BD	Disodium EDTA	1,00
	Tickener	Rheocare XGN	Xanthan Gum	0,5

The formulation was designed taking into consideration the recommendations made by Beiersdorf AG about the ingredients and those concentrations that were beneficial to include in a formulation containing PRE-A. These strategies are described in the patents WO16206961, WO16206962, WO16206963, WO17036662, WO17102300, WO17102301, WO17102302, and WO17129432 (144,192–198) and are summarized in Annex 1. Moreover, the formulation was designed taking into consideration the currently used proportions of ingredient families.

As an example, 5% emulsifier, 15% emollient, 10-20% UV-filters, 0,3-3% thickeners, contained in sunscreen emulsions of SPF 30 (3).

a. Emulsifier system:

The O/W emulsifier made of Cetyl alcohol, Glyceryl stearate, PEG-75 stearate, ceteth-20 and steareth-20 was integrated in the formulation for being widely used in cosmetic formulations. O/W emulsifiers bring both phases together, being the water phase externally with oil droplets inside. An O/W emulsion was preferred for the initial formulation, as it is usually easier to formulate and needs lower shearing velocity when mixing the external and internal phase.

b. UV-filter:

To cover the entire UV spectrum and reaching the SPF 30, UV filters with; broad spectrum, UVA and UVB coverage were chosen, namely BEMT, DPDT and PBSA. While BEMT is lipophilic, PBSA and DPDT are hydrophilic UV filters and therefore they had to be added in the oily and water phase of the formulation, respectively. The UV filters DPDT and PBSA are soluble and therefore effective as UV filters in a basic pH. For this reason, NaOH at 10% in solution was added to distilled water in combination with the hydrophilic UV filters to reach a pH of 7-7,5, as an acid pH would cause a drop in efficacy (a decrease in absorbance of the filter) (199). The use of those UV filters had not only to fulfil the requirement of an in-silico SPF 30 but also were selected because of their physicochemical properties. The use of UV filters in both phases has proved to increase the homogeneity of the formulation film on the skin surface, resulting in a higher performance of the sunscreen (3).

c. Emollient:

The emollients Emollient-B and Decyl Oleate were chosen due to their wide use in cosmetic products. Moreover, Emollient-B is highly efficient at solvent of UV-filters and lets a light and silky feel on the skin with high spreadability.

d. Other ingredients:

- Xanthan gum was selected for its wide use as thickener in sunscreen formulations and due to the recommendations of these ingredients in the patents by Beiersdorf when formulating with PRE-A (144,192–198).

- Phenoxyethanol and Ethylhexylglycerin are together in one final product as current preservative and its beneficial concentration in formulation is between 0,1-1% when the formulation contains PRE-A (144,192–198). Phenoxyethanol is the ingredient with preservative character and Ethylhexylglycerin boosts its effect. It had been proven to be safe and it is well accepted among the public in contrast with other preservatives like parabens. It confers stability to the emulsions even under heating ($> 85\text{ }^{\circ}\text{C}$) and high acid-basic (pH 3-10) conditions (200).

- Glycerin is a well-known moisturizing agent which is effective even at 3% concentration (201). Therefore 5% concentration of glycerin is considered to contribute to the better moisture of the skin.

- Finally, Disodium EDTA is a chelating agent which helps keeping the stabilization of the emulsion for a longer period. Metal ions, which usually concentrate in the water phase of the formulation are neutralized by the protons of disodium EDTA.

Procedure:

The ingredients in Table 5-9 were weighed separately in two different volumetric flasks. The ingredients of the oily phase (A phase) and water phase (B, C phase) were stirred and heated to $80\text{ }^{\circ}\text{C}$ separately. Phase A was added into phase B, C under stirring. The emulsion was homogenized under thurax (Silverson L4R) for 1 min and cooled down to room temperature using a U-shaped stirrer (Yelp scientifica ES overhead stirrer). Finally, the pH was measured with a pH-meter and its pH was adjusted to 7,5. Normally formulations are adjusted to reach a pH of 5,5-6,5. However in this case DPDT and PBS are UV filters which need a higher pH to be effective (90).

Results and discussion

a) Emulsion 1-1

Small lumps were observed in the formulation. This points out the weak stability of the emulsion. The yellow color of the emulsion may be due to the UV filters BEMT and DPDT.

b) Emulsion 1-2

UV-Filters:

It is a fact, that yellowish sunscreens are not that well accepted by customers as white color ones and customers expect some degree of whiteness during rub-out (84). The emulsion 1-1 was yellowish due to the UV-filters BEMT and DPDT. To make a white color emulsion, DPDT was replaced by another UVA-filter: DHHB in emulsion 2. Despite BEMT being yellow, and therefore contributing to the final color of the emulsion, this UV filter has so many advantages, that replacing it was not considered. BEMT is not only a broad-spectrum filter with the highest absorbance capacity, with two peaks with an E_{1,1} of 823 nm and 737 in ethanol (203,204), it has also high stabilization capacity of the emulsion and helps the stabilization of other photo-instable UV-filters like avobenzone. Moreover, as the molecular structure has a high molecular weight (MW= 623,71 g/mol) it is one of the safest UV filters as penetration into the dermis is less likely to occur compared to smaller molecules, whose are found in the plasma after topic exposure on the skin.

To reach an SPF 30 the percentage of BEMT remained unchanged at 5 %, as between the range 2-5% proved to be the most beneficial in formulation together with PRE-A. However, PBS had to be increased to 3 % because of the change in the UVA-filter DPDT for 5 % DHHB. The total filter amount was 13%, which was in line with the typical existing formulations (3).

Emollient:

The emollient decyl oleate was replaced by PEG-7 Glyceryl cocoate for its less greasiness and the concentration of both emollients were increased reaching 15% in total (Emollient-B 10% and PEG-7 Glyceryl cocoate 5%) as this emollient proportion can be found in sunscreens of SPF 30. Other components and the formulation procedure remained unchanged (see Table 5-10).

Table 5-10. Emulsion 1-2. Oil in water (O/W) emulsion.

	Ingredient family	Trade name	INCI	1-2
A	Emulsifier	Emulium delta	Cetyl Alcohol, Glyceryl Stearate, PEG-75 Stearate, Ceteht-20 , Steareth-20	4,00
	Emollient	Emollient-B	Emollient-B	10,00
	Emollient	Cetiol HE	PEG-7 Glyceryl Cocoate	5,00
	Preservative	Euxyl PE9010	Phenolxyethanol, Ethylhexylglycerin	1,00
	Broad spectrum filter	Tinosorb S	Bis-ethylhexyloxyphenol methoxyphenyl Triazone	5,00
	UVA-filter	Uvinul A Plus	Diethylamino Hydroxybenzoyl Hexylbenzoate	5,00
B		water	Aqua	ad. 100
	UVB-filter	Eusolex 232	Phenylbenzimidazole sulfacid	2,00
	Moisturing agent	Glycerin	Glycerin	5,00
	Chelating agent	EDTA BD	Disodium EDTA	0,10
	Thickener	Rheocare XGN	Xanthan Gum	0,50

Procedure:

The procedure was equal to emulsion 1-1.

Results and discussion:

The resulting formulation was homogeneous and very fluid. Some precipitation in the oily phase was observed, which could indicate that the thickener at least could not be integrated into the formulation. The precipitation might indicate a poor solubility of some of the ingredients in PEG-7 Glyceryl Cocoate. To prove this hypothesis, the oily phase was reformulated with Emollient-Be as the only solvent. This time the viscosity increased. In addition, the spreadability and the color were satisfactorily.

Bioadhesive Emulsions O/W, (4-1, 4-2, 4-3)

a) Bioadhesive emulsion O/W 4-1

As the organoleptic properties of emulsion 2 were satisfactory, the bioadhesive agent and booster which can be seen in the formulation developed by the SDM (Internal ref: Internal ref: PLC-19-001-3-1, Table 5-3) were added to accomplish the skin bio-adhesiveness requirement.

Table 5-11. Bioadhesive emulsion 4-1. Oil in water (O/W) emulsion.

	Ingredient family	Trade name	INCI	4-1
A	Emulsifier	Emulium delta	Cetyl Alcohol, Glyceryl Stearate, PEG-75 Stearate, Ceteht-20 , Steareth-20	4,00
	Emollient	Emollient-B	Emollient-B	15,00
	Preservative	Euxyl PE9010	Phenolxyethanol, Ethylhexylglycerin	1,00
	Broad spectrum filter	Tinosorb S	Bis-ethylhexyloxyphenol methoxyphenyl Triazone	5,00
	UVA-filter	Uvinul A Plus	Diethylamino Hydroxybenzoyl Hexylbenzoate	5,00
B		water	Aqua	ad. 100
	UVB-filter	Eusolex 232	Phenylbenzimidazole sulfacid	3,00
	Moisturing agent	Glycerin	Glycerin	5,00
	Bioadhesive agent	BA1	BA1	3,00
	Bioadhesive booster	BA-booster-1	BA-BOOSTER-1	4,00
	Chelating agent	EDTA BD	Disodium EDTA	0,10
	Thickener	Rheocare XGN	Xanthan Gum	0,50

Procedure:

The ingredients were weight separately in two different volumetric flasks (Table 5-11). The ingredients of the water phase (B phase) were stirred together except BA1, which was added once the other components were integrated into the solution. Then, BA1 was added stepwise

into the B phase leading to the formation of the gel. The ingredients of the oily phase (A phase) were stirred and heated to 80 °C. Phase A was let cool down to 25 °C and it was added into phase B under stirring. The emulsion was homogenized under turrax for 1 min. Finally, the pH was adjusted to 7-7,5.

Results and discussion

The water phase was transparent and homogene before mixing both phases. However, with the addition of the oil phase, the emulsion was not homogeneous as lumps of gel were formed, indicating that the two phases did not mix well together. Moreover, the formulation was not adhesive. It is known that the homogenization of the water and the oil phase depends on the emulsifier. Regarding to the poor stability of the two phases, it was decided to replace the emulsifier emulium delta for another O/W emulsifier.

b) Bioadhesive emulsion O/W 4-2

To make the emulsion homogeneous, the emulsifier emulium delta was replaced by tween in the oily phase and Span™ 60 in the water phase. Moreover, the aim was to perform a manufacture procedure which should be as similar as the original bioadhesive gel designed by SDM (int. ref. PLC-3-1 to avoid possible deviations which could lead to incompatibilities affecting the final formulation. Therefore, all ingredients at the same concentration contained in the original formulation (Table 5-3) were selected to design the water phase of the present formulation (Table 5-12), except of crystal menthol. This ingredient was not included as it provides a cooling effect, which was not wanted in the present formulation. Furthermore, the UV filter PBSA was removed so that the gel phase was as similar as possible to the original formulation.

Table 5-12. Bioadhesive emulsion 4-2. Oil in water (O/W) emulsion.

	Ingredient family	Trade name	INCI	4-2
A	Emulsifier	Span™ 60	Sorbitan oleate	2,00
	Emollient	Emollient-B	Emollient-B	15,00
	Preservative	Euxyl PE9010	Phenoxyethanol, Ethylhexylglycerin	1,00
	Broad spectrum filter	Tinosorb S	Bis-ethylhexyloxyphenol methoxyphenyl Triazone	5,00
	UVA-filter	Uvinul A Plus	Diethylamino Hydroxybenzoyl Hexyl benzoate	5,00
B		Water	Aqua	ad. 100
	Emulsifier	Tween™ 20	Polysorbate 20	4,00
	Moisturizing agent	Glycerin	Glycerin	2,00
	Bioadhesive agent	BA1	BA1	3,00
	Bioadhesive booster	BA-booster-1	BA-BOOSTER-1	6,00
	Solvent	Solvent-G	Solvent-G	30,00
		BASE-1	BASE-1	3,00
	Chelating agent	EDTA BD	Disodium EDTA	0,1
	Thickener	Rheocare XGN	Xanthan Gum	0,50

Procedure:

The ingredients were weight separately in two different volumetric flasks corresponding to the water and the oil phase (Table 5-12). The ingredients of the oily phase (A phase) were stirred and heated to 80 °C. In the water phase (B phase) BASE-1 was dissolved in water under U plate stirrer. Once BASE-1 was completely dissolved in water BA-BOOSTER-1 was added to the solution. Then the BASE-1- BA-BOOSTER-1-water solution was added slowly to a beaker with Solvent-G under stirring (using a U plate stirrer). Then, EDTA, xanthan gum, glycerin and Span™ 60 were added in this order. Finally, BA1 was added stepwise waiting until the powder was homogenized in the formulation. Phase A was let cool down to 25 °C and it was

added into phase B under stirring. The emulsion was homogenized under thurax for 1 min. Finally, the pH was adjusted to 5,5-6,5.

Results and discussion:

The emulsion was homogeneous, nevertheless after spreading onto the skin traces of the formulation were formed after scrubbing out the skin. Compared to the water phase of previous formulation 4-1, the gel in the present formulation was white instead of transparent. This could be due to the use of SpanTM 60, which when added into the gel, it changed from transparent to white opaque color.

The previous formulation lost the bioadhesiveness in the gel phase. However, the present emulsion was bioadhesive. Therefore, the manufacturing process of the gel could have an influence on the bioadhesiveness of the emulsion. It is worth outlining, that the temperature of the phase A should be cooled down to 25 °C before mixing both phases. The bioadhesive emulsion 4-2 was overall satisfactory, although the appearance resembled those of mayonnaise, the spreadability should be improved and the viscosity should be decreased.

c) Bioadhesive emulsion O/W 4-3

The aim of the bioadhesive emulsion 4-3 was to improve the appearance of the present emulsion compared to the previous one (Bioadhesive emulsion O/W 4-2). Therefore, the oily phase was reduced by almost the half (30% oily phase in bioadhesive emulsion 4-2; 17,5% oily phase in bioadhesive emulsion 3). Moreover, xanthan gum was removed out of the emulsion to reduce the viscosity and improve the spreadability. During the manufacturing procedure the water phase was sticky enough before the addition of the bioadhesive agent BA1 and consequently the BA1 was reduced to 2 % (Table 5-13).

Table 5-13. Bioadhesive emulsion 4-3. Oil in water (O/W) emulsion.

	Ingredient family	Trade name	INCI	4-3
A	Emulsifier	Span™ 60	Sorbitan oleate	2,00
	Emollient	Emollient-B	Emollient-B	7,50
	Preservative	Euxyl PE9010	Phenoxyethanol, Ethylhexylglycerin	0,50
	Broad spectrum filter	Tinosorb S	Bis-ethylhexyloxyphenol methoxyphenyl Triazone	8,00
B		Water	Aqua	ad. 100
	Emulsifier	Tween™ 20	Polysorbate 20	4,00
	Moisturizing agent	Glycerin	Glycerin	2,00
	Bioadhesive agent	BA1	BA1	2,00
	Bioadhesive booster	BA-booster-1	BA-BOOSTER-1	6,00
		Solvent-G	Solvent-G	30,00
		BASE-1	BASE-1	3,00
	Chelating agent	EDTA BD	Disodium EDTA	0,10

Procedure:

The procedure was equal to bioadhesive emulsion 4-2.

Results and discussion:

Bioadhesive emulsion 4-3 was sticky on the skin and had a better spreadability compared to bioadhesive emulsion 4-2. However, contrary to previously thought the emulsion had an oily texture, which tends to be not well accepted by costumers, as they rather prefer a sunscreen than absorbs onto the skin after its application, reducing the feeling that the cream is still present on the skin.

Bioadhesive emulsions W/O (5-1 & 5-2)

a) Bioadhesive emulsion W/O 5-1

In this formulation the phase was inverted in respect to bioadhesive emulsion 4-3, which was an O/W emulsion, to determine if the base type could have an impact on the organoleptic properties. The proportions of both, the water and the oily phase remained unchanged from 4-3 except for the emulsifiers whose proportion was inverted to form an emulsion W/O). (In 4-3 contained 2% Span™ 60 and 4% Tween™ 20 80. In 5-1 contained 4% Span™ 60 and 2% Tween™ 20 (Table 5-14).

Table 5-14. Bioadhesive emulsion W/O 5-1

	Ingredient family	Trade name	INCI	5-1
A	Emulsifier	Span™ 60	Sorbitan oleate	4,00
	Emollient	Emollient-B	Emollient-B	7,50
	Preservative	Euxyl PE9010	Phenoxyethanol, Ethylhexylglycerin	1,00
	broad spectrum filter	Tinosorb S	Bis-ethylhexyloxyphenol methoxyphenyl Triazone	5,00
	UVA-filter	Uvinul A Plus	Diethylamino Hydroxybenzoyl Hexyl benzoate	5,00
B1		Water	Aqua	ad. 100
		BASE-1	BASE-1	3,00
	Bioadhesive booster	BA-booster-1	BA-BOOSTER-1	6,00
B2		Solvent-G	Solvent-G	30,00
	Moisturizing agent	Glycerin	Glycerin	2,00
	Chelating agent	EDTA BD	Disodium EDTA	0,10
	Emulsifier	Tween™ 20	Polysorbate 20	2,00
	Bioadhesive agent	BA1	BA1	2,00

Procedure:

Firstly, the ingredients of phase A were weight and heated under stirring with an helix stirrer to 80 °C. Secondly, in another beaker BASE-1 was dissolved in water and stirred with a U plate stirrer. Then, BA-BOOSTER-1 was added to the water/BASE-1 dissolution under stirring (phase B1). In a third beaker with Solvent-G the water/BASE-1/BA-BOOSTER-1 solution (phase B1) was added slowly under stirring using the U plate stirrer. Further, glycerin, disodium EDTA and polysorbate 80 were added slowly into the mixture. It is worth underlining, that while adding polysorbate 80 the emulsion turned white. BA1 was added slowly keeping a while between additions to keep the phase homogeneous and it was let under stirring for 10 min. Further, as viscosity increased, the spin was accelerated until it turned out a gel. Finally, the gel was mixed into phase A.

Results and discussion:

The consistency was dense, which could remember those of mayonnaise. The spreadability was significantly higher than 4-3. However, after application onto the skin the emulsion let an oily touch, which is generally not that well accepted among sunscreen consumers compared to “dry touch” (205). Moreover, 24 h later when taking some cream out of the tube, a slight phase separation was observed.

b) Bioadhesive emulsion W/O 5-2)

Taking as a starting point the bioadhesive emulsion W/O 5-1, the oily phase of this emulsion was reduced to the half (Table 5-15). The aim was to reduce the “oily touch” after its application onto the skin.

Table 5-15. Bioadhesive emulsion W/O 5-2

	Ingredient family	Trade name	INCI	5-2
A	Emulsifier	Span™ 60	Sorbitan oleate	2,00
	Emollient	Emollient-B	Emollient-B	3,50
	Preservative	Euxyl PE9010	Phenoxyethanol, Ethylhexylglycerin	0,50
	broad spectrum filter	Tinosorb S	Bis-ethylhexyloxyphenol methoxyphenyl Triazone	2,50
	UVA-filter	Uvinul A Plus	Diethylamino Hydroxybenzoyl Hexyl benzoate	2,50
B1		Water	Aqua	ad. 100
	Puffer	BASE-1	BASE-1	3,00
	Bioadhesive booster	BA-booster-1	BA-BOOSTER-1	6,00
B2	Solvent	Solvent-G	Solvent-G	30,00
	Moisturizing agent	Glycerin	Glycerin	2,00
	Chelating agent	EDTA BD	Disodium EDTA	0,1
	Emulsifier	Tween™ 20	Polysorbate 20	2,00
	Bioadhesive agent	BA1	BA1	2,00

Procedure:

The manufacturing procedure of the bioadhesive emulsion W/O 5-2 was the same as bioadhesive emulsion W/O 5-1.

Results and discussion:

The viscosity of the bioadhesive emulsion W/O 5-2, increased considerably compared to bioadhesive emulsion W/O 5-1, with a potato puree-like texture and the spreadability was slightly decreased. On the other hand, the oily skin touch decreased to a high extent.

Bioadhesive gels (3-2, 3-3)

As the gel and the oil parts were manufactured separately, it was observed, that before adding BA1 the gel was sticky but not adherent. Therefore, some ingredient in the gel was suspected to cause stickiness on the skin. There was the suspect that BA-BOOSTER-1 may have caused the unwanted stickiness of the gels. To prove this hypothesis, two gel formulations were made; Bioadhesive gel 3-2, containing BA-BOOSTER-1 (Table 5-16) and Bioadhesive gel 3-3 without BA-BOOSTER-1 (Table 5-17). Moreover, the manufacturing procedure was modified to evaluate if a phase inversion namely from W/O to O/W, taking propylene glycol as the oily phase could contribute even to increased stickiness.

a) Bioadhesive gel 3-2

Ingredients of Bioadhesive gel 3-2 are listed in Table 5-16.

Table 5-16. Bioadhesive gel 3-2

	Ingredient family	Trade name	INCI	3-2
B1		Water	Aqua	60,00
		BASE-1	BASE-1	3,00
	Bioadhesive booster	BA-booster-1	BA-BOOSTER-1	6,00
B2	Solvent	Solvent-G	Solvent-G	30,00
C	Moisturizing agent	Glycerin	Glycerin	2,00
D	Bioadhesive agent	BA1	BA1	3,00

Procedure:

BASE-1 was dissolved in water and stirred with a U plate stirrer. BA-booster-1 was added to the water/BASE-1 dissolution under stirring (phase B1). In a beaker with Solvent-G (B2) the water/BASE-1/BA-booster-1 solution (phase B1) was added slowly under stirring using the U plate stirrer. Glycerin was added into the mixture. Finally, BA1 was added slowly keeping a while between additions to keep the phase homogeneous and it was let under stirring for 10 min. Further, as viscosity increased, the spin was accelerated until it turned out a gel.

b) Bioadhesive gel 3-3

Ingredients of gel 3-3 are listed in Table 5-17.

Table 5-17. Bioadhesive gel 3-3

	Ingredient family	Trade name	INCI	3-3
B1		Water	Aqua	60,00
		BASE-1	BASE-1	3,00
B2		Solvent-G	Solvent-G	30,00
C	Moisturizing agent	Glycerin	Glycerin	2,00
D	Bioadhesive agent	BA1	BA1	3,00

Procedure:

BASE-1 was dissolved in water and stirred with a U plate stirrer (phase B1). Propilenglycol was added (phase B2) and glycerin were added into the water BASE-1 dissolution, in the order mentioned under U plate stirrer. BA1 was added slowly keeping a while between additions to keep the phase homogeneous and it was let under stirring for 10 min at 70 rpm. Further, as viscosity increased, the spin was increased to 100 rpm until it turned out a gel.

Results and discussion:

Firstly, the bioadhesive gel 3-3 (without BA-BOOSTER-1) was much less sticky than bioadhesive gel 1 (with BA-BOOSTER-1) indicating that BA-BOOSTER-1 has an impact on the stickiness of the gel, which was also observed in previous formulations. Secondly, BA-BOOSTER-1 changed the color of the gel as while bioadhesive gel 3-3 was slightly yellowish, bioadhesive gel 1 was colorless. As the bioadhesive gel 3-3 was preferred for being colorless, non-icky but still highly skin adhesive it was implemented in the next emulsions in the gel part.

Bioadhesive emulsions Oil in Water (O/W) (6-1 to 6-8)

The references of these bioadhesive O/W emulsions is 06-X, which refers to the manufacturing process (process 6) and number of experiments X. The manufacturing process 6 consisted of preparing the water phase and the oil phase independently, then adding the oil phase into the water phase and at the end adding the bioadhesive agent.

a) Bioadhesive emulsion O/W 6-1

In this formulation the importance was set on the organoleptic properties. The aim was to find the correct texture, skin feeling and adhesiveness. To do so the minimal number of ingredients for the necessary ingredient families in a sunscreen were used consisting in two emulsifiers for both, the oil and water phase, an emollient, a preservative, low amount of a UV-filter and the ingredients used in bioadhesive gel 3-3 (Table 5-17) as their organoleptic properties were optimal. These ingredients are listed in Table 5-18.

The emollient Emollient-B was replaced by Caprylic/Capric Triglyceride as the absorbance of BEMT was higher in Caprylic/Capric Triglyceride than in Emollient-B (3).

Table 5-18. Bioadhesive emulsion O/W 6-1

	Ingredient family	Trade name	INCI	6-1
A	Emulsifier	Span™ 60	Sorbitan oleate	2,00
	Emollient	Myritol 318	Caprylic/Capric Triglyceride	15,00
	Preservative	Euxyl PE9010	Phenoxyethanol, Ethylhexylglycerin	1,00
	broad spectrum filter	Tinosorb S	Bis-ethylhexyloxyphenol methoxyphenyl Triazone	5,00
B		Water	Aqua	ad 100
	Emulsifier	Tween™ 20	Polysorbate 20	4,00
	Moisturizing agent	Glycerin	Glycerin	2,00
		Solvent-G	Solvent-G	24,00
		BASE-1	BASE-1	3,00
C	Bioadhesive agent	BA1	BA1	3,00

Procedure:

On the one hand, the ingredients of phase B were mixed with a U plate stirrer. On the other, the ingredients of the phase A were heated to 70 °C and mixed with helix stirrer. Phase A was cooled down to room temperature and added to phase B mixing both phases under stirring. Finally, BA1 was added slowly under stirring with the U plate stirrer.

Results and discussion:

The emulsion was dense. The texture was homogeneous and the feeling on the skin was non oily. This sunscreen had the best organoleptic properties so far. The addition of BA1 in the last step of the process could have led to lower oiliness. The addition of after the emulsification increased the density of the final product. The way it was done in bioadhesive emulsions 4-1, 4-2 & 4-3 (mixing both phases together as the last step, having added BA1 to the water phase beforehand) seemed to break the gel and thus it was possible to find some small parts of gel in the emulsion). Although the emulsion was stable it was more viscous than the commercialized sunscreens.

b) Bioadhesive emulsion O/W 6-2

In this second version of the O/W bioadhesive emulsion Caprylic/Capric Triglyceride and propilenglycol were in a proportion of 1:3. The order in adding the ingredients of the emulsion diverged from 6-1, as while in 6-1 the oil and the water phase were done separately and mixed together before adding acyclic acid polymer, in emulsion 6-2 (Table 5-19) phase A was added while doing phase B (see manufacturing process in section b).

Table 5-19. Bioadhesive emulsion O/W 6-2)

	Ingredient family	Trade name	INCI	6-2
A	Emulsifier hydrophile	Span™ 60	Sorbitan oleate	2,00
	Emollient	Myritol 318	Caprylic/Capric Triglyceride	8,00
	broad spectrum filter	Tinosorb S	Bis-ethylhexyloxyphenol methoxyphenyl Triazone	5,00
	Preservative	Euxyl PE9010	Phenoxyethanol, Ethylhexylglycerin	1,00
B1	Emulsifier	Tween™ 20	Polysorbate 20	4,00
		Solvent-G	Solvent-G	24,00
B2		Water	Aqua	ad. 100
		BASE-1	BASE-1	3,00
	Moisturizing agent	Glycerin	Glycerin	2,00
C	Bioadhesive agent	BA1	BA1	3,00

Procedure:

Phase A was mixed and heated to 70 °C under stirring using a helix stirrer until completely dissolution of the UV-filter. Then the oil phase was homogeneous, phase B1 was added under stirring.

BASE-1 was dissolved in water and stirred with a U plate stirrer (phase B2). First, glycerin and second, phase A-B1 were added slowly into phase B2. After homogenization BA1 was added slowly keeping a while between additions and it was let under stirring for 10 min at 70 rpm. Further, as viscosity increased, the spin was sped up to 100 rpm.

Results and discussion:

The aspect of the emulsion was white yellowish. The spreadability increased compared to the previous formulation (O/W bioadhesive emulsion 6-1). Although there was an oily feeling after spreading on the ski. As a remark the formulation should be at room temperature before adding BA1 to enhance the homogeneity of the final product.

c) O/W bioadhesive emulsion 6-3

The present emulsion was almost identical to emulsion 6-2 since the amount of glycerin was slightly reduced and the emollient content was increased (Table 5-20). The aim of this emulsion was to decrease the stickiness and viscosity.

Table 5-20. O/W bioadhesive emulsion 6-3

	Ingredient family	Trade name	INCI	6-3
A	Emulsifier	Span™ 60	Sorbitan oleate	2,00
	Emollient	Myritol 318	Caprylic/Capric Triglyceride	12,00
	Preservative	Euxyl PE9010	Phenoxyethanol, Ethylhexylglycerin	1,00
	broad spectrum filter	Tinosorb S	Bis-ethylhexyloxyphenol methoxyphenyl Triazone	5,00
B1	Emulsifier	Tween™ 20	Polysorbate 20	4,00
	Solvent	Solvent-G	Solvent-G	24,00
B2		Water	Aqua	ad. 100
		BASE-1	BASE-1	3,00
	Moisturizing agent	Glycerin	Glycerin	1,00
C	Bioadhesive agent	BA1	BA1	3,00

Procedure:

See section b) Bioadhesive O/W emulsion 6-2 as the same manufacturing procedure was used.

Results and discussion

The emulsion was homogeneous and like O/W emulsion 6-2 with some improvements. The viscosity and stickiness were slightly decreased. The decrease of stickiness contributed to a higher dry effect after-feel.

d) Bioadhesive O/W emulsion 6-4

Bioadhesive emulsion O/W 6-4 differs from bioadhesive emulsion O/W 6-3 by the addition of ethanol (Table 5-21). Ethanol was added to the formulation so that the SPF as well as the spreadability could be increased. This can be explained as the addition of ethanol increases the fluidness of the cream and by this a better spreadability is achieved. However, once the

cream is well distributed onto the skin ethanol evaporates and the concentration of the UV-filters increases, which means the SPF of the cream could increase as well.

Table 5-21. O/W bioadhesive emulsion 6-4

	Ingredient family	Trade name	INCI	6-4
A	Emulsifier hydrophile	Span™ 60	Sorbitan oleate	2,00
	Emollient	Myritol 318	Caprylic/Capric Triglyceride	12,00
	Preservative	Euxyl PE9010	Phenoxyethanol, Ethylhexylglycerin	1,00
	broad spectrum filter	Tinosorb S	Bis-ethylhexyloxyphenol methoxyphenyl Triazone	5,00
B1	Emulsifier	Tween™ 20	Polysorbate 20	4,00
	Emollient hydrophile	Solvent-G	Solvent-G	24,00
B2		Water	Aqua	ad. 100
		BASE-1	BASE-1	3,00
	Solvent	Ethanol	Ethanol	30,00
	Moisturizing agent	Glycerin	Glycerin	1,00
C	Bioadhesive agent	BA1	BA1	3,00

Procedure:

See section b) O/W bioadhesive emulsion 6-2 as the same manufacturing procedure was used.

Results and discussion

Smooth consistency and homogeneous, yellowish fluid emulsion. Ethanol smell. It absorbed properly on skin, easy to spread and colorless after its application. The emulsion may decrease skin moisture. To improve the formulation the ethanol content should be decreased.

e) O/W bioadhesive emulsion 6-5

Increase of BA1 content (x2 respect to 6-02) to increase the adhesiveness. The manufacturing procedure was changed (only two phases, see Table 5-22).

Table 5-22. Bioadhesive O/W emulsion 6-5

	Ingredient family	Trade name	INCI	6-5
A	Emulsifier	Span™ 60	Sorbitan oleate	2,00
	Emollient	Myritol 318	Caprylic/Capric Triglyceride	12,00
	Preservative	Euxyl PE9010	Phenoxyethanol, Ethylhexylglycerin	1,00
	broad spectrum filter	Tinosorb S	Bis-ethylhexyloxyphenol methoxyphenyl Triazone	5,00
B		Water	Aqua	ad. 100
		BASE-1	BASE-1	3,00
	Emulsifier	Tween™ 20	Polysorbate 20	4,00
		Solvent-G	Solvent-G	24,00
	Moisturizing agent	Glycerin	Glycerin	1,00
C	Bioadhesive agent	BA1	BA1	6,00

Procedure:

The ingredients of the oily phase (A phase) were stirred and heated to 80 °C. In the water phase (B phase) BASE-1 dissolved in water under U plate stirring. When BASE-1 was completely dissolved in water Tween™ 20, propilenglycol and glycerin were added to the solution. Phase A was added slowly to phase B under stirring (using a U plate stirrer) and let cool down to room temperature. Finally, BA1 was added stepwise waiting until the powder was homogenized in the formulation.

Results and discussion:

The emulsion was highly adhesive. It was considered highly sticky for the skin and did not absorb well. A sticky film was perceived on the skin.

f) Bioadhesive emulsion O/W 6-6

New UV-filters were added to the formulation 6-5; ethylehexyl triazone (EHT), diethylamino hydroxybenzyl hexyl benzoate (DHHB) and tris biphenyl triazine (TPBT), which are a UVB-, UVA and a broad-spectrum filter, respectively. These UV-filters were added to the formulation to achieve the first goal, in which the SPF should be at least 30. With this filter combination, a high filter efficiency was achieved (filter efficiency = 3,7, Table 5-23). Moreover, the UVA/UVB was higher than 1/3 accomplishing the rule to enable the UVA label of the sunscreen (Table 5-24). Two versions of 6-6 were made because of the differences in the last step in the manufacturing procedure consisting in adding BA1 and then tris biphenyl triazine (emulsion 6-6.2) or adding first tris biphenyl triazine and then BA1 (emulsion 6-6.1). These two different versions served to evaluate if the manufacturing procedure could influence the final formulation.

Table 5-23. In silico UV-filter parameters for the filters contained in bioadhesive emulsion O/W 6.6

Parameters	
SPF	59,2
Rating	50
Filter efficiency	3,7
UVA PF	18,9
UVA-PF/SPF	0,32, PASS
Critical Wavelength	373

Table 5-24. Bioadhesive emulsion O/W 6-6).

	Ingredient family	Trade name	INCI	6-6
A	Emulsifier	Span™ 60	Sorbitan oleate	2,00
	Emollient	Myritol 318	Caprylic/Capric Triglyceride	12,00
	Preservative	Euxyl PE9010	Phenoxyethanol, Ethylhexylglycerin	1,00
	UVB-filter	Uvinul T 150	ethylhexyl triazone	4,00
	UVA Filter	Uvinul A Plus	Diethylamino Hydroxybenzoyl Hexyl benzoate	5,00
	broad spectrum filter	Tinosorb S	Bis-ethylhexyloxyphenol methoxyphenyl Triazone	5,00
B		Water	Aqua	ad. 100
	Base	BASE-1	BASE-1	3,00
	Solvent	Solvent-G	Solvent-G	24,00
	Moisturizing agent	Glycerin	Glycerin	1,00
	Emulsifier	Tween™ 20	Polysorbate 20	4,00
D	Bioadhesive agent	BA1	BA1	4,00
C	Broad spectrum filter	Tinosorb 2AB	Tris Biphenyl Triazine	3,00

Procedure:

The ingredients of the oily phase (A phase) were stirred and heated to 80 °C, when the mixture was homogeneous it was let cool down to room temperature. In the water phase (B phase) BASE-1 dissolved in water under U plate stirring. When BASE-1 was completely dissolved in water propilenglycol, glycerin and polysorbate 80 were added to the solution. Phase A was added slowly to phase B under stirring (using a U plate stirrer). The filter The emulsion was divided into two parts to evaluate if the manufacturing procedure in the final.

In version 6-6.1 tris biphenyl triazine was added first to the emulsion and once the emulsion was homogeneous BA1.

In version 6-6.2 BA1 was added first, then tris biphenyl triazine.

The emulsion was homogenized under turrax (Silverson L4R) for 1 min. Finally, the pH was adjusted to 6,5-7.

Results and discussion:

Bioadhesive emulsion O/W 6-6.1 was inhomogeneous. First the emulsion was yellow but after addition of biphenyl triazine turned white grey. After 24 h it had a gel-like texture. Bioadhesive emulsion O/W 6-6.2 had an aspect of a cream and was homogeneous. While in emulsion 6-6.1 4% BA1 was added, in 6-6.2 only 2,8% of the emulsion contained BA1 as with this percentage the emulsion was highly viscous and thus it was considered 2,8 % as enough of the adhesive ingredient. Over all 6-6.2 had better properties than 6-6.1.

6-6.2 was considered a cream with agreeable touch on the skin and good spreadable. Although after application, some whitening of the skin was observed, which may cause drawbacks to some customers, as a transparent layer is preferred over whitening of the skin after sunscreen application. Moreover, when scrubbing the sunscreen on the skin some small lumps formed.

g) Bioadhesive emulsion O/W 6-7

Tween™ 20 and Span™ 60 were replaced by acrylate copolymer to avoid lumps formation after scratching the emulsion on the skin. Moreover, the emollient Emollient-B was added. However, the total emollient concentration in the formulation remained constant. The emulsion was formulated according to emulsion 6-6.2. (see manufacturing procedure in section 3.5.5 f). Ethanol was added to the formulation at 10%, which is less than it was added in emulsion 6-4 (30 %) to decrease the skin dryness of formulation 6-4 (Table 5-25).

Table 5-25. Bioadhesive emulsion O/W 6-7

	Ingredient family	Trade name	INCI	6-7
A	Emollient	Emollient-B	Emollient-B	6,00
	Emollient	Myritol 318	Caprylic/Capric Triglyceride	6,00
	Preservative	Euxyl PE9010	Phenoxyethanol, Ethylhexylglycerin	1,00
	UVB-filter	Uvinul T 150	ethylhexyl triazone	4,00
	UVA Filter	Uvinul A Plus	Diethylamino Hydroxybenzoyl Hexyl benzoate	5,00
	broad spectrum filter	Tinosorb S	Bis-ethylhexyloxyphenol methoxyphenyl Triazone	5,00
B		Water	Aqua	28,40
		Ethanol	Ethanol	10,00
		BASE-1	BASE-1	3,00
	Moisturizing agent	Glycerin	Glycerin	1,00
	Filmformer / Thickener / Increase water resistance	Eudragit	Polymethacrylates	2,00
		Solvent-G	Solvent-G	24,00
D	Bioadhesive agent	BA1	BA1	1,00
C	Broad spectrum filter	Tinosorb 2AB	Tris Biphenyl Triazine	3,00

Procedure:

The ingredients of the oily phase (A phase, Table 5-25) were stirred and heated to 80 °C, when the mixture was homogeneous it was let cool down to room temperature. Polymethacrylates was dissolved into propilenglycol (phase C). BASE-1 was dissolved into water and ethanol with a U plate stirrer (phase B1), and after dilution Glycerin was added to phase B1. Phase C was versed into phase B1-B2, further phase A was versed into phase BC and the resulting emulsion was homogenized with thurax. Phase D was added to the emulsion. After the emulsion was homogenic phase E was added as well and it was homogenized with thurax. Finally, the pH was adjusted to 6,5-7.

It is worth outlining, that acrylate copolymer solubilizes in ethanol, although when adding water to the dissolution it precipitates. Therefore, it was dissolved in propilenglycol.

Results and discussion:

The water phase had a beautiful white color, with a jelly viscosity. Tween™ 20 colored the water part, therefore by replacing Tween™ 20 by acrylate copolymer may have changed the aspect of the water part.

Anyway, by addition of tris biphenyl triazine, the color changed. Opaque white drops of the UV-filter were found on the bottom of the beaker. While mixing it with the plate stirrer the emulsion got broken. However, if keeping stirring, the white crystals of Tinosorb M, finally were soluble in the emulsion and the final sunscreen turned white.

The emulsion was a little sticky and let some whitening of the skin, probably to the use of the white opaque UV-filter tris biphenyl triazine. However, a positive point was that lumps were not formed after scrubbing of the cream on the skin.

h) Bioadhesive emulsion O/W 6-8

The aim was to reduce the whitening effect of the sunscreen on the skin. Therefore, the UV-filter tris biphenyl triazine was replaced by Methylene Bis-Benzotriazolyl Tetramethylbutylphenol (nano) (MBBT), (BEMT) was replaced by the same filter but in water suspension to be added to the water phase of the emulsion. With these UV-filters the label UVA as well as a SPF of 50+ was achieved (Table 5-26).

The decision to use also water-soluble filters was made to reduce the oil phase. Moreover, it has proven to increase the stability, especially in sunscreens with high SPF (3). The proportion of Emollient-B: Caprylic/Capric Triglyceride (50:50) was modified to (42:58) maintaining the total emollient concentration in the emulsion, as Caprylic/Capric Triglyceride has very nice skin feeling.

The thickener xanthan gum was added to the water phase to make the emulsion more viscous than 6-7.

Table 5-26. Bioadhesive emulsion O/W 6-8

	Ingredient family	Trade name	INCI	6-8
A	Emollient	Emollient-B	Emollient-B	5,00
	Emollient	Myritol 318	Caprylic/Capric Triglyceride	7,00
	Preservative	Euxyl PE9010	Phenoxyethanol, Ethylhexylglycerin	1,00
	UVB-filter	Uvinul T 150	ethylhexyl triazone	5,00
	UVA Filter	Uvinul A Plus	Diethylamino Hydroxybenzoyl Hexyl benzoate	4,00
B1		Water	Aqua	ad. 100
		BASE-1	BASE-1	3,00
		EDTA	EDTA	1,00
	Thickener	xanthan gum	xanthan gum	0,50
	broad spectrum filter	Tinosorb S Lite Agua	Bis-ethylhexyloxyphenol methoxyphenyl Triazone	5,00
	broad spectrum filter	Tinosorb M	Methylene/Bisbenzotriazolyl TetraMethylbutylphenol (nano)	5,00
	Moisturizing agent	Glycerin	Glycerin	1,00
B2		Ethanol	Ethanol	10,00
C	Film former / Thickener / Increase water resistance	Eudragit	Polymethacrylates	2,00
		Solvent-G	Solvent-G	24,00
D	Bioadhesive agent	BA1	BA1	1,00

Calculated SPF= 64,1

Rating= 50+

Filter efficiency= 3,37

Procedure:

The ingredients of the oily phase (A phase, Table 5-26) were stirred and heated to 80 °C, when the mixture was homogeneous it was let cool down to room temperature. Polymethacrylates was dissolved into propilenglycol (phase C). In the water phase (phase B1) BASE-1, EDTA, xanthan gum, (MBBT), (BEMT) and Glycerin were dissolved into water with helix stirrer. Further ethanol was added into Phase B1. Phase C was added into phase B and afterwards phase A was given to phase BC. Last, phase D was added slowly to the emulsion (phase ABC), homogenized 1 min with turrax and its pH was adjusted (pH= 6,5-7).

Results and discussion:

The texture of the emulsion was very dense and therefore one of the thickeners should be enough to reach the wanted degree of consistence of the emulsion. However, the emulsion was homogeneous and corresponded with the expectations. First it had an agreeable touch on skin, high spreadable and was well absorbed by the skin without leaving any whitening effect on the skin after its application.

i) Bioadhesive emulsion O/W 6-9

In this emulsion is like emulsion 6-8 as most of the ingredients in 6-9 were already used in emulsion 6-8. However, minor changes were made. Based on emulsion 6-8 the following objectives were set. First, formulate a slightly more fluid emulsion. Therefore, xanthan gum was excluded from the formulation. Second, change the percentages of the two ingredients maintaining the total emollient content. Therefore, the amount of Emollient-B was decreased and Caprylic/Capric Triglyceride increased. Third, compare the stickiness with acrylate polymer (emulsion 6-8) and without the addition of acrylate polymer emulsion (6-9). Fourth, make a colored formulation to be used as BB cream. This was done by adding TiO₂ with a color coating (Table 5-27).

Table 5-27. Bioadhesive emulsion O/W 6-9

	Ingredient family	Trade name	INCI	6-9
A	Emollient	Emollient-B	Emollient-B	3,00
	Emollient	Myritol 318	Caprylic/Capric Triglyceride	9,00
	Preservative	Euxyl PE9010	Phenoxyethanol, Ethylhexylglycerin	1,00
	UVB-filter	Uvinul T 150	ethylhexyl triazone	5,00
	UVA Filter	Uvinul A Plus	Diethylamino Hydroxybenzoyl Hexyl benzoate	4,00
B1		Water	Aqua	ad. 100
		BASE-1	BASE-1	3,00
		EDTA BD	Disodium EDTA	1,00
	broad spectrum filter	Tinosorb S Lite Aqua	Bis-ethylhexyloxyphenol methoxyphenyl Triazone	5,00
	broad spectrum filter	Tinosorb M	Methylene Bis-Benzotriazolyl Tetramethylbutylphenol (nano)	5,00
	Moisturizing agent	Glycerin	Glycerin	1,00
B2		Ethanol	Ethanol	10,00
C	Film former/ Thickener/ Increase water resistance	Eudragit	Polymethacrylates	2,00
		Solvent-G	Solvent-G	24,00
D	broad spectrum filter	TiO2 color	TiO2	0,50

Procedure:

See the manufacturing procedure on section b) O/W bioadhesive emulsion 6-8 as the same manufacturing procedure was used.

Results and discussion:

The emulsion was fluid. Although in this degree was not wanted. Probably the fact that acrylate was not used in this emulsion contributed to the low viscosity of the emulsion. The color coped with the emulsion. All in all, the cream was satisfactorily. However, the viscosity had to be improved (Table 5-28).

W/O bioadhesive emulsions

a) Bioadhesive emulsion W/O 7-1

This emulsion was designed to define the external phase (O/W, W/O) which would be most suitable regarding the organoleptic properties. The same ingredients in the same concentration 6-1 were used except for the emulsifier, which is suited for water in oil. The external phase was oil instead of water (Table 5-28).

Table 5-28. Bioadhesive emulsion W/O 7-1

	Ingredient family	Trade name	INCI	7-1
A	Emulsifier	Stileeze 2000	Vinilpirolidone polimetacrilate Acrylic acid	4,00
	Emollient	Myritol 318	Caprylic/Capric Triglyceride	12,00
	Preservative	Euxyl PE9010	Phenoxyethanol, Ethylhexylglycerin	1,00
	Broad spectrum filter	Tinosorb S	Bis-ethylhexyloxyphenol methoxyphenyl Triazone	5,00
B		Water	Aqua	ad 100
		BASE-1	BASE-1	3,00
	Moisturizing agent	Glycerin	Glycerin	2,00
	Emollient	Solvent-G	Solvent-G	24,00
C	Bioadhesive agent	BA1	Policarbofile	3,00

Procedure:

The ingredients of phase B were mixed with a U plate stirrer.

The ingredients of the phase A were heated to 75 °C and mixed together with an helix stirrer and was let cool down to room temperature. Phase B was added to phase A under stirring. Finally, BA1 was added slowly under stirring with the U plate stirrer.

Results and discussion:

The emulsion was homogeneous and white yellowish (because of the use of the filter, which is yellow). The emulsion highly sticky and the spreadability was very low. According to its organoleptic properties is preferable to use the oil phase as inner phase of the emulsion (O/W) rather than the other way (W/O).

Bioadhesive emulsions O/W non-comedogenic

The aim of emulsions 6-10 to 6-16 was to design and produce non-comedogenic bioadhesive emulsions.

In a previous publication (153) ingredients were tested for their comedogenic potential and graded from 0 to 5 (0-1, no significant increase in follicular keratosis; 2-3, a moderate increase in follicular keratosis; 4-5, an extensive increase in follicular keratosis) according to the degree of comedogenicity (occlusive pore which may develop in acne, black and whitehead induction) (206).

Comedogenic ingredient are those which clog pores avoiding the transpiration of the skin.

The comedogenicity of different types of ingredients was assessed with the rabbit ear assay, as the ear rabbit is a fast method (rabbits develop follicular keratosis much early than humans (2 weeks compared to the six weeks in humans) and are very sensitive to comedogen substances.

This publication covered a wide range of ingredients used in cosmetic. Although since the publication is from 1989 and new ingredients have been marketed some very popular ingredients are missing. However, suspected ingredients for being potential comedogenic are greasy ingredients which cover pores and trigger an inflammation. Therefore, ingredients, especially emollients which were graded with 0-1 were implemented in the emulsions designed to be non-comedogenic.

Therefore, in these formulations some colours were used with different meanings; green stand for a listed con-comedogenic substance, blue meant not listed as non-comedogenic substance but used in a sunscreen labelled non-comedogenic and violet for recommended substance for combining with PRE-A according to the patents WO16206961, WO16206962, WO16206963, WO17036662, WO17102300, WO17102301, WO17102302, and WO17129432 by Beiersdorf (144,192–197,207)

However, for labelling a final product as non-comedogenic, a clinical trial needs to be done to ensure that it is not inducing acne in humans.

O/W non-comedogenic bioadhesive emulsion 6-10, 6-11, 6-12

Based on O/W bioadhesive emulsion 9 three versions of non-comedogenic O/W emulsions were designed.

- 6-10: As emollient caprylic/capric triglyceride was used as it is a listed non-comedogenic emollient (181). (Table 5-29)

- 6-11: The non-comedogenic emollients caprylic/capric triglyceride and Emollient-B, which is an emollient used in non-comedogenic sunscreens, like (208). The same emollient concentration as 6-10 was used (Table 5-29).

- 6-12: This emulsion was similar to 6-11, however the thickener concentration in the oil phase was lower and xanthan gum (the thickener in the water phase) was not used. (Table 5-29).

Table 5-29. Bioadhesive emulsion O/W non-comedogenic 6-10, 6-11 and 6-12

	Ingredient family	Trade name	INCI	6-10	6-11	6-12
A	Emollient	Mygliol 318	Caprylic/capric Triglyceride	10,00	5,00	5,00
	Emollient	Emollient-B	Emollient-B	/	5,00	5,00
	Preservative	Euxyl PE9010	Phenoxyethanol, Ethylhexylglycerin	1,00	1,00	1,00
	UVB-filter	Uvinul T 150	ethylhexyl triazone	5,00	5,00	5,00
	UVA Filter	Uvinul A Plus	Diethylamino Hydroxybenzoyl Hexyl benzoate	4,00	4,00	4,00
B1		Water	Aqua	ad. 100	ad. 100	ad. 100
		BASE-1	BASE-1	3,00	3,00	3,00
		EDTA BD	Disodium EDTA	1,00	1,00	1,00
	Thickener, emulsion stabilizer	xanthan gum	xanthan gum	0,50	0,50	0,20
	broad spectrum filter	Tinosorb S Lite Aqua	Bis-ethylhexyloxyphenol methoxyphenyl Triazone	5,00	5,00	5,00
	broad spectrum filter	Tinosorb M	Methylene Bis-Benzotriazolyl Tetramethylbutylphenol (nano)	5,00	5,00	5,00
	Moisturizing agent	Glycerin	Glycerin	1,00	1,00	1,00
B2		Ethanol	Ethanol	10,00	10,00	10,00
C	Film former/Thickener/ Increase/water resistance	Eudragit	Polymethacrylates	2,00	2,00	2,00
	Solvent	Solvent-G	Solvent-G	24,00	24,00	24,00
D	Bioadhesive agent	BA1	BA1	1,00	1,00	1,00

Procedure

Ingredients in phase A were heated at 70 °C and mixed under stirring with helix stirrer. After phase A was homogeneous it was let cool down. Phase C was mixed under stirring in a

separate beaker. Separately, ingredients of phase B1 were mixed (first BASE-1 was dissolved in water, followed by EDTA, xanthan gum, the UV filters and glycerin (Table 5-29). Ethanol was added to phase B1 slowly under stirring. After the mixture B1-B2 was homogeneous, phase A was added. Further phase C was added to phase AB1-B2. When all components were integrated in the emulsion phase D was added and further the bioadhesive emulsion was homogenized with turrax. Finally, the pH was adjusted between 5,5 and 6,5.

Results:

Emulsion 6-12 was the best formulation compared to the other two 6-10, 6-11 as it was homogeneous and its consistency was fluid (not liquid) but also not very dense. It had an optimal spreadability, the white color of the cream turned transparent on skin after application. While the cream was a little sticky after immediate application, after 20 minutes the sticky feeling disappeared leaving a dry touch-like feeling.

The other two emulsions 6-10, 6-11 were of high quality as well. Formulation 6-11 had a nicer touch on skin and better spreadability than 6-10. However, its density was very high compared to 6-12.

a) Bioadhesive emulsion O/W non-comedogenic 6-13

Based on the composition of formulation 6-12, some changes were made (Table 5-30) which were:

- Replacing Polymethacrylates by a combination of emulsion stabilizers, viscosity controlling agents and emulsifier, to increase its stability consisting of:
 - Arachidyl Alcohol: emulsion stabilizers and viscosity controlling agent.
 - Behenyl Alcohol: emulsion stabilizers, viscosity controlling agent
 - Arachidyl Glucosidase: emulsifier

This combination is non-comedogenic, hypoallergenic and has a matte finish: Moreover, it is certified with COSMOS approval as it is 100% natural origin (209).

Polymethacrylates was replaced for its stickiness on the skin (causing an unagreeable sensation on the skin), its white appearance (producing slight whitening of the skin) and some toxicological issues (mostly irritation) (210).

- The addition of the emollient Emollient-C and the decrease of the concentration of caprylic/capric triglyceride and Emollient-B. Emollient-C is an emollient with a dry touch feeling and therefore it was added into the formula. The overall emollient concentration increased only 1%.
- The thickener concentration decreased to decrease emulsion's 6-12 viscosity.
- Safic alcan was added to the formulation as it absorbs sebum, reducing the greasiness of the emulsion. It has a mattifying effect on skin.
- Glycerin concentration was slightly reduced to decrease the stickiness of the emulsion, although preserving their adherence on the skin.
- Diethylamino hydroxybenzoyl hexyl benzoate (DHHB) was discarded. Nevertheless, to achieve an SPF of 50+ BEMT and MBBT were increased, both to 7%. These changes were made as it has been shown that DHHB interacts with avobenzone causing a destabilization of DHHB thus reducing its photostability (140), see explanation in section 1.3.3 photodegradation. As the final version of the emulsion will contain PRE-A, which is a precursor of avobenzone, DHHB should be avoided.

Table 5-30. Bioadhesive emulsion O/W non-comedogenic 6-13

	Ingredient family	Trade name	INCI	6-13
	Emulsion stabilizer and viscosity controller, emulsifier	Emulsifier-A	Emulsifier-A	3,00
A	Emollient	Mygliol 318	Caprylic/capric Triglyceride	3,00
	Emollient	Emollient-B	Emollient-B	3,00
	Emollient	Emollient-C	Emollient-C	4,00
	Preservative	Euxyl PE9010	Phenoxyethanol, Ethylhexylglycerin	1,00
	UVB-filter	Uvinul T 150	ethylhexyl triazone	5,00
	Oil control	Dry flo plus	Aluminum Starch Octenylsuccinate	0,05
B1		Water	Aqua	ad. 100
		BASE-1	BASE-1	2,40
		EDTA BD	Disodium EDTA	1,00
	broad spectrum filter	Tinosorb S Lite Aqua	Bis-ethylhexyloxyphenol methoxyphenyl Triazone	7,00
	broad spectrum filter	Tinosorb M	Methylene Bis-Benzotriazolyl Tetramethylbutylphenol (nano)	7,00
	Moisturizing agent	Glycerin	Glycerin	0,80
B2		Ethanol	Ethanol	10,00
		Solvent-G	Solvent-G	24,00
D	Bioadhesive agent	BA1	BA1	1,00

Calculated SPF= 68,5

Rating= 50+

Filter efficiency= 3,61

UVA-PF= 0,34, PASS

Results:

The result was a smooth emulsion with a pleasant and dry touch with optimal spreading on the skin, thanks to its emollients. The sunscreen was white in color and fluent however not dense or viscous. While spreading some whiteness was noticed. However, its slightly, almost imperceptible whitening effect disappeared very quickly. Some stickiness was perceived after application pointing out their bioadhesiveness and water resistance. The formulation was paraben and silicone free, however the emulsion was able to feel in some skin imperfections as scars (like post-acne scars), pores or wrinkles. The emulsion is non comedogenic as well as non-irritant. Moreover, it offers a very high protection (SPF 50+) covering the entire UVA and UVB spectra with UVA labeling. Regarding the UV filters they are ones of the safest for humans as well as for marine animals or coral reefs. In humans, their penetration onto the skin is very low, linked to their chemical structure. It is ocean safe as the three UV filters are photostable and therefore they do not break or form second metabolites that could interfere with other substances causing toxicological issues.

5.3.3 Formulation process: Organoleptic evaluation

After this exploration on the formulation type and ingredients to match best with the bioadhesive gel in developing a bioadhesive sunscreen a more systematic formulation development was done based on previous findings:

a Bioadhesive gels

Bioadhesive gels (Table 5-31) were formulated with minimal differences. Bioadhesive gel 1 was adapted from the original bioadhesive gel (Table 5-16).

Phase B ingredients were added slowly into phase A using a U-shape stirrer (Table 5-31). Phase BCD were added to the mixture. Finally, Phase E was added slowly under stirring, keeping sometime between additions until the phase was homogeneous.

Table 5-31. Ingredients of bioadhesive gel 1 and 2. Modifications on the formulation on Table 5-16.

	INCI ¹ name	Bioadhesive gel 1	Bioadhesive gel 2
Phase A	Deionized water	ad 100	ad 100
	BASE-1	3	3
Phase B	BA-booster-1	6	-
Phase C	Solvent-G	30	30
Phase D	Glycerin	2	2
Phase E	BA1	3	3

¹ International nomenclature of cosmetic ingredients

b Bioadhesive emulsions

Four emulsions containing a water and an oily phase with different formulation process (A-type, B-type) and base (W/O, O/W) containing the same ingredients and concentrations (Table 5-32).

Table 5-32. Bioadhesive emulsions (O/W and W/O) and bio-adhesive emulsions (O/W and W/O).

	INCI ¹ name	O/W Emulsion A	W/O Emulsion A	O/W Emulsion B	W/O Emulsion B
Phase A	Sorbitan stearate	-	-	2	4
	Caprylic/capric Triglyceride	12	12	12	12
	Penoxyethanol & Ethylhexylglycerin	1	1	1	1
	BEMT	4	4	4	4
Phase B	Deionized water	ad 100	ad 100	ad 100	ad 100
	BASE-1	2,4	2,4	2,4	2,4
	Polysorbate 80	-	-	4	2
	Solvent-G	24	24	24	24
	Glycerin	1,6	1,6	1,6	1,6
Phase C	BA1	2	2	2	2

¹ International nomenclature of cosmetic ingredients.

O/W emulsion A:

1. The ingredients were weighed separately in two different volumetric flasks. The ingredients of the oily phase (A phase) were stirred and heated to 75 °C.
2. In the gel phase (B phase) BASE-1 was dissolved into water under U-shape stirring. When the BASE-1 was dissolved, the other ingredients of the phase B were added.
3. Phase C was added stepwise to phase B until the powder was homogenized in the formulation.
4. Phase A was cooled down to 25 °C and was added into phase B-C under stirring. The lipogel was homogenized under Turrax for 1 min. Finally, the pH was adjusted to 5,5-6,5.

W/O emulsion A

Steps 1, 2 and 3 were equal as in O/W emulsion. However, phase B-C was added to phase A

O/W emulsion B

Steps 1 and 2 were equal as in O/W emulsion.

1. Phase A was let to cool down to 25 °C and was then added into phase B under stirring.
2. Then polycarbophil was added stepwise to phase A-B waiting until the powder was homogenized in the formulation. The emulsion was homogenized under thurax for 1 min. Finally, the pH was adjusted to 5,5-6,5.

W/O emulsion B

Steps 1, 2 and 4 were equal to the O/W emulsion. However, in step 3 phase B was added to phase A.

c Oil in water (O/W) emulsions (B-type)

The SPF was increased to a rating of 50+ (Table 5-33). Therefore UV-filters were added to the bioadhesive emulsion O/W B, which was the start for further formulation developments (see Table 5-33).

Emulsion 2: The filters EHT, DHHB and BEMT in the oil part and TBPT were added to O/W bioadhesive emulsion. Because TBPT is adhesive itself, BA1 was slightly decreased.

Emulsion 3: The filters EHT, DHHB, BEMT and TBPT were at the same concentration as in Emulsion 2. In addition, BA1 was five times decreased, sorbitan oleate and polysorbate 80 were replaced by Polymethacrylates and ethanol was added aiming to increase spread ability.

Emulsion 4: The UV-filters EHT and DHHB were added at the same concentration as in emulsion 1,2. However, the filter BEMT aqua was added in the water phase together with MBBT to reduce the oil phase and increase the formulation stability (3). Acrylic acid was added instead of sorbitan oleate and polysorbate 80 and BA1 was decreased (equal to emulsion 3). In addition, small amounts xanthan gum was added.

Emulsion 5: Xanthan gum was excluded from the formulation. The emollient concentration was slightly decreased.

Emulsion 6: Emollient-B was added, and Caprylic/capric Triglyceride was reduced, keeping the total concentration constant.

Oil in water (O/W) emulsions (B-type)

The formulation process of Emulsion 2 and 3 was the same:

1. The ingredients of the oily phase (phase A) were stirred and heated to 75 °C until the mixture was homogeneous and let cool down to 25 °C.
2. Meanwhile ingredients of phase C were mixed.
3. The ingredients in phase B1 were mixed with U plate stirrer, and after dilution glycerin (B2), was added to phase B1.
4. Phase C was versed into phase B1-B2
5. Phase A was versed into phase BC, further phase D
6. After the emulsion was homogeneous, phase E was added as well.
7. The emulsion was homogenized with turrax and the pH was adjusted to 5,5-6,5.

O/W emulsions (B-type)

Formulation procedure: Ingredients in phase A were heated at 75 °C and mixed under stirring with helix stirrer. After phase A was homogeneous it was cooled down. Phase C was mixed under stirring in a separate beaker. Separately, ingredients of phase B1 were mixed. Ethanol was added to phase B1 slowly under stirring. After the mixture B1-B2 was homogeneous, phase A was added. Further phase C was added to phase A-B1-B2. When all components were integrated in the emulsion phase D was added and further the bioadhesive emulsion was homogenized with turrax. Finally, the pH was adjusted between 5,5 and 6,5.

Table 5-33. Oil in water (O/W) emulsions(B-type).

	INCI ¹ name	O/W Emulsion 1		INCI ¹ name	Emulsion 2	Emulsion 3		INCI ¹ name	Emulsion 4	Emulsion 5	Emulsion 6
Phase A	Sorbitan stearate	4	Phase A	Sorbitan stearate	2	-	Phase A				
	Caprylic/capric Triglyceride	12		Caprylic/capric Triglyceride	16	16		Caprylic/capric Triglyceride	14	10	5
	Phenoxyethanol & Ethylhexylglycerin	1		Phenoxyethanol & Ethylhexylglycerin	1	1		Emollient-B Phenoxyethanol & Ethylhexylglycerin	- 1	- 1	5 1
	BEMT	5		BEMT	5	5					
				EHT	4	4		EHT	5	5	5
				DHHB	5	5		DHHB	4	4	4
Phase B	Deionized water	ad 100	Phase B1	Deionized water	ad 100	ad 100	Phase B1	Deionized water	ad 100	ad 100	ad 100
	BASE-1	2		BASE-1	2	2		BASE-1	2	2	2
	Glycerin	2	Phase B2	Glycerin	2	2		Glycerin	2	2	2
	Polysorbate 20	4	Phase C	Polisorbate 80	4	-		Xanthan gum	0,1	-	-
				Polymethacrylates	-	2		BEMT (aqua)	7	7	7
	Solvent-G	24		Solvent-G	24	24		MBBT	7	7	7
							Phase B2	Ethanol	10	10	10
Phase C	BA1	2	Phase D	BA1	4	1	Phase C	Polymethacrylates	2	2	2
								Solvent-G	24	24	24
			Phase E	TBPT	1	1	Phase D	BA1	1	1	1

¹ International nomenclature of cosmetic ingredients, ² *in silico* SPF = 43; rating 30; FE = 2,89, UVA-PF= 0,42, PASS,

³ *In silico* SPF = 79,1; rating 50+; FE = 3,44; UVA-PF= 0,52, PASS

Results: Organoleptic properties

In this study the organoleptic properties of a sunscreen product were determinant for its compliance and therefore after each formulation or group of formulations (gels and lipogels/emulsions) the six selected properties (see section 5.2.6) were evaluated to adapt and improve the sunscreen product.

a Gels

Between the two gels gel 2 (without BA-BOOSTER-1) was selected for being colorless, and non-sticky. Therefore, it was implemented in the subsequent formulations as the gel part.

b Emulsions A and B-type

The four emulsions performed well as for the lack of a white cast effect on skin after application. The emulsions type A, however, underperformed by showing poor homogeneity (caused by the presence of gel residues). Both emulsions type A and emulsions type B presented a yellowish color. The formulations with an oily base were highly spreadable unlike the W/O emulsion, which presented poor fluidity and left an unpleasant feeling on skin. Given that the O/W emulsion performed better overall, it was selected as the base for the subsequent stages in the development of the sunscreen product.

c O/W emulsions B-type

The results are presented in Figure 5-5. Starting with emulsion 1, gradual steps were made to improve the sensory performance. Volunteers did not know that emulsion 1 was the O/W emulsion they had previously evaluated. Therefore, their evaluation of emulsion 1 was unbiased; unlike that of emulsion 2 and all subsequent emulsions, which were compared to their predecessors. Emulsion 1 scored 2 points on fluidity, 3 points on spreadability, non-stickiness, pleasant skin feeling, and appearance, and 4 points on white cast effect. For emulsion 2, volunteers reported a decrease in spreadability and stickiness and an increase in white cast effect capacity compared to emulsion 1 ($2,4 \pm 0,6$, $2,0 \pm 0,6$ and $3,1 \pm 0,7$, respectively). Other organoleptic properties remained constant.

For emulsion 3 volunteers reported an increase in spreadability ($3,6 \pm 0,6$), non-stickiness ($3,0 \pm 0,5$), skin feeling ($3,0 \pm 0,4$) and appearance ($3,6 \pm 0,6$) compared to emulsion 2. The biggest improvement on emulsion 3 was its appearance, since emulsion 2, had caused some rashes on some participant's skin. In fact, rashes appeared following the application of all formulations containing sorbitan stearate and polysorbate 20, except in emulsion 3, as it did not contain these two ingredients. The other properties remained constant. In emulsion 4 the fluidity, non-stickiness, white cast effect, appearance and skin feel were improved ($2,4 \pm 0,7$, $3,9 \pm 0,4$, $4,6 \pm 0,5$, $4,6 \pm 0,5$ and $4,0 \pm 0,5$). In emulsion 5 had better organoleptic properties compared to emulsion 4 as the individual scores in the 6 categories were higher

Finally, no big differences were mentioned by volunteers between emulsion 5 and 6. However, more than half the participants praised the pleasant skin feel of emulsion 6, giving it the highest score ($4,7 \pm 0,7$). Emulsion 6 achieved the highest score in spreadability, fluidity, white cast effect, skin feel and appearance. Results are presented as the mean values of 20 volunteers, which were rounded to non-decimal numbers (Figure 5-5). The average values and standard deviation of the sensory results for type B emulsions 1-6 are listed in Table B3.

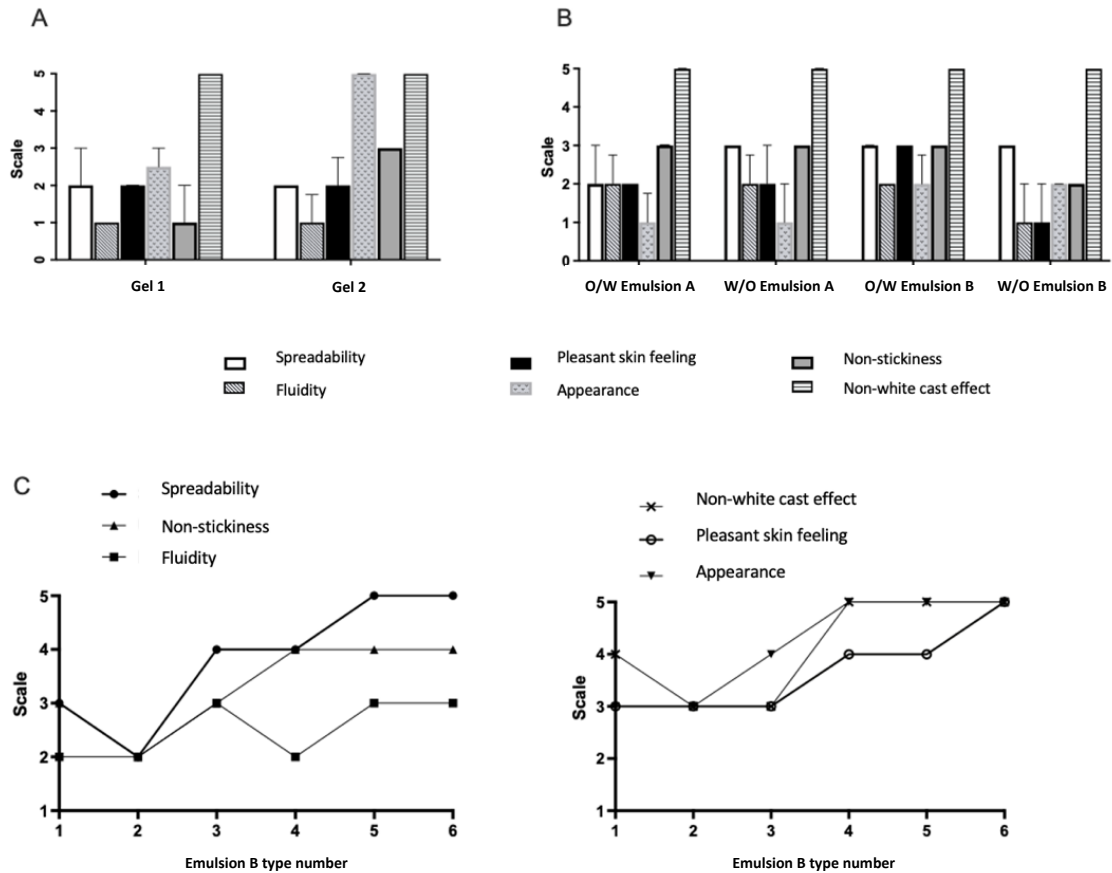


Figure 5-5. Organoleptic properties evaluated during the sensory test. The parameters evaluated were: spreadability, fluidity, pleasant feeling on skin, appearance, non-stickiness and non-white cast effect.

The formulation process of emulsion 6 is shown in Figure 5-6. The increase in the viscosity during the formulation steps was observed in all the emulsions. Such increment was gradual and can be divided into three parts. The oil and water phase had originally shown very low viscosity (Figure 5-6A). The viscosity increased following the mixture of the oil and water phase (Figure 5-6B). However, the highest increase in viscosity was observed after the addition of polycarbophil (Figure 5-6C).

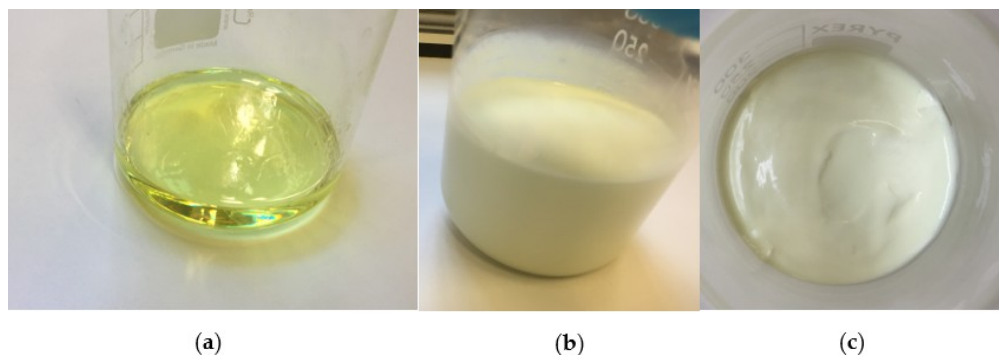


Figure 5-6. Formulation process of emulsion 6. (a) Oily phase (Phase A); (b) Phase ABC, after mixing all the ingredients except for polycarbophil (c) Final formulation

Discussion

Various formulations were developed from a gel (Table 5-3) with high skin retention. We reasoned that the incorporation of an oil phase was necessary since most organic UV filters are soluble in lipophilic solvents. The formulation ingredients were also carefully selected for safety reasons. After some initial testing, two gel ingredients were excluded from the formulation: BA-BOOSTER-1 and menthol. BA-BOOSTER-1 was sticky, thus causing an unpleasant feeling on the skin. Menthol caused a cooling effect on the skin, which was not considered a priority in the proposed product.

The selected volunteers evaluated the properties of various lipogels and emulsions in detail. In general, the O/W lipogel showed the best organoleptic properties among the O/W, W/O lipogels and the O/W, W/O emulsions. These properties were: spreadability, fluidity, pleasant sensation on the skin, appearance of the formulation, non-white cast and non-stick effect. Typically, O/W emulsions pleasant skin sensation is higher than W/O emulsion emulsions. Since water is in the external phase, when the emulsion is applied to the skin, water evaporates, producing a cooling effect on the skin. Volatile ingredients, such as ethanol, can also enhance this feeling of freshness. Otherwise, when the oil is in the external phase, which is the case with W/O formulations, a greasy texture is frequently reported (84).

The O/W emulsion (or emulsion 1) was further developed with the addition of UV filters to achieve SPF 30 with UVA protection according to COLIPA guidelines. In emulsion 2, the observed increase in the white cast effect may have been due to the addition of TBPT (given

that this UV filter has a grey tone). In turn, the addition of UV filters (5% in emulsion 1 vs. 15% in emulsion 2) and the increase in polycarbophil content in emulsion 2 may have contributed to a decrease in spreadability (compared to emulsion 1). The increase in non-stickiness, spreadability and fluidity in emulsion 3 were attributed to the addition of ethanol as well as the decrease in polycarbophil content.

Furthermore, in emulsion 4, a change in the development process and the selection of UV-filters may have affected the spreadability, non-stickiness and non-white cast effect. First, the replacement of TBPT by MBBT could have contributed to the improvement in non-stickiness and non-white cast effect because of the change in the formulation process. While TBPT was added in the last step of the formulation process, MBBT was added in the water phase together with ethanol. This different approach may have contributed to less stickiness as this UV filter is sticky by itself.

Second, the improvement in the formulation appearance may have been the result of replacing BEMT with BEMT aqua, after participants reported that emulsion 4 was whiter/less yellow than emulsion 3. This finding is not surprising, since the BEMT UV filter is characteristically yellow, while the BEMT aqua UV filter is optically much whiter. The decrease in thickeners in emulsion 5 may have been the cause for the increase in fluidity and spreadability. Finally, the increase in the beneficial feeling on skin in emulsion 6 may have been due to the partial replacement of caprylic/capric triglyceride with Emollient-B, as the latter emollient has a light, silky feeling (211). This may contribute to a better feeling on skin and therefore better improve user compliance.

Finally, the emulsion 6 was compared with bioadhesive O/W non-comedogenic emulsion 6-13 with almost identical scores on the six evaluated organoleptical properties (see Table A 4, Annex 2).

The bioadhesive O/W non-comedogenic emulsion 6-13 from now on named as bioadhesive emulsion 6-13 was stored in plastic tubes and glass jars for 12 months at real temperature conditions and humidity of Barcelona. After 12 months the bioadhesive emulsion 6-13 was assessed for its stability.

Evaluation of O/W emulsion 6-13: 24 h and 12 months post-manufacturing stored in a plastic tube.

5.3.4 Absorbance profile and stability of UV filters

The UV filters: Tinosorb T150, an UVB filter together with Tinosorb M and Tinosorb S Aqua Lite covered the UV spectrum (from 290-400 nm). The absorbance of the mixture of UV filters in bioadhesive emulsion 6-13 was measured on five difference positions of an PMMA plate before and after irradiation. The procedure was done on four different plates and the average is presented in Figure 5-7.

Bioadhesive emulsion 6-13 stored for 12 months was measured before and after irradiation using the same procedure, measuring the absorbance spectra of the average at five different positions and four different PMMA plates.

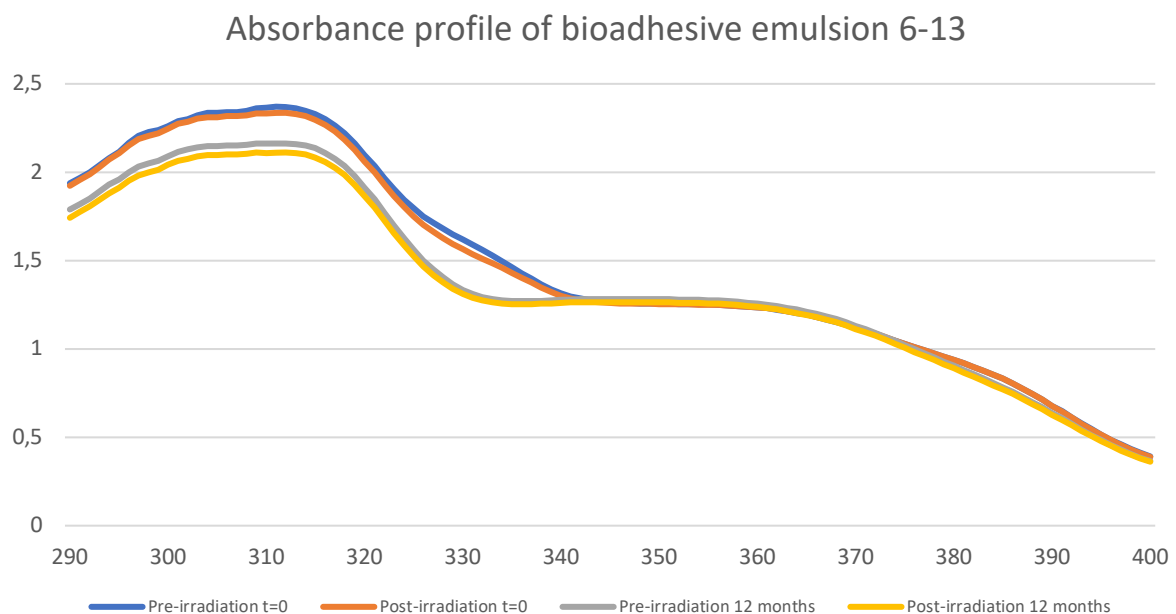


Figure 5-7. Spectra of the bioadhesive emulsion 6-13 at 24 h ($t=0$) and 12 months after formulation. Results before irradiation and after irradiation.

As results show, the four plates were included to the results as the coefficient “C” accomplished the ranges of 0.8 and 1,6 (Table 5-34).

Table 5-34. C coefficients, irradiation doses and exposure time of irradiation of the four plates included in the calculations.

t=0				
Plate	C Coeff.	Irradiation Dose (d)	Exposure Time (min)	Plate included in method results
1	0,89	12,75	28,1	True
2	0,92	13,77	30,4	True
3	0,85	13,62	30	True
4	0,91	14,12	31,1	True
t=12 months				
Plate	C Coeff.	Irradiation Dose (d)	Exposure Time (minutes)	Plate included in method results
1	1,03	14,76	32,5	True
2	0,95	14,86	32,8	True
3	0,95	17,24	38	True
4	0,92	16,62	36,6	True

Bioadhesive emulsion 6-13 was very photostable, both after 24 h and 12 months stored at 25 °C (Figure 5-7). The absorbance recovery after irradiation (28-31 min depending on the plate at 75,6 W/m², Table 5-34) for the emulsion measured 24 h after formulation at the wavelengths 310 nm and 377 nm were 98,7% and 100,1%, respectively. Similar results were observed for the bioadhesive emulsion 6-13 after 12 months of storage, as the difference in recovery between pre- and post- irradiation absorbances were 97,6% at 310 nm and 98,4% at 377 nm (Table 5-35).

Table 5-35. Extinction and recoveries of pre- and post-irradiated PMMA plates from the emulsion 6-13 after formulation (t=0) and after 12 months of storage at 25 °C.

Sample	Wavelength (λ)	Extinction	Recovery (%)
t=0 pre irradiation	310	2,36	100
t=0 post irradiation	310	2,33	98,7
t=0 pre irradiation	377	0,99	100
t=0 post irradiation	377	0,99	100,1

t=12 months pre irradiation	310	2,16	100
t=12 months post irradiation	310	2,10	97,6
t=12 months pre irradiation	377	0,97	100
t=12 months post irradiation	377	0,96	98,4

The content of the UV filters was determined by the resulting spectral absorbance of the bioadhesive emulsion 6-13 after 12 months storage at 25 °C compared to t=0. It was concluded that the bioadhesive emulsion 6-13 after 12 months storage at 25 °C was stable, as there was a difference not greater than 10% in the absorbance between the freshly made emulsion and after 12 months. The higher variation for the two timepoints was observed for the UVB, this accomplished the standards of the FDA on drug release (212). The recovery at the wavelength at the maximal extinction (310 nm) of the bioadhesive emulsion 6-13, which had the greatest divergence to the freshly made formulation showed 90,3% recovery (Table 5-36). Moreover, the recovery at the critical wavelength was 96,7%, which was only 3,3% difference to the freshly made formulation (Table 5-37).

Table 5-36. Absorbance and recovery of emulsion at t=0 and t=12 months at the wavelength at maximal extinction (post-irradiation absorbances).

Sample	Wavelength at maximal extinction (λ)	Maximal Extinction (at post-irradiation)	Recovery (%)
t=0	310	2,33549076	100
12 months	310	2,11028068	90,3570556

Table 5-37. Absorbance and recovery of emulsion at t=0 and t=12 months at lambda critical (post-irradiation absorbances).

Sample	Lambda critical (λ)	Maximal Extinction (at post-irradiation)	Recovery (%)
t=0	377	0,9930665	100
12 months	377	0,9603404	96,7

5.3.5 SPF, UVA-PF and other parameters

The SPF of the bioadhesive emulsion 6-13 was initially calculated with the amount of UV filter product weather than the active substance. The correct calculation procedure was later clarified by the supplier. In the case of Tinosorb 150 the amount of UV filter product equals the amount of active substance. However, for Tinosorb M and Tinosorb S, 1 g UV filter product equals 0,5 g and 0,2 g active substance, respectively. Therefore, the 7 g of Tinosorb M and 7 g of Tinosorb S inside the formulation contained 3,5 g and 1,4 g of active substance, respectively. This led to overrating of the absorbance and therefore to an overrating of the SPF and UVA *in vitro* values (Table 5-38 and Table 5-39).

Table 5-38. Calculated *in vitro* data at t=0 of the formulation 6-13. Pre and post irradiation results.

	t=0									
	PRE- irradiation (nr. of plates)					POST- irradiation (nr. of plates)				
	1	2	3	4	Average	1	2	3	4	Average
SPF Mean	116	101	144	105	116	88	104	141	105	110
SPF SD	31	10	28	9	19	17	10	8	11	11
SPF CoV	27	10	20	8	16	19	9	6	10	11
Lambda Critical Mean	377	377	377	378	377	377	377	378	377	377
Lambda Critical SD	0	0	1	0	0	1	0	1	0	0
Lambda Critical CoV	0	0	0	0	0	0	0	0	0	0
UVAPF Mean	11	12	11	12	11	10	11	12	11	11
UVAPF SD	2	1	2	1	1	1	1	1	1	1
UVAPF CoV	19	7	16	8	12	11	6	5	8	7
SPF/UVAPF Ratio Mean	11	9	12	9	10	9	9	12	9	10
SPF/UVAPF Ratio SD	1	0	1	0	1	1	0	1	0	0
SPF/UVAPF Ratio CoV	9	3	7	2	5	8	4	6	2	5
UVA/UVB Ratio Mean	1	1	1	1	1	1	0	1	0	1
UVA/UVB Ratio SD	0	0	0	0	0	0	0	0	0	0
UVA/UVB Ratio CoV	3	1	3	2	2	1	1	2	2	1

Table 5-39. Calculated *in vitro* data at t=12 months of the formulation 6-13. Pre and post irradiation results.

	t=12 months									
	PRE- irradiation (nr. of plates)					POST- irradiation (nr. of plates)				
	1	2	3	4	Average	1	2	3	4	Average
SPF Mean	65	89	89	101	86	57	92	75	91	79
SPF SD	10	17	24	14	16	11	16	0	23	13
SPF CoV	15	19	27	14	19	19	18	0	25	16
Lambda Critical Mean	377	376	378	378	377	377	377	378	378	378
Lambda Critical SD	0	1	0	0	0	0	0	0	0	0
Lambda Critical CoV	0	0	0	0	0	0	0	0	0	0
UVAPF Mean	12	12	15	14	13	12	13	13	13	13
UVAPF SD	1	2	3	1	2	1	2	0	2	1
UVAPF CoV	10	14	18	8	13	12	12	0	17	10
SPF/UVAPF Ratio Mean	5	7	6	7	6	5	7	6	7	6
SPF/UVAPF Ratio SD	0	0	0	0	0	0	0	0	1	0
SPF/UVAPF Ratio CoV	5	7	7	6	6	7	7	0	10	6
UVA/UVB Ratio Mean	1	1	1	1	1	1	1	1	1	1
UVA/UVB Ratio SD	0	0	0	0	0	0	0	0	0	0
UVA/UVB Ratio CoV	1	1	1	1	1	1	1	0	1	1

All in all, the average post-irradiation SPF of the bioadhesive emulsion 6-13 measured at t=0 was 110. On the other hand, the average SPF 12 months later was 79. This SPF values may be overrated as they were calculated from the adjustments from the C value, and a great difference is accepted (from 0,8-1,6). According to the results the average UVA PF at t=0 was 11 while at 12 months storage the UVA PF was 13 (values post irradiation). This increment in the UVA PF is beneficial for the emulsion. Other than a real increment in the UVA PF, it must have been the consequence of some small difference in weighting the amount of the filters Tinosorb S and Tinosorb M. Lambda critical was at 377 nm and the UVA/UVB ratio was 1.

As previously explained in the method subsection in this chapter 5.2.12, the “C” value is needed to fit the absorbance curve *in vitro* to the SPF *in vivo* value. The *in vitro* absorbance values are multiplied by the “C” value until the SPF *in vitro* equals the SPF *in vivo*. Therefore, the values of the absorbance curve obtained *in vitro* by the spectrophotometer are multiplied by the “C” value and the result of the multiplication is the adjusted curve (164).

To solve the problem with the “wrong” SPF, the “C” value was corrected. For this, the absorbance curve obtained by the spectrophotometer Labsphere 2000S (Figure 5-8) was adapted to the real “C” value by a factor of 1,6. This resulted in similar spectra compared to the results reported by the solar simulator (Figure 5-9).

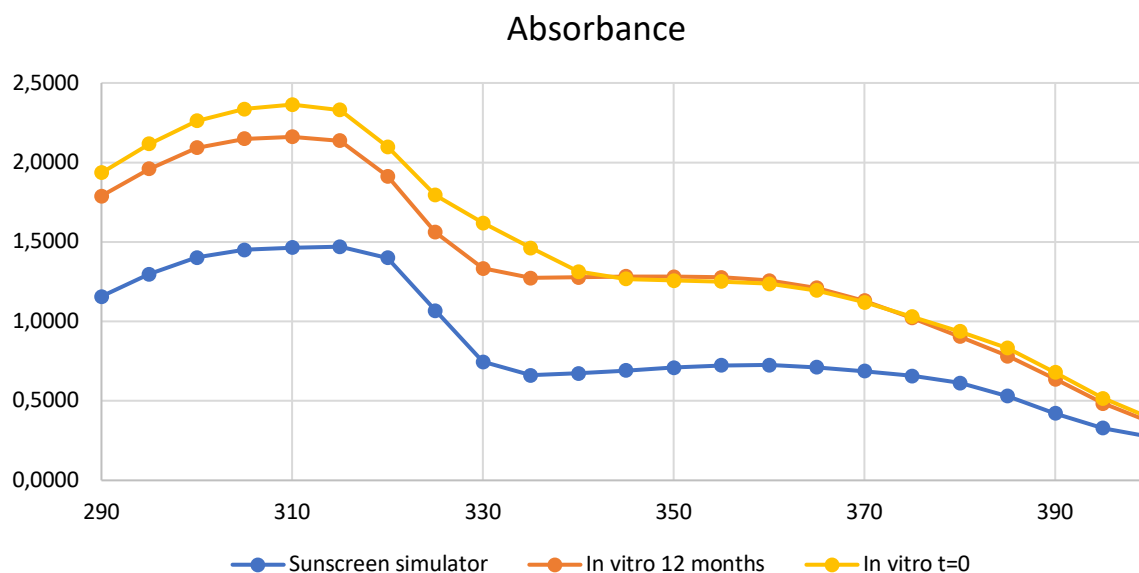


Figure 5-8. Absorbance spectra with the overestimated SPF of bioadhesive emulsion 6-13 at t=0 and at t=12 months (in vitro values) and the theoretical value given by the solar simulator.

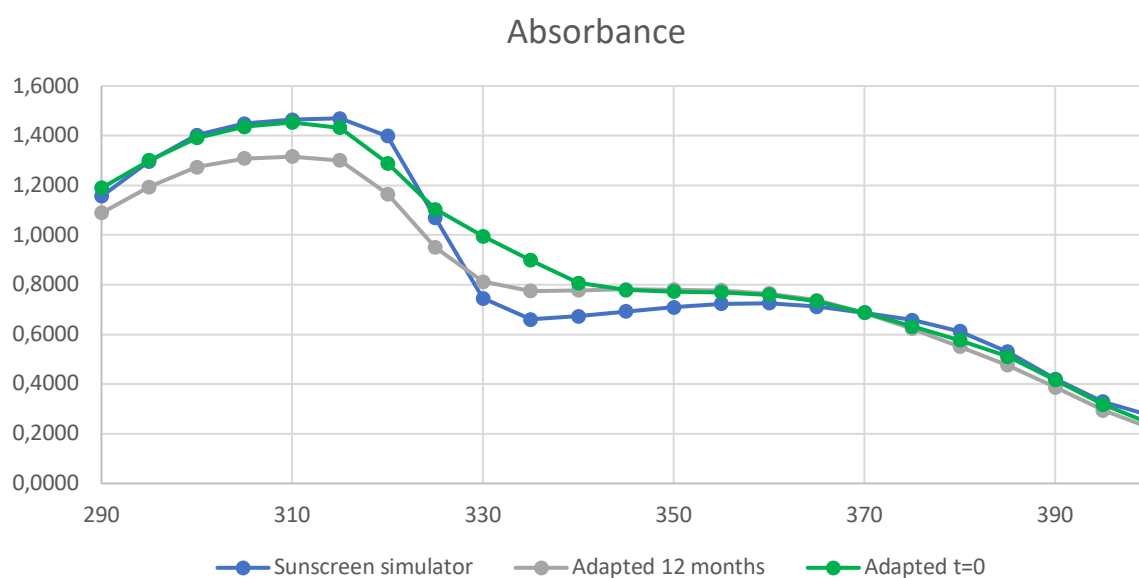


Figure 5-9. Absorbance spectra with the computer adjustment of the absorbance curves in vitro measurements at t=0 and at t=12 months of the bioadhesive emulsion 6-13 and its theoretical value given by the solar simulator.

According to Figure 5-9 the absorbance curve of the bioadhesive emulsion 6-13 is very similar to the theoretical value on the filter mixture given by the sunscreen simulator. Therefore, a similar SPF was estimated. A small difference in the absorbance spectra were noticed between 325 and 340 nm. The absorbance area of the bioadhesive emulsion 6-13 at t=0 was

higher in this section compared to the sunscreen simulator absorbance curve. This difference could be due to the absorbance effect of other ingredients contained in the emulsion. However, after 12 months this increased absorbance in this section was less pronounced.

With the application of Equation 5-16, the resulting SPF of the bioadhesive emulsion 6-13 was 34,3 at t=0 and 26,9 after 12 months storage. Otherwise, the UVA-PF was constant in time with an UVA-PF of 8,2 at t=0 and 8,4 for the 12 months formulation (Table 5-40).

$$SPF \text{ in vitro} = \frac{\int_{290 \text{ nm}}^{400 \text{ nm}} E(\lambda) * I(\lambda) * d\lambda}{\int_{290 \text{ nm}}^{400 \text{ nm}} E(\lambda) * I(\lambda) * T(\lambda) * d\lambda} \quad \text{Equation 5-16}$$

Table 5-40. Calculated SPF and UVA-PF of formulation 6-13 t=0 and of the one at 12 months.

	SPF	UVA-PF	UVA-PF/ SPF
Sunscreen simulator	33,5	7,5	0,23
t=0	34,3	8,2	0,23
12 months	26,9	8,5	0,31

On the other hand, the ratio UVA-PF/SPF was 0,23 and 0,31 for the bioadhesive emulsion 6-13 at t=0 and for this at 12 months, respectively. Therefore, it was not a broad-spectrum sunscreen. However, this was known and made on purpose as this formulation was designed as a base to contain the mixture of the filter avobenzone and PRE-A. However, the proportion of the two active ingredients was at that time still under investigation. However, this formulation was designed with the aim to be a broad-spectrum sunscreen product and have the UVA labelling on the packaging. According to the sunscreen simulator, the addition of 5% avobenzone should provide the necessary UVA PF to accomplish the 1/3 UVA PF/SPF ratio in order for the present emulsion to be a broad spectrum emulsion and be labelled as UVA compliant formulation (Figure 5-10 and Table 5-41).

The SPF of the bioadhesive emulsion 6-13 at t=0 was 34,3 and thus would be labelled as SPF 30. However, the absorbance capacity at the UVB fraction seems to slightly decrease after 1 year of storage, which in turn results in the decrease of the SPF (SPF=26,9), Table 5-41. Therefore, The UVB fraction of the absorbance spectra in (Figure 5-9) corresponds to Tinosorb T 150. This UV filter can crystallize after long time storage, because of supersaturation (213). Consequently, this may be the reason for the slight decrease in the UVB spectrum fraction of the bioadhesive emulsion 6-13 after 12 months storage.

However, with the addition of the mixture avobenzone and PRE-A should increase the absorbance spectra (Figure 5-10) also contributing to an increased SPF. The SPF would be at least SPF 30, as only with 5% addition of avobenzone an SPF 32,5 for the bioadhesive emulsion 6-13 and even a higher SPF 40 for the formulation at t=0 was reached in the simulation model.

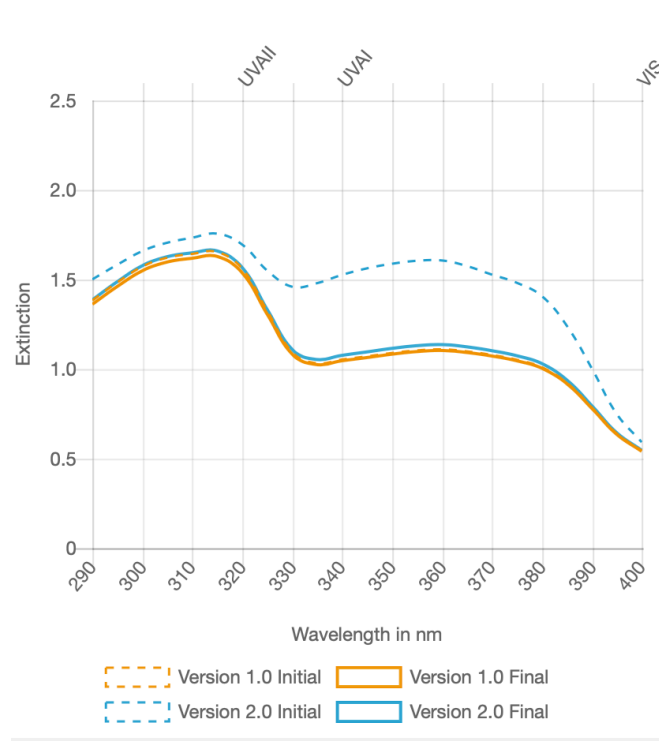


Figure 5-10. Absorbance spectra of Emulsion 6-13 (orange line) and Emulsion 6-13 with the addition of avobenzone (blue dots) (151).

Further, the bioadhesive emulsion 6-13 would have a constant UVA-PF 14,4 (UVA-PF 14,7 if the predictions of bioadhesive emulsion 6-13 are considered) and it would be broad-spectrum with the UVA label on the packaging. The UVA-PF/SPF would be according to the predictions

0,36 and 2,2 for the freshly prepared and the same emulsion after 1 year, respectively (Table 5-41).

Table 5-41. Theoretical values on SPF, UVA-PF, UVA-PF/SPF, UVA labelling and critical wavelength of the emulsion 6-13 without and with the addition of 5% avobenzone (151).

	Emulsion 6-13			Emulsion 6-13 with 5% avobenzone		
	sunscreen simulator	<i>In vitro</i> t=0	<i>In vitro</i> 12 M	(sunscr. simul.)	<i>In vitro</i> t=0 (simulation)	<i>In vitro</i> 12 M (simulation)
SPF	33,4	34,3	26,9	39	40,0	32,5
UVA-PF	7,6	8,2	8,5	13,8	14,4	14,7 (14,4)
UVA-PF/SPF	0,23	0,23	0,31	0,35	0,36	2,2
UVA labelling	No	No	No	Yes	Yes	Yes
Critical wavelength (nm)	379	377	378	379	377	378

5.3.6 pH

The pH of the bioadhesive emulsion 6-13 after 24 h storage was 5,7. Considering that the pH of the skin goes from 5,4 to 5,9 (176) , the obtained value fits the requirements.

5.3.7 Microscopy

In the microscopical view of the bioadhesive emulsion 6-13 after 24 h storage without the polycarbophil was observed that the droplets of oil phase were dispersed in the aqueous phase with droplets of a size between around 1-10 μm (Figure 5-11A). However, after the addition of the polycarbophil an only one phase was observed with structures which might correspond to the polycarbophil. The system was therefore more homogenic (Figure 5-11B). Therefore, the use of polycarbophil might enhance the physic-chemical system by homogenizing it and promoting the bond of the oil and aqueous phase. After 12 months stored at 25 °C no clumps or crystals were observed (Figure 5-11C).

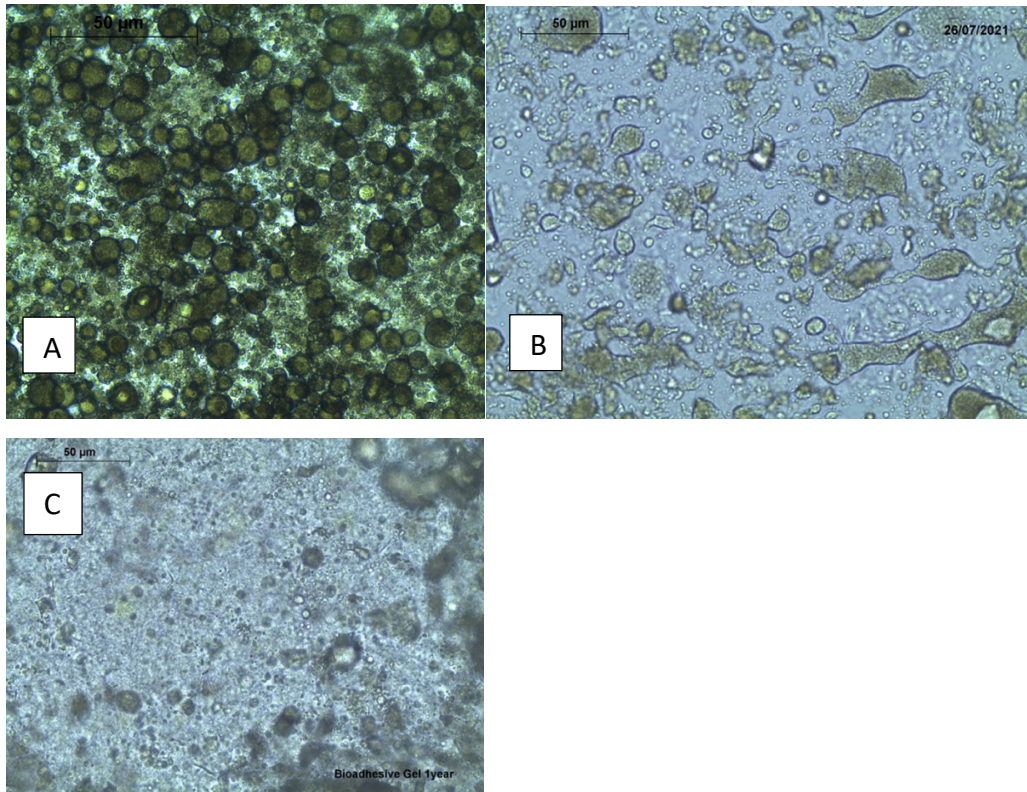


Figure 5-11. Microscopical view of the bioadhesive emulsion 6-13 A) without and B) with polycarbophil at $t=0$ (24 h post formulation) and C) after 12 months at 25 °C with polycarbophil

5.3.8 Rheology and viscosity

The results of the rheology and viscosity for the two measurements of the bioadhesive emulsion 6-13 are depicted in Figure 5-12A and Table 5-42 (corresponding to the first measurement) and Figure 5-12A and Table 5-43 (corresponding to the second measurement). The shear stress curve is present in light blue in Figure 5-12A and in dark blue Figure 5-12B in and can be expressed as the force applied on an area. On the other hand, the viscosity is the orange Figure 5-12A and red Figure 5-12B curves.

Both measurements show almost identical graphs in respect of shear stress and viscosity. This indicates a high reproducibility of the results (Figure 5-12A and Figure 5-12B).

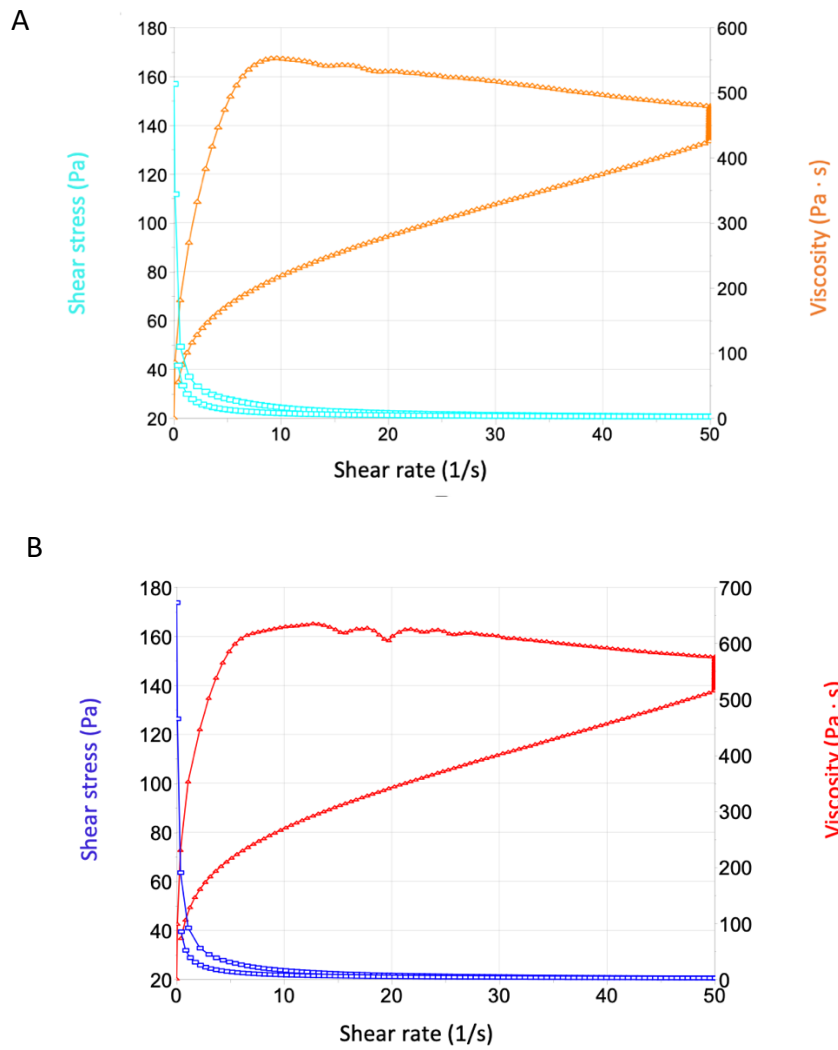


Figure 5-12. Graphical representation of the viscosity and shear stress of the bioadhesive emulsion. A) First measurement B) Second measurement

The flow curve is defined as the shear stress as a function of a shear rate (see section 5.2.9) with a is obtained ramp-up period, constant shear rate period and ramp-down period.

The data from the flow curves are fitted to different mathematical models listed in Table 5-42 and Table 5-43.

Table 5-42. Rheology: Mathematical model equation with ramp up and ramp down period results.

Model	Ramp up	Ramp down
Newton	-3,137 (out of range)	-0,8501 (out of range)
Bingham	0,2264	0,9785
Ostwald de Waele	0,6806	0,9946
Casson (lin)	0,4396	0,9933
Herschel-Bulkley	0,7422	0,9982
Cross	0,9821	0,9998

In the first measurement the correlation which fits best the curve corresponds to the Cross model, with a correlation coefficient equal to $r = 0,9821$ in the ramp-up period and $r = 0,9998$ in the ramp-down period (Table 5-42).

The average **viscosity** at 50 s^{-1} in the first measurement was $2,790 \pm 0,07930 \text{ Pa.s}$, which equals to **$2790 \pm 79,30 \text{ mPa.s}$** and has a **thixotropy of 2904 Pa/s** .

Table 5-43. Rheology: Mathematical model equation with ramp up and ramp down period results.

Model	Ramp up	Ramp down
Newton	3,304 (out of range)	0,8953
Bingham	0,2671	0,9781
Ostwald de Waele	0,7292	0,9946
Casson (lin)	0,4626	0,9932
Herschel-Bulkley	0,7917	0,9983
Cross	0,9901	0,9999

In the second measurement it was observed that the sample fits best to the **Cross model** as well, as confirmed by the correlation constants in Table 5-53 with a ramp-up period constant equal to $r = 0,9901$ and a ramp-down period equal to $r = 0,9999$.

The average **viscosity** at 50 s^{-1} in the first measurement was $2,874 \pm 0,07603 \text{ Pa}\cdot\text{s}$, which equals to **$2874 \pm 76,03 \text{ mPa}\cdot\text{s}$** and has a **thixotropy** of **2809 Pa/s** .

The similarity of both results indicates a very good reproducibility. Both measurements fit the cross model very well. However, the second measurement shows a slightly better correlation to the cross model with an $r = 0,9901$ in the ramp up period and an $r = 0,9999$ in the ramp down period compared to the first measurement ($r = 0,9821$ ramp up period, $r = 0,9998$ in the ramp down period). Only cross was taken into consideration as other models (Newton, Bingham, Ostwald de Waele, Casson and Herschel-Bulkley) did not fit that well compared to the cross model.

The cross model is indicative of pseudoplastic fluids. Pseudoplastic fluids are characterized by a viscosity decrease upon increase of shear rate: a so-called shear thinning behavior. This behavior is depicted in Figure 5-12A and Figure 5-12B. Therefore, the bioadhesive emulsion is a pseudoplastic (non-Newtonian) fluid, which is very common in face creams.

In addition, the bioadhesive emulsion shows thixotropy as the «up-curve» in the Figure 5-12A and Figure 5-12B do not overlap with the «down-curve» and the magnitude of the area that surrounds the hysteresis between these curves is defined as apparent thixotropy. In the bioadhesive emulsion the thixotropy is 2809 mPa/s (second measurement). Paints and glues are typical examples for thixotropic fluids. Therefore, it is not surprising that the bioadhesive emulsion presents thixotropy due to its adherent characteristics. Another characteristic of thixotropic behavior is that the three-dimensional structure that changed during the shear stress is restructured when keeping the fluid free of stress. It comes to its original conformation and therefore this process is probably reversible (214).

Finally, the viscosity of the bioadhesive emulsion is $2874 \pm 76,03 \text{ mPa}\cdot\text{s}$ (second measurement). The *ICH Harmonised tripartite guideline: stability testing of new drug substances and products Q1A(R2)* (169) classifies the viscosity of gels in three groups: low, medium and high viscosity. The limit the viscosity ranges of the different viscosities are listed in Table 5-44.

Table 5-44. Viscosity grades of gels (169).

Type of gel	Limits
Low viscosity	100-1000 mPa.s
Medium viscosity	1000-10000 mPa.s
High viscosity	10000-100000 mPa.s

The bioadhesive emulsion viscosity with $2874 \pm 76,03$ mPa.s is in the limit viscosity range of 1000 and 10000 mPa.s and therefore corresponds to a medium viscosity of a semi-solid gel.

5.3.9 Extensibility

The extensibility (single measurements and average of three measurements) of the bioadhesive emulsion 6-13 is shown in Table 5-45.

Table 5-45. Extensibility of the bioadhesive emulsion after 12 months post-manufacturing

Extensibility	
	S (mm ²)
	706,86
	706,86
	706,86
Average	706,86

The extensibility results were equal in the three measurements with an extensibility of 706,86 mm² for the bioadhesive emulsion 6-13 stored in a plastic tube and measured after 1 year Table 5-45. The standard deviation was 0 as the result for all the measurements was the same. In view of the results, the bioadhesive emulsion has a medium-to-high extensibility as the average extensibility of the sample is between 100 and 1000 which corresponds to a poor and high extensibility, respectively. Nevertheless 706,86 is (by a factor of 0,7) closer to 1000 than to 100 and therefore the extensibility of the sample tends to have high extensibility properties.

5.3.10 Bioadhesion

Ear skin is the *in vitro* substrate which was proven to be most effective to simulate human skin in terms of histological and physiological properties (215). Therefore, pig ear skin was used in the present method to assess bioadhesion as a substrate simulating human skin *in vitro*. The bioadhesive emulsion 6-13 tested right away and after 1-year post-manufacturing, here named as bioadhesive emulsion 2020 and bioadhesive cream 2021, respectively. A control positive, which was the bioadhesive gel (see Table 5-3, section 5.2.5) was tested. The bioadhesive behavior of the bioadhesive emulsion was compared with a commercial sunscreen product of SPF 50 with the label of water resistance. Finally, the bioadhesive emulsion 2021 was tested in wet environment to assess the bioadhesive behavior after being in contact with water. Therefore, the skin was wheaten with 5 mL of distilled water after spreading the bioadhesive emulsion 2021 into the skin.

The results of the bioadhesive test are presented in Table 5-46 (force of all sample measurements and average values within the vehicle) and Figure 5-13. Results show that there were significant differences ($p \leq 0.05$) between the blanc and the bioadhesive emulsions and gel and no significant difference was observed with the commercial sunscreen (represented with *). Moreover, when comparing the commercial sunscreen with the bioadhesive emulsions and gel, significant differences were observed at the level $p \leq 0.05$ (represented as #). This proves that the bioadhesive behavior is present in the bioadhesive emulsions and gel. Although the commercial sunscreen showed some bioadhesive behavior compared to the blanc it made such a small difference, that was concluded to be insufficient and therefore not bioadhesive. This finding was supported by the fact there were significant differences between the commercial sunscreen and all the bioadhesive vehicles as well, including the bioadhesive sunscreen after wet conditions.

In the box and whisker chart (Figure 5-14), it can be seen, that the bioadhesive emulsions are not overlaying with the results of the commercial sunscreen. There is a clear difference between of the gel and the bioadhesive emulsions 2020 and 2021. The wet bioadhesive

emulsion is also not overlapping with the commercial sunscreen. Therefore, the wet bioadhesive emulsion also shows bioadhesion.

Table 5-46. Bioadhesiveness test with pig ear skin substrates; samples measured, cream vehicles, and the results of bioadhesion: force, work and fracture strength.

Sample	Vehicle	Force (N)	Average (N)
0	Blank	0,08	0,08
1-5	Bioadhesive emulsion 2021	0,32 0,47 0,38 0,43 0,40	0,40
6-8	Bioadhesive emulsion 2020	0,33 0,42 0,38	0,38
9-11	Commercial sunscreen (water resistant)	0,08 0,16 0,11	0,12
12-14	Bioadhesive emulsion 2021 "wet skin"	0,17 0,23 0,24	0,21
15-17	Bioadhesive gel	0,45 0,43 0,36	0,41

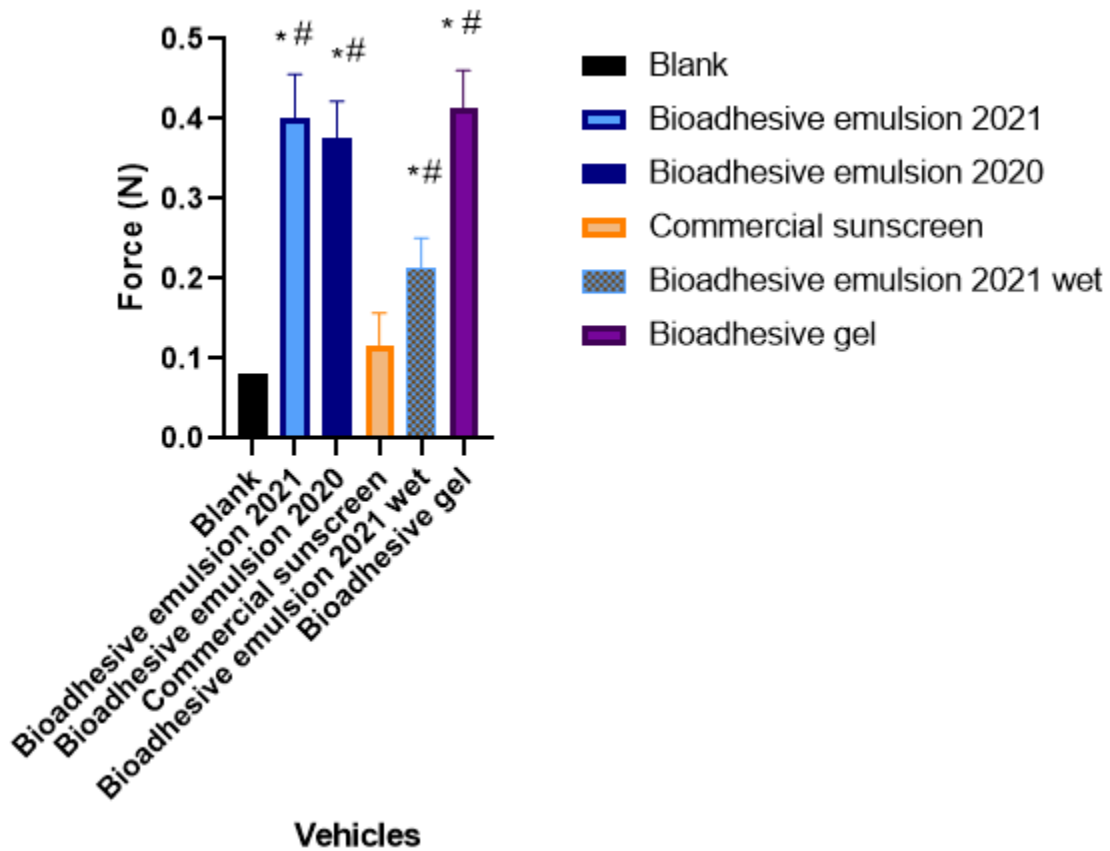


Figure 5-13. Force of the vehicles: bioadhesive emulsion 2021, bioadhesive emulsion 2020, commercial sunscreen “water-resistant”, bioadhesive emulsion 2021 at wet conditions and bioadhesive gel

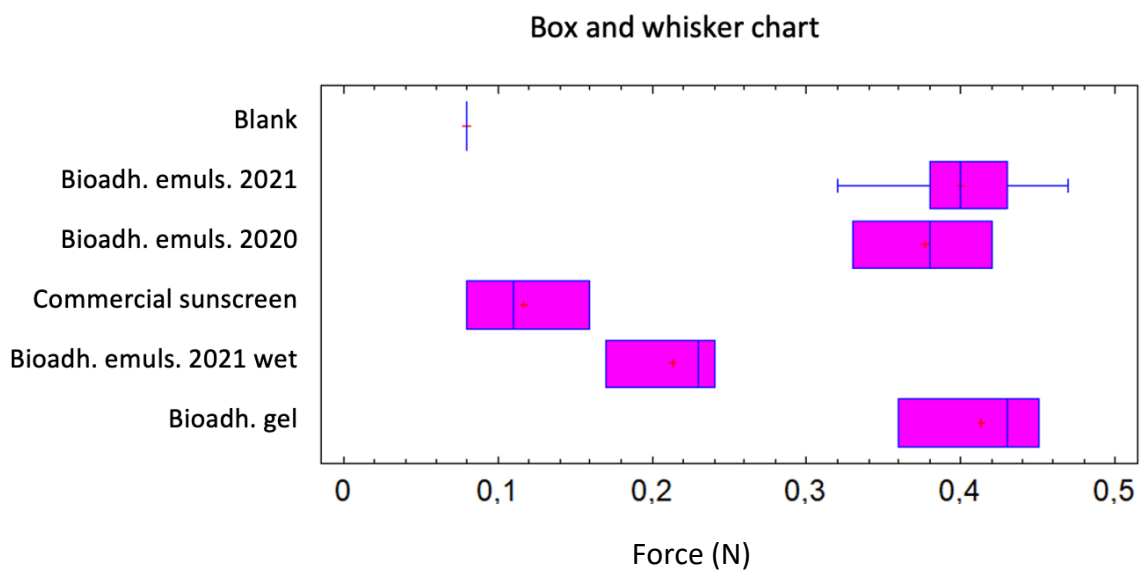


Figure 5-14. Force of the vehicles: bioadhesive emulsion 2021, bioadhesive emulsion 2020, commercial sunscreen “water-resistant”, bioadhesive emulsion 2021 at wet conditions and bioadhesive gel as box and whisker chart.

5.3.11 Water resistance

The water resistance of the bioadhesive emulsion 6-13 was assessed after 12 months of storage. Table 5-47 shows the SPF values within a single PMMA plate (average of the measures = \bar{X} , standard deviation= SD, and covariance= CoV) and the λ Critical of every single PMMA plate with its standard deviation= λ Critical, and covariance= λ Crit CoV. The SPF average values of the four PMMA plates and variance between the four plates are listed. Also the average on the four PMMA plates on the SPF SD, SPF CoV, λ Critical, λ Crit SD and λ Crit CoV are given for the plates measured before the water immersion (pre immersion) and after the water immersion (post immersion).

Table 5-47. SPF and λ Critical of pre immersion and post immersion of four PMMA plates of the bioadhesive emulsion 6-13 12 months after formulation.

	Pre immersion						Post immersion				
	Plate 1	Plate 2	Plate 3	Plate 4	Average	Plate 1	Plate 2	Plate 3	Plate 4	Average	
SPF \bar{X}	74,9	99,7	73,7	74,9	80,8	24,7	119,6	113,4	122,0	94,9	
Variance					159,1					2207,5	
SPF SD	13,6	6,6	14,3	13,2	11,9	6,1	23,6	23,6	17,9	17,7	
SPF CoV	18,2	6,6	19,4	17,6	15,5	24,6	19,7	20,8	14,7	21,7	
λ Critical	377,6	377,8	377,6	377,6	377,7	379,6	377,2	376,6	376,6	377,8	
λ Crit SD	0,5	0,4	0,5	0,5	0,5	0,9	0,8	0,5	0,5	0,8	
λ Crit CoV	0,1	0,1	0,1	0,1	0,1	0,2	0,2	0,1	0,1	0,2	

$$\% WR = \frac{\text{Post immersion SPF}-1}{\text{Pre immersion SPF}-1} = 1,18 \%$$

Equation 5-17

The average SPF of the bioadhesive emulsion 6-13 for the four plates was 80 before immersion of the plates. However, after 20 min immersion of the plate under stirring conditions and subsequent drying of the wet plates the average SPF increased to 94, 9 Table 5-47. The resulting water resistance results (WR= 1,18%) show that there was not only no lose in the SPF but also there was an SPF increase meaning that the sunscreen product maintained attached to the PMMA plate after immersion, as well as the filters which were contained in it (Equation 5-17).

5.3.12 Centrifugation

The Figure 5-15 shows the bioadhesive emulsion 6-13 after 24 h storage ($t=0$) and after 12 months storage after centrifugation at 500 rpm during 15 min.

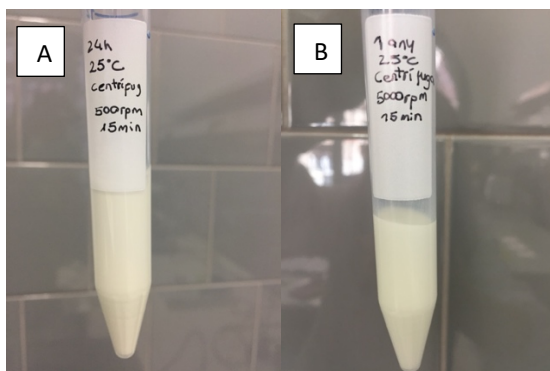


Figure 5-15: Bioadhesive emulsion 6-13 at A) $t=0$ and b) 12 months storage after centrifugation.

No phase separation observed after 15 min centrifugation at 5000 rpm for $t=0$ and after 12 months at 25°C storage on a plastic tube (Figure 5-15).

5.3.13 Stability

The in-use stability of the bioadhesive emulsion 6-13 stored in glass jars was assessed with the parameters listed in Table 5-48 (pH, rheology, viscosity, extensibility, and rheology).

Table 5-48. Stability of the bioadhesive emulsion 6-13 for the parameters: pH, rheology, viscosity, extensibility, and rheology (t=0).

	Parameters	Limit value	Experimental value	RSD (%)	Conversion to radius	Radius value
Finished product	Organoleptic properties	0-10	9,0	10	$eV=r=P_1+P_2+P_3+P_4+P_5^*$ ($eV=r=2+2+1+2+2$)	9,0
	pH	4-7	5,7	-	$r=10, pH_2= \pm 1pH_1$ $r=5, pH_2 >1pH_1$ $r=0, pH_2 <4 \text{ or } >7$	10,0
	Extensibility	1000 mm ²	962,11 mm ²	0	$r= 10- (E^2/100- E^1/100)$	9,6
	Viscosity	1000 mPa·s	2642 mPa·s	9,2	$r= 10- ((v^2-v^1)/1000)$	8,3
	Rheology	0-10	10,0	-	$r=10$	10,0

* P1=Homogeneity, P2=Color, P3=Flowability, P4= Absence of air, P5= Texture

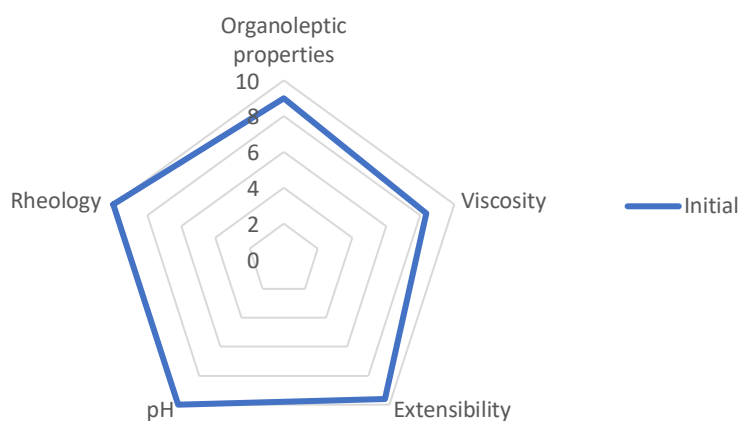


Figure 5-16. Radius diagram of the bioadhesive emulsion 6-13 at t=0 (initial).

Stability test at t=0

The results of the stability test for t=0 was equal for the three conditions (5 °C, 25 °C and 40 °C) as at t=0 there were no differences in treatment yet. After performing the tests, the emulsion was divided into three glass jars with the labeling of 5 °C, 25 °C and 40 °C, respectively. The results of the t=0 is listed below and are classified in organoleptic properties, pH, rheology and viscosity and extensibility (Table 5-48, Figure 5-16).

1. Organoleptic Properties

a. Homogeneity

After analyzing the formulation spread on a glass plate and no physical discontinuities (oil, water) and no clumps were observed in the sample with naked eye.

The formulation had the maximum homogeneity was scored with **2 eV**.

b. Color:

The color was uniform throughout the sample; therefore it was scored with **2 eV**.

c. Flowability:

The emulsion passed smoothly through a cannula with a diameter of 4.80 mm using manual force. **2 eV**.

d. Absence of air:

There was absence of air with the naked eye and under a microscope: **2 eV**.

e. Texture

The texture was as expected and it could be spread properly: **2 eV**

$$eV=r=(P_1+P_2+P_3+P_4+P_5)$$

Equation 5-18

The eV of homogeneity, color, flowability, absence of air and texture were calculated using Equation 5-18. The final score for organoleptic properties of the final product was **9,0**.

2. & 3. Rheology and Viscosity

The viscosity and rheology of the bioadhesive emulsion 6-13 are shown in Table 5-49. The viscosity was 2629 mPa·s in the first measurement and 2642 mPa·s for the second measurement, showing a high reproducibility of the results. The mathematical model, that fitted the best was the Cross model, showing correlation coefficients close to 1, (Table 5-49).

Table 5-49. Viscosity and rheology of the bioadhesive emulsion 6 -13.

Rheology	Viscosity	Ascendent Cross	Descendent Cross
Measurement 1	2629 mPa·s	r= 0,9974	r= 0,9999
Measurement 2	2642 mPa·s	r= 0,9985	r= 1

Fluids, that fit the Cross model are **pseudoplastic**, which is common in face creams. Pseudoplastic fluids show a shear thinning behaviour characterised by a viscosity decrease upon shear rate increase. Finally, thixotropy was reported with values of 1185 and 985 Pa/s for the first and second measurement, respectively.

Extensibility

The results of three measurements on extensibility are listed in Table 5-50.

Table 5-50. Extensibility bioadhesive emulsion 6-13 at t=0.

d(mm)	S(mm ²)	SD
35	962,11	0
35	962,11	0
35	962,11	0

The extensibility results were equal in the three measurements with an extensibility of 962,11 mm². The standard deviation was 0 as the result for all the measurements was the same. In view of the results, the final product has a high extensibility as the average extensibility of the sample is close to 1000 which corresponds to a high extensibility.

pH

The ideal pH range for an emulsion would be between 5,5 and 5,9. The pH of the bioadhesive emulsion 6-13 at t=0 was 5,7. Therefore, it falls within the range of values. **10 eV**

a *In-use stability*

- **Stability at 5 °C**

A summary of the results obtained in-use stability assessment of the bioadhesive emulsion 6-13 for 0-6 months storage at the 5 °C temperature is shown in Table 5-51.

For each time period (t=0, 1, 2, 3 and 6 months) the parameters to assess the in-use stability are given with its limit value, experimental value, relative standard deviation (RSD) in percent and the radius value Table 5-51.

Table 5-51. Stability of the bioadhesive emulsion 13-6 for the parameters: pH, rheology, viscosity, extensibility and rheology for the finished product (t=0) and after 0-6 months at 5 °C.

	Parameters	Limit value	Experimental value	RSD (%)	Conversion to radius	Radius value
Bioadhes. Emulsion 6-13 (t=0)	Organoleptic properties	0-10	9	-	$eV=r=P_1+P_2+P_3+P_4+P_5$	9,0
	pH	4-7	5,7	-	$r=10$	10.0
	Extensibility	100-1000 mm ² (1000 mm ²)	962,11 mm²	0	$r= 10- \left(\frac{E^2}{100} - \frac{E^1}{100} \right)$	9,6
	Viscosity	100-10000 mPas (1000 mPas)	2642 mPa·s	9,2	$r= 10- \left(\frac{v^2-v^1}{1000} \right)$	8,3
	Rheology	0-10	10	-	$r=10$	10.0
After 1 months at 5 °C	Organoleptic properties	0-10	9	-	$eV=r=P_1+P_2+P_3+P_4+P_5$	9,0
	pH	4-7	5,7	-	$r=10$	10.0
	Extensibility	100-1000 mm ² (1000 mm ²)	935,02 mm²	38,3	$r= 10- \left(\frac{E^2}{100} - \frac{E^1}{100} \right)$	9,3
	Viscosity	100-10000 mPas	2287 mPa·s	188,1	$r= 10- \left(\frac{v^2-v^1}{1000} \right)$	8,7

		(1000 mPas)				
	Rheology	0-10	10	-	r=10	10.0
After 2 months at 5 °C	Organoleptic properties	0-10	9	-	eV=r=P ₁ +P ₂ +P ₃ +P ₄ +P ₅	9,0
	pH	4-7	5,6	-	r=10	10.0
	Extensibility	100-1000 mm ² (1000 mm ²)	947,66 mm²	20,4	$r = 10 - \left(\frac{E^2}{100} - \frac{E^1}{100} \right)$	9,4
	Viscosity	100-10000 mPas (1000 mPas)	2394 mPa·s	184,5	$r = 10 - \left(\frac{v^2 - v^1}{1000} \right)$	8,6
	Rheology	0-10	10	-	r=10	10.0
After 3 months at 5 °C	Organoleptic properties	0-10	9	-	eV=r=P ₁ +P ₂ +P ₃ +P ₄ +P ₅	9,0
	pH	4-7	5,9	-	r=10	10.0
	Extensibility	100-1000 mm ² (1000 mm ²)	706,86 mm²	0	$r = 10 - \left(\frac{E^2}{100} - \frac{E^1}{100} \right)$	7,0
	Viscosity	100-10000 mPas (1000 mPas)	3037 mPa·s	118,1	$r = 10 - \left(\frac{v^2 - v^1}{1000} \right)$	8
	Rheology	0-10	10	-	r=10	10.0
After 6 months at 5 °C	Organoleptic properties	0-10	9	-	eV=r=P ₁ +P ₂ +P ₃ +P ₄ +P ₅	10.0
	pH	4-7	6	-	r=10	10.0
	Extensibility	100-1000 mm ² (1000 mm ²)	706,86 mm²	0	$r = 10 - \left(\frac{E^2}{100} - \frac{E^1}{100} \right)$	7,0
	Viscosity	100-10000 mPas (1000 mPas)	3080 Pa·s	9,2	$r = 10 - \left(\frac{v^2 - v^1}{1000} \right)$	7,9
	Rheology	0-10	10	-	r=10	10.0

The parametric index (PI), parametric profile index (PPI), good quality index (GQI) and limit of acceptance (LioA) of the bioadhesive emulsion 6-13 at 5 °C storage for t=0, 1, 2, 3 and 6 months are listed in Table 5-52.

Table 5-52. PI, PPI, GQI and LioA-values of the bioadhesive emulsion 6-13 for 0 to 6 months at 5 °C.

5 °C	t=0	1 month	2 months	3 months	6 months
PI	1	1	1	1	1
PPI	9,3916	9,41263	9,41651	8,80632	8,79772
GQI	7,0437	7,0594725	7,0623825	6,60474	6,59829
LioA	Yes	Yes	Yes	Yes	Yes

The formulation at 5°C kept high stability parameters from 0 to 6 months of storage. No signs of instability were observed. Still after six months the bioadhesive emulsion maintained the same pH, rheology and organoleptic properties. Only some increase in the viscosity and decrease in extensibility were observed. However, these were small.

- Stability at 25 °C

A summary of the results obtained in-use stability assessment of the bioadhesive emulsion 6-13 for 0-6 months storage at the 25 °C temperature is shown in Table 5-53.

For each time period (t=0, 1, 2, 3 and 6 months) the parameters to assess the in-use stability are given with its limit value, experimental value, relative standard deviation (RSD) in percent and the radius value Table 5-53.

Table 5-53. Stability of the bioadhesive emulsion 6-13 for the parameters: pH, rheology, viscosity, extensibility and rheology for the finished product (t=0) and after 0-6 months at 25 °C.

	Parameters	Limit value (E1 or V1)	Experimental value (E2 or V2)	RSD (%)	Conversion to radius	Radius value
Bioadhes. Emulsion 6-13 (t=0)	Organoleptic properties	0-10	9,0	-	$eV=r=P_1+P_2+P_3+P_4+P_5$	9,0
	pH	4-7	5,7	-	$r=10$	10,0
	Extensibility	100-1000 mm ² (1000 mm ²)	962,11 mm²	0	$r= 10- (E^2/_{100}- E^1/_{100})$	9,6
	Viscosity	100-10000 mPas (1000 mPas)	2642 mPa·s	18,4	$r= 10- ((v^2-v^1)/_{1000})$	8,4
	Rheology	0-10	10	-	$r=10$	10.0

After 1 month at 25 °C	Organoleptic properties	0-10	9,0	-	$eV=r=P_1+P_2+P_3+P_4+P_5$	9,0
	pH	4-7	5,7	-	$r=10$	10.0
	Extensibility	100-1000 mm ² (1000 mm ²)	962,11 mm²	0	$r=10- (E^2/100- E^1/100)$	9,6
	Viscosity	100-10000 mPas (1000 mPas)	2618 mPa·s	45,3	$r=10- ((v^2-v^1)/1000)$	8,3
	Rheology	0-10	10	-	$r=10$	10.0
After 2 months at 25 °C	Organoleptic properties	0-10	9,0	-	$eV=r=P_1+P_2+P_3+P_4+P_5$	9,0
	pH	4-7	5,7	-	$r=10$	10.0
	Extensibility	100-1000 mm ² (1000 mm ²)	962,11 mm²	0	$r=10- (E^2/100- E^1/100)$	9,6
	Viscosity	100-10000 mPas (1000 mPas)	2773 mPa·s	45,3	$r=10- ((v^2-v^1)/1000)$	8,2
	Rheology	0-10	10	-	$r=10$	10.0
After 3 months at 25 °C	Organoleptic properties	0-10	9,0	-	$eV=r=P_1+P_2+P_3+P_4+P_5$	9,0
	pH	4-7	6,2	-	$r=10$	10.0
	Extensibility	100-1000 mm ² (1000 mm ²)	706,9 mm²	0	$r=10- (E^2/100- E^1/100)$	7,1
	Viscosity	100-10000 mPas (1000 mPas)	3818 mPa·s	66,4	$r=10- ((v^2-v^1)/1000)$	7,2
	Rheology	0-10	10	-	$r=10$	10.0
After 6 months at 25 °C	Organoleptic properties	0-10	3,0	-	$eV=r=P_1+P_2+P_3+P_4+P_5$	3,0
	pH	4-7	6,5	-	$r=10$	10.0
	Extensibility	100-1000 mm ² (1000 mm ²)	706,9 mm²	0	$r=10- (E^2/100- E^1/100)$	7,1
	Viscosity	100-10000 mPas (1000 mPas)	3823 mPa·s	393,2	$r=10- ((v^2-v^1)/1000)$	7,2
	Rheology	0-10	10	-	$r=10$	10.0

The parametric index (PI), parametric profile index (PPI) good quality index (GQI) and limit of acceptance (LioA) of the bioadhesive emulsion 6-13 at 25 °C storage for t=0, 1, 2, 3 and 6 months are listed in Table 5-54.

Table 5-54. PI, PPI, GQI and LioA-values of the bioadhesive emulsion 6-13 or 0 to 6 months at 25 °C

25 °C	Initial	1 month	2 months	3 months	6 months
PI	1	1	1	1	0,8
PPI	9,3916	9,40062	9,36962	8,65012	7,44912
GQI	7,0437	7,050465	7,027215	6,48759	5,58684
LioA	Yes	Yes	Yes	Yes	Yes

The bioadhesive emulsion after 6 months at 25 °C was not completely stable as on the surface of the cream some oil was observed on the surface. Therefore, there formulation was slight signs of phase separation. Although the GQI of the emulsion is higher than 5, the emulsion was not completely stable.

- **Stability at 40 °C**

A summary of the results obtained in-use stability assessment of the bioadhesive emulsion 6-13 for 0-6 months storage at the 40 °C temperature is shown in Table 5-55.

For each time period (t=0, 1, 2, 3 and 6 months) the parameters to assess the in-use stability are given with its limit value, experimental value, relative standard deviation (RSD) in percent and the radius value Table 5-55.

Table 5-55. Stability of the bioadhesive emulsion 6-13 for the parameters: pH, rheology, viscosity, extensibility and rheology for the finished product (t=0) and after 1-6 months at 40 °C.

	Parameters	Limit value	Experimental value	RSD (%)	Conversion to radius	Radius value
Bioadhes. Emulsion 6-13 (t=0)	Organoleptic properties	0-10	9	-	$eV=r=P_1+P_2+P_3+P_4+P_5$	9,0
	pH	4-7	5,7	-	$r=10$	10.0
	Extensibility	100-1000 mm ² (1000 mm ²)	962,11 mm²	0	$r= 10- (E^2/100- E^1/100)$	9,6
	Viscosity	100-10000 mPas (1000 mPas)	2642 Pa·s	9,2	$r= 10- (v^2-v^1)/1000$	8,3
	Rheology	0-10	10	-	$r=10$	10.0
After 1 month at 40 °C	Organoleptic properties	0-10	9	-	$eV=r=P_1+P_2+P_3+P_4+P_5$	9,0
	pH	4-7	5,7	-	$r=10$	10.0
	Extensibility	100-1000 mm ² (1000 mm ²)	706,86 mm²	0	$r= 10- (E^2/100- E^1/100)$	7,1
	Viscosity	100-10000 mPas (1000 mPas)	3495 Pa·s	9,2	$r= 10- (v^2-v^1)/1000$	7,5
	Rheology	0-10	10	-	$r=10$	10.0
After 2 months at 40 °C	Organoleptic properties	0-10	9	-	$eV=r=P_1+P_2+P_3+P_4+P_5$	9,0
	pH	4-7	5,7	-	$r=10$	10.0
	Extensibility	100-1000 mm ² (1000 mm ²)	706,8 mm²	0	$r= 10- (E^2/100- E^1/100)$	7,06
	Viscosity	100-10000 mPas (1000 mPas)	1951 Pa·s	9,2	$r= 10- (v^2-v^1)/1000$	9,04
	Rheology	0-10	10	-	$r=10$	10.0

After 3 months at 40 °C	Organoleptic properties	0-10	9	-	$eV=r=P_1+P_2+P_3+P_4+P_5$	9,0
	pH	4-7	6,3	-	$r=10$	5,0
	Extensibility	100-1000 mm ² (1000 mm ²)	660,5 mm²	0	$r=10- \left(\frac{E^2}{100} - \frac{E^1}{100} \right)$	9,6
	Viscosity	100-10000 mPas (1000 mPas)	4123 Pa·s	9,2	$r=10- \left(\frac{v^2-v^1}{1000} \right)$	6,8
	Rheology	0-10	10	-	$r=10$	10,0
After 6 months at 40 °C	Organoleptic properties	0-10	9	-	$eV=r=P_1+P_2+P_3+P_4+P_5$	9,0
	pH	4-7	6,6	-	$r=10$	10,0
	Extensibility	100-1000 mm ² (1000 mm ²)	962,11 mm²	0	$r=10- \left(\frac{E^2}{100} - \frac{E^1}{100} \right)$	9,6
	Viscosity	100-10000 mPas (1000 mPas)	2642 Pa·s	9,2	$r=10- \left(\frac{v^2-v^1}{1000} \right)$	8,3
	Rheology	0-10	10	-	$r=10$	10,0

The parametric index (PI), parametric profile index (PPI) good quality index (GQI) and limit of acceptance (LioA) of the bioadhesive emulsion 6-13 at 40 °C storage for t=0, 1, 2, 3 and 6 months are listed in Table 5-56.

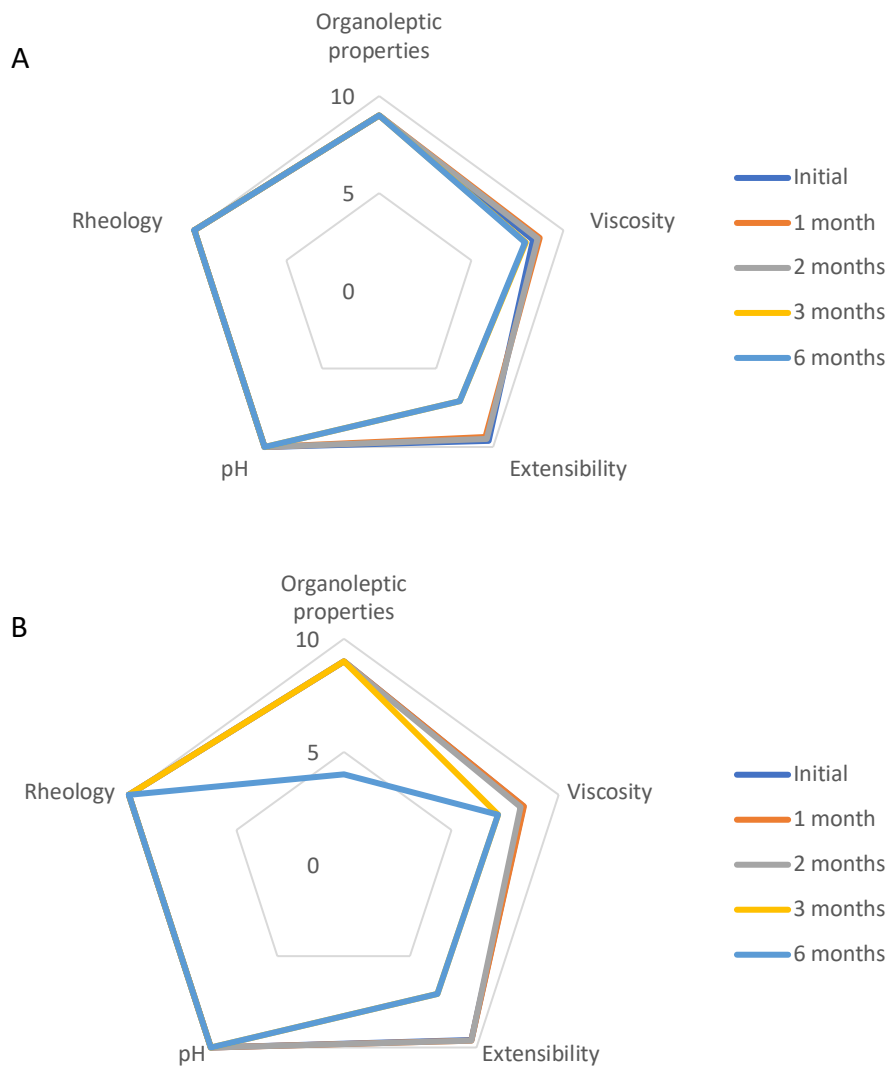
Table 5-56. PI, PPI, GQI and LioA-values of the bioadhesive emulsion 6-13 at 40 °C for 0 to 6 months.

40 °C	Initial	1 month	2 months	3 months	6 months
PI	1	1	1	0,8	0,8
PPI	9,3916	8,51472	8,42352	7,17744	7,41052
GQI	7,0437	6,38604	6,31764	5,38308	5,55789
LioA	Yes	Yes	Yes	No	No

Stability Diagram

The stability diagram is a graphical representation of the in-use stability of the bioadhesive emulsion 6-13 for the different time sets (t=0, 1, 2, 3 and 6 months). It summarizes the in-use stability for each temperature condition (5 °C, 25 °C, and 40 °C), which is represented by a pentagon. In every corner of the pentagon, a parameter is shown. The higher the area of the pentagon, the higher the in-use stability.

Figure 5-17 shows the in-use stability from 0 to 6 months stored at 5 °C (Figure 5-17A), at 25 °C (Figure 5-17B) and at 40 °C (Figure 5-17C).



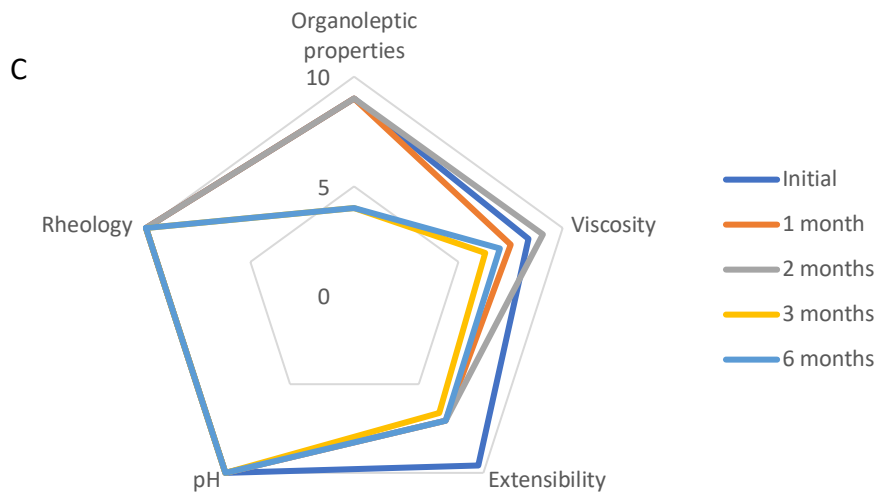


Figure 5-17. Stability diagram of the bioadhesive emulsion 6-13 from 0 to 6 months at A) 5 °C B) 25 °C C) 40 °C.

Figure 5-18 and Figure 5-20 show the progression of the in-use stability of the bioadhesion emulsion 6-13 after 2- and 6-months storage, respectively at 5 °C, 25 °C and 40 °C, while in Figure 5-19 the bioadhesive emulsion after 3 months is shown at 40 °C storage.

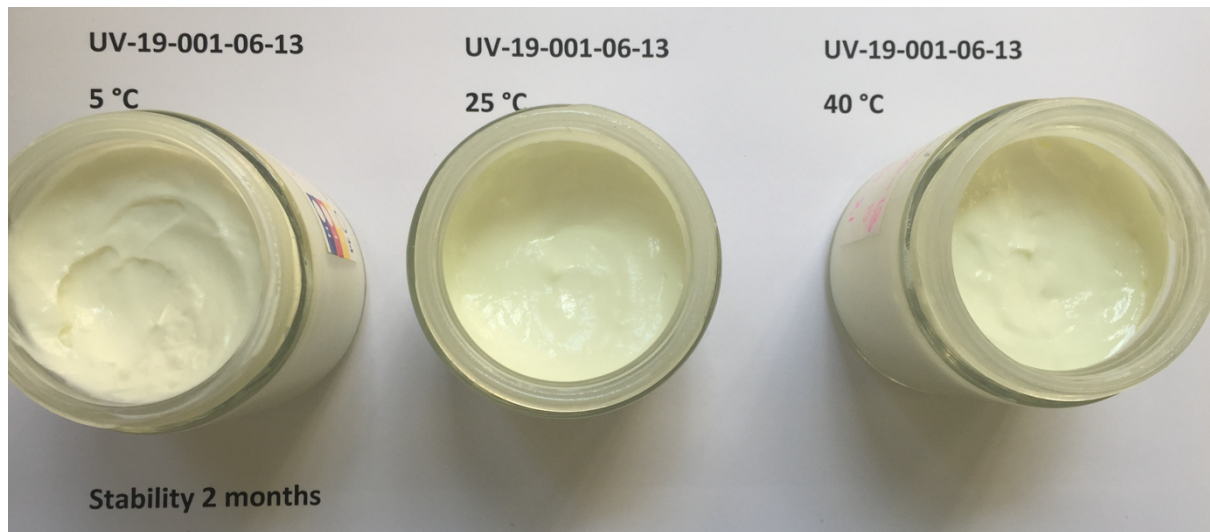


Figure 5-18: In-use stability of the bioadhesive emulsion 6-13 after 2 months storage at 5 °C, 25 °C and 40 °C.



Figure 5-19: In-use stability the bioadhesive emulsion 6-13 after 3 months storage at 40 °C.

The bioadhesive emulsion 6-13 after 3 months at 40 °C at in-use conditions was not completely stable. On the surface of the emulsion some oil was observed (Figure 5-19). Signs of phase separation were observed. The instability increased after six months storage at 40 °C under in-use conditions. For 25 °C storage some slight oil discontinuities were observed. Due to these were very small, they could not be correctly captured by the camera. The bioadhesive emulsion at 5 °C maintained the initial organoleptic properties (Figure 5-20).

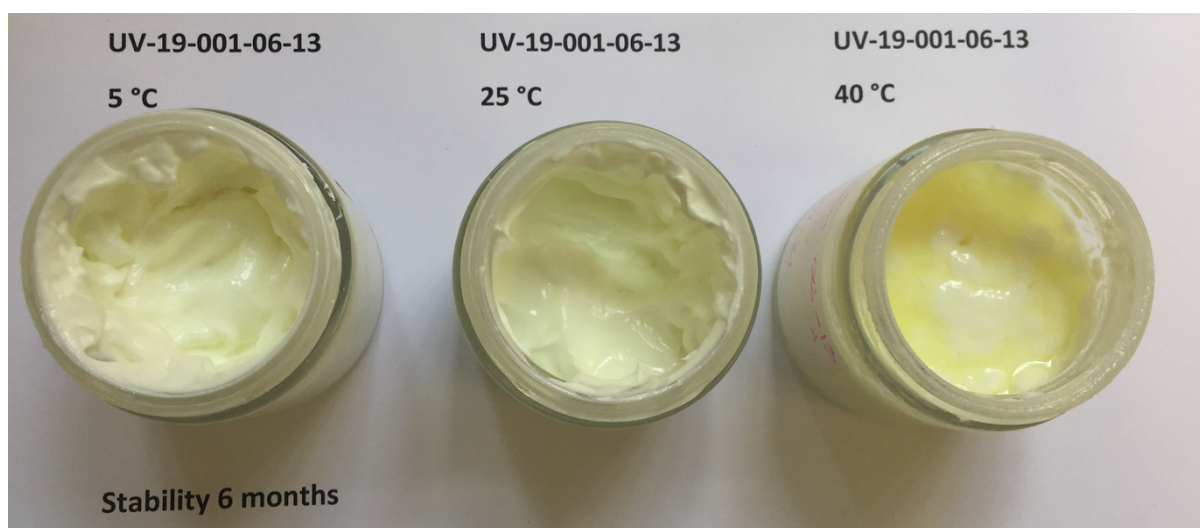


Figure 5-20: In-use stability of the bioadhesive emulsion 6-13 after 6 months storage at 5 °C, 25 °C and 40 °C.

The formulation at 5 °C had significant changes at 3 and 6 months only in **extensibility**. The extensibility decreased from 962,1 mm² to 706,9 mm².

The **viscosity** increased slightly; from the initial viscosity: 2642 mPa to 3080 mPa at 6 months. However, the pH, organoleptic properties, and rheology with a pseudoplastic behavior fitting to cross type and thixotropy were constant. All in all, the bioadhesive emulsion after 6 months at 5 °C maintained a good quality at all the levels with a PI 1 a PPI 8,8 and a GQI 6,6. Therefore, it was within the limit of acceptance (Table 5-51 and Table 5-52).

The formulation at 25 °C had significant changes at 3 months in viscosity and extensibility and at 6 months in organoleptic properties, viscosity, and extensibility. Until 2 months there were no significant differences. However, at 3 months the **extensibility** decreased from the 962,1 mm² to 706,9 mm² and remained at 6 months. Therefore, the stability diagram decreased from 9 to 7, according to the extensibility results.

The **viscosity** at 3 months increased to 3818 mPa (initial value 2642 mPa) and no significant difference was observed for 6 months. Consequently, the score in viscosity dropped to 7,2 and 7,1 for 3 and 6 months, respectively (initial score was 8,3).

There was also a decrease in **organoleptic properties** at 6 months, as since there was some slight phase separation on the surface of the emulsion. The homogeneity obtained 0 points as oil discontinuities were visible with the naked eye. The color scored with a 0 as since there was phase separation, some oil drops were visible on the surface. The flow through a cannula was like the initial formulation and therefore was scored with a 1. No presence of air was observed visually or under the microscope and therefor it was scored with a 2. Finally, the texture on a glass was scored with 1 as although it was not difficult to spread the emulsion, the viscosity increased compared to the emulsion at t=0.

The **pH** remained 10 as the variation remained less than 1 (5,7 initial, 6,2 at 3 months and 6,5 at 6 months). The **rheology** was also constant with a pseudoplastic behavior and thixotropy (Table 5-53 and Table 5-54).

The formulation at 40 °C had significant changes from the first month in viscosity and extensibility:

The increase in the **viscosity** was gradual. At 1 month the viscosity increased to 3495 mPa (initial value 2642 mPa), at 2 months the viscosity decreased unexpectedly to 1951 mPa, a second experiment was done to verify the result and a viscosity of 1075 mPa was obtained. A possible explanation for this low viscosity could be due to at the time of the measurement the temperature was still not at room temperature. This higher temperature could have contributed on the low viscosity. At 3 months the viscosity increased to 4123 mPa and was constant as after 6 months (4016 mPa). The final score is therefore 7.

The **extensibility** decreases after the first month from 962,1 mm² (initial value) to the 706,8 mm². Afterwards and until the end of the experiment the extensibility was constant. All in all, the final score is 7,1.

The total **organoleptic properties** score also decreased with increasing time. At 3 months some oil on the surface of the emulsion was observed (Figure 5-19) corresponding to a slight phase separation. This tendency increased at 6 months (Figure 5-20, Figure 5-17 and Table 5-56).

b *Stability*

- **Stability at 5 °C**

A summary of the results obtained stability assessment of the bioadhesive emulsion 6-13 for 0-3 months storage in independent vials at 5 °C temperature is shown in Table 5-57.

For each time period (t=0, 1, 2 and 3 months) the parameters to assess the stability are given with its limit value, experimental value, relative standard deviation (RSD) in percent and the radius value Table 5-57.

Table 5-57. Stability of the bioadhesive emulsion 6-13 for the parameters: organoleptic properties, pH, extensibility, rheology, viscosity, and rheology for the finished product (t=0) and after 2 and 3 months at 5 °C.

	Parameters	Limit value	Experimental value	RSD (%)	Conversion to radius	Radius value
Bioadhes. Emulsion 6-13 (t=0)	Organoleptic properties	0-10	9	-	$eV=r=P_1+P_2+P_3+P_4+P_5$	9,0
	pH	4-7	5,7	-	$r=10$	10.0
	Extensibility	100-1000 mm ² (1000 mm ²)	567 mm²	0	$r= 10-((E^2/100-E^1/100) $	5,67
	Viscosity	100-10000 mPas (1000 mPas)	3202 mPa·s	165,4	$r=10-((v^2-v^1)/1000)$	7,80
	Rheology	0-10	10	-	$r=10$	10.0
After 2 months at 5 °C	Organoleptic properties	0-10	9	-	$eV=r=P_1+P_2+P_3+P_4+P_5$	9,0
	pH	4-7	5,7	-	$r=10$	10.0
	Extensibility	100-1000 mm ² (1000 mm ²)	601 mm²	0	$r= 10-((E^2/100-E^1/100) $	6,01
	Viscosity	100-10000 mPas (1000 mPas)	3436 mPa·s	0	$r=10-((v^2-v^1)/1000)$	7,56
	Rheology	0-10	10	-	$r=10$	10.0
After 3 months at 5 °C	Organoleptic properties	0-10	9	-	$eV=r=P_1+P_2+P_3+P_4+P_5$	9,0
	pH	4-7	5,7	-	$r=10$	10.0
	Extensibility	100-1000 mm ² (1000 mm ²)	739 mm²	0	$r= 10-((E^2/100-E^1/100) $	7,39
	Viscosity	100-10000 mPas (1000 mPas)	2653 mPa·s	156,3	$r=10-((v^2-v^1)/1000)$	8,3
	Rheology	0-10	10	-	$r=10$	10.0

The parametric index (PI), parametric profile index (PPI) good quality index (GQI) and limit of acceptance (LioA) of the bioadhesive emulsion 6-13 at 5 °C storage for t=0, 2 and 3 months are listed in Table 5-58.

Table 5-58. PI, PPI, GQI and LioA-values of the bioadhesive emulsion 6-13 at 5 °C for 0, 2 and 3 months.

5 °C	t=0	2 months	3 months
PI	1	1	1
PPI	9,28	8,51	8,95
GQI	6,96	6,39	6,71
LioA	Yes	Yes	Yes

- Stability at 25 °C

A summary of the results obtained stability assessment of the bioadhesive emulsion 6-13 for 0-6 months storage in independent vials at 25 °C temperature is shown in Table 5-59.

For each time period (t=0, 2, 3 and 12 months) the parameters to assess the stability are given with its limit value, experimental value, relative standard deviation (RSD) in percent and the radius value Table 5-59.

Table 5-59. Stability of the bioadhesive emulsion 6-13 for the parameters: organoleptic properties, pH, extensibility, rheology, viscosity, and rheology for the finished product (t=0) and after 2, 3 and 12 months at 25 °C.

	Parameters	Limit value	Experimental value	RSD (%)	Conversion to radius	Radius value
Bioadhesive Emulsion 6-13 (t=0)	Organoleptic properties	0-10	9	-	$eV=r=P_1+P_2+P_3+P_4+P_5$	9,0
	pH	4-7	5,7	-	$r=10$	10.0
	Extensibility	100-1000 mm ² (1000 mm ²)	567 mm²	0	$r=10- \left(\frac{E^2}{100} - \frac{E^1}{100} \right) l$	5,67
	Viscosity	100-10000 mPas (1000 mPas)	3202 mPa·s	165	$r=10- \left(\frac{v^2-v^1}{1000} \right)$	7,80
	Rheology	0-10	10	-	$r=10$	10.0

After 2 months at 25 °C	Organoleptic properties	0-10	9	-	$eV=r=P_1+P_2+P_3+P_4+P_5$	9,0
	pH	4-7	5,7	-	$r=10$	10,0
	Extensibility	100-1000 mm ² (1000 mm ²)	587 mm²	0	$r=10- \left(\frac{E^2}{100} - \frac{E^1}{100} \right) l$	5,87
	Viscosity	100-10000 mPas (1000 mPas)	3390 Pa·s	32,5	$r=10- \left(\frac{v^2-v^1}{1000} \right)$	7,61
	Rheology	0-10	10	-	$r=10$	10,0
After 3 months at 25 °C	Organoleptic properties	0-10	10	-	$eV=r=P_1+P_2+P_3+P_4+P_5$	9,0
	pH	4-7	5,6	-	$r=10$	5,0
	Extensibility	100-1000 mm ² (1000 mm ²)	723 mm²	0	$r=10- \left(\frac{E^2}{100} - \frac{E^1}{100} \right) l$	7,23
	Viscosity	100-10000 mPas (1000 mPas)	3202 Pa·s	9,2	$r=10- \left(\frac{v^2-v^1}{1000} \right)$	7,80
	Rheology	0-10	10	-	$r=10$	10,0
After 12 months at 25 °C	Organoleptic properties	0-10	10	-	$eV=r=P_1+P_2+P_3+P_4+P_5$	8,0
	pH	4-7	5,6	-	$r=10$	10,0
	Extensibility	100-1000 mm ² (1000 mm ²)	731 mm²	11,3	$r=10- \left(\frac{E^2}{100} - \frac{E^1}{100} \right) l$	7,31
	Viscosity	100-10000 mPas (1000 mPas)	3000 Pa·s	277,2	$r=10- \left(\frac{v^2-v^1}{1000} \right)$	8,00
	Rheology	0-10	10	-	$r=10$	10,0

The parametric index (PI), parametric profile index (PPI) good quality index (GQI) and limit of acceptance (LioA) of the bioadhesive emulsion 6-13 at 25 °C storage for t=0, 2, 3 and 12 months are listed in Table 5-60.

Table 5-60. PI, PPI, GQI and LioA-values of the bioadhesive emulsion 6-13 at 25 °C for 0, 2,3 and 12 months.

25 °C	t=0	2 months	3 months	12 months
PI	1	1	1	0,8
PPI	9,28	8,50	8,81	8,26
GQI	6,96	6,37	6,60	6,20
LioA	Yes	Yes	Yes	Yes

- **Stability at 40 °C**

A summary of the results obtained stability assessment of the bioadhesive emulsion 6-13 for 0-3 months storage in independent vials at 40 °C temperature is shown in Table 5-61.

For each time period (t=0, 2 and 3 months) the parameters to assess the stability are given with its limit value, experimental value, relative standard deviation (RSD) in percent and the radius value Table 5-61.

Table 5-61. Stability of the bioadhesive emulsion 6-13 for the parameters: organoleptic properties, pH, extensibility, rheology, viscosity, and rheology for the finished product (t=0) and after 2 and 3 months at 40 °C.

	Parameters	Limit value	Experimental value	RSD (%)	Conversion to radius	Radius value
Bioadhes Emulsion 6-13 (t=0)	Organoleptic properties	0-10	9	-	$eV=r=P_1+P_2+P_3+P_4+P_5$	9,0
	pH	5-7	5,7	-	$r=10$	10.0
	Extensibility	100-1000 mm ² (1000 mm ²)	567 mm²	0	$r= 10- \left(\frac{E^2}{100}- \frac{E^1}{100}\right) $	5,67
	Viscosity	100-10000 mPas (1000 mPas)	3202 mPa·s	165	$r= 10- \left(\frac{v^2-v^1}{1000}\right)$	7,80
	Rheology	0-10	10	-	$r=10$	10.0
After 2 months at 40 °C	Organoleptic properties	0-10	9	-	$eV=r=P_1+P_2+P_3+P_4+P_5$	9,0
	pH	5-7	5,7	-	$r=10$	10.0
	Extensibility	100-1000 mm ² (1000 mm ²)	587 mm²	0	$r= 10- \left(\frac{E^2}{100}- \frac{E^1}{100}\right) $	5,87
	Viscosity	100-10000 mPas (1000 mPas)	4330 mPa·s	184,5	$r= 10- \left(\frac{v^2-v^1}{1000}\right)$	6,67
	Rheology	0-10	10	-	$r=10$	10.0

After 3 months at 40 °C	Organoleptic properties	0-10	9	-	$eV=r=P_1+P_2+P_3+P_4+P_5$	9,0
	pH	5-7	5,6	-	$r=10$	10.0
	Extensibility	100-1000 mm ² (1000 mm ²)	739 mm²	0	$r= 10-((E^2/100-E^1/100)) $	7,39
	Viscosity	100-10000 mPas (1000 mPas)	3350 mPa·s	75,66	$r=10-((v^2-v^1)/1000)$	7,65
	Rheology	0-10	10	-	$r=10$	10.0

The parametric index (PI), parametric profile index (PPI) good quality index (GQI) and limit of acceptance (LioA) of the bioadhesive emulsion 6-13 at 40 °C storage for t=0, 2 and 3 months are listed in Table 5-58.

Table 5-62. PI, PPI, GQI and LioA-values of the bioadhesive emulsion 6-13 at 40 °C for 0,2 and 3 months.

40 °C	t=0	2 months	3 months
PI	1	1	1
PPI	9,28	8,31	8,81
GQI	6,96	6,23	6,61
LioA	Yes	Yes	Yes

The bioadhesive emulsion 6-13 had a higher viscosity and decreased extensibility compared with the batch that was tested in the in-use stability. This might be caused due to the stability batch was stirred 5 h more with a plate stirrer in the last step of the manufacturing process. This difference in the procedure might have increase the viscosity and decrease the extensibility. Therefore, the radius value in this batch was 5,67 for extensibility and 7,8 for the viscosity. The other parameters (organoleptic properties, pH and rheology) were the same as for the previous batch in which the in-use stability of the bioadhesive emulsion 6-13 was assessed (see section 5.3.13a).

The bioadhesive emulsion 6-13 was stable at all measured conditions (5 °C, 25 °C and 40 °C). The PI, PPI, GQI parameters were satisfactorily. After 3 months the GQI factor at 5 °C and 40 °C was 6,71 and 6,61, respectively. After 12 months at 25 °C the GQI was 6,20. These

indexes indicated a good quality of the product, as after the stability test the GQI were above the value of 5. Therefore, the bioadhesive emulsion 6-13 was within the limit of acceptance. At 5 °C and 40 °C storage until 3 months and at 25 °C storage until 12 months, the formulation was stable. There was no phase separation in any of the conditions as shown in Figure 5-21.



Figure 5-21. Stability of the bioadhesive emulsion 6-13 after 3 months storage at 5 °C, 25 °C and 40 °C.

The pH was constant for at all three measured temperatures and the rheological behavior and organoleptic properties did not change. Viscosity was constant and extensibility improved over time.

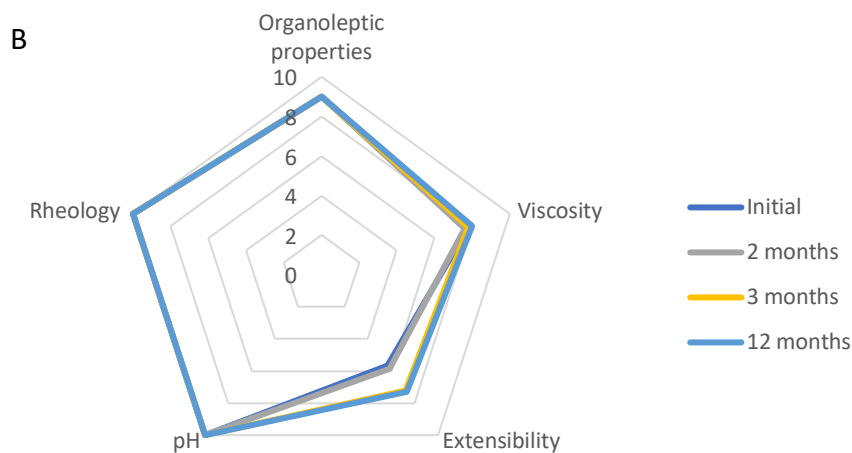
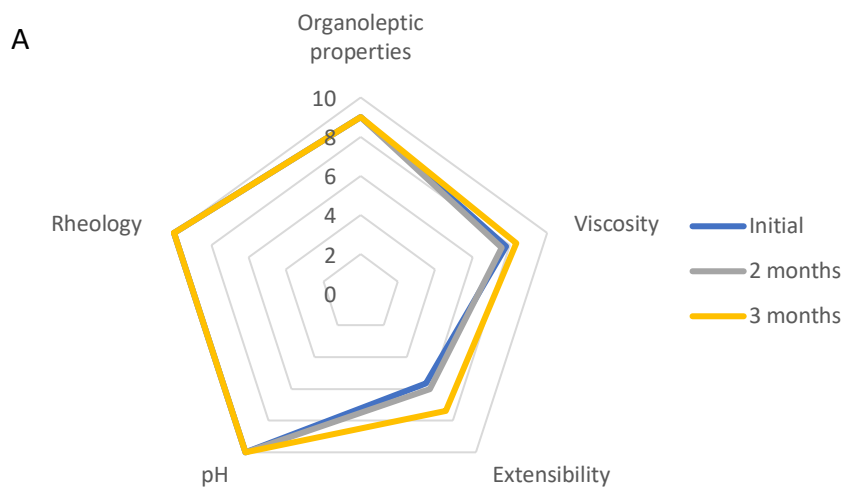
At 5 °C the extensibility after storage of 3 months increased from a radius value of 5,67 (t=0) to a radius value of 7,39. At 25 °C the extensibility after storage of 12 months increased from a radius value of 5,67 (t=0) to a radius value of 7,31. Finally, at 40 °C the extensibility after storage of 3 months increased from a radius value of 5,67 (t=0) to a radius value of 7,39. This increase in extensibility improved the formulation (Table 5-57, Table 5-59 and Table 5-61).

The viscosity after 3 months at and 40 °C storage decreased, and at 5 °C and after 12 months at 25 °C storage decreased. This decrease in the viscosity improved the formulation, obtaining higher radius values. At 5°C and 25 °C the radius values increased from 7,8 (t=0) to 8,3 and 8,0, respectively. At and 40 °C the viscosity decreased to 7,65. However, the viscosity was relatively constant during its respective storage times (Table 5-57, Table 5-59 and Table 5-61).

Stability Diagram

The stability diagram is a graphical representation of the stability of the bioadhesive emulsion 6-13 for the different time sets ($t=0, 1, 2$ and 3 months for $5\text{ }^{\circ}\text{C}$ and $40\text{ }^{\circ}\text{C}$; $t=0, 1, 2, 3$ and 12 months for $25\text{ }^{\circ}\text{C}$). It summarizes the stability for each temperature condition ($5\text{ }^{\circ}\text{C}$, $25\text{ }^{\circ}\text{C}$, and $40\text{ }^{\circ}\text{C}$), which is represented by a pentagon. In every corner of the pentagon, a parameter is shown. The higher the area of the pentagon, the higher the stability.

Figure 5-22 shows the stability from 0 to 3 months stored at $5\text{ }^{\circ}\text{C}$ (Figure 5-22A), from 0 to 12 months stored at $25\text{ }^{\circ}\text{C}$ (Figure 5-22B) and from 0 to 3 months stored at $40\text{ }^{\circ}\text{C}$ (Figure 5-22C).



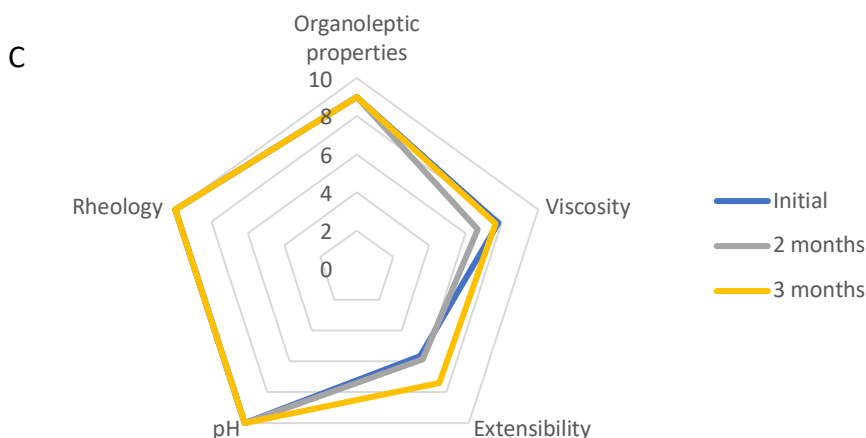


Figure 5-22. Stability diagram of the emulsion 6-13 from 0 to 12 months at A) 5 °C B) 25 °C C) 40 °C

The stability diagram represented graphically the data in Table 5-57, Table 5-59 and Table 5-61. As shown in Figure 5-22, the organoleptic properties, rheology and pH showed identical position on the stability diagram for all the temperature conditions at the tested time points.

Further, although the viscosity was not exactly the same for 0-3 months (5 °C and 40 °C) and for 0-12 months (25 °C), there were not big differences between the times tested. At 5 °C the viscosity slightly increased at 3 months, however for 25 °C and 40 °C the differences from the initial value ($t=0$) until the last time set did almost not change. Therefore, the viscosity was constant.

The extensibility slightly increased, which was a good because the area of the pentagram was bigger, indicating better properties of the product.

All in all, the parameters were constant during the assay. By this it was stated, that the bioadhesive emulsion 6-13 had a stability of 3 months at 5 °C and 40 °C, and a stability of 12 months at 25 °C, at least.

5.4 Conclusion

- 5.4.1 A bioadhesive SPF 30 sunscreen product with non-comedogenic ingredients was designed. The UV filters were not suspected for being endocrine disruptors, allergic potential and skin penetration.
- 5.4.2 According to the evaluation of 20 volunteers, the O/W emulsion performed better compared to W/O emulsion and emulgels on the six organoleptic properties assessed.
- 5.4.3 The resulting emulsion was at a neutral skin pH, was white, homogeneous, with a medium density, pseudoplastic with thixotropy and with a pleasant skin feeling.
- 5.4.4 Homogeneous formulation optically and under the microscope with one phase visualisation under the microscope
- 5.4.5 Bioadhesion emulsion with similar bioadhesion to the bioadhesive gel from which the bioadhesive sunscreen product was developed
- 5.4.6 Extensibility of 700-900 mm² and viscosity equal to 2800 mPa with thixotropy 2800-2904 Pa/s
- 5.4.7 One year stability of the bioadhesive emulsion stored in a plastic tube showed similar results to the bioadhesive emulsion after 24 h after formulation on viscosity, extensibility, visual and microscopical homogeneity, pseudoplastic, bioadhesive and stability after centrifugation.
- 5.4.8 The bioadhesive emulsion was water resistant after 12 months at 25°C
- 5.4.9 The formulation according to the ISO 24443:2012 was photostable, had an SPF 34, UVA-PF 8 and a lambda critical of 378 nm. The formulation with the addition of 5% avobenzone using computational predictions was expected to fulfil the SPF/UVA-PF of 1/3 with an SPF 30 also after one year storage.
- 5.4.10 6 months in use stability at 25 °C was not fulfilled because of slight phase separation. However, one year stability at room temperature and 3 months at 40°C was confirmed by the stability diagram.

6. GLOBAL DISCUSSION

Photocharacterisation of progressive and classical UV filters

The progressive UV filters were studied with the focus on the development of a suitable sunscreen formulation.

Preformulating studies were conducted with PRE-B, PRE-C and PRE-A. Solubilities of PRE-B and PRE-A were performed in different solvents according to its polarity and both PRE-B and PRE-A reflected a complete solubility at 5% in Emollient-A at ambient temperature. This makes Emollient-A a good solvent for PRE-B and PRE-A, as 5% is the maximal permitted amount of most of the crystalline UV filters, including avobenzone (5% in Europe, 3% in US). This guarantees the same or higher solubility at high temperature. This is of importance as formulators increase temperature to 70-80 °C of the oil phase of a formulation during the formulation process. Propilenglycol, which was praised for its 90% maximal yield of PRE-A (73), would have been a suitable solvent had it not been a weak solvent (1% solubility of PRE-A). Methanol, in which PRE-A showed a 46% yield (73), was discarded to be used as solvent of PRE-A in cosmetic formulation for its toxicity.

The smallest the concentration of the progressive UV filter molecule, the higher the activation to the active molecule in Emollient-A solution. This phenomenon was observed in all three progressive UV filters: PRE-A, PRE-B and PRE-C. PRE-B and PRE-C showed almost any activation at 1% but at 0,008%.

All three progressive UV filters showed activation at 0,008%. Therefore, they were combined, at this concentration in solution, to cover the entire UV spectra. The combinations of UVA with UVB filters was proposed to study its activation in view of a future implementation in cosmetical formulation. On the one side, PRE-C and PRE-A are UVA filters. On the other PRE-B has a UVB protective action. Therefore, the following combinations were studied: PRE-A & PRE-B, PRE-B & PRE-C, and a combination of the three progressive UV filters.

As previously thought, the combination of the UV filters had an additive effect. The absorbance of the combinations had an increased absorbance compared to the absorbance of the single UV filters. The objective of assessing the absorbance of the mixture, was the identification of synergies. The absorbance from the single UV filters were added to obtain the so called *in silico* mixture of UV filters. The *in-silico* absorbance of the mixtures was compared with the experimental absorbances. Statistical analysis was performed by two-way ANOVA for the mixture and irradiation time. Synergies of the mixtures were not statistically significant and the combination PRE-C and PRE-B was antagonistic. However, this might be attributed to the lower effectiveness of higher concentration of progressive UV filter in solution.

Another priority of the study was not only to study the activation of the progressive UV filters itself but also to assess the relevance in photoprotection of the progressive UV filters respect to classical UV filters. For this reason, a first screening on the activation of the progressive and classical UV filters was done. Both types of UV filters were irradiated to simulated solar light at 765 W/m^2 (300-800 nm) at 0,008% concentration and its absorbance was measured spectroscopically. The absorbance was converted into the E1,1 value, as this value is used as a parameter to compare the absorbance of UV filters.

Within the progressive UV filters, PRE-A showed a two times increased absorbance compared to PRE-B and PRE-C after 10 h irradiation. It is well known, that avobenzone, the active molecule of PRE-A, is the most efficient UVA sunscreen (216). On the other hand, the four classical UV filters were chosen for its wide use in sunscreen products: Avobenzone (AVO), Ethylhexyl methoxycinnamate (EHMC), Diethylamino Hydroxybenzoyl Hexyl Benzoate (DHHB) and Ethylhexyl Salicylate (EHS). On the one side AVO and DHHB are UVA filters. On the other, EHMC and EHS are UVB filters. Moreover, AVO and EHMC are photoinstable UV filters, which are degraded by UVR. It was interesting to study the effect of the degradation in terms of absorbance and compare it with the activation of the progressive UV filters. In the present study the recovery of avobenzone after 2 h irradiation was 52% in Emollient-A solution. Many factors play a role in the degradation of avobenzone. Some examples are different; method, solvent, type of irradiation, irradiation wavelength and intensity of irradiation.

Interlaboratory variation have been demonstrated for avobenzone, showing recoveries between 64-27% by the same method (217). More relevant is the consistency of the method within the different measurements. In this study, in a block of experiments (for example within the cuvette method), all measurements were performed by the same procedure and by the same person. For this reason, the measurements can be easily compared. The increased recovery of avobenzone in Emollient-A could have benefited PRE-A as well by avoiding the degradation of the active substance, PRE-A.

PRE-B and PRE-C at the maximal irradiation (10 h) had an absorbance high comparable to EHS for 2 h irradiation. PRE-A showed a higher activation compared to PRE-B and PRE-C. Therefore, it was further studied.

PRE-A was characterized photochemically by different methods: HPLC, IR, UV, DSC and solubility in water a different pH. Three different batches were analysed by HPL. Batch 1 had the highest purity (94% purity). Therefore, it was used for further photoactivation experiments. IR confirmed the structure of PRE-A for the batches R-80 and R-81= batch 1. In view of the results, batch 1 was further analyzed. UV confirmed two peaks at 204 nm and 247 nm for PRE-A in ethanol. DCS peaks were obtained a 73 and 232 °C. Finally, PRE-A solubility was classified as not soluble in water. Therefore, PRE-A, like avobenzone must be solubilized in lipophilic medium.

PRE-A was completely soluble at 5% in Emollient-A at ambient temperature. As Emollient-A proved to be a good solvent for PRE-A, activation studies with different batches of PRE-A were performed. Among all the batches, batch 3 and batch 7 performed the highest absorbance. On the one hand, batch 3 showed a higher absorbance at 20 min. On the other, batch 7 achieved higher absorbances at 2 h and 10 h irradiation compared to batch 3. At 4 h the absorbance high of batch 3 and 7 was almost the same. The increased absorbance may be linked to the purity of PRE-A. HPLC studies were conducted in another laboratory and are not included in this thesis.

More specifically, the absorbance of the batches of PRE-A increased with increasing irradiation energy. While in batch 1 and 2 the maximal absorbance was at 10 h, batch 3 and 7 had a maximal absorbance at 4 h and between 4 h and 10 h absorbance decreased. It turns out that batch 3 and 7 reach its maximal absorbance faster than batches 1 and 2. Moreover, the absorbance high was superior in batch 3 and 7 (E1,1 between 700-800) than in batch 1 and 2 (E1,1 between 500-600).

It is important mentioning, that PRE-A at 0 h has a little absorbance reaching its maximum at 327-329 nm. However, after 5 min irradiation its absorbance decreases and shows a maximum at 359 nm. From 5 min on, its maximal absorbance is at 359 nm. This could be attributed to the conversion from PRE-A to avobenzene. Finally, avobenzene and the active molecule of PRE-A (avobenzene) show both a peak at 359 nm. The spectroscopical results confirms the phototransposition of PRE-A to avobenzene. Moreover, batches 1-7 presented a characteristic second peak between 270-290 nm. This is characteristic for the keto form of avobenzene, which is produced upon phototautomerization of the enol form of avobenzene, which is the predominant form in the ground state (218). These both peaks indicate that the phototransposition of PRE-A to avobenzene is being produced.

In view of the results, batch 7 of PRE-A was solubilized in solvents with different viscosity and the activation high during 4 h was measured spectroscopically. Ethanol was the solvent in which PRE-A had the highest absorbance at different irradiation times followed by Emollient-A, cocoglycerides, myritol and PEG 400. The viscosity of the solvents was inversely proportional to the activation of PRE-A. As ethanol is not a suitable solvent for solubilizing PRE-A due to PRE-A solubility in ethanol is only 2%, see section 2.2.2, Emollient-A was established as a suitable solvent for PRE-A activation.

PRE-A (batch 3 and 7) activation and avobenzene activation degradation at 4 h irradiation at 765 W/m² (nearly 20 MED) in solution. As 4 h was initially considered a slow activation it was considered to employ PRE-A as booster for avobenzene. A booster is a compound that helps maintaining the photoprotection for a longer time or helps achieving a higher absorbance (23). Avobenzene and PRE-A (batch 7) were combined in different proportions to boost the

effect of avobenzone. From all the proportions, the combination at 2:1 (avobenzone : PRE-A) achieved a constant absorbance from 0 to 4 h and a higher absorbance at 4 h irradiation, compared to avobenzone alone.

The possibility of a synergy for the combination avobenzone: PRE-A in solution was studied. However, no synergistic effect was observed at the maximal absorbance of avobenzone and PRE-A. This time the concentration was the same for all the combinations. Therefore, no differences in activation because of the concentration were expected, as was later concluded either by an synergistic effect nor an antagonistic effect.

With the arrival of the equipment Labsphere 200S, it was possible to measure the absorbance of PRE-A in emulsion as a thin film in a synthetic substrate simulating human skin. Although the *in vitro* measurement of the SPF is not a validated method, it is the UVA-PF measurement. Both factors are directly measured by the Labsphere 200S software. PRE-A and avobenzone were formulated at 5% concentration as this is the maximal allowed amount of avobenzone in Europe. Firstly, it was interesting to find out that the activation of PRE-A as thin film was faster than in cuvette. While a maximal PRE-A activation in cuvette was near 20 MED, the activation in a PMMA plate was at only 7,5 MED. This positive aspect made PRE-A more attractive in photoprotection. The combination used beforehand of 2:1 avobenzone: PRE-A was also formulated in emulsion. The two versions of the 2:1 combination were subjected to the regulatory requirements. Therefore, the formulations were 1) 3,3% avobenzone and 1,6% PRE-A and 2) 5% avobenzone and 2,5% PRE-A, corresponding to: 1) the possibility that PRE-A could be classified as avobenzone (therefore the sum of both ingredients would not surpass the permitted amount of avobenzone, equal to 5%) and 2) PRE-A would be seen simply as a booster.

Avobenzone and the combinations had a similar behavior. The maximal activation of the three (5% avobenzone, 5% avobenzone & 2,5% PRE-A, and 3,3% avobenzone & 1,6% PRE-A) was at 2,5 MED. Afterwards, degradation was observed. In both combinations, the absorbance was higher compared to avobenzone alone. Therefore, PRE-A contributed to avobenzone stabilization. The increased absorbance in the combinations was reflected in higher SPF and UVA-PF values.

The different behaviour of PRE-A and avobenzone in cuvette and plate can be explained by different ways. First, it could be that the concentration of the ingredients in which they were tested might exert an influence on the degradation of avobenzone and activation-degradation profile of PRE-A. In the cuvette, the ingredient concentration was 0,001% while in the emulsion the concentration of the ingredients was 5%. The lower concentration of ingredients could be the cause for the slowly activation of PRE-A in the cuvette. Also, the degradation of PRE-A and avobenzone was slowly in the cuvettes. It could be that since the concentration in the cuvettes was smaller, the molecules of avobenzone had less chance to interact with themselves, resulting in less degradation.

It is unexpected, that in the PMMA plate avobenzone experience until 2,5 MED an increase in absorbance, as in theory a decrease in absorbance from the $t=0$ irradiation would be expected. Moreover, this was not observed in the cuvette method. This gives a misleading sense of activation of avobenzone, which is not expected for this molecule. This effect is most probably due to a change in the structure of the emulsions-film on the PMMA HD 6 plates, making the surface more evenly distributed due to direct heat. This uniformity of the layer increases the SPF value (149).

All in all, the degradation of avobenzone in emulsion might be closer to real conditions. Not only the concentration 5% is used in formulations, while 0,001% is not appropriate for sunscreen products but also the film thickness ($1,3 \text{ mg/cm}^2$) is closer to real sunscreen applications doses rather than 1 cm thickness of cuvette measurements.

While some photodegradation studies have been performed with glass plate method (219), *Granoli et al. 2009* showed that PMMA plates are also suitable to study the photodegradation of UV filters but there is no clear optimum thickness (220).

Comparing the degradation of avobenzone 5% in the present study, avobenzone recovered 59% after approximately 2 h at 765 W/m^2 while in another study avobenzone 3% in caprylic/capric triglyceride spread as thin film (approximately $2 \mu\text{L/cm}^2$) film on quartz cells recovered 44% after 4 h at 765 W/m^2 (45). The photodegradation of avobenzone might therefore depend on more variables like the concentration, substrate (PMMA plate, quartz

cell), formulation form (solution, emulsion), optical thickness, emollient in which it was solubilized, etc.

Bioadhesive Sunscreen product

The aim of the thesis was the development of a sunscreen formulation with bioadhesive properties (great retention properties on the skin). Sunscreen product manufacturers recommend reapplication of the product every 2 h and after bathing. It is important mentioning, that according to the water-resistant test in Europe, a sunscreen product is considered water resistant if after the test, 50% of the initial SPF recovers. Therefore, a water-resistant sunscreen product does ensure full protection after bathing. Sunscreen with SPF 30 could be reduced to an SPF 15.

The reapplication of the sunscreen product might be inconvenient to users and forget reapplication. In these cases, users could be overestimating their protection giving them a false sense of photoprotection. *In vitro* studies of the developed sunscreen formulation in this study revealed that the product was intact after the test, achieving slightly more than a 100% of the original SPF.

Another requisite in the design was a high SPF of 30 at least using UV filters under no suspicion of penetration into the dermis. The penetration into the dermis of UV filters might produce contact dermatitis, different allergic reactions and suspected UV filters for endocrine disruption were found in plasma, human milk and urine. Although there is no evidence of harm in human, many users are concerned for the possible harm of these UV filters. This is why, in this thesis the UV filters were carefully selected. The final product contained only UV filters with a mass higher than 500 Da in which suspicion of allergy, endocrine effects and photodegradation were excluded. Moreover, different to ZnO and TiO₂ which produce photocatalysis in combination with avobenzone, the selected UV filters: Uvinul T150[®], Tinosorb S Aqua[®] and Tinosorb M[®] can be combined with avobenzone. The compatibility of the filters with avobenzone was also studied, with the possibility to add PRE-A, alone or in combination with avobenzone, in the future.

Finally, it was extremely important, that the sunscreen product had optimum organoleptic properties on skin. Compliance of a sunscreen product is widely subjected to aesthetic appealing. The consumer usually prefers non-oily textures, which are normally achieved in O/W emulsions. Cosmetic agreeable formulations was a priority from the beginning of the design. Moreover, ingredients with comedogenic potential were avoided and small amounts of emollients were used for this purpose. All in all in a survey with 20 volunteers the final sunscreen product achieved in 5/6 organoleptic properties (spreadability, fluidity, pleasant feeling on skin, appearance, non-stickiness and non-white cast effect) the maximal score.

In addition to the good organoleptic properties, the bioadhesiveness was proved measuring the detachment force and work of the emulsion. The formulation had a skin neutral pH, a medium extensibility and pseudoplastic behaviour with thixotropy. This shear thinning behaviour is desirable in creams, as while spreading the cream on the skin, its viscosity decreases and spreadability increases. Finally, the SPF 30 was confirmed *in vitro* at 24 h and *in silico* after 1 year storage with the addition of 5% avobenzone.

A centrifugation assay was performed at 24 h and after 1 year storage. In both cases the formulation was stable. In view of the favorable results, an in-use stability test was performed. In use conditions are normally not evaluated in a stability test. However, this method guarantees the stability of the emulsion at hard conditions.

The stability at in use conditions tended to increase in viscosity and extensibility the longer it was exposed to higher temperatures. A decrease in extensibility can be explained by the increase in viscosity. The decrease in extensibility was however stable at 706,8 mm² during the period of six months independently of the storage temperature. Also, the formulation stored at 5°C until the 3rd month showed an extensibility of 706,8 mm² and was stable at 6 months. Therefore, a decrease in extensibility may not be a sign of instability.

However, an increase in the viscosity is in some cases showed when the formulation has signs of instability (3 months and 6 months at 40 °C and 3 months at 25 °C). However, the

rheological behavior was constant with all the formulations showing a cross-like pseudoplastic behavior with thixotropy.

Although the GQI of the bioadhesive emulsion 6-13 was higher than 5, the emulsion was not stable. Therefore, under the evaluated conditions the emulsion was not within the limits of acceptance.

The cause for instability could be due to the formulation was exposed to continuous temperature changes (especially for the formulation at 40 °C but also the formulation at 5 °C) as the tests were performed at ambient temperature. Another added stability issue could have been the constant manipulation of the emulsions. By opening the jar and taking out product about five times almost every month for conducting the experiments, the oxidation would have contributed to an increased instability.

In view of the results, a standard stability test with sealed glass vials was performed. It was not possible to perform the stability of 6 months. However, the bioadhesive emulsion was stable after 12 months storage at room temperature and after 3 months storage at 5 °C and 40 °C.

Novel method to assess bioadhesiveness/mucoadhesiveness applicable to various pharmaceutical dosage forms

Although some methods for measuring bioadhesion/mucoadhesion have been proposed, a standardized method has not been identified in the literature. This is expected to hinder systematic comparisons of results across studies.

In particular, most of the published studies on bioadhesion have been performed using mucosa. The choice of substrate usually depends on the route of administration of the product. In cases where the product is intended for oral, nasal, or intravaginal use, the use of mucosal tissue is the norm, and numerous studies have described the development of these bioadhesive products. However, few studies have addressed bioadhesion for skin

administration. This external part of the body may be a target for semisolid formulations (with bioadhesive properties carrying one or more active substances). The methods for bioadhesion have been described in the literature for both the mucosa and the skin, but separately. However, a method compatible with different pharmaceutical dosage forms and skin/mucosa substrates has not yet been established. Therefore, as previously stated, this study proceeded to select two solid products for oral administration and a semisolid form for topical administration in an attempt to develop an *in vitro* method for measuring bioadhesion and mucoadhesion that is applicable to a variety of pharmaceutical dosage forms.

The bioadhesive product was compared with a non-bioadhesive formulation, in contrast to other studies in which the substrate without any product was the mock. Thus, the bioadhesive material itself was assessed as the formulation without the bioadhesive film may have an independent measure of adhesion. However, as was demonstrated in the case study, there were only small differences in peak force and work of adhesion between the skin without emulsion and the non-bioadhesive formulation. Therefore, both skin without emulsion and non-bioadhesive emulsion were deemed valid mocks.

Regarding the product use, it was important to assess bioadhesion with amounts as close as possible to the actual conditions of use. While package leaflets do not establish single-dose prescriptions for topical formulations, a patent for a bioadhesive gel product containing acyclovir selected 8.3 mg/cm² as the appropriate amount of gel product for topical use. However, sunscreen products have clear standards for measuring sun protection factors (SPF) *in vivo* and do specify an amount of 2 mg/cm² to achieve the labeled SPF. This is equivalent to 50 mg of the product homogeneously spread on a 5 × 5 cm skin sheet section. In the present study, 80 mg of the emulsion was spread on 3 × 3 cm skin sheet sections. This corresponds to 5.3 mg/cm². This amount was selected because it lies between 2 mg/cm² and 8.3 mg/cm². The amount used in this study is therefore closer to that of actual applications of topical formulations compared with other studies in the same field.

The parameters of peak force and work of adhesion were both valid for determining the bioadhesion of the formulation. Significant differences were observed between bioadhesive

and non-bioadhesive formulations when any of these parameters were used. The high standard deviation of the work of adhesion can be explained by the fact that the work of adhesion is the result of two factors, namely force and distance, whereas peak force is a direct measure. Furthermore, contact time and contact force were determining factors for bioadhesion.

The method proposed here was found to work on formulations of different natures, namely, solid formulations (minitablets and pellets) and semi-solid formulations (emulsions). Minitablets and pellets were chosen because they are representatives of solid formulations, and an emulsion is representative of a semi-solid formulation. It should, however, be emphasized that the test must be performed under the same conditions for all measurements as minor changes may result in variations. For instance, in our study, the bioadhesive emulsion was moistened with 5 mL of water prior to the bioadhesive test, and consequently, the bioadhesion decreased compared with the unmoistened bioadhesive emulsion. This further illustrates the challenge of extrapolating results performed under different settings.

7. CONCLUSIONS

- 7.1 Emollient-A solubilizes PRE-A and PRE-B at 5% concentration.
- 7.2 At 0,008% concentration, representative wavelength for the activation were 335 nm, 366 nm and 360 nm for PRE-B, PRE-C and PRE-A, respectively in Emollient-A solution. The E_{1,1} at the maximal wavelength after 10 h irradiation was 210,5, 167,9 and 449,5 for PRE-B, PRE-C and PRE-A.
- 7.3 After 10 h irradiation PRE-A (batch 1) showed a higher E_{1,1} than PRE-C and PRE-B and a lower absorbance than avobenzene after 2 h irradiation, at the same concentration. Therefore, the absorbance capacity of PRE-A (batch 1) was higher than PRE-B and PRE-C but lower than avobenzene.
- 7.4 References R-81 (batch 1) and (B) of PRE-A showed similar retention times in the HPLC. In both references the peak came after 7,9 min. However, in reference R-81 this peak was higher corresponding to a higher pureness of PRE-A.
- 7.5 PRE-A's was practically insoluble in water. Absorbance peaks in ethanol were at 204 and 247 nm.
- 7.6 The quality of a batch could be determined by measuring the absorbance capacity resulting higher efficiency of PRE-A batch 7 compared to batches 1, 2 and 3.
- 7.7 In Emollient-A solution, the proportion 2:1 of avobenzene and PRE-A until 4 h (20 MED) irradiation, showed a greater E_{1,1}. PRE-A was used in combination with avobenzene as booster ingredient.
- 7.8 In formulation PRE-A has a maximal increase at 7,5 MED in emulsion. Avobenzene showed overall higher absorbances than PRE-A. This states that at equal concentrations avobenzene has a higher SPF value than PRE-A.

- 7.9 The absorbance of the plate method showed a faster activation of PRE-A and a faster degradation of avobenzene and PRE-A compared to the cuvette method. The plate method is closer to the conditions of use of sunscreens and therefore it is nearer to real conditions.
- 7.10 A synergistic effect for 2:1 avobenzene: PRE-A (3,3%: 1,6%) was observed in emulsion. Therefore, the use of both provides a higher solar protection.
- 7.11 A bioadhesive SPF 30 sunscreen product with non-comedogenic ingredients was designed. The UV filters were not suspected for being endocrine disruptors, allergic potential and skin penetration.
- 7.12 According to the evaluation of 20 volunteers, the O/W emulsion B performed better compared to the W/O emulsion B, O/W emulsion A and W/O emulsion A on the six organoleptic properties assessed.
- 7.13 The bioadhesive emulsion 6-13 had a neutral skin pH, was white, homogeneous, with a medium density, pseudoplastic with thixotropy and with a pleasant skin feeling. Therefore, it can be concluded, that it is correct and fulfils the established objectives.
- 7.14 One-year stability of the bioadhesive emulsion 6-13 stored in a plastic tube at 25 °C showed similar results to the bioadhesive emulsion after 24 h after formulation on viscosity, extensibility, visual and microscopical homogeneity, pseudoplastic, bioadhesive and stability after centrifugation. Therefore, it was stable compared to at 24 h.
- 7.15 The bioadhesive emulsion was water resistant after 0 and 12 months at 25 °C
- 7.16 The formulation according to the ISO 24443:2012 was photostable, had an SPF 34, UVA-PF 8 and a lambda critical of 378 nm. The formulation with the addition of 5% avobenzene using computational predictions fulfilled the SPF/UVA-PF of 1/3 with an SPF 30 also after 1 year storage.
- 7.17 The bioadhesive emulsion 6-13 is stable at in-use during 3 months and is perfectly stable during 1 year at 25 °C at least.

8. REFERENCES

1. Pelizzo M, Zattra E, Nicolosi P, Peserico A, Garoli D, Alaibac M. In Vitro Evaluation of Sunscreens: An Update for the Clinicians . *ISRN Dermatol*. 2012 Nov 27;2012:1–4.
2. [REDACTED]
[REDACTED]
[REDACTED]
3. Osterwalder U, Sohn M, Herzog B. Global state of sunscreens. *Photodermatol Photoimmunol Photomed*. 2014;30(2–3):62–80.
4. Lawrence K, Al-Jamal M, Kohli I, Hamzavi I. Clinical and Biological Relevance of Visible and Infrared Radiation. *Principles and Practice of Photoprotection* [Internet]. 2016 Jan 1 [cited 2022 Apr 29];3–22. Available from: https://link.springer.com/chapter/10.1007/978-3-319-29382-0_1
5. Madronich S, McKenzie RL, Björn LO, Caldwell MM. Changes in biologically active ultraviolet radiation reaching the Earth’s surface. *J Photochem Photobiol B*. 1998 Oct 1;46(1–3):5–19.
6. D’Orazio J, Jarrett S, Amaro-Ortiz A, Scott T. UV radiation and the skin. Vol. 14, *International Journal of Molecular Sciences*. MDPI AG; 2013. p. 12222–48.
7. Adler Y. Hautnah, alles über unser grösstes Organ. 2016. 160–174
8. Herzog B, Hüglin D, Borsos E, Stehlin A, Luther H. New UV Absorbers for Cosmetic Sunscreens – A Breakthrough for the Photoprotection of Human Skin. *Chimia (Aarau)* [Internet]. 2004 Jul 1 [cited 2022 Apr 28];58(7–8):554. Available from: <https://www.chimia.ch/chimia/article/view/3869>
9. [REDACTED]
[REDACTED]
10. Suozzi K, Turban J, Girardi M. Cutaneous Photoprotection: A Review of the Current Status and Evolving Strategies. Vol. 93, *YALE JOURNAL OF BIOLOGY AND MEDICINE*. 2020.
11. Biniak K, Levi K, Dauskardt RH. Solar UV radiation reduces the barrier function of human skin. *Proc Natl Acad Sci U S A* [Internet]. 2012 Oct 16 [cited 2022 May 6];109(42):17111–6. Available from: www.pnas.org/cgi/doi/10.1073/pnas.1206851109

12. Scherer D, Kumar R. Genetics of pigmentation in skin cancer--a review. *Mutat Res* [Internet]. 2010 Oct [cited 2022 May 4];705(2):141–53. Available from: <https://pubmed.ncbi.nlm.nih.gov/20601102/>
13. Dutra EA, Gonçalves Da Costa E Oliveira DA, Rosa E, Kedor-Hackmann M, Rocha MI, Santoro M, et al. Determination of sun protection factor (SPF) of sunscreens by ultraviolet spectrophotometry. *Revista Brasileira de Ciências Farmacêuticas Brazilian Journal of Pharmaceutical Sciences*. 2004;40.
14. Phan TA, Halliday GM, Barnetson RSC, Damian DL. Melanin differentially protects from the initiation and progression of threshold UV-induced erythema depending on UV waveband. *Photodermatol Photoimmunol Photomed*. 2006 Aug;22(4):174–80.
15. Brenner M, Hearing VJ. The Protective Role of Melanin Against UV Damage in Human Skin†. *Photochem Photobiol* [Internet]. 2008 May 1 [cited 2022 May 6];84(3):539–49. Available from: <https://onlinelibrary.wiley.com/doi/full/10.1111/j.1751-1097.2007.00226.x>
16. Kockott D, Herzog B, Reichrath J, Keane K, Holick MF. New Approach to Develop Optimized Sunscreens that Enable Cutaneous Vitamin D Formation with Minimal Erythema Risk. *PLoS One* [Internet]. 2016 Jan 1 [cited 2022 May 5];11(1):e0145509. Available from: <https://journals.plos.org/plosone/article?id=10.1371/journal.pone.0145509>
17. Griffith JL, Al-Jamal M, Lim HW. Photoprotection and Vitamin D. Principles and Practice of Photoprotection [Internet]. 2016 Jan 1 [cited 2022 May 5];95–104. Available from: https://link.springer.com/chapter/10.1007/978-3-319-29382-0_6
18. Kannan S, Lim HW. Photoprotection and vitamin D: a review. *Photodermatol Photoimmunol Photomed* [Internet]. 2014 Apr 1 [cited 2022 May 5];30(2–3):137–45. Available from: <https://onlinelibrary.wiley.com/doi/full/10.1111/phpp.12096>
19. COLIPA. ISO 24444:2019 Sun protection test methods: In vivo determination of the sun protection factor. 2019.
20. Schalka S, dos Reis VMS. Sun protection factor: meaning and controversies. *An Bras Dermatol* [Internet]. 2011 May [cited 2022 May 4];86(3):507–15. Available from: <https://pubmed.ncbi.nlm.nih.gov/21738968/>
21. ISO 24443: 2012 Determination of sunscreen UVA photoprotection in vitro. 2012.

22. Herzog B, Giesinger J, Settels V. Insights into the stabilization of photolabile UV-absorbers in sunscreens. *Photochemical & Photobiological Sciences* [Internet]. 2020 Dec 18 [cited 2022 May 3];19(12):1636–49. Available from: <https://pubs.rsc.org/en/content/articlehtml/2020/pp/d0pp00335b>
23. Sohn M. UV Booster and Photoprotection. *Principles and Practice of Photoprotection* [Internet]. 2016 Jan 1 [cited 2022 Apr 29];227–45. Available from: https://link.springer.com/chapter/10.1007/978-3-319-29382-0_13
24. Uitto J. Understanding Premature Skin Aging. <http://dx.doi.org.sire.ub.edu/101056/NEJM199711133372011> [Internet]. 2009 Aug 20 [cited 2022 May 7];337(20):1463–5. Available from: <https://www-nejm-org.sire.ub.edu/doi/10.1056/NEJM199711133372011>
25. Fisher GJ, Kang S, Varani J, Bata-Csorgo Z, Wan Y, Datta S, et al. Mechanisms of photoaging and chronological skin aging. *Arch Dermatol* [Internet]. 2002 Nov 1 [cited 2022 May 7];138(11):1462–70. Available from: <https://pubmed.ncbi.nlm.nih.gov/12437452/>
26. Ezzedine K, Mauger E, Latreille J, Jdid R, Malvy D, Gruber F, et al. Freckles and solar lentigines have different risk factors in Caucasian women. *Journal of the European Academy of Dermatology and Venereology* [Internet]. 2013 Mar 1 [cited 2022 May 6];27(3):e345–56. Available from: <https://onlinelibrary-wiley-com.sire.ub.edu/doi/full/10.1111/j.1468-3083.2012.04685.x>
27. Friedman BJ, Lim HW, Wang SQ. Photoprotection and Photoaging. *Principles and Practice of Photoprotection* [Internet]. 2016 Jan 1 [cited 2022 May 6];61–74. Available from: https://link.springer.com/chapter/10.1007/978-3-319-29382-0_4
28. Effects of smoking, sun and stress on the skin of twins [Internet]. [cited 2022 May 6]. Available from: <https://www.today.com/slideshow/today/effects-of-smoking-sun-and-stress-on-the-skin-of-twins-33422340/>
29. Hibler BP, Dusza SW, Wang SQ. Photoprotection and Skin Cancer Prevention. *Principles and Practice of Photoprotection* [Internet]. 2016 Jan 1 [cited 2022 May 5];23–38. Available from: https://link.springer.com/chapter/10.1007/978-3-319-29382-0_2
30. Non-melanoma skin cancer - NHS [Internet]. [cited 2022 May 5]. Available from: <https://www.nhs.uk/conditions/non-melanoma-skin-cancer/>

31. Rosso S, Zanetti R, Pippione M, Sancho-Garnier H. Parallel risk assessment of melanoma and basal cell carcinoma: Skin characteristics and sun exposure. *Melanoma Res.* 1998;8(6):573–83.
32. Holman CD arcy J, Armstrong BK. Cutaneous Malignant Melanoma and Indicators of Total Accumulated Exposure to the Sun: An Analysis Separating Histogenetic Types. *JNCI: Journal of the National Cancer Institute* [Internet]. 1984 Jul 1 [cited 2022 May 5];73(1):75–82. Available from: <https://academic.oup.com/jnci/article/73/1/75/900678>
33. Rastrelli M, Tropea S, Rossi CR, Alaibac M. Melanoma: epidemiology, risk factors, pathogenesis, diagnosis and classification. *In Vivo* [Internet]. 2014 Nov 1 [cited 2022 May 5];28(6):1005–12. Available from: <https://pubmed.ncbi.nlm.nih.gov/25398793/>
34. Sander M, Sander M, Burbidge T, Beecker J. The efficacy and safety of sunscreen use for the prevention of skin cancer. *CMAJ* [Internet]. 2020 Dec 14 [cited 2022 May 5];192(50):E1802–8. Available from: <https://www.cmaj.ca/content/192/50/E1802>
35. Green AC, Williams GM, Logan V, Strutton GM. Reduced melanoma after regular sunscreen use: Randomized trial follow-up. *Journal of Clinical Oncology.* 2011 Jan 20;29(3):257–63.
36. Green A, Williams G, Neale R, Hart V, Leslie D, Parsons P, et al. Daily sunscreen application and betacarotene supplementation in prevention of basal-cell and squamous-cell carcinomas of the skin: a randomised controlled trial. *The Lancet* [Internet]. 1999 Aug 28 [cited 2022 May 5];354(9180):723–9. Available from: <http://www.thelancet.com/article/S0140673698121682/fulltext>
37. INCI - Personal Care Products Council [Internet]. [cited 2022 Apr 29]. Available from: <https://www.personalcarecouncil.org/resources/inci/>
38. Shaath NA. The Chemistry of Ultraviolet Filters. *Principles and Practice of Photoprotection* [Internet]. 2016 Jan 1 [cited 2022 May 10];143–57. Available from: https://link.springer.com/chapter/10.1007/978-3-319-29382-0_9
39. Mancuso JB, Maruthi R, Wang SQ, Lim HW. Sunscreens: An Update. Vol. 18, *American Journal of Clinical Dermatology.* Springer International Publishing; 2017. p. 643–50.
40. Manaia EB, Kaminski RCK, Corrêa MA, Chivavacci LA. Inorganic UV filters. *Brazilian Journal of Pharmaceutical Sciences.* 2013 Jan;49(2):201–9.

41. Kim EJ, Kim MJ, Im NR, Park SN. Photolysis of the organic UV filter, avobenzone, combined with octyl methoxycinnamate by nano-TiO₂ composites. *J Photochem Photobiol B*. 2015 Jun 19;149:196–203.
42. Nery ÉM, Martínez RM, Velasco MVR, Baby AR. A short review of alternative ingredients and technologies of inorganic UV filters. *J Cosmet Dermatol* [Internet]. 2021 Apr 1 [cited 2022 May 25];20(4):1061–5. Available from: <https://onlinelibrary.wiley.com/doi/full/10.1111/jocd.13694>
43. Osterwalder U, Hareng L. Global UV Filters: Current Technologies and Future Innovations. *Principles and Practice of Photoprotection* [Internet]. 2016 Jan 1 [cited 2022 Apr 29];179–97. Available from: https://link.springer.com/chapter/10.1007/978-3-319-29382-0_11
44. Amorós-Galicia L. Investigations of spectral performance of photostability of UV absorbers used in sunscreens. 2018.
45. Mortimer RG. Spectroscopy and Photochemistry. *Physical Chemistry*. 2000 Jan 1;751–815.
46. Wolf R, Wolf D, Morganti P, Ruocco V. Sunscreens. *Clin Dermatol*. 2001 Jul 1;19(4):452–9.
47. Herzog B, Schultheiss A, Giesinger J. On the Validity of Beer–Lambert Law and its Significance for Sunscreens. *Photochem Photobiol* [Internet]. 2018 Mar 1 [cited 2022 Apr 29];94(2):384–9. Available from: <https://onlinelibrary-wiley-com.sire.ub.edu/doi/full/10.1111/php.12861>
48. Cosmetics - Sun protection test methods - In vivo determination of the sun protection factor (SPF). ISO 24444:2010. 2010.
49. Lott DL, Stanfield J, Sayre RM, Dowdy JC. Uniformity of sunscreen product application: a problem in testing, a problem for consumers. *Photodermatol Photoimmunol Photomed* [Internet]. 2003 Feb 1 [cited 2022 May 4];19(1):17–20. Available from: <https://onlinelibrary.wiley.com/doi/full/10.1034/j.1600-0781.2003.00007.x>
50. ISO - ISO 16217:2020 - Cosmetics — Sun protection test methods — Water immersion procedure for determining water resistance [Internet]. [cited 2022 May 5]. Available from: <https://www.iso.org/standard/61437.html>

51. ISO - ISO 18861:2020 - Cosmetics — Sun protection test methods — Percentage of water resistance [Internet]. [cited 2022 May 5]. Available from: <https://www.iso.org/standard/63659.html>
52. Romeu X. Fotoprotección, Parte 1: Efectos de la radiación electromagnética y su medida- Master en dermofarmacia y cosmetología UB. 2021.
53. COSMETICS EUROPE: GUIDELINES FOR EVALUATING SUN PRODUCT WATER RESISTANCE. 2005.
54. Deckner G (Prospector). Avobenzone: A Globally Approved UVA Absorber [Internet]. 2015. Available from: <https://knowledge.ulprospector.com/2232/pcc-avobenzone-globally-approved-uva-absorber/>
55. Herzog B, Amorós-Galicia L, Sohn M, Hofer M, Quass K, Giesinger J. Analysis of photokinetics of 2'-ethylhexyl-4-methoxycinnamate in sunscreens. *Photochemical and Photobiological Sciences*. 2019;18(7).
56. Abid AR, Marciniak B, Pędziński T, Shahid M. Photo-stability and photo-sensitizing characterization of selected sunscreens' ingredients. *J Photochem Photobiol A Chem*. 2017;332:241–50.
57. Lhiaubet-Vallet V, Marin M, Jimenez O, Gorchs O, Trullas C, Miranda MA. Filter-filter interactions. Photostabilization, triplet quenching and reactivity with singlet oxygen. *Photochemical and Photobiological Sciences*. 2010;9(4):552–8.
58. Chatelain E, Gabard B. Photostabilization of Butyl methoxydibenzoylmethane (Avobenzone) and Ethylhexyl methoxycinnamate by Bis-ethylhexyloxyphenol methoxyphenyl triazine (Tinosorb S), a New UV Broadband Filter. *Photochem Photobiol*. 2001;74(3):401.
59. Lionetti N, Rigano L. The new sunscreens among formulation strategy, stability issues, changing norms, safety and efficacy evaluations. *Cosmetics*. 2017;4(2).
60. L'Alloret F, Candau D, Seité S, Pygmalion MJ, Ruiz L, Josso M, et al. New combination of ultraviolet absorbers in an oily emollient increases sunscreen efficacy and photostability. Vol. 2, *Dermatology and Therapy*. 2012. p. 1–10.
61. Herzog B, Sommer K. Investigations on photostability of UV-absorbers for cosmetic sunscreens. In: XXlth IFSCC Int Congr, Berlin. 2000. p. 1–7.

62. Kockler J, Oelgemöller M, Robertson S, Glass BD. Photostability of sunscreens. *Journal of Photochemistry and Photobiology C: Photochemistry Reviews* [Internet]. 2012;13(1):91–110. Available from: <http://dx.doi.org/10.1016/j.jphotochemrev.2011.12.001>
63. Molins-Delgado D, Olmo-Campos M del M, Valeta-Juan G, Pleguezuelos-Hernández V, Barceló D, Díaz-Cruz MS. Determination of UV filters in human breast milk using turbulent flow chromatography and babies' daily intake estimation. *Environ Res*. 2018 Feb 1;161:532–9.
64. León Z, Chisvert A, Tarazona I, Salvador A. Solid-phase extraction liquid chromatography-tandem mass spectrometry analytical method for the determination of 2-hydroxy-4-methoxybenzophenone and its metabolites in both human urine and semen. *Anal Bioanal Chem* [Internet]. 2010 Sep [cited 2022 May 24];398(2):831–43. Available from: <https://pubmed.ncbi.nlm.nih.gov/20625888/>
65. Hayden CGJ, Roberts MS, Benson HAE. Systemic absorption of sunscreen after topical application. *The Lancet* [Internet]. 1997 Sep 20 [cited 2022 May 24];350(9081):863–4. Available from: <http://www.thelancet.com.sire.ub.edu/article/S0140673605620326/fulltext>
66. Matta MK, Zusterzeel R, Pilli NR, Patel V, Volpe DA, Florian J, et al. Effect of Sunscreen Application Under Maximal Use Conditions on Plasma Concentration of Sunscreen Active Ingredients: A Randomized Clinical Trial. *JAMA* [Internet]. 2019 Jun 4 [cited 2022 May 24];321(21):2082–91. Available from: <https://jamanetwork.com/journals/jama/fullarticle/2733085>
67. Fda, Cder, Beitz, Julie G. Nonprescription Sunscreen Drug Products— Safety and Effectiveness Data Guidance for Industry. 2016 [cited 2022 May 24]; Available from: <http://www.fda.gov/Drugs/GuidanceComplianceRegulatoryInformation/Guidances/default.htm>
68. Food Additives; Threshold of Regulation for Substances Used in Food-Contact Articles.
69. Matta MK, Florian J, Zusterzeel R, Pilli NR, Patel V, Volpe DA, et al. Effect of Sunscreen Application on Plasma Concentration of Sunscreen Active Ingredients: A Randomized Clinical Trial. *JAMA* [Internet]. 2020 Jan 21 [cited 2022 May 24];323(3):256–67. Available from: <https://jamanetwork.com/journals/jama/fullarticle/2759002>

70. Bos JD, Meinardi MMHM. The 500 Dalton rule for the skin penetration of chemical compounds and drugs. *Exp Dermatol*. 2000;9(3):165–9.
71. Lorigo M, Mariana M, Cairrao E. Photoprotection of ultraviolet-B filters: Updated review of endocrine disrupting properties. *Steroids*. 2018 Mar 1;131:46–58.
72. Nonell S, Teixidó J, Raga M, Giuglietta A. EP1707558A1 Benzoic acid ester compounds, compositions, uses and methods related threto. 2005.
73. [REDACTED]
74. Gallardo A, Teixidó J, Miralles R, Raga M, Guglietta A, Marquillas F, et al. Dose-dependent progressive sunscreens. A new strategy for photoprotection? *Photochemical and Photobiological Sciences*. 2010;9(4):530–4.
75. Gallardo Sánchez A, Nonell Marrugat S, Marquillas Olondriz F, Miralles Bacete R. WO2015177064A1 Silylated imine and carbamate polymeric benzoate compounds, uses, and compositions thereof.
76. Espacenet – search results [Internet]. [cited 2022 Sep 21]. Available from: <https://worldwide.espacenet.com/patent/search/family/047520732/publication/ES2608794T3?q=ES2608794T3>
77. Boreu MB. EMULSIONES COSMÉTICAS. FUNDAMENTOS GENERALES DE FORMULACIÓN (I) Definición. Tipos de Emulsiones. Composición. 2019.
78. Boreu MB. EMULSIONES COSMÉTICAS. FUNDAMENTOS GENERALES DE FORMULACIÓN (II) Emulsificación. Caracterización de una emulsión. Proceso de fabricación de una emulsión. 2019.
79. Borda Boreu M. EMULSIONES COSMÉTICAS. FUNDAMENTOS GENERALES DE FORMULACIÓN Y SELECCIÓN DE INGREDIENTES. (III) Bases Autoemulsionables Emulsionantes comerciales. 2019.
80. Vila-Jato JL. Tecnología Farmacéutica. Volumen I: Aspectos fundamentales de los sistemas farmacéuticos y operaciones básicas. 1a ed. Madrid: Editorial Sínteis S.A.,2001. ISBN 8.
81. Bustamante-Martinez P. Emulsiones. In: *Tratado de Farmacia galenica*. 1993. p. 423–46.
82. Imanidis G. Vorlesung Halbfeste / Disperse Arzneiformen.

83. Raeisi F, Mousavi SM, Hashemi SA, Malekpour L, Bahrani S, Lai CW, et al. Application of biosurfactant as a demulsifying and emulsifying agent in the formulation of petrochemical products. In: Green Sustainable Process for Chemical and Environmental Engineering and Science. Elsevier; 2021. p. 399–422.
84. Hewitt JP. Sunscreen Formulation: Optimising Aesthetic Elements for Twenty-First-Century Consumers. In: Wang SQ, Lim HW, editors. Principles and Practice of Photoprotection. Cham: Springer International Publishing; 2016. p. 289–302.
85. [REDACTED]
86. Sohn M, Amorós-Galicia L, Krus S, Martin K, Herzog B. Effect of emollients on UV filter absorbance and sunscreen efficiency. *J Photochem Photobiol B*. 2020;205.
87. Yeah-Young B. BASF Emollients-Choosing the right Emollient, Technical document. 2012.
88. Borda Boreu M. GELES Y CREMIGELES CONCEPTOS GENERALES, FORMULACIÓN Y APLICACIONES COSMÉTICAS. 2019.
89. 5.1.4. Microbiological quality... - European Pharmacopoeia 10.7 [Internet]. [cited 2022 May 17]. Available from: <https://pheur.edqm.eu/app/10-7/content/10-7/50104E.htm?highlight=on&terms=cutaneous>
90. Ethylhexylglycerin (Explained + Products) [Internet]. [cited 2022 May 18]. Available from: <https://incidecoder.com/ingredients/ethylhexylglycerin>
91. Disodium EDTA (Explained + Products) [Internet]. [cited 2022 May 18]. Available from: <https://incidecoder.com/ingredients/disodium-edta>
92. Borda-Boreu M. Emulsificación. Caracterización de una emulsión. Proceso de fabricación de una emulsión. In: Master Dermofarmacia y Cosmetología. 2021. p. 1–28.
93. Borda Boreu M. ESTABILIDAD EMULSIONES Y OTRAS FORMAS COSMÉTICAS. 2019.
94. Tadros TF. Emulsions [Internet]. De Gruyter; 2016 [cited 2022 May 13]. Available from: <https://www.degruyter.com/document/doi/10.1515/9783110452242/html>
95. Osterwalder U, Herzog B. The long way towards the ideal sunscreen - Where we stand and what still needs to be done. *Photochemical and Photobiological Sciences*. 2010;9(4):470–81.

96. Nash JF, Tanner PR. The Controversy of Sunscreen Product Exposure: Too Little, Too Much, or Just Right. *Principles and Practice of Photoprotection* [Internet]. 2016 Jan 1 [cited 2022 Apr 30];125–39. Available from: https://link.springer.com/chapter/10.1007/978-3-319-29382-0_8
97. Diffey BL. When should sunscreen be reapplied? *J Am Acad Dermatol*. 2001 Mar;45(6):882–5.
98. Geoffrey K, Mwangi AN, Maru SM. Sunscreen products: Rationale for use, formulation development and regulatory considerations. *Saudi Pharmaceutical Journal* [Internet]. 2019;27(7):1009–18. Available from: <https://doi.org/10.1016/j.jsps.2019.08.003>
99. Suozzi K, Turban J, Girardi M. Cutaneous photoprotection: A review of the current status and evolving strategies. *Yale Journal of Biology and Medicine*. 2020;93(1):55–67.
100. Briasco B, Capra P, Mannucci B, Perugini P. Stability study of sunscreens with free and encapsulated UV filters contained in plastic packaging. *Pharmaceutics*. 2017;9(2).
101. Kumar K, Dhawan N, Sharma H, Vaidya S, Vaidya B. Bioadhesive polymers: Novel tool for drug delivery. *Artif Cells Nanomed Biotechnol*. 2014;42(4):274–83.
102. da Silva JB, de Souza Ferreira SB, de Freitas O, Bruschi ML. A critical review about methodologies for the analysis of mucoadhesive properties of drug delivery systems. Vol. 43, *Drug Development and Industrial Pharmacy*. Taylor and Francis Ltd.; 2017. p. 1053–70.
103. Hägerström H, Edsman K. Interpretation of mucoadhesive properties of polymer. *Journal of Pharmacy and Pharmacology*. 2001;53:1589–99.
104. Djekic L, Martinovic M. In Vitro, Ex Vivo and In Vivo Methods for Characterization of Bioadhesiveness of Drug Delivery Systems. p. 57–98.
105. Carvalho FC, Calixto G, Hatakeyama IN, Luz GM, Gremião MPD, Chorilli M. Rheological, mechanical, and bioadhesive behavior of hydrogels to optimize skin delivery systems. Vol. 39, *Drug Development and Industrial Pharmacy*. 2013. p. 1750–7.
106. Palacio MLB, Bhushan B. Bioadhesion: A review of concepts and applications. *Philosophical Transactions of the Royal Society A: Mathematical, Physical and Engineering Sciences*. 2012;370(1967):2321–47.
107. Wong R, Geyer S, Weninger W, Guimberteau JC, Wong JK. The dynamic anatomy and patterning of skin. *Exp Dermatol*. 2016;25(2):92–8.

108. [REDACTED]
[REDACTED]
[REDACTED]
109. Hägerström H, Bergström CAS, Edsman K. The importance of gel properties for mucoadhesion measurements: a multivariate data analysis approach. *Journal of Pharmacy and Pharmacology*. 2004;56(2):161–8.
110. Tuğcu-Demiröz F, Acartürk F, Erdoğan D. Development of long-acting bioadhesive vaginal gels of oxybutynin: Formulation, in vitro and in vivo evaluations. *Int J Pharm*. 2013;457(1):25–39.
111. EL Hosary R, El-Mancy SMS, El Deeb KS, Eid HH, EL Tantawy ME, Shams MM, et al. Efficient wound healing composite hydrogel using Egyptian *Avena sativa* L. polysaccharide containing β -glucan. *Int J Biol Macromol*. 2020;149:1331–8.
112. [REDACTED]
[REDACTED]
[REDACTED]
113. [REDACTED]
[REDACTED]
[REDACTED]
114. [REDACTED]
[REDACTED]
115. Duchene, D.; Ponchel G. Bioadhesion: a new pharmacotechnical method for improving therapeutic efficiency. *S T D Pharma*. 1989;5:830–8.
116. Piérard-Franchimont C, Piérard GE. Comedogenesis. *Cosmetics* [Internet]. 1999 [cited 2022 May 8];268–74. Available from: https://link.springer.com/chapter/10.1007/978-3-642-59869-2_23
117. Titus S, Hodge J. Diagnosis and treatment of acne. *Am Fam Physician* [Internet]. 2012 Oct 15 [cited 2022 May 8];86(8):734–40. Available from: <https://pubmed.ncbi.nlm.nih.gov/23062156/>
118. Thielitz A, Helmdach M, Röpke EM, Gollnick H. Lipid analysis of follicular casts from cyanoacrylate strips as a new method for studying therapeutic effects of antiacne

- agents. *Br J Dermatol* [Internet]. 2001 [cited 2022 May 8];145(1):19–27. Available from: <https://pubmed.ncbi.nlm.nih.gov/11453902/>
119. Gollnick H, Cunliffe W, Berson D, Dreno B, Finlay A, Leyden JJ, et al. Management of acne: a report from a Global Alliance to Improve Outcomes in Acne. *J Am Acad Dermatol* [Internet]. 2003 Jul 1 [cited 2022 May 8];49(1 Suppl). Available from: <https://pubmed.ncbi.nlm.nih.gov/12833004/>
120. Tan J, Bourdès V, Bissonnette R, Petit L, Reynier P, Khammari A, et al. Prospective Study of Pathogenesis of Atrophic Acne Scars and Role of Macular Erythema. *J Drugs Dermatol* [Internet]. 2017 Jun 1 [cited 2022 May 8];16(6):566–72. Available from: <https://pubmed.ncbi.nlm.nih.gov/28686774/>
121. Draelos ZD, DiNardo JC. A re-evaluation of the comedogenicity concept. *J Am Acad Dermatol* [Internet]. 2006 [cited 2022 May 8];54(3):507–12. Available from: <https://pubmed.ncbi.nlm.nih.gov/16488305/>
122. Fulton JE. Comedogenicity and irritancy of commonly used ingredients in skin care products. *J Soc Cosmet Chem*. 1989;40(6):321–33.
123. Mills OH, Kligman AM. A human model for assessing comedogenic substances. *Arch Dermatol* [Internet]. 1982 [cited 2022 May 8];118(11):903–5. Available from: <https://pubmed.ncbi.nlm.nih.gov/7138047/>
124. O’Riordan DL, Steffen AD, Lunde KB, Gies P. A Day at the Beach While on Tropical Vacation. *Arch Dermatol*. 2008;144(11):1449–55.
125. Gallardo-Sánchez A. *Filtros solares progresivos*. [Barcelona]; 2012.
126. CSIC. *CROMATOGRÁFIA LIQUIDA DE ALTA EFICACIA*.
127. [REDACTED]
128. Beer-Lambert Law | Technical Note 120 [Internet]. [cited 2022 Mar 14]. Available from: <https://www.denovix.com/tn-120-smartpath%C2%AE-and-high-absorbance/>
129. Akash MSH, Rehman K. Differential Scanning Calorimetry. In: *Essentials of Pharmaceutical Analysis*. Singapore: Springer Singapore; 2020. p. 199–206.
130. Suñé-Pou M. Cholesteryl oleate-loaded solid lipid nanoparticles for the vectorization of nucleic acids [Internet]. Available from: www.tdx.cat

131. [REDACTED]
[REDACTED]
132. [REDACTED]
133. Miralles R, Nonell S, Raga MM, Giuglietta A, Teixidó J. Benzoic acid ester compounds, compositions, uses and methods related thereto. Spain; US 8,545,816 B2, 2013. p. 1–29.
134. Gallardo A, Teixidó J, Miralles R, Raga M, Guglietta A, Marquillas F, et al. Dose-dependent progressive sunscreens. A new strategy for photoprotection? *Photochemical and Photobiological Sciences*. 2010;9(4):530–4.
135. Brooke DN, Burns J. S., Crooke M. J., Great Britain. Environment Agency. UV-filters in cosmetics : prioritisation for environmental assessment. Environment Agency; 2008. 112 p.
136. US EPA. Estimation Program Interface (EPI) Suite. <https://www.epa.gov/oppt/exposure/pubs/episuitedl.htm>. 2012.
137. 01 General notices - European Pharmacopoeia 10.6 [Internet]. 2022. Available from: <https://pheur.edqm.eu/app/10-6/content/10-6/10000E.htm?highlight=on&terms=solubility&terms=solubility>
138. European chemicals agency. Cosmetic Products Regulation, Annex VI - Allowed UV Filters. 1223/2009/EC on Cosmetic Products, as corrected by Corrigendum to Commission Regulation (EU) 2021/850. 2021.
139. [REDACTED]
[REDACTED]
[REDACTED]
140. [REDACTED]
[REDACTED]
141. Garbutcheon-Singh KB, Dixit S, Lee A, Brown P, Smith SD. Assessment of attitudes towards sun-protective behaviour in Australians: A cross-sectional study. *Australasian Journal of Dermatology*. 2016 May 1;57(2):102–7.
142. Ethanol - Dynamic and Kinematic Viscosity vs. Temperature and Pressure [Internet]. [cited 2022 May 31]. Available from: https://www.engineeringtoolbox.com/ethanol-dynamic-kinematic-viscosity-temperature-pressure-d_2071.html

143. Poly(ethylene glycol) 400 | Sigma-Aldrich [Internet]. [cited 2022 May 31]. Available from: <https://www.sigmaaldrich.com/ES/es/product/sial/81170>
144. WILLE, Charlotte; BLECKMANN A, SCHLAGER T. WO 2016/206962 A1. [DE/DE]; Unnastrasse 48, 20253 Hamburg (DE); 2016.
145. Sohn M, Amorós-Galicia L, Stanislaw K, Martin K, Herzog B. Effect of emollients on UV filter absorbance and sunscreen efficiency. *J Photochem Photobiol.* 2020;205(1):1–8.
146. Herzog B, Mongiat S, Deshayes C, Neuhaus M, Sommer K, Mantler A. In vivo and in vitro assessment of UVA protection by sunscreen formulations containing either butyl methoxy dibenzoyl methane, methylene bis-benzotriazolyl tetramethylbutylphenol, or microfine ZnO. *Int J Cosmet Sci.* 2002;24(3):170–85.
147. O’Riordan DL, Steffen AD, Lunde KB, Gies P. A Day at the Beach While on Tropical Vacation. *Arch Dermatol.* 2008;144(11):1449–55.
148. Roell KR, Reif DM, Motsinger-Reif AA. An introduction to terminology and methodology of chemical synergy-perspectives from across disciplines. Vol. 8, *Frontiers in Pharmacology.* Frontiers Research Foundation; 2017.
149. Herzog B, Osterwalder U. Simulation of sunscreen performance. In: *Pure and Applied Chemistry.* Walter de Gruyter GmbH; 2015. p. 937–51.
150. [REDACTED]
151. BASF. Sunscreen simulator [Internet]. Available from: https://www.sunscreensimulator.basf.com/Sunscreen_Simulator/computation
152. [REDACTED]
153. [REDACTED]
154. Commission E. https://ec.europa.eu/health/scientific-committees/scientific-committee-consumer-safety-sccs_es.
155. Review CI. <https://www.cir-safety.org>.
156. cancer prevention partners- Campaign for safe cosmetics B. <https://www.safecosmetics.org>.
157. (EPA) USEPA. 1-(4-tert-Butylphenyl)-3-(4-methoxyphenyl)propane-1,3-dione 70356-09-1 | DTXSID9044829, Property Summary [Internet]. Available from:

- <https://comptox.epa.gov/dashboard/dsstoxdb/results?search=avobenzene#properties>
158. EDGAR DOOLEY LAUREN M. ; ADHIKARI KC. A GENERAL LEXICON FOR SENSORY ANALYSIS OF TEXTURE AND APPEARANCE OF LIP PRODUCTS. *J Sens Stud.* 2009;(24):581–600.
 159. Terescenco D, Hucher N, Picard C, Savary G. Sensory perception of textural properties of cosmetic Pickering emulsions. *Int J Cosmet Sci.* 2020;42(2):198–207.
 160. Rafferty DW, Dupin L, Zellia J, Giovannitti-Jensen A. Predicting lipstick sensory properties with laboratory tests. *Int J Cosmet Sci.* 2018;40(5):451–60.
 161. Marto J, Pinto P, Fitas M, Gonçalves LM, Almeida AJ, Ribeiro HM. Safety assessment of starch-based personal care products: Nanocapsules and pickering emulsions. *Toxicol Appl Pharmacol* [Internet]. 2018;342(January):14–21. Available from: <https://doi.org/10.1016/j.taap.2018.01.018>
 162. Del Pozo Ojeda A, Suñé Arbussà JM. Extensibilidad en pomadas. I. Definición y determinación. *Galen Acta.* 1955;VIII:7–26.
 163. Del Pozo Carrascosa A, Suñé Negre J, Faulí trillo C. Diseño de los modelos matemáticos que rigen los fenómenos de extensibilidad de pomadas. *Boll Chim Farm.* 1987;126(8):330–5.
 164. ISO 24443: 2012 Determination of sunscreen UVA photoprotection in vitro. 2012.
 165. ISO 16217:2020 Cosmetics — Sun protection test methods — Water immersion procedure for determining water resistance. 2020.
 166. ISO 18861:2020 Cosmetics — Sun protection test methods — Percentage of water resistance. 2020.
 167. Sohn M, Malburet C, Caliskan G, Büchse A, Grumelard J, Chambert M, et al. In vitro water resistance testing using SPF simulation based on spectroscopic analysis of rinsed sunscreens. *Int J Cosmet Sci.* 2018;40(3):217–25.
 168. ISO 24444:2010 - Cosmetics - Sun protection test methods - In vivo determination of the sun protection factor (SPF). 2010.
 169. Nardi-Ricart A, Linares MJ, Villca-Pozo F, Pérez-Lozano P, Suñé-Negre JM, Bachs-deMiquel L, et al. A new design for the review and appraisal of semi-solid dosage forms:

Semi-solid Control Diagram (SSCD). Kizilel S, editor. PLoS One. 2018 Sep 7;13(9):e0201643.

170. ICH HARMONISED TRIPARTITE GUIDELINE : STABILITY TESTING OF NEW DRUG SUBSTANCES AND PRODUCTS Q1A(R2). 2003.

171. [REDACTED]

172. Protocolo de estudio de estabilidad para productos hidroalcoholicos-Puig Research Center.

173. Estabilidad y especificaciones de producto acabado-Laboratorios Myrurgia.

174. Kim E, Kim S, Nam GW, Lee H, Moon S, Chang I. The alkaline pH-adapted skin barrier is disrupted severely by SLS-induced irritation. *Int J Cosmet Sci.* 2009;31(4):263–9.

175. Proksch E. pH in nature, humans and skin. *Journal of Dermatology.* 2018;45(9):1044–52.

176. Lukić M, Pantelić I, Savić SD. Towards optimal ph of the skin and topical formulations: From the current state of the art to tailored products. Vol. 8, *Cosmetics.* 2021.

177. cancer prevention PB. *CHEMICALS OF CONCERN-Page Under Scientific Review.*

178. [REDACTED]

179. [REDACTED]

180. [REDACTED]

181. Lees M. *Clearing Concepts: A Guide to Acne Treatment.* 2013.

182. [REDACTED]

183. [REDACTED]

184. Becker LC. Safety Assessment of Glycerin as Used in Cosmetics Status. Cosmetic Ingredient Review. 2014;202–331.
185. Shank C, Ph D, Slaga TJ, Ph D, Snyder PW, The PD, et al. Safety Assessment of Microbial Polysaccharide Gums as Used in Cosmetics Status : Release Date : Panel Meeting Date : Final Report for public distribution. 2012.
186. Colipa C. Scientific Committee on Consumer Safety Phenoxyethanol. 2012;(March).
187. CIR expert panel. Safety Assesment of Alkyl Glycery Ethers as used in Cosmetics. Int J Toxicol. 2013;32 (suplem:5S-21S.
188. Stiefel C, Schwack W. Photoprotection in changing times - UV filter efficacy and safety, sensitization processes and regulatory aspects. Int J Cosmet Sci. 2015;37(1):2–30.
189. Bp D, Continental J, Hydrochloride D, Simone G, Tpo D. Safety data sheet Safety data sheet. Carbon N Y. 2005;1173(i):1–8.
190. EVONIK. Safety data sheet EUDRAGIT L 100. 2017.
191. Partners Breast cancer prevention. CHEMICALS OF CONCERN-Page Under Scientific Review.
192. WILLE, Charlotte; BLECKMANN, Andreas; SCHLÄGER T. WO2016/206961 A1. [DE/DE]; Unnastrasse 48, 20253 Hamburg (DE); 2016.
193. WILLE C, BLECKMANN A, SCHLAGER T. WO 2016/206963 A1. [DE/DE]; Unnastrasse 48, 20253 Hamburg (DE); 2016.
194. WILLE, Charlotte; Babentwiete; BLECKMANN, Andreas; SCHERNER C, DINGLER C. WO 2017/036662 A1. [DE/DE]; Unnastrasse 48, 20253 Hamburg (DE); 2017.
195. BORCHERS, Kathrin; BLECKMANN, Andreas; ZIPPEL J. WO 2017/102300 A1. [DE/DE]; Unnastrasse 48, 20253 Hamburg (DE); 2017.
196. BORCHERS, Kathrin; LERG, Heike; BLECKMANN A, ZIPPEL J. WO 2017/102301 A. [DE/DE]; Unnastrasse 48, 20253 Hamburg (DE); 2017.
197. BORCHERS, Kathrin; LERG H, BLECKMANN A, ZIPPEL J. WO 2017/102302 A1. [DE/DE]; Unnastrasse 48, 20253 Hamburg (DE); 2017.
198. BORCHERS, Kathrin; LERG, Heike; BLECKMANN A, ZIPPEL J. WO 2017/129432 A1. [DE/DE]; Unnastrasse 48, 20253 Hamburg (DE); 2017.
199. Romeu X. Fotoprotección-Fotoprotectores-Los Filtros UV. 2021. p. 1–76.

200. Phenoxyethanol properties [Internet]. Available from: <https://incidecoder.com/ingredients/phenoxyethanol>
201. Glycerin properties [Internet]. Available from: <https://incidecoder.com/ingredients/glycerin>
202. [REDACTED]
203. Certificate of Analysis BTC Europe GmbH. 2019.
204. Amorós-Galicia L. Investigations of spectral performance of photostability of UV absorbers used in sunscreens. University of Basel; 2018.
205. Hewitt JP. Sunscreen Formulation: Optimising Aesthetic Elements for Twenty-First-Century Consumers. Henry S, editor. Principle and Practice of Photoprotection. 2016. p. 290–303.
206. Acne.org. What Is Comedogenicity, and What Ingredients Are Comedogenic?
207. WILLE C, BLECKMANN A, SCHLAGER T, WILLE, Charlotte; Babentwiete; BLECKMANN, Andreas; SCHERNER C, DINGLER C, BORCHERS, Kathrin; BLECKMANN, Andreas; ZIPPEL J, et al. WO 2017/129432 A1. [DE/DE]; Unnastrasse 48, 20253 Hamburg (DE); 2017.
208. Ducray. MELASCREEN UV CREMA LIGERA SPF50+ UVA [Internet]. Available from: <https://www.ducray.com/es-es/melascreen/melascreen-uv-crema-ligera-spf-50-uva>
209. [REDACTED]
[REDACTED]
[REDACTED]
[REDACTED]
210. [REDACTED]
[REDACTED]
211. [REDACTED]
212. Food and Drug Administration. International Conference on Harmonisation; Guidance on Q6A Specifications: Test Procedures and Acceptance Criteria for New Drug Substances and New Drug Products: Chemical Substances. 2000 p. 83041–63.
213. Properties C, Properties T. Technical data sheet Technical data sheet. Cell. 2005;123(May):98–9.
214. Québatte G. Viscosity, FS 2015, Nr. 12523-02 Arzneiformenlehre II. 2015.

215. Dick IP, Scott RC. Pig Ear Skin as an In-vitro Model for Human Skin Permeability. *Journal of Pharmacy and Pharmacology*. 1992 Aug 1;44(8):640–5.
216. Daly S, Ouyang H, Maitra P. *Chemistry of Sunscreens. Principles and Practice of Photoprotection* [Internet]. 2016 Jan 1 [cited 2022 Jun 2];159–78. Available from: https://link.springer.com/chapter/10.1007/978-3-319-29382-0_10
217. Berset G, Gonzenbach H, Christ R, Martin R, Deflandre A, Mascotto RE, et al. Proposed protocol for determination of photostability. Part I: Cosmetic UV filters. *Int J Cosmet Sci*. 1996;18(4):167–77.
218. Yamaji M, Kida M. Photothermal tautomerization of a UV sunscreen (4-tert -butyl-4'-methoxydibenzoylmethane) in acetonitrile studied by steady-state and laser flash photolysis. *Journal of Physical Chemistry A* [Internet]. 2013 Mar 7 [cited 2022 May 30];117(9):1946–51. Available from: <https://pubs.acs.org/doi/pdf/10.1021/jp312774e>
219. Diffey BL. A method for broad spectrum classification of sunscreens. *Int J Cosmet Sci*. 1994 Apr;16(2):47–52.
220. Hojerová J, Medovčíková A, Mikula M. Photoprotective efficacy and photostability of fifteen sunscreen products having the same label SPF subjected to natural sunlight. *Int J Pharm*. 2011 Apr 15;408(1):27–38.

ANNEXES

Annex 1

Table A 1. Summary of ingredients and concentrations of beneficial, recommended and detrimental ingredients for PRE-A in formulation, formulation patents by Beiersdorf.

Ingredient Type	Ingredient Family	Ingredient	Beneficial ingredient concentration in Emulsion (M ingredient/M total) in %	Preferred ingredient concentration in Emulsion (M ingredient/ M total) in %		
UVA Filter precursor	pre-avobenzene		0,1-6	1-4,75		
	Ethanol		0,1-99	2-60		
Emollient	C 12-C 15 Alkylbenzoat		0,1-20			
			0,5-3			
		Dialkyladipate	Dimethyladipat Diethyladipat Dipropyladipat Diisopropyladipat Diisobutyladipat Di-n-butyladipat Di-2- ethylhexyladipat Dicyclohexyladipat Dialkyladipat Di-n-butyladipat	as total concentration of Dialkyladipates		
			Dialkylcarbonate	Dicaprylylcarbonat Dimethylcarbonat. Diethylcarbonat. Diisopropylcarbonat. Di-n-butylcarbonat.	1-20 as total concentration of Dialkylcarbonates	
Natural/Synthetic Oils, Grease, Wax	Dimethicone free!					
	alpha-Liponacid					
	Folic acid					
	Phytoen					
	D-Biotin					
	Cienzym Q 10					
	alpha-Glucosylrutin					
	Carnosin					
	natural and/or synthetic Isoflavonoids					
	Flavonoids					
	Kreatin					
	Kreatinin					
	Taurin					
	beta-Alanin					
	Panthenol					
	Magnolol					
	Honokiol					
	Tocopherylacetate					
	Dihydroxyacetone					
	8-Hexadecen-1,16-dicarbonacid					
	Glycerylglycose					
	(2-Hydroxyethyl) urea					
	Vitamin E					
Hyaluronic acid						
Preservatives	Alkandiol	1,2-Pentandiol	0,1-2,5	as total concentration of Alkandiol		
		1,2-Hexandiol				
		1,2-Octandiol				
		1,2-Decandiol				
		2-Methyl-1,3-propandiol				
	Phenoxyethanol		0,1-1 alone or in combination			
	Ethylhexylglycerin					

UV-filters	2-Phenylbenzimidazol-5-sulfonacid and/or its salts	1-4	
	Phenylen-1,4-bis-(2-benzimidazol-3,3'-5,5'-tetrasulfonsauresalze	2-Phenylbenzimidazol-5-sulfonacid salt	
	1,4-di-(2-oxo-10-Sulfo-3-borylidenmethyl)-Benzol and their salts		
	4-(2-Oxo-3-borylidenmethyl)benzolsulfonacid salts		
	2-Methyl-5-(2-oxo-3-borylidenmethyl)sulfonsauresalze		
	2,2'-Methylen-bis-(6-(2H-benzotriazol-2-yl)-4-(1,1,3,3-tetramethylbutyl)-phenol		
	2-(2H-benzotriazol-2-yl)-4-methyl-6-[2-methyl-3-[1,3,3,3-tetramethyl-1-(trimethylsilyloxy)disiloxanyl]propyl]-phenol		
	3-(4-Methylbenzyliden)campher		
	3-Ben-zylidencampher		
	Ethylhexylsalicylat	3-5%, in case of combination with homosalate, then 2-5%	
	Terephthalidencamphersulfonacid		
	2-Ethylhexyl-2-cyano-3,3-diphenylacrylat (INCI: Octocrylen)		
	4-(Dimethylamino)-benzoesaure(2-ethylhexyl)ester		
	4-(Dimethylamino)benzoesaure-amyester		
	4-Methoxybenzalmon-sauredi(2-ethylhexyl)ester;		
	Methoxzimtsaure(2-ethylhexyl)ester		
	2-Hydroxy-4-methoxybenzophenon (INCI: Oxybenzone)		
	2-Hydroxy-4-methoxy-4'-methylbenzophenon		
	2,2'-Dihydroxy-4-methoxybenzophenon		
	Homomenthylsalicylat	3-10%, in case of combination with Ethylhexylsalicylat, then 2-10%	
	2-Ethylhexyl-2-hydroxybenzoat		
	Dmethicodimethylbenzalmalonat		
	3-(4-(2,2-bis-Ethoxycarbonylvinyl)-phenoxy)propenyl-methoxysila-xan 1		
	Dimethylsiloxan- Copolymer		
	4-(tert.-Butyl)-4'-methoxydibenzoylmethan		
	2-(4'-Diethylamino-2'-hydroxybenzoyl)-benzoesacidhexylester		
	Diethylhexyl-Butamidotriazone		
	2,4-bis-[5-(1(dimethylpropyl)benzoxazol-2-yl-(4-phenyl)-imino)-6-(2-ethylhexyl)-imino-1,3,5-triazin mit der (CAS Nr. 288254-16-0)		
	2,4-Bis-[4-(2-Bis-Ethylhexyloxyphenol Methoxyphenyl) Triazin		2-5%
	Ethylhexyl Triazone	2-5%	
	2,4,6-Tribiphenyl-4-yl-1,3,5-triazin		
	Merocyanine		
	Titanoxid		
	Zinkoxid		
	Natriumsalts		
	Kaliumsalts		

Annex 2

Table A 2. Average values and standard deviations of organoleptic evaluations for gel formulations, n=20

Gel nr.	Spreadability	Non-stickiness	Fluidity	Non-white cast effect	Skin feeling	Appearance
1	2,2± 0,8	1,4± 0,5	1,2± 0,4	3,1± 0,7	1,6± 0,5	2,5± 0,8
2	2,1± 0,8	3,1± 0,4	1,3± 0,4	3,1± 0,6	2,1± 0,7	4,7± 0,5

Table A 3. Average values and standard deviations of organoleptic evaluations for emulsion type, n=20

Type.	Spreadability	Non-stickiness	Fluidity	Non-white cast effect	Skin feeling	Appearance
O/W Em. A	2,3± 0,7	2,9± 0,5	2,2± 0,6	4,6± 0,7	2,2± 0,5	1,3± 0,6
W/O Em. A	2,9± 0,5	2,9± 0,5	2,2± 0,6	4,7± 0,5	2,3± 0,6	1,5± 0,6
O/W Em. B	2,8± 0,6	3,1± 0,4	2,2± 0,4	4,8± 0,5	2,8± 0,6	2,3± 0,4
W/O Em. B	3,0± 0,5	2,1± 0,6	1,3± 0,5	4,8± 0,4	1,4± 0,6	1,8± 0,5

Table A 4. Average values and standard deviations of organoleptic evaluations for different emulsions, n=20

Emulsion nr.	Spreadability	Non-stickiness	Fluidity	Non-white cast effect	Skin feeling	Appearance
1	2,8± 0,6	2,8± 0,6	2,5± 0,7	4,2± 0,7	2,8± 0,5	3,2± 0,5
2	2,4± 0,5	2,0± 0,5	2,4± 0,6	3,1± 0,7	2,7± 0,7	3,0± 0,4
3	3,6± 0,6	3,0± 0,5	2,2± 0,5	3,1± 0,6	3,0± 0,4	3,6± 0,6
4	4± 0,4	3,9± 0,4	2,4± 0,7	4,6± 0,5	3,9± 0,5	4,6± 0,5
5	4,6± 0,5	4,2± 0,6	2,9± 0,6	4,7± 0,5	4,0± 0,6	4,9± 0,4
6	4,7± 0,5	4,4± 0,5	3,2± 0,7	4,8± 0,4	4,7± 0,7	4,9± 0,3
06-13	4,5± 0,8	4,6± 0,9	3,1± 0,5	4,8± 0,3	4,8± 0,4	4,9± 0,5

Resolució parcial definitiva de la convocatòria de doctorats industrials (DI) 2019. (2n termini)

Fets

1. La Resolució EMC/394/2019, de 19 de febrer (DOGC núm. 7817 – 25.2.2019), aprova les bases reguladores dels ajuts a doctorats industrials (DI).
2. La Resolució EMC/581/2019, de 28 de febrer (DOGC núm. 7829 – 13.3.2019), obre la convocatòria de doctorats industrials (DI) 2019 (ref. BDNS 443065).
3. El 9 de juliol de 2019 es reuneix la comissió de selecció de la convocatòria de doctorats industrials (DI) 2019.

Fonaments de dret

1. És d'aplicació la Llei 38/2003, de 17 de novembre, general de subvencions i el Reial decret 887/2006, de 21 de juliol pel qual s'aprova el Reglament de la Llei 38/2003, de 14 de novembre.
2. El capítol IX del Decret legislatiu 3/2002, de 24 de desembre, pel qual s'aprova el Text refós de la Llei de finances públiques de Catalunya, regula el règim jurídic de les subvencions i les transferències de la Generalitat de Catalunya.
3. La Resolució UNI/962/2005, d'1 de febrer, per la qual s'aproven les bases generals que han de regir la concessió de beques i ajuts convocats per l'AGAUR.
4. El Decret 223/2013, de 15 d'octubre, crea la Seu electrònica de la Generalitat de Catalunya i en regula el funcionament, així com el del Registre electrònic i el Tauler electrònic.
5. L'Ordre ECO/172/2015, de 3 de juny, (DOGC núm. 6890, de 11.6.2015), regula les formes de justificació de subvencions.
6. La base 15.1 de la Resolució EMC/394/2019, de 19 de febrer, preveu que es podran dictar resolucions parcials definitives en les dates que es faran constar a la convocatòria corresponent.
7. L'article 5.2 de la Resolució EMC/581/2019, de 28 de febrer, estableix el següent:
“ Es preveu dictar quatre resolucions parcials definitives en les dates següents:
– Segona resolució parcial: segona quinzena de juliol de 2019
[...]

8. L'article 6.2 de la Resolució EMC/581/2019, de 28 de febrer, estableix que la resolució de concessió correspon al Consell de Direcció de l'AGAUR i, per delegació, a la CEAR i al CEAU o la persona que n'ocupa la presidència, segons l'acord del Consell de Direcció de 5 de desembre de 2002 (Resolució UNI/73/2003, de 14 de gener, DOGC núm. 3808, de 27.1.2003).
9. El president de la Comissió Executiva d'Ajuts Universitaris i el president de la Comissió Executiva d'Ajuts de Recerca, en l'ús de les funcions que els han estat delegades pel Consell de Direcció de l'Agència, en sessió de 5 de desembre de 2002, i atesa la Proposta de Resolució definitiva de l'òrgan instructor de la convocatòria DI (2019);

Resolen:

1. Concedir els ajuts que es detallen en el document adjunt: Sol·licituds Concedides, per un import de 1.226.136,00€ a càrrec de les partides: 409.0001, 440.0001, 442.0001, 449.0001, 470.0001, 482.0001 del pressupost de l'Agència per als anys 2019, 2020 i 2021, en el marc de la convocatòria de doctorats industrials (DI) 2019, en els termes que s'hi fan constar.
2. Sotmetre l'atorgament dels ajuts al compliment per part dels seus destinataris de les condicions i obligacions previstes a la Resolució EMC/394/2019, de 19 de febrer, per la qual s'aproven les bases reguladores dels ajuts a doctorats industrials (DI), i a la Resolució EMC/581/2019, de 28 de febrer, per la qual s'obre la convocatòria de doctorats industrials (DI) 2019.

Contra aquesta resolució, que exhaureix la via administrativa, es pot interposar un recurs potestatiu de reposició davant la presidenta de la Comissió Executiva d'Ajuts Universitaris i el president de la Comissió Executiva d'Ajuts de Recerca de l'AGAUR, en el termini d'un mes, a comptar des de l'endemà de la seva publicació al tauler electrònic de l'Administració de la Generalitat de Catalunya, o bé es pot interposar directament recurs contenciós administratiu davant el jutjat contenciós administratiu de Barcelona, en el termini de dos mesos, a comptar des de l'endemà de la seva publicació al tauler esmentat, de conformitat amb el que preveuen els articles 123 i 124 de la Llei 39/2015, d'1 d'octubre, del Procediment Administratiu Comú de les Administracions Públiques, i els articles 8, 14 i 46 de la Llei 29/1998, de 13 de juliol, reguladora de la jurisdicció contenciosa administrativa.

Signat a Barcelona,

P. d (Resolució UNI/73/2003, de 14 de gener, DOGC de 27.1.2003)

La presidenta de la Comissió Executiva
d'Ajuts Universitaris
M. Victòria Girona Brumós

El president de la Comissió Executiva
d'Ajuts de Recerca
Joan Gómez Pallarès

ANNEX: Sol·licituds concedides

Núm. d'exp.	Empresa	CIF	Import atorgat empresa	Organisme de recerca	CIF	Import atorgat org. recerca	Identificació Candidat/a
28	SENSING SOLUTIONS	B66724568	21.600,00 €	Consell Superior d'Investigacions Científiques	Q0818002D	33.960,00 €	Marta Mañez Alambiaga
29	Onalabs Inno-Hub SL	B66905936	21.600,00 €	Universitat de Barcelona	Q0818001J	33.960,00 €	Javier Aguilar Torán
30	Acsa, Obras e Infraestructuras S.A.U	A08112716	21.600,00 €	Universitat de Barcelona	Q0818001J	33.960,00 €	Karin Florencio Pérez
31	Ingeniería Física de Alta Tecnología, S.L. (INFISAT)	B63378616	21.600,00 €	Universitat Politècnica de Catalunya	Q0818003F	33.960,00 €	Adil Rachid
32	Etticas Research and Innovation (ETTCAS FOUNDATION)	G66592817	21.600,00 €	Universitat Autònoma de Barcelona	Q0818002H	33.960,00 €	Alba Molina Serrano
33	SEAT S.A.	A28049161	21.600,00 €	Universitat Politècnica de Catalunya	Q0818003F	33.960,00 €	Jessica Ferrelira Vicente
34	SEAT S.A.	A28049161	21.600,00 €	Universitat Ramon Llull	G59069740	33.960,00 €	Juan Manuel Garcia Sánchez
35	DARES TECHNOLOGY S.L.	B66557844	21.600,00 €	Universitat Politècnica de Catalunya	Q0818003F	33.960,00 €	Marta Monfort Codinach
36	JG INGENIEROS S.A.	A08606410	21.600,00 €	Universitat Politècnica de Catalunya	Q0818003F	33.960,00 €	Gil Vinyeta Medina
37	Roka Furadada S.L.	B67401505	21.600,00 €	Universitat de Barcelona	Q0818001J	33.960,00 €	Adriana Solange Maddaleno
38	Roka Furadada S.L.	B67401505	21.600,00 €	Universitat de Barcelona	Q0818001J	33.960,00 €	Lola Amorós Galicia
39	Dena Desarrollos S.L.	B08306052	21.600,00 €	Universitat Politècnica de Catalunya	Q0818003F	33.960,00 €	Poi Fontanes Molina
40	SEAT S.A.	A28049161	21.600,00 €	Universitat Politècnica de Catalunya	Q0818003F	33.960,00 €	Joan Orti Navarro
41	BRUDY TECHNOLOGY S.L.	B61886214	21.600,00 €	Universitat Rovira i Virgili	Q9350003A	33.960,00 €	Carmen Méndez Sánchez
42	PROTEODESIGN SL	B65915167	21.600,00 €	Universitat Pompeu Fabra	Q5850017D	33.960,00 €	Núria Rafel Millan
43	Gestió de Serveis Sanitaris	Q7555308A	21.600,00 €	Universitat de Lleida	Q7550001G	33.960,00 €	Didac Florensa Cazorla
45	Aigües de Barcelona, E.M.G.C.I.A., S.A	A66098435	21.600,00 €	Universitat Ramon Llull	G59069740	33.960,00 €	Ferran Gras Traveset
46	Sonora System SL (Mercurio Distribuciones)	B82807082		Universitat de Lleida	Q7550001G	8.472,00 €	Núria Vita Barrull
47	Medtep Inc. Sucursal en España	W4007663J	21.600,00 €	Fundació Institut Mar d'Investigacions Mèdiques	G60072253	33.960,00 €	Natàlia Soldevila Domènech
48	QUSIDE TECHNOLOGIES SL	B67074849	21.600,00 €	Institut de Ciències Fotòniques	G62819537	33.960,00 €	David Cirauqui García
49	Institut Català de la Salut	Q5855029D		Universitat Rovira i Virgili	Q9350003A	8.472,00 €	Josep Zaragoza Brunet
50	Associació Jeroni de Moragas	C43036565		Universitat Rovira i Virgili	Q9350003A	33.960,00 €	Marta Torra Moreno
51	Aigües de Barcelona, E.M.G.C.I.A., S.A	A66098435	21.600,00 €	Consell Superior d'Investigacions Científiques	Q2818002D	33.960,00 €	Joan Dalmau Soler
52	INSTITUT MUNICIPAL DE L'HABITATGE I REHABILITACIÓ	P5801915I	21.600,00 €	Universitat Pompeu Fabra	Q5850017D	33.960,00 €	Eduardo González De Molina Soler
53	FACEBOOK FRANCE	530085802		Universitat Pompeu Fabra	Q5850017D	8.472,00 €	Roberto Dessi

Article

Development of a Standardized Method for Measuring Bioadhesion and Mucoadhesion That Is Applicable to Various Pharmaceutical Dosage Forms

Lola Amorós-Galicia ¹, Anna Nardi-Ricart ¹, Clara Verdugo-González ¹, Carmen Martina Arroyo-García ¹, Encarna García-Montoya ^{1,2}, Pilar Pérez-Lozano ^{1,2}, Josep M^a Suñé-Negre ^{1,2} and Marc Suñé-Pou ^{1,2,*}

¹ Department of Pharmacy and Pharmaceutical Technology and Physical Chemistry, Faculty of Pharmacy and Food Sciences, University of Barcelona, Av. Joan XXIII, 27-31, 08028 Barcelona, Spain

² Pharmacotherapy, Pharmacogenetics and Pharmaceutical Technology Research Group, Bellvitge Biomedical Research Institute (IDIBELL), Av. Gran via de l'Hospitalet, 199-203, 08908 Hospitalet de Llobregat, Spain

* Correspondence: marcsune@ub.edu

Abstract: Although some methods for measuring bioadhesion/mucoadhesion have been proposed, a standardized method is not yet available. This is expected to hinder systematic comparisons of results across studies. This study aimed to design a single/systematic in vitro method for measuring bioadhesion/mucoadhesion that is applicable to various pharmaceutical dosage forms. To this end, we measured the peak force and work of adhesion of minitables, pellets, and a bioadhesive emulsion using a texture analyzer. Porcine tissue was used to simulate human stomach/skin conditions. The results of these formulations were then compared to those for formulations without the bioadhesive product. We conducted a case study to assess the stability of a bioadhesive emulsion. The results for the two parameters assessed were contact time = 60 s and contact force = 0.5 N at a detachment speed of 0.1 mm/s. Significant differences were observed between the bioadhesive and control formulations, thus demonstrating the adhesive capacity of the bioadhesive formulations. In this way, a systematic method for assessing the bioadhesive capacity of pharmaceutical dosage forms was developed. The method proposed here may enable comparisons of results across studies, i.e., results obtained using the same and different pharmaceutical formulations (in terms of their bioadhesion/mucoadhesion capacity). This method may also facilitate the selection of potentially suitable formulations and adhesive products (in terms of bioadhesive properties).

Keywords: bioadhesion; mucoadhesion; standardized method; pharmaceutical forms; texture analyzer



Citation: Amorós-Galicia, L.; Nardi-Ricart, A.; Verdugo-González, C.; Arroyo-García, C.M.; García-Montoya, E.; Pérez-Lozano, P.; Suñé-Negre, J.M.; Suñé-Pou, M. Development of a Standardized Method for Measuring Bioadhesion and Mucoadhesion That Is Applicable to Various Pharmaceutical Dosage Forms. *Pharmaceutics* **2022**, *14*, 1995. <https://doi.org/10.3390/pharmaceutics14101995>

Academic Editor: Giulia Bonacucina

Received: 21 July 2022

Accepted: 17 September 2022

Published: 21 September 2022

Publisher's Note: MDPI stays neutral with regard to jurisdictional claims in published maps and institutional affiliations.



Copyright: © 2022 by the authors. Licensee MDPI, Basel, Switzerland. This article is an open access article distributed under the terms and conditions of the Creative Commons Attribution (CC BY) license (<https://creativecommons.org/licenses/by/4.0/>).

1. Introduction

The term bioadhesion was first introduced in the 1980s when formulations with great retention on biological surfaces started to gain attention. It is defined as the process by which natural and synthetic materials adhere to biological surfaces [1]. Similarly, mucoadhesion (a word derived from bioadhesion) refers to the process by which a bioadhesive substance adheres to the mucosal surfaces of the body [2].

Bioadhesive substances (polymers) are often added to pharmaceutical formulations to enable their adhesion to biological membranes when prolonged contact on the skin is desired [3]. An advantage of increasing the retention time of formulations is that API absorption by biological membranes is enhanced. Thus, pharmacological treatments require less reapplication to be effective, which may increase user compliance. Bioadhesive formulations require a smaller amount of API to ensure a stable therapeutic concentration. This is an advantage, particularly if the therapeutic effect is achieved systemically, since fluctuations in plasma API concentration may cause toxicity. Thus, bioadhesive formulations offer a precise systemic API concentration compared to non-bioadhesive formulations, where values below and above the therapeutic range may occur [4].

Polymers are three-dimensional structures that crosslink and increase in volume in the presence of solvents. Several forces affect the formation of polymer structures that, in turn, enable bioadhesion. The most common are covalent bonds, as well as physical entanglement, ionic forces, hydrophilic interactions, and van der Waals forces [5]. The implications of polymers (as bioadhesive excipients) in formulations are vital in medicine. Bioadhesive formulations are not only beneficial for drug delivery but also for dental (e.g., reattachment of tooth fragments) and surgical treatments (e.g., attachment of a surgical mesh to the peritoneum using fibrin glue), as is noted in the literature [6].

In drug delivery, the most common application sites include dermal, buccal, peroral, nasal, ocular, rectal, and vaginal, and the pharmacologic effect may be local or systemic. The conditions of the various application sites may differ substantially from each other. For example, the gastric mucosa differs from the epidermis. The intestinal epithelium has a mucosal layer (which is mainly composed of water and is in constant contact with an acidic medium, pH 1.2). The skin epidermis, however, has a dry environment and is composed of a lipidic barrier consisting of ceramides, cholesterol, and fatty acids [7]. Since these differences impact the measurement of bioadhesion, the test conditions should be as close as possible to the application site to simulate actual conditions. The animal selected for the bioadhesion test is also an important factor. Pig/rat mucosa and excised vaginal skin (from cow/pig) are generally preferred and are suggested in the literature [4].

Various methods have been used to assess the degree of bioadhesion of finished products or excipients, including both *in vitro* and *in vivo* methods. *In vitro* methods are generally preferred, as they are cost-effective, relatively easy to perform, and less time-consuming. They are often used to screen bioadhesive excipients prior to formulation development or to test potential bioadhesive products with different bioadhesive agents [4].

The vertical detachment strength test is a commonly employed *in vitro* test. This test can be employed by means of modified balance, a tensile device, a dynamic contact angle analyzer, or an electromagnetic transducer system (though a texture analyzer is perhaps the most employed method) [2,4]. This test quantifies the strength needed to break the internal forces binding the material to the biological surface; that is, to detach the material from the biological surface. Two parameters are commonly measured: detachment or peak force and work of adhesion. Detachment force is the maximal force required to detach the surface from the bioadhesive material. The work of adhesion is calculated from the area of the force–distance curve, following the contact of the bioadhesive material and the biological surface under a constant force during a fixed time. However, some critical factors can influence results and negatively impact the standardization of a method. Parameters used to assess bioadhesive capacity may differ across studies, which makes comparisons between different formulations and adhesive polymers difficult [2]. Some of the critical parameters mentioned in the literature include (1) contact time, (2) the force applied, (3) detachment speed [2], and (4) amount of test material [8] as potential factors affecting bioadhesion.

Some researchers have addressed some of the critical issues related to the development of an optimal standardized method of measuring bioadhesion. Hägeström et al. [8], for instance, concluded that a small amount of bioadhesive gel in contact with two mucosa sheets was preferred to a large volume of bioadhesive gel in contact with one piece of the mucosa. They also concluded, after testing different detachment speeds (0.1–0.5 mm/s), that a lower speed of 0.1 mm/s led to higher precision in terms of detachment force and work of adhesion compared with 0.5 mm/s [8]. However, although some studies [3,9] have suggested that the work of adhesion may have a higher predictive value compared to peak force, the opposite seems to be true for small samples, for which the literature reports that detachment force is more determinant [8]. Furthermore, although some studies [3,8] have been conducted on the bioadhesive capacity of topical forms, the focus has mainly been on intestinal mucoadhesion rather than on the skin [5]. These studies [3,8] have suggested methods for measuring bioadhesion. However, they have predominantly focused on examining the bioadhesive behavior of a single pharmaceutical dosage form. A standardized method to assess bioadhesion is not yet available [8]. In particular, a study

with a defined setup and test conditions would enable the development of a systematic method for measuring bioadhesion and mucoadhesion that is applicable to a variety of pharmaceutical dosage forms.

Accordingly, this study sought to design an *in vitro* method for measuring bioadhesion and mucoadhesion that is applicable to a variety of pharmaceutical dosage forms. In particular, this method aims to simulate the conditions of the human topical and gastric environments.

2. Materials and Methods

2.1. Materials

The following materials were used: a bioadhesive emulsion, bioadhesive minitables and pellets, and control minitables and pellets (with no adhesive properties). Pig ear skin and porcine stomach (obtained from the animal facility of the University of Barcelona, Bellvitge campus) were used as substrates. The following instruments were used to dissect the skin: a disposal sterile scalpel (Sheffield Morton, Sheffield S6 2BJ, England), tweezers (JP Selecta), and scissors. Distilled water was used in the saline solution (0.1% NaCl). An acidic solution with HCl was used to obtain a pH of 1.2. A material texture analyzer (and software) was also used in the experiment: MT-LQ (Stable Micro Systems, Surrey, England).

2.2. Formulations

2.2.1. Pellets

Non-bioadhesive pellets were formulated according to Table 1.

Table 1. Preparation of non-bioadhesive pellets.

Ingredients	%
Vinylpyrrolidone–vinyl acetate copolymer	5.0
Hypromellose	5.0
Sodium bicarbonate	30.0
Barium sulfate	20.0
Microcrystalline cellulose	40.0

To formulate bioadhesive pellets, the non-bioadhesive pellets listed in Table 1 were coated in a fluidized bed with a double coating of 10% polyacrylic acid. See Table 2 for details.

Table 2. Preparation of bioadhesive pellets.

Ingredients	%
Pellets in Table 1	70
Acrylic acid polymer solution (10%) (polycarbophil USP)	30

2.2.2. Minitables

Non-bioadhesive (no film coating placebo minitables) and bioadhesive minitables (film-coated placebo minitables with bioadhesive polyacrylic acid) were formulated with the ingredients in Tables 3 and 4, respectively.

Table 3. Preparation of non-bioadhesive minitables.

Ingredients	%
Sodium croscarmellose	2.0
Magnesium stearate	2.0
Talc	4.0
Isomaltose	ad 100

Table 4. Preparation of bioadhesive minitables.

Ingredients	%
Non-bioadhesive minitables	98.0
Acrylic acid polymer solution (1%) (polycarbophil USP)	2.0

2.2.3. Emulsions

A non-bioadhesive emulsion and a bioadhesive emulsion were formulated as stipulated in Table 5.

Table 5. Preparation of bioadhesive emulsions.

Phase	Ingredients	%
A	Behenyl alcohol	3.0
	Caprylic/capric triglyceride	3.0
	Dodecyl benzoate	3.0
	7-methyloctanoate	4.0
	Phenoxyethanol	0.8
B	Benzoic acid 2-ethylhexyl ester	5.0
	Distilled water	ad 100
	Disodium EDTA	1.0
	Tris(hydroxymethyl)aminomethane	2.4
C	Glycerine	0.8
	Acrylic acid polymer (polycarbophil USP)	X ¹
	Ethylhexyloxy hydroxyphenyl methoxyphenyl triazine	7.0
	Benzotriazolyl tetramethylbutylphenol	7.0
	Ethanol	10.0
	Propylenglycol	24.0

¹ x = 0, 1.

The ingredients in phase A were heated to 75 °C and mixed under stirring with a helix stirrer until complete homogenization. Phase B was heated to 75 °C and mixed under stirring in a separate beaker until homogenization. Phase B was added to phase A under stirring until complete homogenization with turrax and then cooled down to room temperature. Phase C was added slowly under stirring (Table 5). Finally, the pH was adjusted to between 5.5 and 6.5.

2.3. Gastric Mucoadhesion

The porcine stomach was defrosted and put into a saline solution (0.1% NaCl) 24 h before the start of the experiment. The stomach mucosa was cut into similar portions and placed on a Petri dish along with the saline solution. Care was taken to ensure that the contact area was completely smooth. Another piece of stomach mucosa was attached to the lower end of the cylindrical probe by means of a piece of cellulose paper and a rubber ring. The cylindrical probe measured 1 cm in diameter and was oriented downward, facing the stomach piece in the Petri dish. Excess saline was withdrawn from the Petri dish, and ten pellets of similar size and weight (87 mg ± 5%) were placed on top of the stomach mucosa. Furthermore, 1 mL of the acid solution was added to the mucosa and pellets. The Petri dish (containing the mucosa and pellets) was placed at the bottom of the texture analyzer.

The same procedure was repeated for the minitables (ten minitables of similar size and weight (49.5 mg ± 5%) were used in each experiment).

2.4. Topical Bioadhesion

For the topical bioadhesion test, a bioadhesive emulsion (emulsion containing a bioadhesive polymer) was compared with a non-bioadhesive emulsion (emulsion without a bioadhesive polymer).

Pig ear skin (as a substrate simulating human skin *in vitro*) was used to assess bioadhesion. This choice was informed by reported evidence that it is the most effective *in vitro*

substrate to simulate human skin in terms of its histological and physiological properties [10]. The ears of young pigs (40 kg) were collected from a laboratory animal facility (University of Barcelona, Bellvitge campus). They were cleaned with water at room temperature, and the hairs were trimmed. A scalpel was used to separate the skin (epidermis and dermis) from the pig ear cartilage. The ears were stored in a freezer at $-20\text{ }^{\circ}\text{C}$ for two weeks.

The skins were defrosted 24 h before the start of the study. They were cut into square pieces ($3 \times 3\text{ cm}$) and placed on Petri dishes. These skin portions were the substrates for the sample vehicles. A total of 80 mg of the emulsion was spread homogeneously on the substrate skin sheets. In addition, another skin sheet was attached to the lower end of a cylindrical probe (1 cm in diameter) facing downward, opposite the substrate skin with a rubber ring (attached skin) (Figure 1).

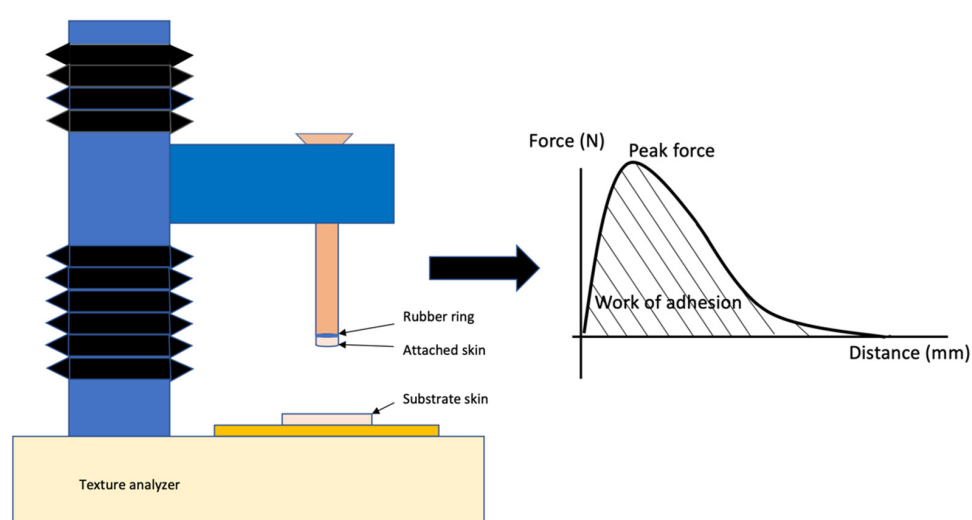


Figure 1. Experimental settings: Schematic illustration of the texture analyzer. The peak force and work of adhesion provided by the texture analyzer software Materials Master (SET19002, Stable Micro Systems, Surrey, England). Illustration based on Carvalho et al., 2013 [5] and Hägeström et al., 2004 [8].

2.5. Texture Analyzer

A texture analyzer was used to measure the bioadhesion of pellets, minitables, and emulsions. This device is commonly used to measure bioadhesion/mucoadhesion [11]. The method and experiment settings are described in Section 2.5.1 (and the preliminary method settings are described in Section 2.5.2).

2.5.1. Experimental Settings

The upper part of the texture analyzer (with the attached skin) was placed as close as possible to the substrate skin. Contact was avoided between the two skin sheets (porcine stomach for the pellets and minitables and porcine ear skin for the emulsions). In this position, the texture analyzer was lowered to 0.1 mm/s until contact between the substrate skin and the attached skin was made. The triggering force (by which the contact with the sample was calculated) was 0.01 N . The two skin pieces were in contact for 60 s under a force of 0.5 N . The upper part of the texture analyzer was lifted at a speed of 0.1 mm/s until the separation of the two skin sheets occurred. Figure 1 illustrates the peak force and the work of adhesion, which are the force needed to separate the two skin sheets and the area under the force–distance curve, respectively.

2.5.2. Method Development

Preliminary experiments were conducted to establish the best conditions for performing the test described in Section 2.5.1. Porcine stomach was used as a substrate. Three critical parameters were selected to determine the conditions of the test: (1) the contact time between the attached and the substrate skin, (2) the force exerted during contact time, and (3) the detachment speed. The test conditions for contact time were 15, 20, 60, and 900 s. The test conditions for contact force were 0.3, 0.5, and 1 N. The detachment speed was set to 0.1 mm/s according to Hägerström et al. [3]. Hägerström et al. studied different speeds and concluded that the one that gave the best discriminative values was 0.1 mm/s. The findings of this author on the detachment speed were taken into account in the present article.

The test was performed at controlled room temperature (25 ± 2 °C) according to the Eur Ph [12].

The peak force of ten pellets with the bioadhesion film was compared with the same number of pellets without the bioadhesion film. The increase difference was determined by the percentage increase of the two types of pellets and calculated with Equation (1).

$$\text{Percentage increase (\%)} = \frac{\bar{F}_{(Film-No\ film)}}{\bar{F}_{No\ film}} \times 100 \quad (1)$$

where F stands for the peak force (N) of the average results obtained for the pellets with the bioadhesive film and those without the bioadhesive film.

The same calculation was used to assess the percentage increase in the work of adhesion (calculated with Equation (2)).

$$\text{Percentage increase (\%)} = \frac{\bar{W}_{(Film-No\ film)}}{\bar{W}_{No\ film}} \times 100 \quad (2)$$

where W stands for the work of adhesion (mJ) of the average results obtained for the pellets with the bioadhesive film and those without the bioadhesive film.

After establishing the method for the pellets, Equations (1) and (2) were used to calculate the force and work percentage increase of the minitables and emulsions.

A stability test was also performed for the bioadhesive emulsion. The bioadhesive emulsion was assessed immediately after and one year after manufacturing. The bioadhesive behavior of the bioadhesive emulsions (1 and 2) was then compared with (1) a non-bioadhesive emulsion and (2) the substrate skin alone. Moreover, the bioadhesive emulsion was tested in a wet environment so that the bioadhesive behavior could be assessed following exposure to water. For this purpose, the skin was moistened with 5 mL of distilled water (following the application of the bioadhesive emulsion to the skin).

2.6. Statistical Analysis

The bioadhesive emulsions were assessed five times ($n = 5$), and the following emulsions were assessed three times ($n = 3$): non-bioadhesive emulsions, bioadhesive emulsions after 1 year, and bioadhesive emulsions at wet conditions. Bioadhesive and control pellets were assessed nine times ($n = 9$), and bioadhesive minitables and control minitables were assessed six times ($n = 6$). Statistical relevance was established at $p < 0.05$ for all statistical tests performed. GraphPad Prism version 9.0.0 for Windows Harvey Motulsky (GraphPad Software, San Diego, CA, USA) was used as a statistical tool. Data are expressed as mean \pm SD, and statistical significance was measured using the unpaired t -test (two measurement datasets), one-way ANOVA, and multiple comparison tests (more than two datasets).

3. Results

3.1. Parameters Analysis

Unlike trigger force, withdrawal speed, contact force, and contact time have been reported as key factors influencing the design of an in vitro method for measuring bioadhe-

sion and mucoadhesion [13]. To determine the best conditions for measuring bioadhesion using a texture analyzer, the current study combined some of the factors that could affect it. In particular, the velocity was set to 0.1 mm/s as a result of findings in the literature [3] that 0.1 mm/s led to less variability in the measurements.

As has previously been described, the bioadhesion of ten pellets (ten with and ten without the bioadhesive film) was compared. Three different contact forces were applied: 0.3, 0.5, and 1 N. While the bioadhesive pellets showed higher force peaks at 0.3 and 0.5 N contact forces, at 1 N, the opposite effect was observed, i.e., a negative percentage increase. Of the two other forces tested, 0.5 N showed a higher force value. Although the percentage differences were small, the bioadhesive pellets at 0.5 N showed a marginally higher force value compared with the non-bioadhesive pellets.

Having determined the contact force as 0.5 N, the contact time was assessed. A force of 0.5 N was applied at 0.01 mm/s in this experiment. The following contact times were assessed: two short contact times (15 s and 20 s), an intermediate contact time of 60 s, and a long contact time of 900 s. Among these, 15 s was immediately discarded, as the percentage increase was negative. However, a positive percentage increase was obtained with the 20 s test, although the results showed large deviations. Additionally, a high deviation of the results was observed with the high contact time (900 s). The contact time of 60 s was thus selected as the most suitable contact time for testing, as this contact time showed positive percentage increase values with only small deviations (Figure 2).

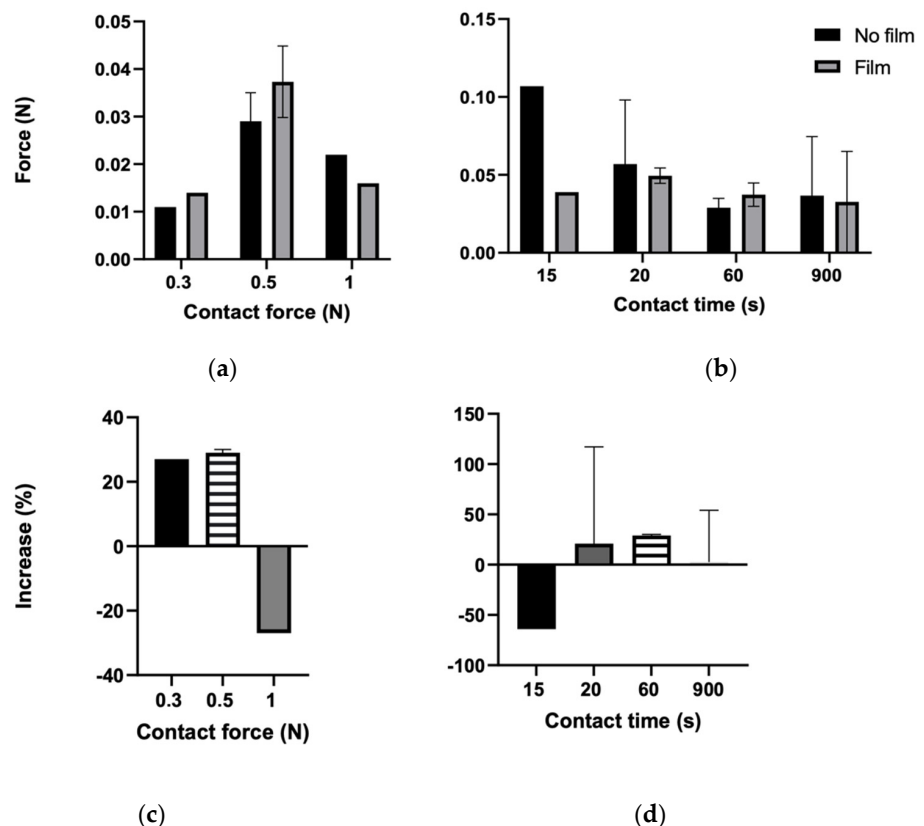


Figure 2. Adhesion force applied to pellets with (a) different contact forces and (b) different contact times. (c) Percentage increases at different contact forces and (d) percentage increases at different contact times.

3.2. Gastric Mucoadhesion and Statistical Study

3.2.1. Pellets

The results in Table 6 show that there are significant differences in terms of both studied parameters (peak and work forces) between the bioadhesive and non-bioadhesive pellets. The difference between both types of pellets was 0.048 N in terms of peak force and 0.119 mJ in terms of work force. The similarity in the peak force and work force of both types of pellets was also reflected in the percentage increase (187.8% and 179.8%, respectively). Thus, both parameters confirmed bioadhesion (Figure 3, with raw data being listed in Table A1).

Table 6. Peak force (F) and work of adhesion (W) of pellets without the mucoadhesive film (control) and with the mucoadhesive film. Differences between the two groups shown as mean \pm SD, ($n = 9$).

Pellets	F (N)	W (mJ)
No film	0.025 \pm 0.012	0.066 \pm 0.070
Film	0.073 \pm 0.053	0.185 \pm 0.135
Difference (film–no film)	0.048	0.119
Increase (%)	187.8	179.8

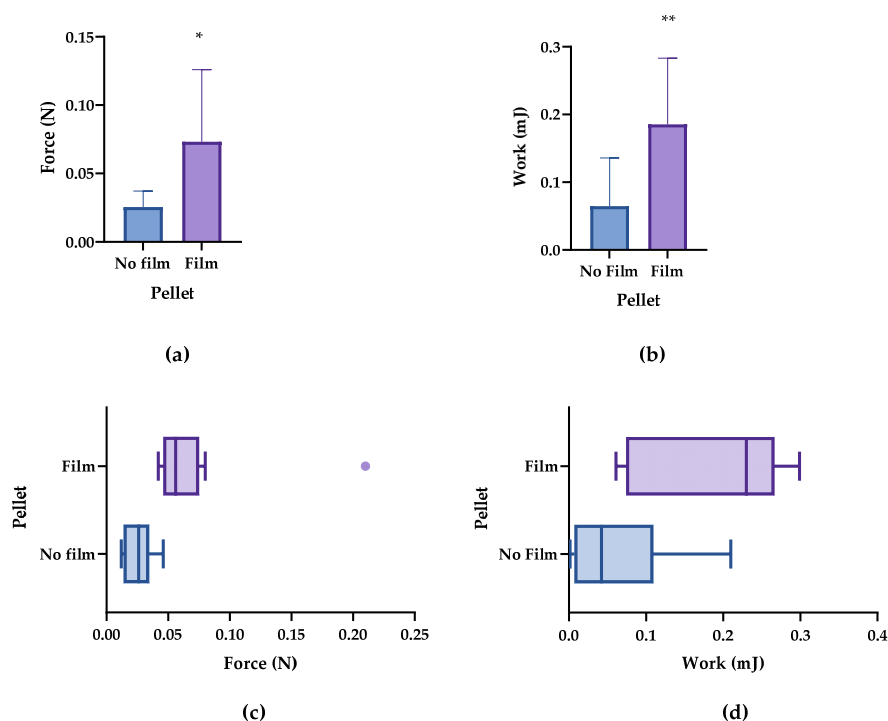


Figure 3. Bioadhesion parameters of the bioadhesive and non-bioadhesive pellets. (a) Peak adhesion force and (b) work of adhesion. (c) Box plot of the peak of adhesion and (d) work of adhesion. * $p < 0.5$, ** $p < 0.01$.

It is worth mentioning that the relatively high standard deviation (± 0.053) in the force of the bioadhesive pellets was the result of a single value exceeding the mean (Figure 3a,c). However, this was not observed in the work of adhesion (Figure 3b,d). Moreover, the results of the work of adhesion were more dispersed for both pellet types compared with the peak force values.

3.2.2. Minitablets

Greater differences were observed for the work of adhesion compared with the peak force between the two types of minitables (with film and no film) (Table 7). While the

difference in the peak force for both minitab types was 0.015 N, the difference in the work force was 0.065 mJ. This represented more than twice the increase in the work of adhesion compared with the peak force of adhesion (60% peak force increase compared with 141.3% work increase). The raw data are listed in Table A2.

Table 7. Peak force (F) and work of adhesion (W) of minitabets without the mucoadhesive film (control) and with the mucoadhesive film. Differences between the two groups shown as mean \pm SD, ($n = 6$).

Minitabets	F (N)	W (mJ)
No film	0.025 \pm 0.006	0.046 \pm 0.022
Film	0.040 \pm 0.007	0.111 \pm 0.060
Difference (film–no film)	0.015	0.065
Increase (%)	60	141.3

Again, the work of adhesion showed a higher statistical value compared with the peak force. However, both parameters were optimal predictors for assessing the bioadhesion of the minitabets. Therefore, despite the differences in the magnitude of the increase, both parameters showed high statistical differences for the two minitab types with $p < 0.01$ and $p < 0.001$ for peak force and work of adhesion, respectively (Figure 4a,b). This difference in bioadhesive results for both parameters (peak force and work of adhesion) is shown in the box plots; peak force and work of adhesion results for the second and third quartiles are separated from each other (Figure 4b,d).

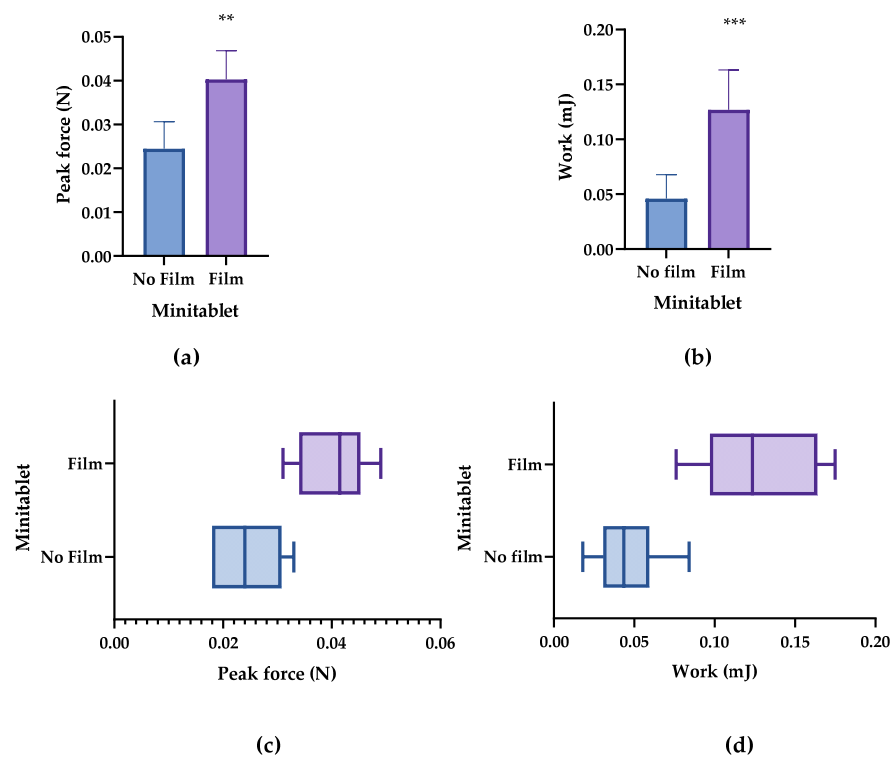


Figure 4. Bioadhesion parameters of the bioadhesive and non-bioadhesive minitabets. (a) Peak force and (b) work of adhesion. (c) Box plot of the peak force and (d) work of adhesion. ** $p < 0.01$, and *** $p < 0.001$.

3.3. Emulsions

The peak force and work of adhesion results for both the bioadhesive (BE) and the non-bioadhesive (non-BE) emulsions are shown in Figure 5a–d and Table 3. While the

average peak force difference between both emulsion types was 0.283 N, the average work of adhesion difference between both emulsions was 0.375 mJ. The peak force of the bioadhesive emulsion resulted in more than three times the peak force of the non-bioadhesive emulsion. However, the bioadhesive emulsion increased more than 20 times compared with the non-BE for the work of adhesion.

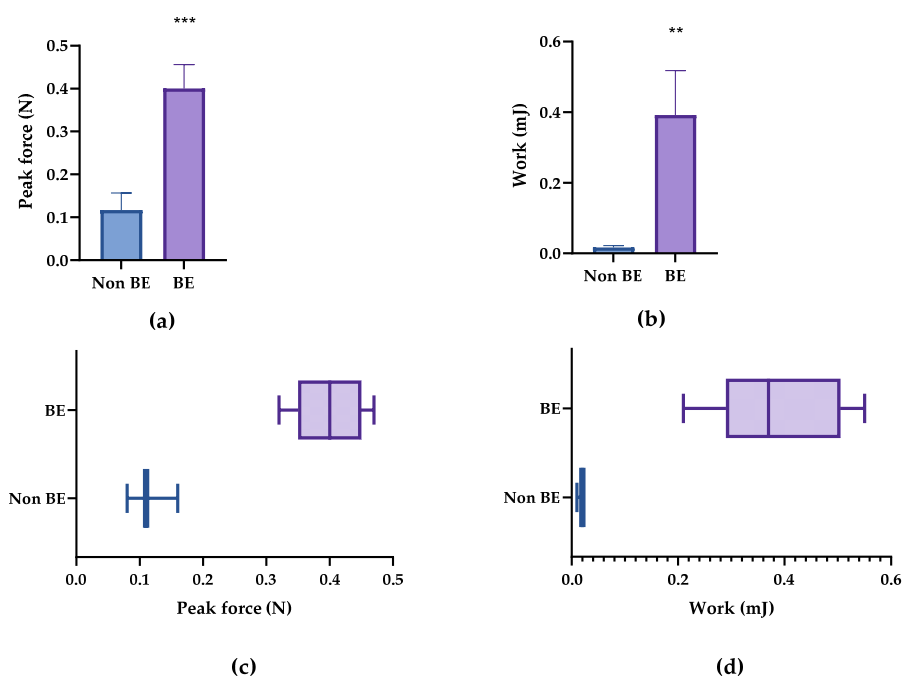


Figure 5. Bioadhesion parameters of the bioadhesive and non-bioadhesive emulsions (BE and non-BE). (a) Peak and (b) work of adhesion. (c) Box plot of the peak force and (d) work of adhesion. ** $p < 0.01$, and *** $p < 0.001$.

The percentage increase in the work of adhesion was nearly eight times higher compared with the percentage increase in the peak force (241.9% peak force vs. 2205% work force, Table 8). The raw data are listed in Table A3.

Table 8. Peak force (F) and work of adhesion (W) of the bioadhesive (BE) and non-bioadhesive (Non-BE) emulsions. Differences between the two groups shown as mean \pm SD, ($n = 5$ for BE and $n = 3$ for non-BE).

Samples	F (N)	W (mJ)
Non-BE	0.117 \pm 0.040	0.017 \pm 0.009
BE	0.400 \pm 0.056	0.392 \pm 0.126
Difference (BE–Non-BE)	0.283	0.375
Increase (%)	241.9	2205.9

Despite these differences in the magnitudes of the increase, both parameters were equally valid for predicting the bioadhesion of emulsions. This was because the peak force and work of adhesion of the bioadhesive emulsions were significantly different from the non-bioadhesive ones with p -values of < 0.001 and 0.01 , respectively (Figure 5a,b). The high statistical significance is visible in Figure 5c,d; the box plots of the bioadhesive emulsions do not overlap with those of the non-bioadhesive ones for either the peak force or work of adhesion.

Regarding the precision of the measurements, the peak force had a smaller standard deviation for the bioadhesive emulsion compared with the work of adhesion. However,

this effect was the opposite for the non-bioadhesive emulsion, where the standard deviation for the work of adhesion was smaller.

3.4. Case Study

The results of the bioadhesive test are presented in Table 9 and Figure 6a–d. The peak force and work of adhesion were measured for each emulsion type. The results showed that there were significant differences ($p \leq 0.05$) between the bioadhesive emulsion and the mock (skin without emulsion) in terms of both the peak force and work of adhesion. As was mentioned in Section 3.2, the bioadhesive emulsion was statistically different to the non-bioadhesive emulsion. Additionally, no significant difference was observed between the mock and the non-bioadhesive emulsion (Table 4). The raw data are listed in Table A3.

As has previously been stated, the bioadhesive emulsion was then compared with the same emulsion after one year of storage. Figure 6a–d show very similar peak forces and work of adhesion after one year of storage. The peak force of the bioadhesive emulsion was originally 0.40 ± 0.056 N, and after one year the peak force was 0.377 ± 0.045 N. There was only a 0.023 N difference after one year, which represents roughly a 5% decrease. Additionally, the bioadhesive emulsion that had been manufactured one year earlier (BE 1 year) was compared with the mock and the non-bioadhesive emulsion (non-BE). Both the mock and the non-bioadhesive emulsion showed statistical differences compared with BE 1 year. While the differences observed for the mock in terms of peak force and work of adhesion were 0.297 N and 0.308 mJ (a 371% and 2803% increase, respectively), the difference observed for the non-bioadhesive emulsion was 0.260 N and 0.302 mJ (a 222.3% and 1776% increase, respectively). We can observe that the percentage increases were similar for peak force and greater for work of adhesion. In addition, the results of the percentage increase obtained for work of adhesion showed higher standard deviations than those obtained for peak force.

This measurement precision is shown in the box plots (Figure 6c,d). The results on the work of adhesion were more spread out, especially for the emulsions showing bioadhesive behavior: BE and BE 1 year (* in Figure 6a,b). The results for bioadhesive emulsions did not overlap with the results for the non-bioadhesive emulsion or the mock.

Table 9. Peak force (F) and work of adhesion (W) of the bioadhesive (BE), non-bioadhesive (Non-BE) emulsions, BE after one year (ba.em-1y) and Bioadhesive emulsion wet (ba.em-wet). Differences between the groups shown as mean \pm SD, ($n = 5$ for BE and $n = 3$ for non-BE, ba.em-1y and ba.em-wet).

Samples	F (N)	W (mJ)
Mock	0.080	0.011
Non-BE	0.117 ± 0.040	0.017 ± 0.009
BE	0.400 ± 0.056	0.392 ± 0.126
Difference (BE–mock)	0.320	0.381
Increase (%)	400.0	3463.6
Difference (BE–Non-BE)	0.283	0.375
Increase (%)	241.8	2205.9
BE after 1 year	0.377 ± 0.045	0.319 ± 0.152
Difference (ba.em-1y–mock)	0.297	0.308
Increase (%)	371.3	2803.0
Difference (ba.em-1y–Non-BE)	0.260	0.302
Increase (%)	222.2	1776.0
Bioadhesive emulsion wet	0.212 ± 0.041	0.081 ± 0.004
Difference (ba. em-wet–mock)	0.132	0.070
Increase (%)	165.0	638.8
Difference (ba. em-wet–Non-BE)	0.095	0.064
Increase (%)	81.2	376.0

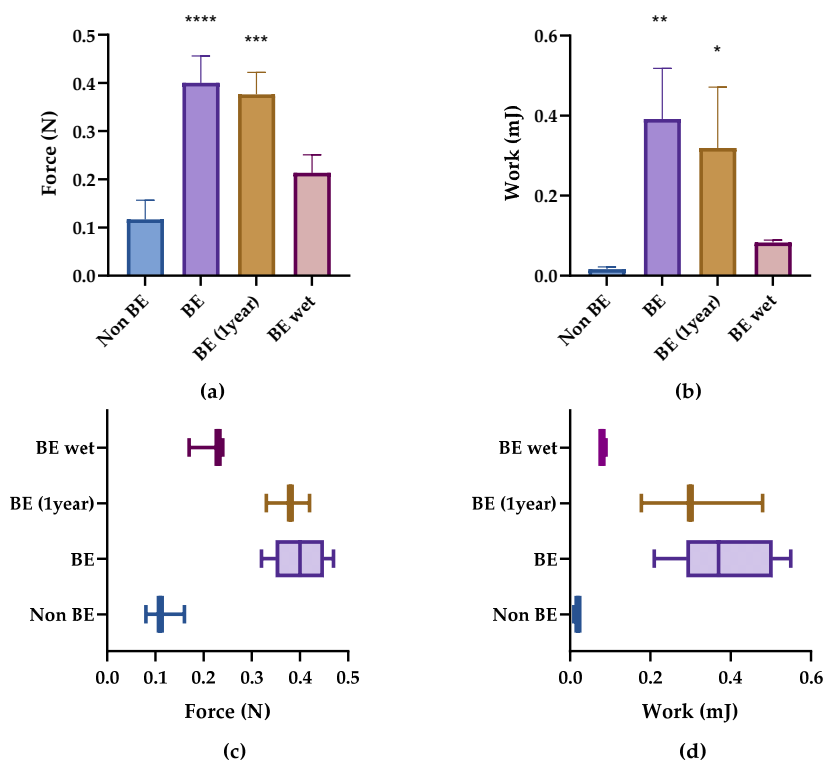


Figure 6. The bioadhesion parameters of the non-bioadhesive emulsion (non-BE), bioadhesive emulsion (BE), bioadhesive emulsion after one year, and bioadhesive emulsion in wet conditions (BE 1 year). (a) Peak adhesion force and (b) work of adhesion. (c) Box plot of the peak of adhesion and (d) work of adhesion. * $p < 0.5$, ** $p < 0.01$, and *** $p < 0.001$, **** $p < 0.0001$.

Finally, the moistened bioadhesive emulsion was compared with the non-bioadhesive emulsion and mock in terms of peak force and work of adhesion. There was no significant difference between the bioadhesive emulsion that was moistened with 5 mL of water and the mock in relation to peak force and work of adhesion, as is shown in Figure 6a,b. This confirms that the bioadhesive emulsion that was moistened with 5 mL was not bioadhesive. The percentage increase was higher for the work of adhesion compared with the peak force: 638.8% and 165% compared with the mock and 376% and 81.2%, respectively, compared with the non-BE.

4. Discussions

As was mentioned in the introduction (Section 1), although some methods for measuring bioadhesion/mucoadhesion have been proposed, a standardized method has not been identified in the literature. This is expected to hinder systematic comparisons of results across studies.

In particular, most of the published studies on bioadhesion have been performed using mucosa. The choice of substrate usually depends on the route of administration of the product. In cases where the product is intended for oral, nasal, or intravaginal use, the use of mucosal tissue is the norm, and numerous studies have described the development of these bioadhesive products [4]. However, few studies have addressed bioadhesion for skin administration. This external part of the body may be a target for semisolid formulations (with bioadhesive properties carrying one or more active substances). The methods for bioadhesion have been described in the literature for both the mucosa and the skin, but separately. However, a method compatible with different pharmaceutical dosage forms and skin/mucosa substrates has not yet been established. Therefore, as previously stated, this study proceeded to select two solid products for oral administration and a

semisolid form for topical administration in an attempt to develop an *in vitro* method for measuring bioadhesion and mucoadhesion that is applicable to a variety of pharmaceutical dosage forms.

The bioadhesive product was compared with a non-bioadhesive formulation, in contrast to other studies [3,8,14] in which the substrate without any product was the mock. Thus, the bioadhesive material itself was assessed as the formulation without the bioadhesive film may have an independent measure of adhesion. However, as was demonstrated in the case study (Section 3.3), there were only small differences in peak force and work of adhesion between the skin without emulsion and the non-bioadhesive formulation. Therefore, both skin without emulsion and non-bioadhesive emulsion were deemed valid mocks.

Regarding the product use, it was important to assess bioadhesion with amounts as close as possible to the actual conditions of use. While package leaflets do not establish single-dose prescriptions for topical formulations, a patent for a bioadhesive gel product containing acyclovir selected 8.3 mg/cm^2 as the appropriate amount of gel product for topical use [15]. However, sunscreen products have clear standards for measuring sun protection factors (SPF) *in vivo* and do specify an amount of 2 mg/cm^2 to achieve the labeled SPF [16]. This is equivalent to 50 mg of the product homogeneously spread on a $5 \times 5 \text{ cm}$ skin sheet section. In the present study, 80 mg of the emulsion was spread on $3 \times 3 \text{ cm}$ skin sheet sections. This corresponds to 5.3 mg/cm^2 . This amount was selected because it lies between 2 mg/cm^2 and 8.3 mg/cm^2 . The amount used in this study is therefore closer to that of actual applications of topical formulations compared with other studies in the same field [3,8,17,18].

The parameters of peak force and work of adhesion were both valid for determining the bioadhesion of the formulation. Significant differences were observed between bioadhesive and non-bioadhesive formulations when any of these parameters were used. The high standard deviation of the work of adhesion can be explained by the fact that the work of adhesion is the result of two factors, namely force and distance, whereas peak force is a direct measure. Furthermore, contact time and contact force were determining factors for bioadhesion.

The method proposed here was found to work on formulations of different natures, namely, solid formulations (minitablets and pellets) and semi-solid formulations (emulsions). Minitablets and pellets were chosen because they are representatives of solid formulations, and an emulsion is representative of a semi-solid formulation. It should, however, be emphasized that the test must be performed under the same conditions for all measurements as minor changes may result in variations. For instance, in our study, the bioadhesive emulsion was moistened with 5 mL of water prior to the bioadhesive test, and consequently, the bioadhesion decreased compared with the unmoistened bioadhesive emulsion. This further illustrates the challenge of extrapolating results performed under different settings.

5. Conclusions

A systematic method for measuring the bioadhesive capacity of pharmaceutical dosage forms (for topical and internal mucosa applications) was successfully developed. The method proposed here may enable the comparison of results across studies, *i.e.*, results obtained using the same and different pharmaceutical formulations (in terms of bioadhesion/mucoadhesion capacity). This method could also facilitate the selection of potentially suitable formulations and adhesive products (in terms of their bioadhesive properties).

Future research may wish to further verify the applicability of such a method to other pharmaceutical dosage forms (*e.g.*, gels, lipogels, emulgels, patches, and capsules).

Author Contributions: Conceptualization, J.M.S.-N.; methodology, C.V.-G., C.M.A.-G. and L.A.-G.; software, L.A.-G.; validation, J.M.S.-N. and M.S.-P.; formal analysis, J.M.S.-N., M.S.-P., E.G.-M. and P.P.-L.; investigation, L.A.-G. and A.N.-R.; resources, L.A.-G.; data curation, J.M.S.-N. and M.S.-P.; writing—original draft preparation, L.A.-G.; writing—review and editing, M.S.-P. and J.M.S.-N.; supervision, J.M.S.-N.; project administration, J.M.S.-N.; funding acquisition, J.M.S.-N. All authors have read and agreed to the published version of the manuscript.

Funding: This research was funded by the Industrial Doctorate Program of the Agency for the Management of University and Research Grants (Agència de Gestió d’Ajuts Universitaris i de Recerca (AGAUR)), Grant number 2019 DI 38.

Institutional Review Board Statement: Not applicable.

Informed Consent Statement: Not applicable.

Acknowledgments: The authors thank Albert Manich of the advanced Chemical Institute of Catalonia (IQAC-CSIC), Barcelona for training in the measurements of bioadhesion and Marta Lamana for her assistance during the measurement of the topical bioadhesion.

Conflicts of Interest: The authors declare no conflict of interest.

Appendix A

Table A1. The force of adhesion (N) and work of adhesion (mJ) of pellets without the mucoadhesive film (control) and with the mucoadhesive film. The differences between the two groups and the percentage increase in adhesion force.

Assay Number	Force of Adhesion		Work of Adhesion	
	No Film (N)	Film (N)	No Film (mJ)	Film (mJ)
1	0.031	0.056	0.058	0.137
2	0.014	0.049	0.011	0.273
3	0.012	0.043	0.003	0.260
4	0.046	0.21	0.150	0.299
5	0.038	0.058	0.210	0.063
6	0.029	0.07	0.042	0.085
7	0.014	0.08	0.038	0.061
8	0.019	0.051	0.069	0.230
9	0.026	0.042	0.015	0.260
Average	0.025	0.073	0.07	0.19
DS	0.012	0.053	0.07	0.10
CV	0.460	0.720	1.05	0.53

Table A2. The force of adhesion (N) and work of adhesion (mJ) of minitables without the mucoadhesive film (control) and with the mucoadhesive film. The differences between the two groups and the percentage increase in adhesion force.

Assay Number	Fore of Adhesion		Work of Adhesion	
	No Film (N)	Film (N)	No Film (mJ)	Film (mJ)
1	0.018	0.044	0.018	0.175
2	0.033	0.049	0.051	0.123
3	0.018	0.043	0.045	0.124
4	0.023	0.031	0.042	0.076
5	0.025	0.035	0.035	0.010
6	0.030	0.040	0.084	0.160
Average	0.025	0.040	0.046	0.111
DS	0.006	0.007	0.022	0.060
CV	0.251	0.161	0.477	0.541

Table A3. The force of adhesion (N) of emulsions (bioadhesive, non-bioadhesive (t = 0), after one year of storage, and in wet conditions) and mock (no sample). The differences between two groups and the percentage increase in adhesion force.

Assay Number	Force of Adhesion					Work of Adhesion				
	Mock (N)	Non-BE Emulsion (N)	BE (N)	BE 1 Year (N)	BE Wet (N)	Mock (mJ)	Non-BE Emulsion (mJ)	BE (mJ)	BE 1 Year (mJ)	BE Wet (mJ)
1	0.080	0.080	0.320	0.330	0.170	0.01	0.007	0.21	0.178	0.09
2		0.160	0.470	0.420	0.230		0.020	0.37	0.480	0.08
3		0.110	0.380	0.380	0.240		0.023	0.37	0.300	0.08
4			0.430					0.55		
5			0.400					0.46		
Average		0.12	0.40	0.38	0.21	0.01	0.02	0.39	0.32	0.08
DS		0.04	0.06	0.05	0.04	0.0001	0.01	0.13	0.15	0.00
CV		0.35	0.14	0.12	0.19		0.51	0.32	0.48	0.05

References

- Kumar, K.; Dhawan, N.; Sharma, H.; Vaidya, S.; Vaidya, B. Bioadhesive Polymers: Novel Tool for Drug Delivery. *Artif. Cells Nanomed. Biotechnol.* **2014**, *42*, 274–283. [CrossRef] [PubMed]
- Bassi da Silva, J.; de Ferreira, S.B.S.; de Freitas, O.; Bruschi, M.L. A Critical Review about Methodologies for the Analysis of Mucoadhesive Properties of Drug Delivery Systems. *Drug Dev. Ind. Pharm.* **2017**, *43*, 1053–1070. [CrossRef] [PubMed]
- Hägerström, H.; Edsman, K. Interpretation of Mucoadhesive Properties of Polymer. *J. Pharm. Pharmacol.* **2001**, *53*, 1589–1599. [CrossRef] [PubMed]
- Djelic, L.; Martinovic, M. In Vitro, Ex Vivo and In Vivo Methods for Characterization of Bioadhesiveness of Drug Delivery Systems. In *Bioadhesives in Drug Delivery*; Scrivener Publishing LLC: Beverly, MA, USA, 2020.
- Carvalho, F.C.; Calixto, G.; Hatakeyama, I.N.; Luz, G.M.; Gremião, M.P.D.; Chorilli, M. Rheological, Mechanical, and Bioadhesive Behavior of Hydrogels to Optimize Skin Delivery Systems. *Drug Dev. Ind. Pharm.* **2013**, *39*, 1750–1757. [CrossRef] [PubMed]
- Palacio, M.L.B.; Bhushan, B. Bioadhesion: A Review of Concepts and Applications. *Philos. Trans. R. Soc. A* **2012**, *370*, 2321. [CrossRef] [PubMed]
- Wong, R.; Geyer, S.; Weninger, W.; Guimberteau, J.C.; Wong, J.K. The Dynamic Anatomy and Patterning of Skin. *Exp. Dermatol.* **2016**, *25*, 92–98. [CrossRef]
- Hägerström, H.; Bergström, C.A.S.; Edsman, K. The Importance of Gel Properties for Mucoadhesion Measurements: A Multivariate Data Analysis Approach. *J. Pharm. Pharmacol.* **2004**, *56*, 161–168. [CrossRef] [PubMed]
- Duchene, D.; Ponchel, G. Bioadhesion: A New Pharmacotechnical Method for Improving Therapeutic Efficiency. *STD Pharma* **1989**, *5*, 830–838.
- Dick, I.P.; Scott, R.C. Pig Ear Skin as an In-Vitro Model for Human Skin Permeability. *J. Pharm. Pharmacol.* **1992**, *44*, 640–645. [CrossRef] [PubMed]
- Bruschi, M.L.; Jones, D.S.; Panzeri, H.; Gremiao, M.P.D.; de Freitas, O.; Lara, E.H.G. Semisolid Systems Containing Propolis for the Treatment of Periodontal Disease: In Vitro Release Kinetics, Syringeability, Rheological, Textural, and Mucoadhesive Properties. *J. Pharm. Sci.* **2007**, *96*, 2074–2089. [CrossRef] [PubMed]
- 01 General Notices—European Pharmacopoeia 10.8. Available online: <https://pheur.edqm.eu/app/10-8/content/10-8/10000E.htm?highlight=on&terms=1.2.3%20temperature&terms=temperature&terms=temperature&terms=temperature&terms=temperature&terms=temperature&terms=1.2.3%20temperature&terms=temperature&terms=temperature&terms=temperature&terms=temperature&terms=temperature> (accessed on 31 August 2022).
- Woertz, C.; Preis, M.; Breikreutz, J.; Kleinebudde, P. Assessment of test methods evaluating mucoadhesive polymers and dosage forms: An overview. *Eur. J. Pharm. Biopharm.* **2013**, *85*, 843–853. [CrossRef] [PubMed]
- Hägerström, H.; Edsman, K. Limitations of the Rheological Mucoadhesion Method: The Effect of the Choice of Conditions and the Rheological Synergism Parameter. *Eur. J. Pharm. Sci.* **2003**, *18*, 349–357. [CrossRef]
- Gonzalez-Ojer, C.; Costa-Martins, D.; Maria, R.; Miñarro-Carmona, M.; Ticó-Grau, J.R.A.; García-Montoya, E.; Pérez-Lozano, P.; Roig-Carreras, M.; Sánchez-Porqueres, N. ES2608794T3_Original_document_20200610102618.Pdf 2013, 29. Available online: <https://worldwide.espacenet.com/patent/search/family/047520732/publication/ES2608794T3?q=ES2608794T3> (accessed on 16 September 2022).
- ISO 24444:2019 (SPF), Cosmetics—Sun Protection Test Methods—In Vivo Determination of the Sun Protection Factor 2019. Available online: <https://www.iso.org/standard/72250.html> (accessed on 16 September 2022).
- Karakucuk, A.; Tort, S.; Han, S.; Oktay, A.N.; Celebi, N. Etodolac Nanosuspension Based Gel for Enhanced Dermal Delivery: In Vitro and in Vivo Evaluation. *J. Microencapsul.* **2021**, *38*, 218–232. [CrossRef] [PubMed]
- Ivarsson, D.; Wahlgren, M. Comparison of in Vitro Methods of Measuring Mucoadhesion: Ellipsometry, Tensile Strength and Rheological Measurements. *Colloids Surf. B Biointerfaces* **2012**, *92*, 353–359. [CrossRef]

